Distributed control of deregulated electrical power networks

Distributed Control of Deregulated Electrical Power Networks

PROEFSCHRIFT

ter verkrijging van de graad van doctor aan de
Technische Universiteit Eindhoven, op gezag van de
rector magnificus, prof.dr.ir. C.J. van Duijn, voor een
commissie aangewezen door het College voor
Promoties in het openbaar te verdedigen op
dinsdag 20 november 2012 om 14.00 uur

door

Rudolf Michiel Hermans

geboren te Stein

Dit proefschrift is goedgekeurd door de promotor:

prof.dr.ir. P.P.J. Van den Bosch

Copromotoren:
dr. M. Lazar
en
dr. A. Jokić

A catalogue record is available from the Eindhoven University of Technology Library.

Distributed Control of Deregulated Electrical Power Networks /
by Ralph Hermans. – Eindhoven : Technische Universiteit Eindhoven, 2012.
Proefschrift.

ISBN: 978-90-386-3275-9
NUR 959

Trefw.: elektrische energiesystemen; regeling / elektriciteitsvoorziening; economie / gedistribueerde regelsystemen; optimalisering / energiemarkt / dynamische netwerken; stabiliteit.
Subject headings: power system control / power generation economics / distributed control / power markets / stability of networked dynamical systems.

to my parents

Samenstelling promotiecomissie

Promotor:	Prof.dr.ir. P. P. J. Van den Bosch
Copromotors:	Dr. M. Lazar Dr. A. Jokić
Kerncommissie:	Prof.dr.-ing. F. Allgöwer Prof.dr.ir. G.L. Doorman Prof.ir. W.L. Kling

Agentschap NL

This work is part of the Energie Onderzoek Subsidie Lange Termijn (EOS-LT) Regelduurzaam project that is funded by Agentschap NL, an agency of the Dutch Ministry of Economic Affairs.

disc

This dissertation has been completed in fulfillment of the requirements of the Dutch Institute of Systems and Control (DISC).

This thesis was prepared using the LaTeX typesetting system.
Printed by: Printservice, Eindhoven University of Technology.
Cover design: Vespaget & Bruinink Vormgeving, Nuenen, The Netherlands.

Summary

A prerequisite for reliable operation of electrical power networks is that supply and demand are balanced at all time, as efficient ways for storing large amounts of electrical energy are scarce. Balancing is challenging, however, due to the power system's dimensions and complexity, the low controllability and predictability of demand, and due to strict physical and security limitations, such as finitely fast generator dynamics and finite transmission-line capacities.

The need for efficient and secure balancing arrangements grows stronger with the increasing integration of distributed generation (DG) and the ongoing deregulation of production and consumption of electrical energy — and thus, also, the provision of many of the ancillary services that are essential for network stability. DG is mostly based on renewable, intermittent sources such as wind and sun, and consequently, it is associated with a much larger uncertainty in supply than conventional, centralized generation. Moreover, with the emergence of deregulated energy markets as core operational mechanism, the prime goal of power system operation is shifted from centralized minimization of costs to the maximization of individual profit by a large number of competing, autonomous market agents.

The main objective of this thesis is to investigate the control-technical possibilities for ensuring efficient, reliable and stable operation of deregulated and badly predictable electrical power networks. Its contributions cover aspects of power system operation on a time scale ranging from day-ahead trading of electrical energy to second-based load-frequency control.

As a first contribution, we identify the maximization of security of supply and market efficiency as the two main, yet conflicting objectives of power sys-

tem operation. Special attention is paid to congestion management, which is an aspect of power system operation where the tension between reliability and efficiency is particularly apparent. More specifically, the differences between locational pricing and cost-based congestion redispatch are analyzed, followed by an assessment of their effects on grid operation.

Next, we show that the current synchronous, energy-based market and incentive system does not necessarily motivate producers to exchange power profiles with the electricity grid that contribute to network stability and security of supply. The thesis provides an alternative production scheduling concept as a means to overcome this issue, which relies on standard market arrangements, but settles energy transactions in an asynchronous way. Theoretical analysis and simulation results illustrate that by adopting this method, scheduling efficiency is improved and the strain on balancing reserves can be reduced considerably.

A major part of this thesis is dedicated to real-time, i.e., closed-loop, balancing or load-frequency control.

With the increasing share of badly predictable DG, there is a growing need for efficient balancing mechanisms that can account for generator and transmission constraints during the operational day. A promising candidate solution is model predictive control (MPC). Because the large dimensions and complexity of electrical power networks hamper a standard, centralized implementation of MPC, we evaluate a number of scalable alternatives, in which the overall control action is computed by a set of local predictive control laws, instead. The extent of inter-controller communication is shown to be positively correlated with prediction accuracy and, thus, attainable closed-loop performance. Iterative, system-wide communication/coordination is usually not feasible for large networks, however, and consequently, optimal performance with respect to a system-wide objective function and coupled-constraint handling are currently out of reach. This also hampers the application of standard cost-based stabilization schemes, in which closed-loop stability is attained via monotonic convergence of a single, optimal system-wide performance cost.

Motivated by the observations regarding non-centralized MPC, the focus is then shifted to distributed control methods for networks of interconnected dynamical systems, with power systems as particular field of application, that can ensure stability based on local model and state information only.

First, we propose a non-centralized, constraint-based stabilization scheme, in which the set of stabilizing control actions is specified via separable convergence conditions for a collection of a-priori synthesized structured max-control Lyapunov functions (max-CLFs). The method is shown to be non-conservative, in the sense that non-monotonic convergence of the structured functions along

closed-loop trajectories is allowed, whereas their construction establishes the existence of a control Lyapunov function, and thus, stability, for the full, interconnected dynamics. Then, an alternative method is provided in which also the demand for a monotonically converging full-system CLF is relaxed while retaining the stability certificate. The conditions are embedded in an almost-decentralized Lyapunov-based MPC scheme, in which the local control laws rely on neighbor-to-neighbor communication only.

Secondly, a generalized theorem and example system are provided to show that stabilization methods that rely on the off-line synthesis of fixed quadratic storage functions (SFs) fail for even the simplest of linear, time-invariant networks, if they contain one or more subsystems that are not stable under decoupled operation. This may also impede the application of max-CLF control. As key contribution of this thesis, to solve this issue, we endow the storage functions with a finite set of state-dependent parameters. Max-type convergence conditions are employed to construct a Lyapunov function for the full network, whereas monotonic convergence of the individual SFs is not required. The merit of the provided approach is that the storage functions can be constructed during operation, i.e., along a closed-loop trajectory, thus removing the impediment of centralized, off-line LF synthesis associated with fixed-parameter SFs.

It is shown that parameterized-SF synthesis conditions can be efficiently exploited to obtain a scalable, trajectory-dependent control scheme that relies on non-iterative neighbor-to-neighbor communication only. For input-affine network dynamics and quadratic storage functions, the procedure can be implemented by solving a single semi-definite program per node and sampling instant, in a receding horizon fashion. Moreover, by interpolating a collection of so-obtained input trajectories, a low-complexity explicit control law for linear, time-invariant systems is obtained that extends the trajectory-specific convergence property to a much stronger guarantee of closed-loop asymptotic stability for a particular set of initial conditions.

Finally, we consider the application of max-CLF and parameterized SFs for real-time balancing in multimachine electrical power networks. Given that generators are operated by competitive, profit-driven market agents, the stabilization scheme is extended with the competitive optimization of a set of arbitrarily chosen, local performance cost functions over a finite, receding prediction horizon. The suitability of the distributed Lyapunov-based predictive control and parameterized storage function algorithms is evaluated by simulating them in closed-loop with the 7-machine CIGRÉ benchmark system.

The thesis concludes by summarizing the main contributions, followed by ideas for future research.

Samenvatting

Door het gebrek aan middelen voor het efficiënt opslaan van grote hoeveelheden elektrische energie, dienen, voor een juist functioneren van het elektriciteitsnetwerk, vraag en aanbod van vermogen voortdurend op elkaar te worden afgestemd. Balancering is echter een technisch uitdagend probleem, vanwege de grote afmetingen en complexiteit van electriciteitsnetwerken, de matige beheersbaarheid en voorspelbaarheid van geconsumeerd vermogen, en stricte fysieke en veiligheidsbeperkingen, zoals generatortraagheid en eindige transmissiecapaciteiten.

De behoefte aan efficiënte en betrouwbare balansregelingen groeit met het toenemende belang van decentrale opwekking, de deregulering van de productie en consumptie van elektrische energie, en dientengevolge, ook de levering van veel van de ondersteunende diensten die essentieel zijn voor netwerkstabiliteit. Decentrale opwekking is vooral gebaseerd op hernieuwbare, fluctuerende bronnen zoals wind en zon, en wordt daarom geassocieerd met een veel grotere onzekerheid in opgewekt vermogen dan bij conventionele energiecentrales het geval is. Met de komst van gedereguleerde energiemarkten als belangrijkste stuurmechanisme, is het hoofddoel van elektriciteitsnetwerkbeheer verschoven van de gecentraliseerde minimalisatie van operationele kosten naar individuele winstmaximalisatie door een groot aantal concurrerende, autonome marktpartijen.

Doel van dit proefschrift is het onderzoeken van regeltechnische methoden die bij kunnen dragen aan een efficiënte, betrouwbare en stabiele werking van gedereguleerde en moeilijk voorspelbare elektriciteitsnetwerken. Het beschreven onderzoek bestrijkt een tijdschaal variërend van day-ahead handel in elek-

trische energie tot load-frequentieregeling met tijdconstantes in de orde van secondes.

Als eerste bijdrage, identificeren we het vergroten van systeemveiligheid en marktefficiëntie als de twee belangrijkste, maar tegenstrijdige doelstellingen van elektriciteitsnetwerkbeheer. Speciale aandacht wordt besteed aan congestiemanagement, waar het spanningsveld tussen betrouwbaarheid en efficiëntie bijzonder zichtbaar is. De verschillen tussen *locational pricing* en *cost-based redispatch* worden onderzocht, gevolgd door een analyse van hun effect op het functioneren van elektriciteitsmarkt en -netwerk.

Vervolgens wordt aangetoond dat het huidige synchrone, energiegebaseerde markt- en prijsprikkelsysteem marktpartijen niet noodzakelijkerwijs stimuleert tot het leveren van vermogensprofielen die bijdragen aan de netwerkstabiliteit en de continuïteit van elektrische energievoorziening. Een alternatieve productieplanningsmethode die berust op standaard marktregelingen, maar waarbij energietransacties op een asynchrone manier worden verrekend, wordt voorgesteld als oplossing voor dit probleem. Theoretische onderbouwing en simulatieresultaten illustreren dat deze methode de planningsefficiëntie verhoogt en de benodigde hoeveelheid regelreserves aanzienlijk kan doen afnemen.

Een groot deel van dit proefschrift is gewijd aan real-time, oftewel, closed-loop, balancering/frequentieregeling.

Door het toenemende belang van moeilijk voorspelbare gedistribueerde opwekking, is er een groeiende behoefte aan efficiënte balanceringsmechanismen die expliciet, in real-time, rekening houden met generator- en transmissiebeperkingen. Een veelbelovende mogelijke oplossing is *model predictive control (MPC)*. Omdat de afmetingen en complexiteit van het elektriciteitsnetwerk de implementatie van een standaard, gecentraliseerde vorm van MPC bemoeilijken, richten we onze aandacht op een aantal schaalbare alternatieve technieken, waarbij de totale regelactie wordt berekend door een verzameling van lokale modelvoorspellende regelaars. De mate van inter-controller communicatie blijkt positief gecorreleerd te zijn met de nauwkeurigheid van toestandsvoorspellingen, en dus, closed-loop performance. Grootschalige netwerken staan iteratieve, systeembrede communicatie/coördinatie echter niet toe, en dus zijn optimale netwerkprestaties en gekoppelde constraint handling op dit moment technisch niet haalbaar. Dit belemmert ook de toepassing van standaard, kostengebaseerde stabilisatiemethoden, waarbij closed-loop stabiliteit wordt bereikt via monotone convergentie van de optimale waarden van een enkel netwerkbreed optimalisatiecriterium.

Gegeven de beperkingen van gedecentraliseerde MPC, verleggen we vervolgens onze aandacht naar gedistribueerde regelmethoden voor generieke netwerken van gekoppelde dynamische systemen, met elektriciteitsnetwerken als

specifiek toepassingsgebied, die stabiliteit garanderen op basis van slechts lokale model- en toestandsinformatie.

Eerst wordt een decentrale, constraintgebaseerde stabilisatietechniek beschreven, waarbij de verzameling van stabiliserende systeemspecifieke regelacties gekarakteriseerd wordt door convergentievoorwaarden voor een aantal apriori gesynthetiseerde *structured max-control Lyapunov-functies (max-CLFs)*. Deze methode is niet conservatief, in die zin dat niet-monotone convergentie van de max-CLFs is toegestaan. De functies worden echter op een dusdanige manier geconstrueerd, dat dit het bestaan van een systeembrede control Lyapunov-functie, en dus closed-loop stabiliteit van het volledige netwerk, garandeert. Vervolgens wordt een alternatieve stabilisatiemethode beschreven, waarin ook de netwerkbrede CLF niet meer monotoon, maar slechts asymptotisch hoeft te convergeren. De stabilisatiecondities worden daarna ingesloten in een gedistribueerde modelvoorspellende regeling, die volledig berust op communicatie tussen directe buursystemen.

Ten tweede wordt theoretisch bewezen en een voorbeeldnetwerk beschreven dat aantoont dat stabilisatiemethodes die gebaseerd zijn op off-line synthese van fixed-parameter kwadratische *storagefuncties (SFs)* niet geschikt zijn voor zelfs de eenvoudigste lineaire, tijdinvariante netwerken, indien deze één of meer subsystemen bevatten die niet stabiel zijn wanneer ze worden ontkoppeld. Dit bemoeilijkt ook de toepassing van max-CLF control. Het vinden van een oplossing voor dit probleem is een belangrijke bijdrage van dit proefschrift. De oplossing wordt verkregen door de storagefuncties te voorzien van een eindige verzameling aan toestandsafhankelijke parameters. Max-type convergentievoorwaarden worden gebruikt om een netwerkbrede Lyapunovfunctie te construeren, zonder monotone convergentie van de afzonderlijke SFs te eisen. Deze aanpak heeft als voornaamste voordeel dat de storagefuncties in real-time kunnen worden gesynthetiseerd, aan de hand van feedback/een specifieke closed-loop trajectory. Zodoende kunnen de belemmeringen van gecentraliseerde, off-line Lyapunov-functiesynthese, zoals benodigd bij het gebruik van fixed-parameter SFs, worden vermeden.

We beschrijven vervolgens hoe geparametriseerde SF-synthese kan worden benut om een gedistribueerde trajectoryspecifieke regelwet te verkrijgen, die op niet-iteratieve communicatie tussen direct gekoppelde systemen berust. Voor input-affiene netwerken en kwadratische storagefuncties, kan de regelactie worden berekend door elk bemonstertijdstip één semidefiniet programma per subsysteem op te lossen, op een *receding horizon* manier. Middels interpolatie van een verzameling regelactietrajectory's wordt een eenvoudig te implementeren, expliciete regelwet voor lineaire, tijdinvariante systemen verkregen die de trajectoryspecifieke convergentieëigenschap uitbreidt naar een veel sterkere garantie

van closed-loop asymptotische stabiliteit voor een bepaalde verzameling van begincondities.

Tot slot beschouwen we de toepassing van max-CLF en geparametriseerde storagefuncties voor het real-time balanceren van elektriciteitsnetwerken. Omdat generatoren beheerd worden door concurrerende, winstgedreven marktpartijen, wordt de stabilisatiemethode uitgebreid met niet-coöperatieve optimalisatie van een aantal willekeurig gekozen lokale kostenfuncties over een eindige predictiehorizon. De geschiktheid van de gedistribueerde Lyapunov-MPC regeling en de geparametriseerde storagefunctie-algoritmes wordt geëvalueerd aan de hand van closed-loop simulaties van een CIGRÉ benchmarksysteem.

Het proefschrift eindigt met een samenvatting van de belangrijkste wetenschappelijke bijdragen, gevolgd door ideeën voor toekomstig onderzoek.

Contents

1 Introduction

In its early days, electrical power supply was inefficient and costly. The use of direct-current (DC) transmission of electrical power at the same, low voltage as required by the loads put a severe restriction on the distance between generators and consumers, and resulted in a vast range of voltage-specific networks designed for different types of applications, such as lighting, railway systems and fixed motors.

However, by the end of the nineteenth century, electrical engineers and investors began to realize that alternating current (AC), which enabled the use of transformers, and thus the use of different voltages for transmission and different classes of loads, provided a solution to the above issues. High-voltage transmission is much more efficient over long distances, and by employing common, centralized generators for every type of load, economies of scale became possible, overall capital investments were lowered, and the costs of electricity consumption were decreased considerably.

The adoption of AC transmission marked the beginning of an era of large-scale electrification. Today, the electrical power network has become a vital part of the economic infrastructure in most of the industrialized world, and, even now, the overall use of electrical energy is increasing still. The modern electrical power system consists of thousands of generators and millions of consumers

that are interconnected via a continent-spanning grid of transmission lines and transformers. Power system dynamics cover an extensive time scale that includes both microsecond-order electromagnetic phenomena, yearly variations in energy demand and decades of investment planning, which is reflected by a multi-layered control infrastructure that has evolved over more than 100 years through research efforts in technological as well as economic, social, environmental and political disciplines.

Throughout most of its existence, power systems have been operated by a small number of regulated utilities that were responsible for the generation, transmission and distribution of electricity within a certain area. However, today, the electrical power system is going through a new restructuring process that gives rise to many questions, some of which will be addressed in this thesis.

Firstly, with the growing complexity of the electrical power system, the lack of efficiency and scalability associated with the traditional, centralized and monopolistic way of operating the electricity grid was identified as becoming problematic, and by the end of the twentieth century the first steps were taken to establish continent-wide, liberalized markets for electrical energy. Today, the system is restructured to allow for many parties competing for the production and consumption of electrical energy, as well as the provision of many of the services that are necessary for safe and reliable system operation (Stoft, 2002).

The second important change that power system operators face today is the ongoing integration of distributed generators (DG), many of which are based on intermittent renewable sources such as wind an sun. Driven by environmental concerns and concerns about the dependency on fossil fuels, many countries have posed ambitious targets for the share of renewable-based electrical energy generation over 10–50 year horizons, see, e.g., (European Commission, 2011).

Deregulation and the increasing share of distributed generation have a considerable impact on nearly all aspects of power system operation. It is therefore necessary to reconsider many of the arrangements that are used for power network operation today, to guarantee efficient and reliable operation of tomorrow's electrical power system. Because this thesis covers only very specific parts of electrical power system operation, the objective of this introduction is to outline the scope of the research that is presented in the following chapters.

1.1 Operation of the electrical power system

The operation of the electrical power system, and thus the design of competitive markets for electrical energy, is complicated by significant physical restrictions:

- An important prerequisite for reliable and stable operation of the electri-

cal power network is that supply and demand are balanced at all time, as efficient, inexpensive ways of storing large amounts of electrical energy are scarce.

- Finite transmission-line capacity and a lack of power-flow controllability pose strict constraints on electrical power injections (i.e., nodal production/consumption). Violation of network constraints can cause power outages with severe economic consequences.

The physical properties given above are reflected by a tight coupling between the economic and technical control layers of today's electrical power system, and they are the main reason why the straightforward application of knowledge from deregulation and control of other sectors is difficult or simply impossible.

Before presenting the main motivation and outline of this thesis, we provide a brief overview of the key principles of electrical power system operation, a comparison of the operational arrangements before and after restructuring, and a brief account of the problems originating from deregulation and the introduction of DG. More details on these topics can be found in, e.g., (Kundur, 1994; Ilić, 1998; Stoft, 2002; Jokić, 2007; Frunt, 2011).

1.1.1 Balancing supply and demand

An important goal of electrical power system operation is to keep mismatches between the supply and demand of power and energy close to zero, at all time. Before describing the key principles behind this balancing problem, we specify what is meant by supply and demand in this context.

According to the law of conservation of energy, the total amount of energy in an isolated system is constant over time. It can only be converted into different forms, e.g., electrical energy can be transformed into kinetic energy or heat. Thus, the amount of power produced in an electrical power network is always equal to the power consumed by the loads and the power losses in the grid. In this perspective, the electrical power system is always in balance. However, with balancing supply and demand, we actually mean balancing production and *desired* consumption instead of what is *actually* consumed, which turns out to be an economic or control problem, depending on the time scope involved. To be precise, *power demand* is defined as *the amount of consumed power if the network frequency and voltage are constant over time and equal their nominal values*. In Europe, these nominal values are $f_0 = 50\,\text{Hz}$ for the frequency and $V_0 = 230\,\text{V}$ rms for the voltage (at distribution network level). A very simple analogy of the balancing problem is shown in Figure 1.1, where frequency stabilization is compared with keeping the water level h (cf., *the frequency* f) in a

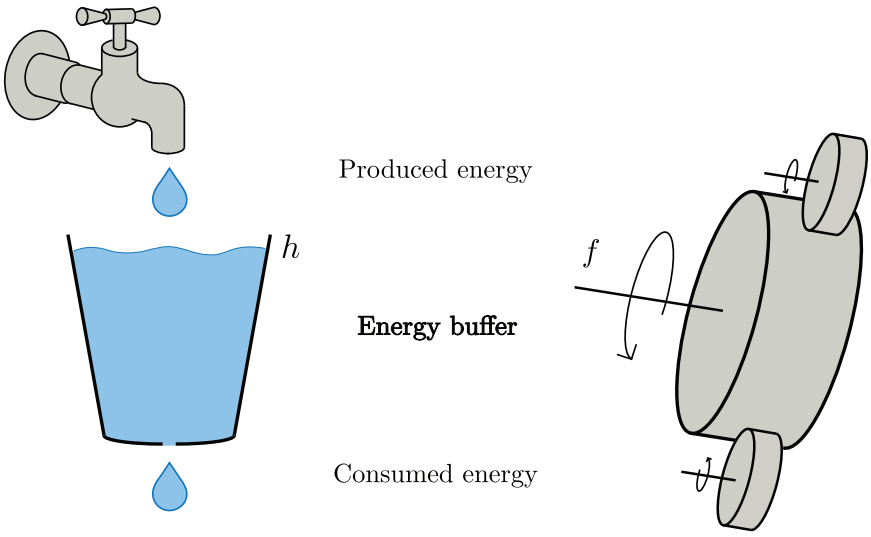

Figure 1.1: A simple analogy of electrical load balancing.

leaky bucket at a constant value, by continuously adjusting the inflow of water (*produced energy*) to the outflow (*consumed energy*).

The mechanism that couples the mismatch in supply and demand with the network frequency is as follows. Whenever there is an excess in electrical power P supplied to the grid, the (open-loop) change in radial frequency $\omega = 2\pi f$ can be approximated by the linear differential equation (Kundur, 1994)

$$\dot{\omega} = \frac{1}{H}(P - D\omega), \tag{1.1}$$

where H is the aggregated equivalent inertia of the load components connected to the grid, D is a damping term originating from frequency-dependent loads (e.g., synchronous generators), and where ω is measured with respect to the nominal value $\omega_0 = 2\pi f_0$.

Remark 1.1.1 Because electrical power networks are AC systems, balancing involves both *active* and *reactive* power. For the class of problems considered in this thesis, these quantities can be studied separately, as the flows of active and reactive power in the transmission network are only loosely coupled and influenced by different control actions. Frequency and active power are closely related to each other, conform (1.1), whereas reactive power is more closely related to the voltage magnitude (Kundur, 1994). Throughout this thesis, we will consider *balancing of active power*. ■

1.1.2 Hierarchical decomposition of power system control

The operation of the electrical power system is characterized by a temporal-decomposition based hierarchical structure, with a number of layers that reflect the decisions and control actions made on particular time scales (Jokić, 2007):

- The slower, upper layers are used for investment planning and to schedule controllable generation and load based on long-term *predictions* of electricity demand. At most of these levels, there is little connection with the physical properties and dynamics of the electrical power system; decisions are made in an open-loop fashion, based on the optimization of static economic and reliability-related objectives. There is plenty of time to compute the upper layer control actions, as they are generated well in advance of operation. Accordingly, the optimization problems considered on the upper layers may be large (e.g., involving the full, continent-wide network) and computationally complex (e.g., involving discrete decision variables and iterative communication).

- The faster, lower layers of power system operation are employed for real-time balancing, based on continuous feedback of system *measurements*, e.g., frequency deviations and power flows. The lower layers thus solve a control problem that explicitly accounts for the prediction errors introduced by the upper decision-making layers and the power system's dynamics to ensure closed-loop stability. The computation of low-level control actions is a time-critical procedure, as the time constants that are relevant for power balancing range from seconds to a few minutes. Consequently, the problems considered on the lower levels are typically solved in a scalable, non-centralized fashion, i.e., by generating the overall control action via a number of local control laws that are assigned to a particular section of the network (e.g., a *control area* or a single network bus).

In what follows, we will describe the key layers of power system operation (i.e., energy/power balancing) in detail, starting with the slow-acting layers and ending with the fast ones.

Investment planning
At the upper-most level of electrical power system operation, decisions are made regarding network expansion and the installment of new power plants, based on uncertain predictions of regional, national and continent-wide developments in electrical energy demand, long-term fuel and electricity price forecasts, govern-

mental policies, the emergence of new technologies (e.g., distributed generation), etc. The time constants associated with this decision layer are in the order of 5 years or longer.

Power scheduling and unit commitment
Typically 1 or 2 days ahead of operation, power system operators decide upon which generators will be switched on or off, to optimize some economic objective while balancing production with the expected electricity demand. The outcome of this unit commitment stage determines the setpoints for the network's transmission-line flows that are used by the faster control layers. System reliability is accounted for by scheduling also the amount of standby capacity that needs to be on-line for providing real-time balancing services and generating support in case of emergency situations, such as sudden network failures or generator tripping. Note that the unit commitment problem involves discrete decisions, and thus its implementation is rather complex and time-consuming. Moreover, because starting up and shutting off large generators can take hours or more, it is not possible to decide upon these actions on lower layers of the operational hierarchy.

Economic dispatch
As the setpoints provided by power scheduling and unit commitment are based on inaccurate day-ahead forecasts, it may be necessary to re-dispatch the power production among generators to improve economic operation. The corresponding (intra-day) economic dispatch (ED) layer is the fastest level dealing explicitly with the utility's economic objectives. ED updates are typically provided each 5 to 15 minutes by solving an optimization problem where the objective is to maximize economic performance, while accounting for the power balance, generator limits and transmission network capacity.

Automatic generation control (secondary control)
The slowest automated control loop in the power system's operational hierarchy is automatic generation control (AGC), load-frequency control (LFC) or secondary control (SC). Each AGC controller is assigned to a specific control area, i.e., a division of the electrical power network that is capable of and responsible for controlling its internal power balance in real-time.[1] The objective of the AGC layer is to stabilize the *area control error (ACE)* at zero. The ACE signal is obtained as a linear combination of the area's measured frequency deviation and

[1] In Europe, for historical and political reasons, control areas typically coincide with individual nations.

the deviation of the nett power exchanged with neighboring areas, measured with respect to the nominal and scheduled setpoints, respectively. If the ACEs of all areas in a network are zero and constant, then both the frequency of all areas and the inter-area power exchanges are kept at their target values. The output of the AGC controller represents the change in the area's total internal power production required to establish this goal. Each area may employ different ways of distributing these setpoints over the various generators in the area. Note that usually, only the largest generators will participate in the AGC loop to provide the corresponding area-balancing service. In classical control schemes, the AGC action is typically computed by an integral control law, to achieve a non-zero ACE and frequency steady state error. The time constants associated with secondary control dynamics are in the order of a few minutes, and AGC setpoints are typically updated and sent to the participating generators each 2 to 5 seconds.

Governor control (primary control)
The fastest automated balancing feedback loop in the power system hierarchy is the governor or primary control (PC) loop, which causes the mechanical power applied to the generator shaft to increase whenever the frequency drops. The governor control law $P_{\mathrm{PC}}(\omega) = -R\omega$ is a proportional function of the *locally measured* frequency deviation ω, that is, the frequency deviation evaluated at the generator bus. Usually, only the largest generators are equipped with a governor controller. Those that are, supply in addition to the basic service of producing power, an additional fast power balancing support to react on imbalances within 30–60 seconds. Although PC is much faster than SC, it induces a non-zero steady state error in terms of the network frequency, and thus it can stabilize only the power, i.e., not the energy, imbalance. Consequently, the PC loop ensures that in case of power imbalance $\dot{\omega}(t) \to 0$ for $t \to \infty$.

Kinetic energy and frequency-dependent synchronous loads
A passive, yet very fast power balancing mechanism originates from the aggregated inertia H of the synchronous generators that are connected to the network. Any real-time power imbalance will immediately be compensated by a change in kinetic energy stored in this rotating mass. For example, an excess in power demand will initially be supported by a decrease in the generators' kinetic energy, causing them to slow down and the network frequency to drop. Apart from functioning as a large buffer for kinetic energy, synchronous generators also tend to draw less power as the network frequency drops, thus providing a passive form of primary control. This phenomenon is described by the damping term $-D\omega$ in (1.1).

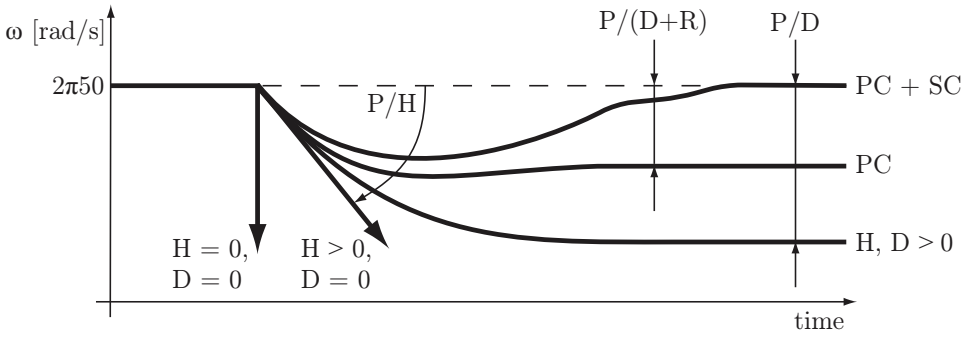

Figure 1.2: Comparison of active and passive balancing mechanisms.

Figure 1.2 illustrates the real-time balancing mechanisms (SC, PC, H, D) for a sudden, unexpected step-wise decrease in power supply P and 5 scenarios: *(i)* $H = 0, D = 0$, no PC/SC; *(ii)* $H > 0$, $D = 0$, no PC/SC; *(iii)* $H, D > 0$ and no control; *(iv)* $H, D > 0$, PC and no SC; and finally, *(v)* $H, D > 0$, PC and SC. Clearly, the inertia H is essential for avoiding sudden drops in frequency. D and PC restrict the steady state frequency error for constant load disturbances *(frequency containment)*. The figure also shows that SC is crucial for returning the frequency deviation to zero *(frequency restoration)*.

1.1.3 Challenges in future power system design

Throughout most of its existence, the power system has been controlled by a small number of regulated utilities responsible for both the generation, transmission and distribution of electricity within a certain area. For many decades, the associated arrangements have proven to be quite reliable and robust, even though even now, many of the complex dynamic phenomena occurring in large power systems are not yet fully understood. However, this robustness did not come for free, but at the cost of conservative engineering and operation, which resulted in economic inefficiency, reduced incentives for innovation and a high resistance towards changes.

With the increasing complexity and growth of the electrical power system, the inefficiency and lack of scalability associated with the traditional, centralized and monopolistic way of operating the electricity grid was becoming increasingly problematic. Given the economic principle that in a competitive market with equally strong players, scarce resources are allocated efficiently, by the end of the twentieth century the first steps were taken to establish liberalized

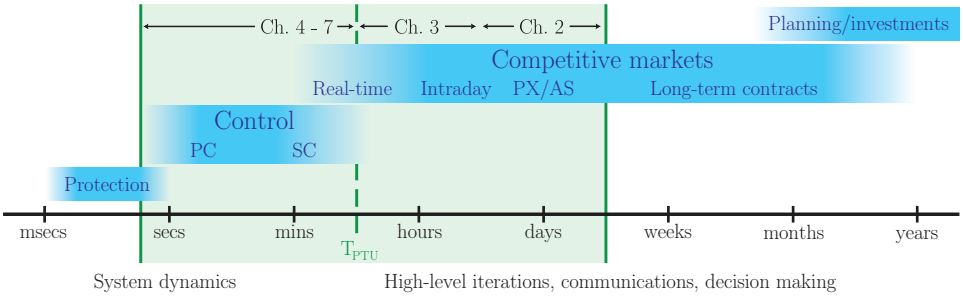

Figure 1.3: Temporal layers of power system operation.

markets for electrical energy.[2] After deregulation, electricity production came in the hands of multiple parties competing for the supply and demand of electrical energy, whereas the transportation, and thus, also the continuous (real-time) balancing of electrical power was entrusted to a regulated *transmission system operator (TSO)*.[3] In contrast to the cost-based objectives that were the main driving forces of the centralized, conventional control arrangements, the operation of the power system now involves a large number of local, competitive profit-driven mechanisms and interests.

The temporal-decomposition based structure of classical power network operation discussed in Section 1.1.2 is also reflected by the market arrangements in today's deregulated power systems. However, many of the decisions that were traditionally made in a centralized fashion by a single network utility, are now established in a decentralized way, by multiple autonomous market actors. Since there are many different approaches to power system restructuring, we only mention the common features that are relevant to the research presented in this thesis. The time-scale decomposition of deregulated systems is summarized by Figure 1.3, which shows that typically, parts of the unit commitment and economic dispatch scheduling layers have been replaced by day-ahead and intra-day markets, respectively. These markets are organized by an independent, neutral entity,[4] and can have several forms (Stoft, 2002). Together with long-term bilateral contracts between the market parties, the ahead and intra-day established energy transactions shape the energy generation schedules for the operational day, all defined with respect to time slots, i.e., *program time*

[2]Convincing arguments for the creation of competitive markets to increase economic efficiency can be found in, e.g., (Nicholson and Snyder, 2012).

[3]In the Netherlands, the maintenance and operation of the high-voltage transmission network is entrusted to TenneT TSO, see `www.tennet.org`.

[4]For example, in the Netherlands, day-ahead and intra-day markets for energy are set up by the Amsterdam Power Exchange (APX), see `www.apx.nl`.

units (PTUs), of length T_{PTU} (typically, in the order of 15–60 minutes).

Because generation has been "unbundled" from transmission, it is no longer possible for the transmission system operator to directly control energy production, which complicates the delivery of many of the services that are necessary for secure network operation. Instead, the TSO has to ensure system reliability by designing appropriate market rules and by coordinating the market participants via the provision of proper incentives, i.e., incentives that motivate behavior that supports the system-wide, societal beneficial goal of stable network operation. In most deregulated systems, there exist several markets for *ancillary services (AS)* in addition to the standard markets for energy production scheduling. The AS markets that are most relevant for the topics discussed in this thesis, are the markets on which the TSO can purchase generation capacity for the support of the primary/secondary control loops during normal system operation. In real-time, these reserves can be activated to maintain the network balance. The generators involved in balancing are then compensated according to a predetermined price. Apart from the balancing markets, in most deregulated systems, the TSO also participates on the day-ahead and intra-day energy markets to avoid overloading of the transmission network. The procurement of reserves for handling (rare, but severe) emergency situations, such as sudden generator tripping, is typically done via long-term contracts with electricity producers.

Besides deregulation, a second important trend that affects power system operation today, is the ongoing integration of distributed generation. This includes micro-turbines, fuel cells, geothermal power plants, tidal power plants, biomass plants, photovoltaic arrays and wind turbines. Conventional power systems are characterized by a highly repetitive daily pattern of power flows, with a relatively small amount of suddenly occurring, uncertain fluctuations on the demand side, and with large, controllable power plants on the supply side. As a consequence, in traditional power systems, a major portion of energy production can be efficiently scheduled in an open-loop fashion (e.g., via unit commitment and economic dispatch), with automatic generation control providing efficient balancing of uncertain variations in real-time power demand. The highly predictable nature of supply and demand allowed network and generator constraints to be fully accounted for during the dispatch/market phase, by introducing security margins that had negligible impact on system efficiency. However, in power systems with significant shares of small-scale distributed generators that are fed by renewable, intermittent energy sources such as wind and sun, power supply is difficult to control and predict, and thus, it is no longer possible to balance a large part of demand and supply based on open-loop

scheduling alone. Instead, there is an increasing need for efficient, distributed real-time balancing arrangements, to deal with the prediction inaccuracy of scheduling during the operational day. Moreover, to avoid the inclusion of conservative constraint margins during scheduling/ahead trade, new real-time control schemes are required that can explicitly take system constraints into account. Finally, the demand for balancing reserves that are able to compensate for fast fluctuations in distributed supply is expected to increase.

There are many other changes in electrical power network design that have considerable impact on future system operation.

- As explained Section 1.1.2, a large part of real-time balancing effort is pretty much given for free, with the kinetic energy buffer of large synchronous generators reducing the need for active control. However, today, increasing numbers of loads and distributed sources are connected to the electrical power network via power-electronic converters, which renders them insensitive to changes in the network frequency and voltage. As a result, the equivalent inertia H and damping D of the network are expected to decrease, which in turn affects passive stability.

- The synchronous grid is increasing in size and complexity, while the demand for electrical energy is rising still. Significant growth of electrical energy consumption is particularly expected from the emergence of plug-in electrical vehicles. The increasing scale of the electrical power system intensifies the need for efficient, competitive operation and non-centralized control.

- With electrical power system operation being increasingly driven by economic objectives, the number of transmission lines that are loaded up to their maximum capacity is expected to increase. Accordingly, network constraints will play an increasingly important role in the future operation of the electrical power system. Already today, TSOs sometimes need to sacrifice market efficiency by allocating sufficient spare capacity on inter-area connections. In future power systems, the spatial dimension of the grid can no longer be ignored during trade and the procurement of balancing reserves.

- The dynamics of generators, loads, control mechanisms and the market are starting to overlap, which complicates the temporal-decomposition based design that has dominated power system operation for over a century.

1.2 Scope and outline of the thesis

The trends and challenges described in the previous section form the main motivation for the research presented in this thesis, and can be summarized as follows.

Future electrical power systems are characterized by decreased predictability at all time scales, and their operation increasingly relies on non-centralized control mechanisms and decentralized, competitive decision-making.

Efficient provision of electrical energy and ancillary services for secure and reliable network operation will require new market and control arrangements that explicitly account for the constraints and dynamics associated with the transmission and generation of electrical power, that are robust against the large fluctuations in supply associated with DG, and that allow for decentralized, autonomous decision-making of the actors involved.

1.2.1 Research scope and goals

The shaded area in Figure 1.3 indicates the time-scale window of interest for the research presented in this thesis. Within this window, new solutions for power system operation and control are needed to deal with:

- the increasing interaction between (energy-driven) market arrangements and (both power- and energy-based) control mechanisms;
- the decreased predictability and controllability of power production and consumption in a competitive market setting;
- the growing complexity and increasing dimensions of the electrical power network.

A trivial solution to many of the issues caused by deregulation and distributed generation is to simply upgrade the power system infrastructure and hardware. For instance, the decrease in passive balancing and the increase of high-frequent, uncertain fluctuations in supply can be compensated by installing energy buffers such as storage lakes, batteries and fly wheels (Atwa and El-Saadany, 2010; Chen et al., 2012; Hill et al., 2012), whereas the need for real-time constraint handling can be alleviated by constructing additional transmission lines. Although these solutions may be technically feasible, their implementation remains questionable due to the associated investment costs and uncertain economic profitability. Therefore, the main objective of this thesis is to investigate the *control-technical* possibilities for ensuring efficient, reliable and stable operation of the

deregulated electrical power system.[5] Control is the natural solution for dealing with network dynamics and uncertain real-time imbalances, and may considerably relieve the need for large power system investments by optimally exploiting the existing sources for balancing.

Note that because active power balancing is a key task of transmission system operators, the findings in this thesis are particularly relevant from a TSO's perspective.

1.2.2 Outline of the thesis

The main results of this thesis are presented in six chapters. Roughly speaking, the thesis consists of two distinct parts; the first part (Chapters 2–3) deals with open-loop energy production scheduling and market design, whereas the second part (Chapters 4–7) concerns real-time power balancing/non-centralized network stabilization and is of a control-theoretical nature.

In Chapter 2 we provide a concise description of the key players on the electricity market. Each of these entities pursues certain goals while accounting for a specific set of technical and economic constraints. Of particular interest are the conflicting objectives of market efficiency and network reliability. These objectives are, for example, relevant to congestion management in deregulated power systems. We therefore investigate the principles and effects of the most common congestion management schemes (i.e., counter-trade and local marginal pricing) on transmission grid operation and market performance, particularly in terms of dispatch efficiency. Moreover, a multiobjective modeling framework is presented to decouple and analyze the effects of TSO and producer behavior on network security and short-run market efficiency.

In Chapter 3, we demonstrate that the currently employed energy-based transaction settlement system does not necessarily induce power exchange profiles that contribute to grid stability and security of supply. State-of-the-art solutions for tackling the inconsistency between energy-based market transactions and power-related frequency-control objectives can constrain trade or increase market complexity. An alternative scheduling concept is provided as a solution to this issue, which relies on the asynchronous settlement of energy transactions between market participants. It is shown that in this way, open-loop scheduling efficiency can be improved, grid operation can become more robust and the strain on balancing reserves can be reduced considerably.

Chapter 4 concerns the application of model predictive control (MPC) for real-time operation of electrical power systems. An attractive feature of MPC

[5] Organizational and juridical considerations are outside the scope of this thesis.

is its capability of explicitly taking state and input constraints into account, and consequently, there has been an increasing interest in the usage of MPC to control constrained electrical power networks. However, a major obstacle lies in the large scale of these systems, which prohibits a standard, centralized predictive control implementation. We therefore assess and compare the suitability of several state-of-the-art non-centralized predictive control schemes, to provide valuable insights that can contribute to the successful application of non-centralized MPC in real-life electrical power systems.

A key observation made in Chapter 4 is that non-iterative, non-centralized MPC schemes, in which the local control actions are computed based on incomplete state information, cannot guarantee system-wide optimal performance. As a consequence, when considering MPC for power systems, cost-based stabilization is not a feasible goal. The design of scalable, *constraint-based* stabilization methods for general networks of dynamical systems (NDS), and power systems in particular, is therefore addressed in Chapters 5 and 6.

The stabilization method considered in Chapter 5 is Lyapunov-based model predictive control (L-MPC). This method relies on a set of structured control Lyapunov functions (CLFs) with a particular type of convergence conditions to characterize the set of stabilizing control actions. While these conditions do not impose that each of the structured functions should decrease monotonously, as typically required for a CLF, they provide a standard control Lyapunov function for the overall network. Still, the conservatism associated with a demand for monotonic convergence of the overall CLF might be restrictive in practice. A solution is therefore provided for relaxing the temporal monotonicity of the global CLF. The proposed control scheme needs no global coordination and can be implemented based on non-iterative, local communication only.

The L-MPC method proposed in Chapter 5 requires the a-priori construction of a set of structured CLFs. The synthesis of such functions is a non-trivial problem. In Chapter 6, a generalized theorem and example network are provided to demonstrate that state-of-the-art, tractable synthesis methods, which typically rely on fixed-parameter local quadratic Lyapunov or storage functions, can fail even for simple unconstrained, linear and time-invariant network dynamics. Then, a solution to this issue is proposed, in which controller synthesis is decentralized via a set of *parameterized* storage functions. The corresponding stability conditions allow for max-type construction of a trajectory-specific Lyapunov function for the full closed-loop network, while neither of the storage functions is required to be monotonically converging. The provided approach is indicated to be non-conservative in the sense that it can generate converging closed-loop trajectories for the motivating example network and a prescribed set of initial conditions. For input-affine dynamics and quadratic parameterized

storage functions (p-qSFs), the synthesis scheme can be formulated as a set of low-complexity semi-definite programs that are solved on-line, in a receding horizon fashion. Moreover, for linear and time-invariant networks an even simpler, explicit control scheme is derived by interpolating a collection of a-priori generated converging state and control trajectories in a decentralized fashion.

In Chapter 7, we consider the application of the L-MPC and p-qSF methods for asymptotic frequency stabilization in multimachine power systems. Moreover, given that electric generators are operated by competitive, profit-driven market agents, a method is provided for improving closed-loop performance, in a Nash fashion, by embedding the p-qSF stability conditions in a distributed, iterative optimal control scheme that relies on neighbor-to-neighbor communication only. The effectiveness of the L-MPC and p-qSF schemes is then illustrated by simulating them in closed loop with a benchmark power system that is often used in frequency control studies.

The main conclusions from this thesis are summarized in Chapter 8. In this final chapter, we also provide a number of starting points and directions for further research.

1.3 Summary of publications

This thesis is mainly based on peer-reviewed, published or submitted articles.

The results presented in Chapter 2 are published in:

- Hermans, R. M., Van den Bosch, P. P. J., Jokić, A., Giesbertz, P., Boonekamp, P., Virag, A., May 2011c. Congestion management in the deregulated electricity market: An assessment of locational pricing, redispatch and regulation. In: International Conference on the European Energy Market. Zagreb, Croatia, pp. 8–13.

Chapter 3 contains results that are presented in:

- Hermans, R. M., Verberk, J. H., Van den Bosch, P. P. J., Jokić, A., Frunt, J., 2012g. Systematic design of market-based balancing arrangements for deregulated power systems: an asynchronous solution, to be submitted to a journal. Based on conference paper (Verberk et al., 2011) that was awarded with an IEEE PES PowerTech'11 High Quality Paper Certificate.

The results in Chapter 4 originate from:

- Hermans, R. M., Jokić, A., Lazar, M., Alessio, A., Van den Bosch, P. P. J., Hiskens, I. A., Bemporad, A., 2012b. Assessment of non-centralised model

predictive control techniques for electrical power networks. International Journal of Control 85 (8), 1162–1177.

Chapter 5 contains the results from:

- Hermans, R. M., Lazar, M., Jokić, A., 2010b. Almost decentralized Lyapunov-based nonlinear model predictive control. In: American Control Conference. Baltimore, MD, USA, pp. 3932–3938.

- Hermans, R. M., Lazar, M., Jokić, A., 2012d. Distributed MPC Made Easy. Springer, Berlin/Heidelberg, Germany, Ch. Distributed Lyapunov-based Model Predictive Control, in press.

The results provided in Chapter 6 are based on:

- Hermans, R. M., Lazar, M., Jokić, A., Gielen, R. H., August 2011b. On parameterized stabilization of networked dynamical systems. In: IFAC World Congress. Milano, Italy, pp. 1416–1421.

- Hermans, R. M., Lazar, M., Jokić, A., 2012e. Stabilization of interconnected dynamical systems by on-line convex optimization. Submitted to a journal.

Finally, the results in Chapter 7 are published in:

- Hermans, R. M., Lazar, M., Jokić, A., Van den Bosch, P. P. J., April 2010c. Almost decentralized model predictive control of power networks. In: IEEE Mediterranean Electrotechnical Conference. Valletta, Malta, pp. 1551–1556.

- Hermans, R. M., Lazar, M., Jokić, A., July 2011a. Distributed predictive control of the 7-machine CIGRÉ power system. In: American Control Conference. San Francisco, CA, USA, pp. 5225–5230.

- Hermans, R. M., Lazar, M., Jokić, A., 2012c. Competitive model predictive control for networks of interconnected dynamical systems, submitted to a conference (invited).

A few other results on related topics, which are not included in this thesis, can be found in (Hermans et al., 2010a; Van den Bosch et al., 2011; Driessen et al., 2012; Hermans et al., 2012a).

1.4 Notation and definitions

In this section, we specify the basic mathematical notation and standard definitions that are used throughout the thesis.

A. Electrical power systems

- Power and energy can both be positive or negative; they are either delivered (>0) to or withdrawn (<0) from the grid.
- *Prosumer* is a portmanteau formed by contracting 'producer' and 'consumer'. This term is used to denote market actors that can both inject and withdraw power or energy to/from the grid.
- The electrical power network models considered in this thesis are dimensioned using a *per unit* system: physical quantities are expressed as fractions of pre-defined base units (which are generally derived after selecting a certain base value for voltage and power).
- A list of employed acronyms is given in Table 1.1.

B.1 Sets and operations on sets

- Let $\mathbb{C}$, $\mathbb{R}$, $\mathbb{R}_+$, $\mathbb{Z}$ and $\mathbb{Z}_+$ denote the sets of complex numbers, reals, non-negative reals, integers and non-negative integers, respectively.
- For each $c \in \mathbb{R}$ and $\Pi \subseteq \mathbb{R}$ we define $\Pi_{\geq c} := \{k \in \Pi \mid k \geq c\}$ and similarly, $\Pi_{\leq c}$. Let $\mathbb{Z}_\Pi := \mathbb{Z} \cap \Pi$.
- $\emptyset$ denotes the empty set.
- A C-set $\mathbb{X} \subset \mathbb{R}^n$ is a convex and compact subset of $\mathbb{R}^n$ including the origin as an interior point, i.e., $0_n \in \text{int}(\mathbb{X})$.
- The set of solutions to a linear inequality $a^\top x \geq b$ (or $a^\top x > b$), for $a, x \in \mathbb{R}^n$ and $b \in \mathbb{R}$, constitutes a closed (or open) half-space of $\mathbb{R}^n$.
- The set $\mathbb{X} \subset \mathbb{R}^n$ is a polytope (or polytopic set) if it can be described as the intersection of a finite number of open and closed half-spaces.
- For a set $\mathbb{X}$ and some $N \in \mathbb{Z}_+$, $\mathbb{X}^N := \mathbb{X} \times \ldots \times \mathbb{X}$ is the N-th Cartesian power of $\mathbb{X}$.

Table 1.1: List of acronyms

Acronym	Meaning
AC	Alternating current
ACE	Area control error
AGC	Automatic generation control (i.e., SC/LFC)
AS	Ancillary service
BRP	Balance responsible party
DC	Direct current
DG	Distributed generation
E-program	Energy program
LFC	Load-frequency control (i.e., AGC/SC)
LMP	Locational marginal pricing
MPC	Model predictive control
NDS	Network of dynamical systems
ONP	Optimal nodal pricing
OPF	Optimal power flow
PC	Primary control
PTU	Program time unit
PX	Power exchange, energy exchange
SC	Secondary control (i.e., AGC/LFC)
TSO	Transmission system operator

B.2 Vectors, matrices and norms

- Let $\mathbf{z} := \{z(l)\}_{l\in\mathbb{Z}_+}$ with $z(l) \in \mathbb{R}^n$, $l \in \mathbb{Z}_+$, denote an arbitrary sequence. Define $\mathbf{z}_{[0,k]} := \{z(l)\}_{l\in\mathbb{Z}_{[0,k]}}$, $k \in \mathbb{Z}_+$.

- For some $s \in \mathbb{R}$, let $|s|$ denote its absolute value and let $\lfloor s \rfloor := \max\{n \in \mathbb{Z} \mid n \leq s\}$ be the floor function.

- For a finite set of vectors $\{x_i\}_{i\in\mathbb{Z}_{[1,N]}}$, $x_i \in \mathbb{R}^{n_i}$, $N \in \mathbb{Z}_{\geq 1}$, let $\mathrm{col}(\{x_i\}_{i\in\mathbb{Z}_{[1,N]}})$ and $\mathrm{col}(x_1, \ldots, x_N)$ denote the vector $[\, x_1^\top \ \ldots \ x_N^\top \,]^\top$.

- For $n_i = n$, $i \in \mathbb{Z}_{[1,N]}$, the vectors x_i are said to be linearly independent if there are no nonzero $c_i \in \mathbb{R}$, $i \in \mathbb{Z}_{[1,N]}$, such that $\sum_{i\in\mathbb{Z}_{[1,N]}} c_i x_i = 0_n$, where 0_n is the zero vector in $\mathbb{R}^n$.

- The linear span of $\{x_i\}_{i\in\mathbb{Z}_{[1,N]}}$ is denoted by

$$\mathrm{span}\left(\{x_i\}_{i\in\mathbb{Z}_{[1,N]}}\right) := \left\{ x \in \mathbb{R}^n \,\middle|\, x = \sum_{i\in\mathbb{Z}_{[1,N]}} c_i x_i, c_i \in \mathbb{R} \right\}.$$

Similarly, let the convex hull of $\{x_i\}_{i\in\mathbb{Z}_{[1,N]}}$ be

$$\operatorname{conv}\left(\{x_i\}_{i\in\mathbb{Z}_{[1,N]}}\right) := \left\{ x\in\mathbb{R}^n \;\middle|\; x=\sum_{i\in\mathbb{Z}_{[1,N]}} c_i x_i, c_i\in\mathbb{R}_{[0,1]}, \sum_{i\in\mathbb{Z}_{[1,N]}} c_i = 1 \right\}.$$

- For $x\in\mathbb{R}^n$, let $\|x\|$ be an arbitrary p-norm, i.e., $\|x\|_p := \left(\sum_{i=1}^n |[x]_i|^p\right)^{\frac{1}{p}}$ for $p\in\mathbb{Z}_{[1,\infty)}$ and $\|x\|_\infty := \max_{i=1,\dots,n}|[x]_i|$, where $[x]_i$, $i\in\mathbb{Z}_{[1,n]}$, is the i-th component of x.
- For a matrix $M\in\mathbb{R}^{m\times n}$, let $\|M\| := \max_{x\neq 0_n}\frac{\|Mx\|}{\|x\|}$ denote the corresponding induced matrix norm.
- For a square symmetric matrix $M\in\mathbb{R}^{n\times n}$, $M\succeq 0$ and $M\succ 0$ mean that M is positive semi-definite and positive definite, respectively. Similarly, we denote negative (semi-)definiteness of M by $M\prec 0$ ($M\preceq 0$).
- The spectral radius of a square matrix $M\in\mathbb{R}^{n\times n}$ with eigenvalues $\lambda_1,\dots,\lambda_n$ is $\varepsilon_{\max}(M) := \max_{i\in\mathbb{Z}_{[1,n]}}|\lambda_i|$.
- For a finite set of matrices $\{M_i\}_{i\in\mathbb{Z}_{[1,N]}}, M_i\in\mathbb{R}^{n_i\times m_i}$, and $N\in\mathbb{Z}_{\geq 1}$, let $\operatorname{diag}(\{M_i\}_{i\in\mathbb{Z}_{[1,N]}})$ be a $\sum_{i=1}^N n_i$ by $\sum_{i=1}^N m_i$ matrix with diagonal blocks M_i and all-zero off-diagonal blocks.
- The n by n identity matrix is denoted by I_n.

B.3 Functions and mappings

- The first and second order derivatives of a continuous function $f(t)$, $f:\mathbb{R}\to\mathbb{R}$, are denoted by $\frac{\mathrm{d}f}{\mathrm{d}t}$ and $\frac{\mathrm{d}^2 f}{\mathrm{d}t^2}$, respectively. If f is a function of time, we also use the alternative notation $\dot{f}$ and $\ddot{f}$.
- A function $\varphi:\mathbb{R}_+\to\mathbb{R}_+$ is in class $\mathcal{K}$ if it is continuous, strictly increasing and $\varphi(0)=0$; φ is in class $\mathcal{K}_\infty$ if $\varphi\in\mathcal{K}$ and $\lim_{s\to\infty}\varphi(s)=\infty$.
- A function $\beta:\mathbb{R}_+\times\mathbb{R}_+\to\mathbb{R}_+$ is in class $\mathcal{KL}$ if for all $k,s\in\mathbb{R}_+$, $\beta(\cdot,k)\in\mathcal{K}$, $\beta(s,\cdot)$ is decreasing and $\lim_{k\to\infty}\beta(s,k)=0$.
- A set-valued mapping f from set $\mathcal{S}$ to set $\mathcal{P}$ is denoted by $f:\mathcal{S}\rightrightarrows\mathcal{P}$.

2

Congestion management in the deregulated electrical energy market: locational pricing, redispatch and regulation

2.1 Introduction

In the operation of the electrical power system, two key objectives can be identified. Firstly, there is a societal desire for producing and distributing electricity as efficiently as possible (in an economical sense). Secondly, producers and consumers expect the transmission network to deliver high security of supply; in the ideal case, each connection point behaves as a continuously available, reliable source of electrical energy, with nominal frequency and voltage. It is not possible to solely pursue either economic efficiency or reliability: a reliable transmission network is essential for the exchange of electrical energy among market participants, whereas the costs of transmission network operation and expansion need to be recovered from the market. Moreover, a high level of network reliability does not come for free, but may have considerable impact on market performance. The conflicting nature of reliability and economic efficiency is reflected by the actions of the TSO, who is entrusted with the expan-

sion, maintenance and operation of the electricity grid on one hand, and the behavior of profit-driven energy prosumers on the other. In the first part of this chapter, we briefly describe the main drivers and constraints of these and other important actors involved in power system operation, to clarify their decisions and facilitate the design of market arrangements and regulation.

In the second part of this chapter, we consider *congestion management* as an aspect of power system operation where the tension between network reliability and market efficiency is particularly relevant. Congestion management is vital to guarantee secure operation of the electricity grid; finite transmission-line capacity and a lack of power-flow controllability pose strict constraints on electrical power transmission, and persistent violation of these constraints can cause power outages with severe economic consequences.

Before liberalization of the electricity market, network limitations could effectively be taken into account during the dispatch phase, which was centrally coordinated and involved a small number of cooperating parties only. Today, power systems are deregulated and decentralized, and their operation relies on providing market participants with proper incentives for societal beneficial behavior. When congestion management is the main focus, transmission system operators need to design arrangements that maximize market performance while simultaneously motivating producers and consumers to adapt to network restrictions. It is well-known that transmission constraints can induce market inefficiency, because congestion can supply participants with market power. To prevent this, market-based congestion management should be robust, fair and transparent.

Roughly speaking, two different types of congestion management can be distinguished, see, e.g., (Christie et al., 2000; Bompard et al., 2002). Many TSOs correct infeasible outcomes of an unconstrained forward market via congestion redispatch, that is, by requesting counter transactions after market gate closure. As an alternative, operators can employ locational marginal pricing (LMP) such as nodal or zonal pricing to directly influence the energy market during forward trade (Schweppe et al., 1988). Locational prices differ from the unconstrained-market price (determined by the lowest-cost producers) if congestion occurs, thus providing an incentive to schedule generation and load in a way that relieves congestion and contributes to grid security.

We compare the principles and effects of counter-trade and LMP-based congestion management on grid operation and market performance, particularly in terms of dispatch efficiency and total prosumer surplus. We indicate that both schemes can perform equally well from a social welfare point of view, although the associated transactions differ and yield different nett prosumer profits. Then, we present a multiobjective modeling framework to decouple and an-

alyze the effects of TSO and prosumer behavior on network security and short-run market efficiency. All results are illustrated using the IEEE 39-bus New-England benchmark network.

Remark 2.1.1 Although opposed by many economists, prosumers and politicians often regard *fairness* as a third goal of electrical power system (or market) operation, separate from maximizing efficiency and reliability. The meaning of fairness as an objective of control law or market design is unclear and subject to debate, however. In this chapter, we avoid this discussion by considering mechanisms or arrangements that affect overall system efficiency, due to unequal or non-transparent treatment of the participants involved, to be unfair. In this way, (competitive) fairness can be regarded as one of many aspects that contribute to efficient system operation.

For details on this issue, in particular regarding fairness of LMP, the interested reader is referred to (Stoft, 2002; Lévêque, 2006). ■

2.2 Competitive markets for electrical energy

The main reason for deregulating the electricity market is to increase its efficiency through competition. An equilibrium of the electricity market is economically efficient (or *Pareto optimal*) if energy is produced by the cheapest suppliers and is consumed by those that are most willing to pay for it (Stoft, 2002). This outcome is attained by maximizing *social welfare*, which is defined as follows.

Definition 2.2.1 The social welfare associated with a certain market outcome is defined as the sum of the corresponding consumer benefits and negated producer costs. ■

At this point, it is important to stress that economic efficiency only relates to the optimality of a certain market equilibrium, not on the method that was used to establish it.

Apart from the production/consumption of energy, few other aspects of the electrical power system lend themselves for competitive operation. Transmission is particularly unsuited for competition because of its natural monopoly character: duplicated lines are a waste of capital equipment and network expansion involves high investment costs. The monitoring, maintenance, construction and operation of the European transmission system is therefore unbundled from supply and carried out by regulated TSOs.

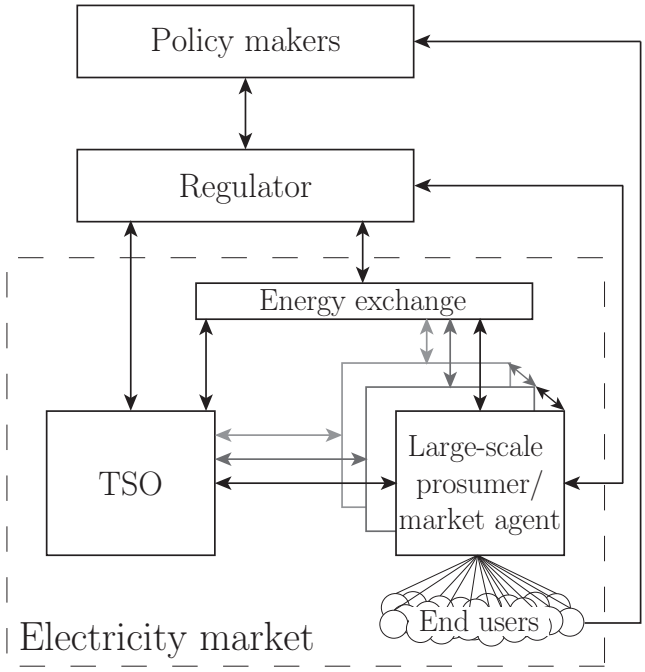

Figure 2.1: Schematic overview of the key actors and interactions on the electrical energy market.

A schematic overview of the key players and their interactions on the electricity market is given in Figure 2.1. Because of electricity's time-critical nature, real-time trading of energy (that is, trade for instantaneous delivery) is difficult. Instead, the bulk of electrical energy is traded on forward markets such as a day-ahead and intra-day markets, i.e., the *power exchange (PX)*,[1] where traders aim to maximize their profit while taking care of their expected internal energy balance (supply + demand + exchange = 0). Together with long-term contracts and bilateral transactions, the PX outcome shapes the energy exchange schedules for the next operational day. Accordingly, all ahead-established energy transactions exist on paper only, as they define contracts to buy specific quantities of energy at a specified price with the supply set at a specified period in the future. There is no direct relation with the real-time, TSO-monitored state of the electricity grid.

[1] Or, equivalently, *energy exchange*. The commonly used term *power exchange* is somewhat confusing, as trade involves electrical energy rather than power.

Large-scale producers and consumers (prosumers) usually directly participate on forward markets such as the PX. This is not the case for small-scale end users, whose individual demand is too small and uncertain for effective trade. Instead, they are represented on the PX by specific market agents. This relation is typically established via long-term (e.g., monthly/yearly) contracts. Note that market agents may not own production capacity themselves; if this is the case, they have to ensure delivery of energy to their contracted end users by purchasing it from suppliers on the market. It is advantageous for market agents to have a large number of contracted prosumers, because the corresponding extent of aggregation facilitates the prediction of energy demand during forward trade. Similar to large-scale prosumers, market agents are driven mainly by a desire to maximize profit.

To optimize economic efficiency, regulators and policy makers aim to design markets for the supply and demand of electricity in such a way that they are as competitive as possible. Regulation is therefore also needed to make sure that TSOs do not benefit from their monopoly on power transmission. Typically, a TSO's income is not allowed to be higher than what is necessary to cover the cost of its lawfully assigned tasks, under the assumption that these are carried out efficiently and adequately. In the Netherlands, this is achieved by imposing an upper bound on the transmission tariffs requested from prosumers for use of the transmission network.[2] These tariffs are the TSO's main source of income. Because there are no possibilities for making profit, the decisions and actions taken by a TSO are usually driven by a desire to minimize long-run costs instead. These costs are associated with network investments, maintenance, and operation. Because a TSO has no direct control over power prosumption, a considerable part of its operational costs originates from purchasing the services that are necessary for secure network operation on the energy market.

In competitive markets, producers adjust price and supply until the market reaches an equilibrium. Competitive market equilibriums can be short-run and long-run optimal, as defined below (see Stoft (2002) for more details).

Definition 2.2.2 A *short-run/dispatch-efficient market equilibrium* is attained when marginal cost/benefit equals the market price and supply equals demand. This outcome optimizes social welfare given fixed productive resources. Under competition, the following conditions are necessary to guarantee that the market clears at a short-run optimal outcome: *(i)* market liquidity is high, *(ii)* prosumers are price takers with increasing marginal costs/decreasing marginal benefit functions and *(iii)* prices are publicly available. ■

[2]For more details on the Dutch regulator, *De Energiekamer/De Nederlandse Mededingingsautoriteit (NMA)*, we refer the interested reader to `www.nma.nl/regulering/energie/`.

Table 2.1: Characterization of long-term TSO/producer behavior

Actor	Transmission system operator	Large prosumer/market agent
Objective (set by actor)	Minimize long-term costs	Maximize long-term profit
Constraints (set by regulator)	Market rules, general legislation; Lower bound on operational quality/adequacy (e.g., security of supply, reliability); Lower bound on efficiency; Upper bound on transport tariff; Actions/decisions should be fair, transparent, non-discriminatory	Market rules, general legislation
Actions and decisions	Network investments, maintenance and operation; Trade/contracting of ancillary services	Generator investments, maintenance and operation (producers); Trade/contracting of energy transactions

Definition 2.2.3 A *long-run/investment-efficient market equilibrium* guarantees that the right (i.e., cost-minimizing) investments in production capacity have been made, and long-run social welfare has been maximized. Besides fulfilment of conditions *(i)–(iii)*, this requires that *(iv)* there are no barriers for new competitors to enter and exit the market. ■

Note that in the above definitions, short-run and long-run refer to the completion of distinct market processes (that is, dispatch and investment planning, respectively) rather than to different time scales. Moreover, they relate to energy market efficiency in general rather than to the efficiency of transmission system operation and expansion (i.e., whether this contributes to welfare maximization). These aspects have significant influence on the fulfillment of conditions *(i)–(iv)* and thus on market performance, as is illustrated in Section 2.3–2.4.

The characterization of TSO and large-scale energy prosumer/market agent behavior provided above is summarized in Table 2.1.

2.3 Congestion management

During operation, grid users are unavoidably confronted with the physical limitations of electrical power and energy. As a result of imperfect predictions, the ahead-established transactions will deviate from the actual supply and demand of energy, and unscheduled or infeasible power flows need to be counter-

acted immediately, to prevent network overloading. It is thus crucial for TSOs to design ahead-market schemes that are both as accurate and robust as possible, to minimize the need for real-time (fast and expensive) control effort, see, e.g., (Van den Bosch et al., 2011). When market-based congestion management is the main focus, these methods need to maximize social welfare while simultaneously taking limited network capacity and uncertainty of supply/demand into account. In what follows, we will discuss methods for forward-time congestion management in detail.

We begin by introducing the power system modeling framework that is used throughout this chapter. Let graph $\mathcal{G} = (\mathcal{S}, \mathcal{E}, A)$ describe a transmission network, where $\mathcal{S} = \{\varsigma_1, \ldots, \varsigma_n\}$ is a set of nodes/buses, $\mathcal{E} \subseteq \mathcal{S} \times \mathcal{S}$ is a set of undirected edges/bus interconnections, and A is a weighted adjacency matrix. The interconnection between bus ς_i and ς_j is denoted by $e_{ij} = (\varsigma_i, \varsigma_j)$. The adjacency matrix $A \in \mathbb{R}^{n \times n}$ satisfies $[A]_{ij} = -b_{ij} \neq 0 \Leftrightarrow e_{ij} \in \mathcal{E}$ and $[A]_{ij} = 0 \Leftrightarrow e_{ij} \notin \mathcal{E}$, where b_{ij} [Ω^{-1}] is the susceptance of the line(s) associated with edge e_{ij}, see (Christie et al., 2000). Self-connecting edges are not allowed (i.e., $e_{ii} \notin \mathcal{E}$), such that A has zeros on its main diagonal. The set of neighbors of a node $\varsigma_i \in \mathcal{S}$ is denoted by $\mathcal{N}_i := \{\varsigma_j \in \mathcal{S} \mid (\varsigma_i, \varsigma_j) \in \mathcal{E}\}$; the corresponding indices are $I(\mathcal{N}_i) := \{j \mid \varsigma_j \in \mathcal{N}_i\}$. With each $e_{ij} \in \mathcal{E}$, we associate a symmetric power-flow limit $\overline{p}_{ij} = \overline{p}_{ji}$.

The concepts discussed in this chapter are illustrated using the IEEE 39-bus New England test system. Figure 2.2 depicts the corresponding network topology, including price-elastic generators and price-inelastic loads. Line susceptance and load values for the network can be found in (Pai, 1981).

2.3.1 The optimal power flow problem

In conventional, regulated electrical power systems, the productive resources are owned by a small number of cooperating operators, such that power production can be scheduled in a centralized fashion, by solving an *optimal power flow (OPF)* problem. This problem is instrumental to many market-based congestion management schemes and is used to derive the LMP scheme later on.

To define the OPF problem, with each bus $\varsigma_i \in \mathcal{S}$ we associate a singlet $\hat{p}_i$ [MW] and a quadruplet $(p_i, \underline{p}_i, \overline{p}_i, J_i)$, where $p_i, \underline{p}_i, \overline{p}_i, \hat{p}_i \in \mathbb{R}$, $\underline{p}_i < \overline{p}_i$ and $J_i : \mathbb{R} \to \mathbb{R}$ is a strictly convex, differentiable cost function. The values p_i and $\hat{p}_i$ denote the reference values for power injections at each node into the network. Both p_i and $\hat{p}_i$ can take positive as well as negative values, denoting production and consumption, respectively; the only difference is that in contrast to $\hat{p}_i$, the value p_i has an associated cost/benefit function $J_i(p_i)$ [€] and an interconnector capacity constraint $\underline{p}_i \leq p_i \leq \overline{p}_i$. We will thus refer to p_i as the power from a

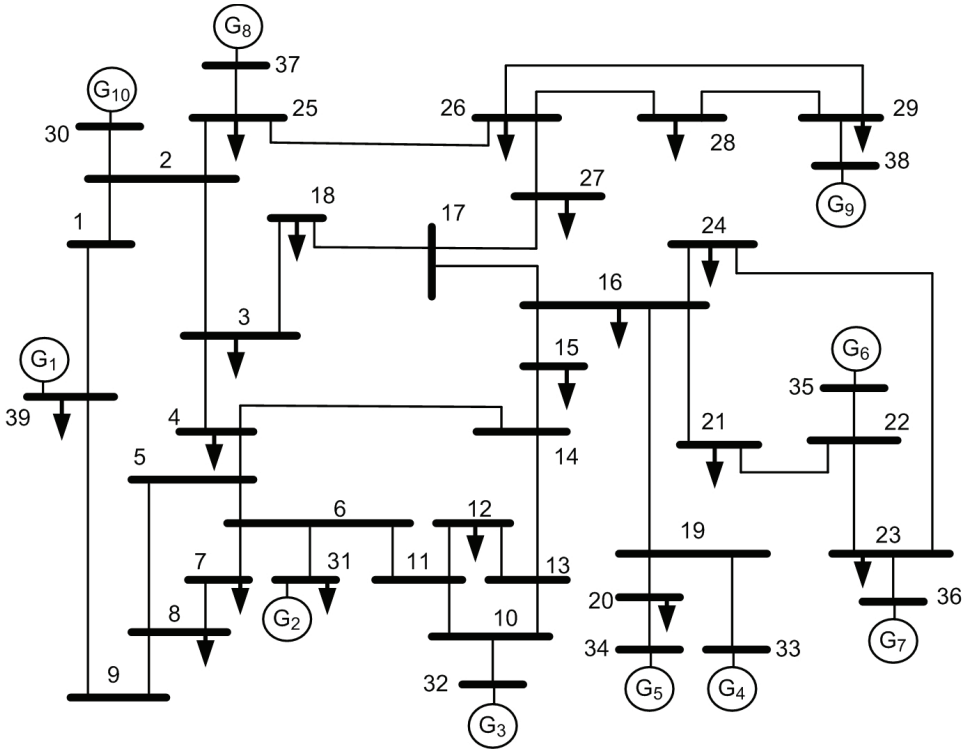

Figure 2.2: The IEEE 39-bus New England test system.

price-elastic prosumer, and to $\hat{p}_i$ as the power from a price-inelastic prosumer. In the case of a positive p_i, the function $J_i(p_i)$ represents the variable costs of production, while for negative values of p_i, it denotes the negated benefit of a consumer. Marginal production costs/benefits are denoted by $\nabla J_i(p_i)$ [€/MW].

A lossless "DC power flow" model is employed to describe the power flows in the network for given nodal power injections. Under certain reasonable assumptions, this model is proven to be a relatively accurate approximation of the more complex "AC power flow" model, see, for instance, (Christie et al., 2000). In particular, convexity of the DC power flow constraints is a crucial property that will be exploited in what follows. With δ_i [rad] denoting the voltage phase angle at node ς_i, the power flow in line $e_{ij} \in \mathcal{E}$ is given by $p_{ij} = b_{ij}(\delta_i - \delta_j) = -p_{ji}$. If $p_{ij} > 0$, power in the line e_{ij} flows from node ς_i to node ς_j. The power balance in a node yields $p_i + \hat{p}_i = \sum_{j \in I(\mathcal{N}_i)} p_{ij}$. With $p := \mathrm{col}(p_1, \ldots, p_n)$, $\hat{p} := \mathrm{col}(\hat{p}_1, \ldots, \hat{p}_n)$, $\delta := \mathrm{col}(\delta_1, \ldots, \delta_n)$ and $\mathbf{1}_n := [1 \ \ldots \ 1]^\top \in \mathbb{R}^n$, the overall network balance condition is $p + \hat{p} = B\delta$, where $B := A - \mathrm{diag}(A\mathbf{1}_n)$. The OPF problem is

defined as follows.

Problem 2.3.1 Optimal power flow problem
For any constant value of $\hat{p} \in \mathbb{R}^n$,

$$\begin{aligned}
&\text{minimize}_{p,\delta} && \textstyle\sum_{i=1}^{n} J_i(p_i) && \text{(2.1a)}\\
&\text{subject to} && p - B\delta + \hat{p} = 0, && \text{(2.1b)}\\
& && \underline{p} \le p \le \overline{p}, && \text{(2.1c)}\\
& && b_{ij}(\delta_i - \delta_j) \le \overline{p}_{ij},\ \forall (i,j \in I(\mathcal{N}_i)), && \text{(2.1d)}
\end{aligned}$$

where $\underline{p} = \text{col}(\underline{p}_1, \ldots, \underline{p}_n)$, $\overline{p} = \text{col}(\overline{p}_1, \ldots, \overline{p}_n)$. ■

We will refer to a vector p^* that solves the OPF problem as a *vector of optimal power injections*. This vector maximizes the (short-run) social welfare $-\sum_{i=1}^{n} J_i(p_i)$ while respecting all balance, generator-capacity and transmission-line constraints, as specified by (2.1b), (2.1c) and (2.1d), respectively.

Remark 2.3.2 In practice, power production schedules need to be robust against contingencies such as outages or equipment failures. Rather than solving Problem 2.3.1, which yields a vector of optimal power injections for nominal operating conditions, this requires the evaluation of a *security-constrained OPF (SC-OPF)*, where the objective function $\sum_{i=1}^{n} J_i(p_i)$ is minimized while ensuring constraint satisfaction both under nominal and perturbed conditions. To limit conservatism and obtain a tractable optimization problem, typically only single outages (i.e., $n-1$ scenarios) are considered (Wood and Wollenberg, 1996). Because SC-OPF is essentially a special version of the OPF problem, for simplicity, we employ the latter as starting point for our comparison of congestion management schemes. ■

2.3.2 Locational pricing

Solving the OPF problem is one of the major operational (short-run) goals in a regulated power system. For liberalized, market-based power systems, the OPF problem is important due to its relation to the optimal nodal price problem (and similar LMP schemes) that is defined next.

In a market-based power system, different generator units are owned and controlled by separate parties; each of them acts autonomously to maximize its profit given the time-varying price for electricity. In other words, when a price-elastic unit at node i receives the price for a certain period in the future, i.e.

λ_i [€/MW], it adjusts its scheduled production p_i to

$$\begin{aligned}\tilde{p}_i = \Upsilon_i(\lambda_i) &:= \arg\min_{p_i \in [\underline{p}_i, \overline{p}_i]} J_i(p_i) - \lambda_i(p_i + \hat{p}_i) \\ &= \arg\min_{p_i \in [\underline{p}_i, \overline{p}_i]} J_i(p_i) - \lambda_i p_i, \end{aligned} \tag{2.2}$$

where $\lambda_i(p_i+\hat{p}_i)-J_i(p_i)$ is the *profit/surplus* of this particular unit. Since J_i is a strictly convex function, the relation $\Upsilon_i : \mathbb{R} \to [\underline{p}_i, \overline{p}_i]$ defines a unique mapping from λ_i to $\tilde{p}_i$ for any $\lambda_i \in \mathbb{R}$. For convenience, let $\Upsilon(\lambda) := \text{col}(\Upsilon_1(\lambda_1), \ldots, \Upsilon_n(\lambda_n))$. Note that if the capacity constraint $p_i \in [\underline{p}_i, \overline{p}_i]$ is ignored, it holds that $\lambda_i = \nabla J_i(\tilde{p}_i)$; since prosumers are price-takers/consider the price as given, they adjust production and consumption until the corresponding marginal cost $\nabla J_i(p_i)$ equals the nodal price λ_i.

The foregoing shows that in a deregulated power system, the TSO cannot directly adjust nodal power injections to achieve a certain objective, e.g., to prevent congestion. Instead, it should provide market participants with price-based incentives for supporting such a system-wide goal. The operational goal in a nodal-pricing based power system is to determine the nodal price λ_i for each node i in the network, in such a way that short-run social welfare is maximized, while fulfilling both balance and network constraints. This *optimal nodal pricing (ONP)* problem is defined as follows (Schweppe et al., 1988).

Problem 2.3.3 Optimal nodal prices problem
For any constant value of $\hat{p} \in \mathbb{R}^n$,

$$\begin{aligned} &\text{minimize}_{\lambda,\delta} && \textstyle\sum_{i=1}^{n} J_i(\Upsilon_i(\lambda_i)) && \text{(2.3a)} \\ &\text{subject to} && \Upsilon(\lambda) - B\delta + \hat{p} = 0 && \text{(2.3b)} \\ & && b_{ij}(\delta_i - \delta_j) \leq \overline{p}_{ij},\ \forall (i,j \in I(\mathcal{N}_i)). && \text{(2.3c)} \end{aligned}$$

where $\lambda = \text{col}(\lambda_1, \ldots, \lambda_n)$ is a vector of nodal prices. ■

We will refer to a vector λ^* that solves the ONP problem with the term *vector of optimal nodal prices*. The OPF and ONP problems are related through Lagrange duality (see, e.g., Jokić (2007)). It thus holds that $\Upsilon(\lambda^*) = p^*$, i.e., both problems implicitly define the vector of optimal nodal power injections that maximizes short-run social welfare.

In ONP-operated networks, the nodal price of electricity at a given time instant and bus reflects the least expensive way to increase the power flow to that particular node from the on-line generators while respecting all network constraints and system limits. Consequently, prices are identical throughout the network only if the transmission system has infinite capacity, or if OPF outcome

Table 2.2: Generator parameters

Bus i	c_i	b_i	Bus i	c_i	b_i
30	0.8	30.00	35	0.8	34.80
31	0.7	35.99	36	1.0	34.40
32	0.7	35.45	37	0.8	35.68
33	0.8	34.94	38	0.8	33.36
34	0.8	35.94	39	0.6	34.00

p^* yields no congestion. In the latter case, the network constraints have no effect on the forward market. It is easy to see that in this *uniform price* scenario, i.e., for $\lambda_i = \lambda_j$, $\forall i, j \in \mathbb{Z}_{[1,n]}$, the sum of producer and consumer surplus $\sum_{i=1}^{n} \big(\lambda_i(p_i + \hat{p}_i) - J_i(p_i)\big)$ is equivalent to the social welfare $-\sum_{i=1}^{n} J_i(p_i)$.[3]

In what follows, we illustrate the nodal pricing concept using the New England test network. For this, the cost functions associated with the price-elastic generators at buses $i = 30, \ldots, 39$ are parameterized as

$$J_i(p_i) = \frac{1}{2} c_i p_i^2 + b_i p_i, \tag{2.4}$$

with $c_i, b_i \in \mathbb{R}$, yielding affine marginal costs or bids $\nabla J_i(p_i) = c_i p_i + b_i$. The values for c_i and b_i are listed in Table 2.2. All generator capacity limits are set to $\underline{p}_i = 0, \overline{p}_i = 10$ (per unit, base value 100 MW). For simplicity, $\overline{p}_{ij}$ was set to infinite for all transmission lines, except for $e_{25,26}$. Figure 2.3 shows the nodal prices for an uncongested (dashed line) and a congested (bars) network scenario, obtained by solving Problem 2.3.3 for $\overline{p}_{25,26} = \infty$ and $\overline{p}_{25,26} = 1.5$, respectively. The corresponding optimal power injections are given in Table 2.3. The unconstrained scenario yields $p_{25,26} = 2.2326 > 1.5$. In the constrained scenario, only the power flow between node 25 to 26 is limited, yet trade is affected at all buses. This effect is typical for highly-interconnected meshed networks such as the 39-bus system. The constrained scenario leads to 21 price areas, i.e., 21 clusters of buses with uniform nodal prices. This division of the network in price areas (or *zones*) is not static, but completely determined by the parameters of the ONP problem (such as the bids ∇J_i).

The 39-bus example shows that transmission-line restrictions may have varying effects on the nodal prices throughout the network. Congested lines do not

[3] This equivalence does *not* hold in case of congestion. Then, the aggregated income of the energy producers deviates from the total consumer cost. This yields a non-zero difference between the nett prosumer surplus and the social welfare, i.e., a *merchandise surplus*, see (Bompard et al., 2002).

Table 2.3: Optimal nodal power injections

$\overline{p}_{25,26}$	$\{p^*_{30},\ldots,p^*_{39}\}$
∞	$\{10.0, 4.70, 5.47, 5.43, 4.18, 5.60, 4.88, 4.50, 7.40, 8.80\}$
1.5	$\{10.0, 4.54, 5.35, 5.56, 4.31, 5.74, 4.99, 3.72, 8.43, 8.33\}$

support additional power flow, such that specific nodes (e.g., bus 38 in the simulation) can be cut off from the cheapest supplier in the network, which results in an increased nodal price (if the unconstrained market is taken as reference). Other prosumers (such as the ones at bus 25) can benefit from congestion, as the least expensive supply is distributed among a smaller number of accessible consumers. Still, since transmission-line restrictions narrow the domain over which the market is optimized, congestion always decreases nett welfare. In the above simulation, for instance, if $\overline{p}_{i,j} = \infty$ for all lines, the optimized cost/negated benefit $J(p^*)$ and nett prosumer surplus $\sum_{i=1}^{n}\left(\lambda_i^*(p_i^*+\hat{p}_i)-J_i(p_i^*)\right)$ amount to €2227.50 and €-2227.50 (with price-elastic component $\sum_{i=1}^{n}\left(\lambda_i^* p_i^*-J_i(p_i^*)\right)$ equal to €167.54), respectively, whereas the constrained scenario yields an optimal cost/negated benefit and surplus of €2228.28 and €-2225.10 (with price-elastic component €165.78), respectively.

Remark 2.3.4 Since ONP may confront prosumers with different prices for electrical energy depending on where they are located in the network, nodal pricing schemes are sometimes considered to be "unfair" (see also Remark 2.1.1). This argument is occasionally used against locational pricing, to support congestion redispatch schemes such as the one discussed in the following subsection. Note, however, that from an objective point of view, optimal nodal prices are in fact competitive prices, i.e., there is no market outcome that yields lower network-wide costs/larger social welfare. More specifically, there is nothing inherently inefficient about the distribution of profit under ONP (Lévêque, 2006). ■

Remark 2.3.5 As indicated by the example, transmission constraints can provide prosumers at badly accessible network locations with market power. If exercised, this power can result in non-optimal local prices and market inefficiency. Adequate regulation of the TSO is therefore crucial to ensure that the operation and expansion of the transmission network contribute to welfare maximization, see Section 2.4. ■

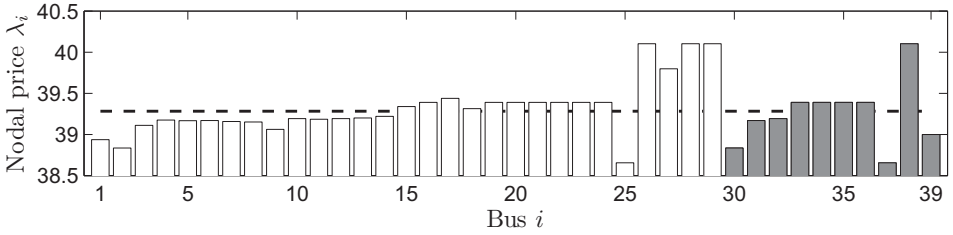

Figure 2.3: Optimal nodal prices for an uncongested (dashed line) and a congested scenario (bars).

2.3.3 Curative congestion management

LMP methods such as ONP explicitly confront market participants with network limitations, that is, with constraint (2.3c), during the ahead-trading stage. Consequently, when supply and demand bids $\nabla J_i(p_i)$ have been exchanged with the market, the optimal nodal prices for the next operational day can be computed in a single optimization run.

However, in practice, such *preventive congestion management* methods, i.e., methods that are employed before market gate closure, may not be sufficient for satisfaction of security criteria during the operational day, see, e.g., (ETSO, 2005). Due to unexpected fluctuations in generation and load, or due to contingencies such as transmission-line outages, power flow limits can be violated even if the market takes reasonable safety margins into account. Moreover, to deal with the complexity of the European power system, in practice, preventive methods only account for a subset of the transmission-line restrictions and evaluate the corresponding flows in an approximate, decentralized fashion. In contrast to ONP, where the clustering of buses with uniform prices may vary over time and is determined by the congested lines, the European energy market relies on a limited number of a-priori fixed price areas (usually defined by political borders), within which Problem 2.3.3 is solved while ignoring internal transmission constraints. Below, we briefly discuss two preventive congestion methods that are currently used or considered for application in practice.

Today, many TSOs reduce the congestion risk between price areas by adjusting the forward-market's *available transfer capacity (ATC)*, which is allocated to market participants on the basis of periodically held auctions, see (ETSO, 2000). ATC values indicate the maximum amount of power that can be exchanged with adjacent areas while ensuring system security. The ATC flow model maps an inter-area energy transaction solely to the aggregated interconnection between the areas involved, and ignores the fact that in reality, the energy transfer

between two neighboring areas actually acts upon the flows throughout the network as a whole. This is a considerable simplification of (2.3c). Moreover, ATC values are conditional upon the actual network-wide distribution of power injections. Since the exact nodal power injections are not known in advance of market clearing, ATC values therefore need to be computed by evaluating a number of "base cases", i.e., a finite set of expected dispatch and contingency scenarios.

Motivated by the conservatism associated with ATC, European TSOs are now considering preventive congestion management via *flow-based market coupling (FMC)*, see (Schavemaker et al., 2008; Aguado et al., 2012). In this scheme, the network-wide effect of inter-area energy transactions is described by a vector of *power transfer distribution factors (PTDFs)*. The PTDFs describe what power flows would be provoked on a limited set of critical branches in the European network by an imbalance in a particular area. Although flow-based congestion management is less conservative than the ATC-based method and thus provides more flexibility and trade opportunities to the market, the corresponding market outcome may still give rise to congestion, as PTDFs strongly depend on the accuracy of the base cases that were used to compute them.

ATC/FMC inaccuracy and intra-area transmission restrictions render *curative congestion management*, i.e., congestion redispatch or counter trade after gate closure, indispensable for secure operation of the European transmission network. Normally, the TSO is the only buyer of curative counter transactions (i.e., supplementary transactions to recover secure network conditions), and their selection is usually based on merit-order criteria or long-term contracts, see (Bompard et al., 2002). Although there are many options for redispatch, in what follows we only consider *pay-as-bid based counter trade*. In such a system, suppliers are exactly paid the price at which they are willing to contribute to the redispatch (as specified by their bids). Moreover, for simplicity, we consider redispatch in combination with an unconstrained forward market, to illustrate the need for countertrading when facing intra-area congestion (recall that in practice, ATC/PTDF-based congestion management is mainly employed to reduce the need for inter-area curative congestion management).

Let $\Delta p_i \in \mathbb{R}$ and $\Delta\delta_i \in \mathbb{R}$ be a power-injection and voltage-angle adjustment at bus i, measured with respect to the unconstrained-market outcome $p_i^{\mathrm{PX}}, \delta_i^{\mathrm{PX}} \in \mathbb{R}$. Suppose that elastic prosumers provide the TSO with knowledge of their adjustment cost/benefit, in the form of strictly convex bid functions $J_i^{\mathrm{CT}} : \mathbb{R} \to \mathbb{R}$. Then, a bid-based intra-area congestion-redispatch procedure is formally defined as follows.

Problem 2.3.6 Curative congestion management
1. The market solves Problem 2.3.3 while ignoring (2.3c) to find the uniform price vector $\bar{\lambda}^{\mathrm{PX}} = \mathrm{col}(\lambda^{\mathrm{PX}}, \ldots, \lambda^{\mathrm{PX}}) \in \mathbb{R}^n$, i.e.,

$$(\bar{\lambda}^{\mathrm{PX}}, \delta^{\mathrm{PX}}) := \arg\min_{\{\lambda,\delta \text{ s.t. (2.3b)}\}} \sum_{i=1}^{n} J_i(\Upsilon_i(\lambda_i)). \tag{2.5}$$

2. If $p^{\mathrm{PX}} := \Upsilon(\bar{\lambda}^{\mathrm{PX}})$ and δ^{PX} violate (2.3c), the TSO employs congestion redispatch:

$$\begin{aligned} &\text{minimize}_{\Delta p, \Delta\delta} && \textstyle\sum_{i=1}^{n} J_i^{\mathrm{CT}}(\Delta p_i) && \text{(2.6a)}\\ &\text{subject to} && \Delta p - B\Delta\delta = 0 && \text{(2.6b)}\\ & && b_{ij}(\delta_i^{\mathrm{PX}} + \Delta\delta_i - \delta_j^{\mathrm{PX}} - \Delta\delta_j) \le \overline{p}_{ij}, && \text{(2.6c)} \end{aligned}$$

for all $(i, j \in I(\mathcal{N}_i))$, where $\Delta p := \mathrm{col}(\Delta p_1, \ldots, \Delta p_n)$ and $\Delta\delta := \mathrm{col}(\Delta\delta_1, \ldots, \Delta\delta_n)$.
3. Given optimal redispatch vector Δp^*, the TSO pays $J_i^{\mathrm{CT}}(\Delta p_i^*)$ to prosumer i as an incentive for adjusting its power injection to $p_i^{\mathrm{PX}} + \Delta p_i^*$. ■

Next, suppose that the cost functions J_i and capacities $\underline{p}_i, \overline{p}_i$ are time invariant,[4] and assume that market participants use these to form the redispatch bids, i.e.,

$$J_i^{\mathrm{CT}}(\Delta p_i) = \begin{cases} J_i(p_i^{\mathrm{PX}} + \Delta p_i) - J_i(p_i^{\mathrm{PX}}), & \Delta p_i \in [\underline{\Delta p}_i, \overline{\Delta p}_i] \\ \infty, & \Delta p_i \notin [\underline{\Delta p}_i, \overline{\Delta p}_i] \end{cases} \tag{2.7}$$

for all i, where $\underline{\Delta p}_i := \underline{p}_i - p_i^{\mathrm{PX}}$ and $\overline{\Delta p}_i := \overline{p}_i - p_i^{\mathrm{PX}}$. In this case, prosumers that are constrained on, i.e., increase production/decrease consumption, are exactly compensated for their increased variable cost/decreased variable benefit, whereas prosumers that are constrained off are financially indifferent between producing p_i^{PX} and participating in redispatch by reducing production with Δp_i^*.[5] Note that under assumption (2.7), we actually obtain *cost-based* redispatch.

Now consider the following result.

Theorem 2.3.7 *Let* (2.7) *hold. Then, Problem 2.3.3 and Problem 2.3.6 (i) define identical nodal power injections and social welfare, but (ii) the transactions needed to establish this market outcome differ and yield different total producer and consumer profits, except for* $p^{PX} = p^*$.

[4] This assumption is nontrivial: depending on the generators and the time frame involved, cost functions and capacities will generally change over time. Consider for instance start/stop times that are irrelevant during forward trade, but that prevent redispatch of the corresponding sources after gate closure.

[5] Note that a small ε [€] term may be added to $J_i^{\mathrm{CT}}(\Delta p_i)$ to provide prosumers with a *strictly positive* incentive for redispatch.

Proof. (i) From (2.7) and the construction of $p_i^{\mathrm{PX}}, \delta_i^{\mathrm{PX}}, \Delta p_i^*$ and $\Delta\delta_i^*$, it straightforwardly follows that $p^{\mathrm{PX}} + \Delta p^*$ and $\delta^{\mathrm{PX}} + \Delta\delta^*$ solve the OPF problem. Thus, the power injections and angles defined by Problem 2.3.6 satisfy $p_i^{\mathrm{PX}} + \Delta p_i^* = p_i^*$ and $J_i(p_i^{\mathrm{PX}}) + J_i^{\mathrm{CT}}(\Delta p_i^*) = J_i(p_i^{\mathrm{PX}} + \Delta p_i^*) = J_i(p_i^*)$ for all i. Both methods attain the same, efficient market equilibrium with optimal social welfare $-\sum_{i=1}^n J_i(p_i^*)$. *(ii)* In case of ONP/Problem 2.3.3, the income and cost of the producers (or, equivalently, the cost and benefit of the consumers) at node i equal $\lambda_i^*(p_i^* + \hat{p}_i)$ and $J_i(p_i^*)$, respectively, whereas in case of Problem 2.3.6, the producer income and cost amount to $\lambda^{\mathrm{PX}}(p_i^{\mathrm{PX}} + \hat{p}_i) + J_i^{\mathrm{CT}}(\Delta p_i^*)$ and $J_i(p_i^*)$, respectively. Thus, the total profit made by the prosumers is

$$\sum_{i=1}^{n} \left(\lambda_i^*(p_i^* + \hat{p}_i) - J_i(p_i^*)\right) \tag{2.8a}$$

for ONP and

$$\sum_{i=1}^{n} \left(\lambda^{\mathrm{PX}}(p_i^{\mathrm{PX}} + \hat{p}_i) - J_i(p_i^{\mathrm{PX}})\right) \tag{2.8b}$$

for cost-based redispatch. These values are not equal, except for $p^{\mathrm{PX}} = p^*$. □

Figure 2.4 provides a schematic illustration of the redispatch procedure, under the assumption that (2.7) holds.

Remark 2.3.8 Theorem 2.3.7 shows that a comparison in terms of social welfare or efficiency is not sufficient for evaluating the performance of different market arrangements. There are many ways to establish an efficient market equilibrium (e.g., the vector of optimal nodal power injections p^* that maximizes social welfare), but this does not imply that all these arrangements are equally desirable from, for example, a societal perspective. ■

Next, we describe a simple curative counter transaction for the 39-bus test network to illustrate the above result and its consequences for the TSO. Recall from Section 2.3.2 that the optimal vector of nodal power injections for the unconstrained market (corresponding to $\lambda^{\mathrm{PX}} = 39.2817$, see Table 2.3) violates the transmission-line constraints. The TSO can ask market participants what compensation they are willing to accept to adjust their prosumption in such a way that the power balance is maintained and the flow $p_{25,26}$ is lowered to $\overline{p}_{25,26} = 1.5$. These conditions are met, e.g., if the generators at buses 37 and 38 decrease and increase their power injections with 0.7326, respectively. Since the generator at node 37 reduces its production with respect to p_{37}^{PX}, it pays $J_{37}(p_{37}^{\mathrm{PX}}) - J_{37}(p_{37}^{\mathrm{PX}} - 0.7326) = €41.6527$ to the TSO, whereas the TSO pays

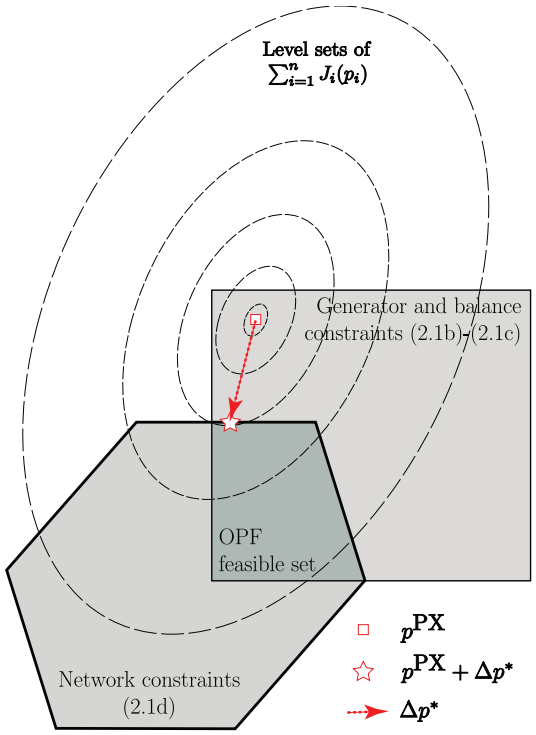

Figure 2.4: A schematic illustration of cost-based redispatch.

$J_{38}(p_{38}^{\mathrm{PX}} + 0.7326) - J_{38}(p_{38}^{\mathrm{PX}}) = €42.5723$ for increasing the generation at bus 38. Thus, the cost associated with this pair of bilateral transactions is €0.9195.

Under assumption (2.7), it can be shown that there is no other feasible pair of bilateral transactions that yields lower redispatch costs than the one described above. However, if the selection of counter transactions is not limited to a subset of the generators, the overall prosumption costs can be lowered to those of the OPF solution, yielding minimum costs for the TSO, i.e., $\sum_{i=1}^{n} J_i^{\mathrm{CT}}(p_i^* - p_i^{\mathrm{PX}})$, which equals €0.7758. Still, by construction, a constrained market (e.g., Problem 2.3.3) cannot outperform the corresponding unconstrained market (e.g., Problem 2.3.3 without constraints (2.3c)), such that the TSO generally suffers losses from counter trade. In case of efficient behavior, the TSO can usually socialize and recover these congestion redispatch costs via a system-wide transmission tariff. This is in contrast to ONP-based networks, where the forward market price may be non-uniform and explicitly confronts prosumers, without intervention by the TSO, with both energy and location-specific transmission costs.

2.4 Market efficiency and network security

Since Problem 2.3.3 implicitly defines the vector of power injections that maximizes short-term social welfare, one might conclude that ONP, and, at best, also OPF-based redispatch, lead to a dispatch efficient market equilibrium. However, since the vector of optimal power injections p^* is a function of network parameters B and $\overline{p}_{ij}$, it is hard to draw firm conclusions on dispatch efficiency without analyzing how these network parameters are obtained. B, $\overline{p}_{ij}$ and ATC/PTDF values are stochastic variables, and only the TSO has sufficient information to predict their value in a reliable fashion.[6] Since the TSO has a natural monopoly on transmission, regulation is required to avoid possible abuse of his powerful position in the market. The monitoring of line-susceptance prediction quality is straightforward, as real-time measurements allow for a-posteriori comparison with the TSO's expectations. This is not the case for transfer-capacity (or ATC) profiles, which consist of both estimated thermal transmission-line limits and safety margins that are selected at the TSO's discretion.

The above described non-transparency provides network operators with the possibility to exploit flow-capacity estimation in their own benefit (see, for example, Glachant and Pignon (2005)). Naturally, TSOs tend to minimize the probability of network overloading by choosing the security margins as large as possible, whereas prosumers demand maximum freedom of trade, i.e., minimum margins, to allow for maximum profits. In what follows, we provide a way to model this trade-off between conflicting short-run security and market efficiency objectives as a *multiobjective optimization problem*, see, for instance, (Sawaragi et al., 1985).

Let l_{ij} [MW] and Δl_{ij} [MW] be the thermal limit (determined by external factors such as weather conditions) and the security margin (set by the TSO) of transmission line e_{ij}, respectively, such that $\overline{p}_{ij} := l_{ij} - \Delta l_{ij}$. Note that $0 \leq l_{ij}$ and $0 \leq \Delta l_{ij} \leq l_{ij}$. Next, let $l := \text{col}(\{l_{ij} \mid e_{ij} \in \mathcal{E}\})$ and $\Delta l := \text{col}(\{\Delta l_{ij} \mid e_{ij} \in \mathcal{E}\})$, and consider an objective function $S(\Delta l)$ [€] that represents the TSO's financial risk of congestion, overloading and line outages/damage associated with a particular set of safety margins Δl. For simplicity, we assume that $S(\Delta l)$ is decreasing in all Δl_{ij}, and that $S(\Delta l) \to 0$ if $\Delta l_{ij} \to l_{ij}$ for all $(i, j \in I(\mathcal{N}_i))$. Moreover, let $J(p) := \sum_{i=1}^{n} J_i(p_i)$ [€] map the vector of nodal power injections $p \in \mathbb{R}^n$ to the corresponding total prosumption cost/benefit. Now consider the following problem.

[6] Note that also in the long-run, the TSO is the only market actor able to adjust B and $\overline{p}_{ij}$ by investing in the transmission infrastructure.

Problem 2.4.1 Power system security/efficiency trade-off
For any constant value of $\hat{p}$ and l,

$$\min_{\Delta l,\lambda,\delta} \begin{bmatrix} S(\Delta l) & J(\Upsilon(\lambda)) \end{bmatrix}^{\top} \tag{2.9}$$

subject to $0 \leq \Delta l \leq l$, (2.3b)-(2.3c), where $\overline{p}_{ij} := l_{ij} - \Delta l_{ij}$. ■

Multiobjective optimization problems such as the one above have an infinite number of solutions, as there are infinitely many ways to trade off two or more conflicting goals. A feasible point $(\Delta l^*, \lambda^*, \delta^*)$ lies within the solution space of Problem 2.4.1 if and only if it is *Pareto optimal*, i.e., if all points corresponding to lower security costs S (or lower prosumption cost J) yield larger J (or S). One way to solve Problem 2.4.1 is to construct a single composite objective function $C(\Delta l, \lambda) := rS(\Delta l) + J(\Upsilon(\lambda))$, with positive scalar weight $r \in \mathbb{R}_+$, and solve

$$\min_{\Delta l,\lambda,\delta} C(\Delta l, \lambda) \tag{2.10}$$

subject to $0 \leq \Delta l \leq l$, (2.3b) and (2.3c). Each outcome of the composite optimization problem corresponds to a particular trade-off that is characterized by r. Thus, the full set of solutions (i.e., the trade-off surface/Pareto frontier) is found by evaluating (2.10) for all $r \in [0, \infty)$.

In what follows, we illustrate the above concept with the 39-bus network. For simplicity, let $\overline{p}_{ij}$ be infinite for all lines except $e_{25,26}$, and let $S(\Delta l) := (\Delta l_{25,26} - l_{25,26})^2$, where $l_{25,26} = 1.5$. Figure 2.5 shows the resulting Pareto frontier in the $J(\cdot), S(\cdot)$-plane. Clearly, minimal network costs $S(\Delta l)$ are attained for $r \to \infty$. This ratio corresponds to a security/efficiency trade-off that is completely in favor of the TSO (i.e., line $e_{25,26}$ is not loaded at all). Social welfare, on the other hand, is maximized for $r = 0$, in which case $\Delta l_{25,26} = 0$ and transmission risks are high.

Figure 2.5 shows that r can have significant effects on market and system performance. The regulator can choose any positive value for r that is in accordance with (inter)national legislation, to trade off security against market efficiency in a way that best fits his priorities. As an example of a point of operation that the regulator can pursue, we mention the *egalitarian solution P*, see (Sawaragi et al., 1985). A power system is operated in an egalitarian fashion if the regulator appreciates system security and market performance to an equal extent, yielding an outcome of Problem 2.4.1 that satisfies $\frac{\mathrm{d}}{\mathrm{d}r} S(\Delta l^*(r)) = -\frac{\mathrm{d}}{\mathrm{d}r} J(p^*(r))$. As shown in Figure 2.5, the egalitarian solution of Problem 2.4.1 is the point $P = (S(\cdot), J(\cdot))$ where the tangent to the Pareto frontier has a slope $\frac{\mathrm{d}S}{\mathrm{d}J}$ of -1.

The above modeling framework provides a transparent way to decouple and analyze the effects of TSO behavior, prosumer bids and network regulation on

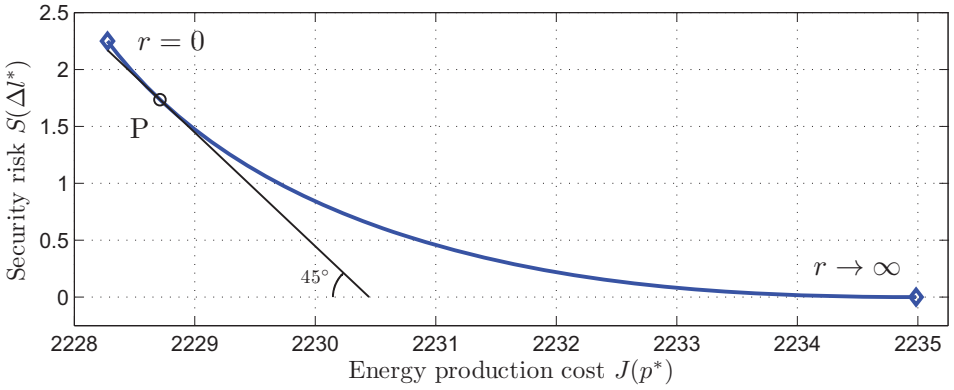

Figure 2.5: Security/efficiency Pareto front for the 39-bus example network.

short-run market efficiency, regardless of the applied congestion management scheme. Moreover, it explicitly associates network reliability (measured in terms of line margins Δl) with the expected costs for the network operator. Note that even though it is difficult to predict network security costs a priori, there are many observation-based methods for approximating them empirically, see, e.g., (Chowdhury and Koval, 2010) and the references therein.

2.5 Conclusions

In this chapter, we identified the maximization of security of supply and market efficiency as the two main objectives of power system operation. The conflicting nature of these objectives is reflected in the decisions and actions taken by the transmission system operator and profit-driven market players.

Particular attention was paid to congestion management, which is an aspect of power system operation where the tension between reliability and economic efficiency is particularly apparent. More specifically, the differences between locational pricing and cost-based congestion redispatch were analyzed, followed by an assessment of their effects on grid operation. It was shown that although optimal nodal pricing and cost-based congestion redispatch can yield identical, economically efficient power injections, they are not equivalent in terms of transaction costs. Moreover, we illustrated that the effects of TSO/regulator and prosumer behavior on short-run power system security and market efficiency can be decoupled and analyzed by employing a multiobjective modeling framework.

3

Asynchronous settlement of energy transactions

3.1 Introduction

In the deregulated market for electrical energy, transmission system operators (TSOs) are no longer able to directly manipulate power supply in a centralized fashion. Instead, they have to provide prosumers with incentives for societal beneficial behavior, e.g., for contributing to the power and energy balance. Since the main electricity market commodity is *energy* rather than power (which is a flow variable of undefined economic value), the market and the TSO can only provide energy-based financial incentives, *even though real-time control objectives actually require balancing of power*. Moreover, because energy transactions are defined with respect to fixed-length time slots or *program time units (PTUs)*, energy imbalances can only be settled at a limited number of discrete-time instants. Recent studies show that already today, the inconsistency between periodic energy-based imbalance settlement on one hand and power-related stability requirements on the other is causing severe frequency deviations in the European power network, particularly at the boundaries of subsequent PTUs, see (UCTE, 2008; Weissbach and Welfonder, 2009; Tractebel Engineering, 2009; Frunt, 2011).

The contribution of this chapter is twofold. Firstly, we analyze the fundamental flaws of the current market arrangements with respect to the TSO's stability and balancing objectives, in particular, by investigating the strong dependency between market-induced generator setpoints and power imbalance fluctuations at PTU transitions. Secondly, it is shown that the coupling between the market/incentive layer and the physical network layer is loosened, by settling the energy transactions of market participants, or more specifically, *balance responsible parties (BRPs)*,[1] in an asynchronous fashion. In this way, a short, virtual PTU length is induced on the aggregated network level, which is independent of the PTU length that is observed by market actors during trade. This enables the TSO to decrease the day-ahead expected open-loop power imbalance, as the energy supply and demand expectations acquired during the scheduling/dispatch phase can be used more efficiently in real-time, with minor consequences for trade complexity and market flexibility. Open- and closed-loop simulation results are provided to compare the performance of the proposed asynchronous settlement mechanism with that of a number of state-of-the-art solutions to the issues described above. We finish with conclusions.

3.2 Inconsistency of market arrangements and balancing objectives

One of the objectives of forward trading/scheduling is to guarantee that for each PTU, there is a balance between *expected* production and consumption. Since energy, rather than power, is traded on the electricity market, the market condition for open-loop balance is formulated in terms of energy, i.e.,

$$\sum_{i=0,\ldots,N-1} E_i[n] = 0, \qquad n \in \mathbb{Z}, \tag{3.1}$$

where $E_i[n]$ [MWh] denotes the nett energy transaction of balance responsible party $i \in \mathcal{I}_{\text{BRP}} :=\in \mathbb{Z}_{[0,N-1]}$ during the n-th PTU.

Let the controllable and uncontrollable power production of BRP $i \in \mathcal{I}_{\text{BRP}}$ at continuous-time instant $t \in \mathbb{R}$ be denoted by $P_i(t)$ [MW] and $\mu_{P_i i}(t)$ [MW], respectively. To comply with the ahead-established market transactions (and thus, to avoid imbalance costs), BRPs can track any power profile $P_i(t)$ that satisfies

$$E_i[n] = \int_{\text{PTU } n} \{P_i(t) + \mu_{P_i i}(t)\} dt. \tag{3.2}$$

[1] A balance responsible party is a reliable, accountable entity that has to and is able to represent its production capacities and demands (including that of contracted prosumers) on the market (Van den Bosch et al., 2011).

However, for BRPs with strictly convex power production costs, the most profitable way to supply a certain amount of energy is to keep controllable power prosumption constant; see, e.g., (Frunt, 2011, Chapter 5). These BRPs therefore attempt to generate the step-wise averaged power profiles

$$\widetilde{P}_i(t) = \widetilde{P}_i[n], \qquad \text{for } t \in [t_n, t_{n+1}), \tag{3.3}$$

where

$$\widetilde{P}_i[n] := \frac{1}{T_{\text{PTU}}} \left(E_i[n] - \int_{t_n}^{t_{n+1}} \mu_{P,i}(t) dt \right),$$

and where T_{PTU} [s] denotes the PTU-length and $t_n := n T_{\text{PTU}}$, $n \in \mathbb{Z}$. Now suppose that all the BRPs are able to track $\widetilde{P}_i(t)$ exactly, and let $\mu_{P,i}(t)$ be piecewise constant, in such a way that its value changes only at time instants t_n, $n \in \mathbb{Z}$. To illustrate this scenario, consider the left-hand side of Figure 3.1, which shows the total controllable power generation $P(t) := \sum_i P_i(t)$, i.e., $\widetilde{P}(t) := \sum_i \widetilde{P}_i(t)$, the total noncontrollable production $\mu_P(t) := \sum_i \mu_{P,i}(t)$ and their sum, i.e., the open-loop aggregated power imbalance

$$\Delta P_{\text{OL}}(t) := P(t) + \mu_P(t). \tag{3.4}$$

In this ideal case, the open-loop *energy balance* condition (3.1) inherently yields open-loop *power balance* (that is, $\Delta P_{\text{OL}} = 0$ for all $t \in \mathbb{R}$). However, in reality, the power demand profiles $\mu_{P,i}(t)$ will never be step-wise; they are usually smooth, due to generator/load inertia and other physical restrictions. This is schematically illustrated in the right-hand side of Figure 3.1, which shows that in practice, $\Delta P_{\text{OL}}(t)$ is nonzero and especially large at setpoint interchange instants t_n, i.e, at PTU boundaries. Thus, although the present market and incentive system complies with requirement (3.1) for open-loop energy balance (at discrete time instants t_n), it introduces large open-loop mismatches in terms of power, which need to be compensated by considerable control effort in real-time, even if no external disturbances act on the system.

Note that the effects caused by the above described inconsistency are already observable today. Figure 3.2 shows a frequency measurement performed in the European/ENTSO-E synchronous grid during the evening (TenneT TSO, 2009).[2] Directly after a change in energy exchange setpoints, which occurs every full hour, large frequency deviations occur. These deviations due to step-wise

[2] *ENTSO-E*, or, the *European Network of Transmission System Operators for Electricity*, is the association of European TSOs, see `www.entsoe.eu`.

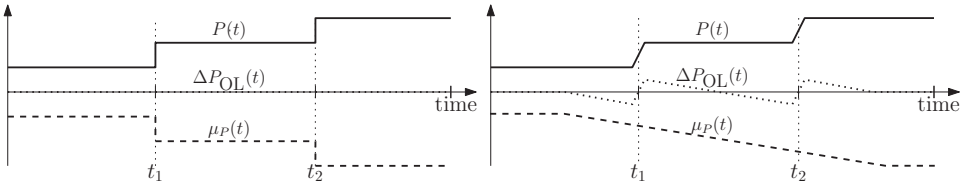

Figure 3.1: Open-loop power imbalance for step-wise (left) and smooth (right) power exchange profiles.

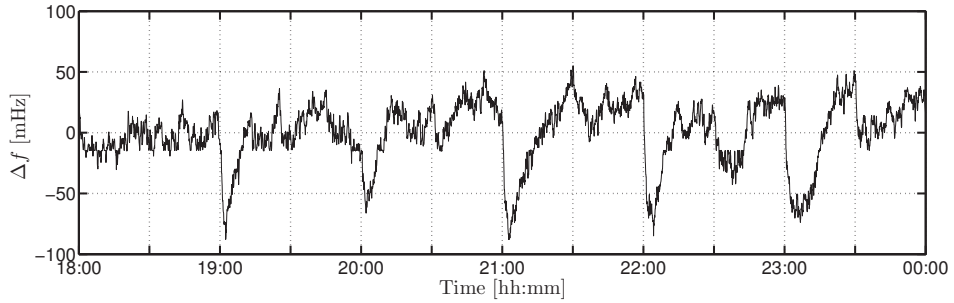

Figure 3.2: Grid frequency measurement, reproduced from (TenneT TSO, 2009).

power reference tracking activate a significant share of primary and secondary control (PC/SC) reserves, such that the system becomes vulnerable to disturbances, see (Weissbach and Welfonder, 2009; UCTE, 2008; Tractebel Engineering, 2009).

3.2.1 State-of-the-art solutions

Because the above explained power imbalance fluctuations are expected to increase in the near future, e.g., due to the ongoing deregulation and the growth of energy trading volumes, a number of solutions have been proposed in the literature, see, for example, (UCTE, 2008; Weissbach and Welfonder, 2009). These approaches are briefly discussed below.

Explicit constraints on power
A natural way to decrease the open-loop power imbalance is to put an upper bound on the ramp rates of $P_i(t)$ (UCTE, 2008). This constraint (on power instead of energy) prevents large step-wise changes in $P(t)$ at PTU boundaries, such that intra-PTU power imbalances can be decreased effectively. However, due to the integral relation of power and energy, this inherently limits market

activity, and the implementation of power-based incentives and verification of the associated conditions (by the TSO) is challenging.

Shorter PTUs
The difference between subsequent energy transactions $E_i[n]$ and $E_i[n+1]$ can be decreased by shortening the interval T_{PTU}. Thus, this is an effective way of reducing the step-wise change in $P_i(t)$ and open-loop imbalance at PTU transitions (Weissbach and Welfonder, 2009). However, as energy transactions are settled on a PTU basis, a decrease in PTU length will increase the number of transactions, and thus, scheduling and trade complexity, correspondingly. Moreover, it is difficult for BRPs to respond to portfolio deviations (and, accordingly, it may be challenging to avoid imbalance costs) within short PTUs during the operational day. As a consequence, the support for decreasing the PTU length may be low, particularly amongst BRPs.

3.3 Asynchronous program time units

To the best of our knowledge, reducing the PTU length is the only state-of-the-art solution that tackles the fundamental flaw of the current forward/open-loop market arrangements, i.e., the inconsistency between energy-based trade and power-based balancing requirements. However, the increase of market complexity associated with straightforwardly shortening the PTU length renders this solution unsuited for implementation. In this section, it is shown that the PTU lattice density, and hence, open-loop balancing performance, can still be increased, without affecting forward trade, by *settling the energy transactions of various market participants in an asynchronous way*.

Let $M \leq N$ partitions or *time frames* $\mathcal{P}_j$, $j \in \mathbb{Z}_{[0,M-1]}$, of the continuous-time axis $\mathbb{T} = \mathbb{R}$ be given such that

$$\mathbb{T} = \{\ldots, \mathbb{T}_j[-1], \mathbb{T}_j[0], \mathbb{T}_j[1], \ldots\}, \tag{3.5}$$

with partition blocks (or time-shifted PTUs)

$$\mathbb{T}_j[n] := \big[(\varphi_j + n)T_{\text{PTU}}, \quad (\varphi_j + n + 1)T_{\text{PTU}}\big), \tag{3.6}$$

for $n \in \mathbb{Z}$, where $\varphi_j := \frac{(1+2j)}{2M}$. Each partition $\mathcal{P}_j$ is assigned to a nonempty set of BRPs $\mathcal{I}_j \subseteq \mathcal{I}_{\text{BRP}}$, where $\mathcal{I}_j$ is constructed in such a way that

$$\bigcup_{j \in \mathbb{Z}_{[0,M-1]}} \mathcal{I}_j = \mathcal{I}_{\text{BRP}} \quad \text{and} \quad \mathcal{I}_j \bigcap \mathcal{I}_l = \emptyset \tag{3.7}$$

Algorithm 1 Asynchronous PTU Method (APM)

1) Trade: Each BRP $i \in \mathcal{I}_{\text{BRP}}$ submits its T_{PTU}-based E-programs/transactions $E_i[n]$ for the upcoming day to the TSO, who performs a consistency check according to (3.1).

2) Scheduling: Given a set of consistent transactions $E_i[n]$, $i \in \mathcal{I}_{\text{BRP}}$, the TSO reschedules them to obtain *E-references* that are defined with respect to the time frames $\mathcal{P}_j$. That is, it expects BRP $i \in \mathcal{I}_j$ to exchange a nett amount of energy with the grid in time interval $\mathbb{T}_j[n]$ of

$$\hat{E}_i[n] := (1-\varphi_j)E_i[n] + \varphi_j E_i[n+1]. \tag{3.8}$$

3) Settlement: Any deviations from $\hat{E}_i[n]$ within $\mathbb{T}_j[n]$ are settled in a fashion that is similar to the present arrangements, except for the different PTUs used per group of BRPs $\mathcal{I}_j$. Thus, the portfolio deviation $\int_{\mathbb{T}_j} P_i^{\text{RT}}(t)dt - \hat{E}_i[n]$ of BRP $i \in \mathcal{I}_j$ is sold to the TSO against a certain ex-post determined price, where $P_i^{\text{RT}}(t)$ is the actual, real-time power exchange of BRP i at time t.

whenever $j \neq l$, for $j, l \in \mathbb{Z}_{[0,M-1]}$. Next, consider Algorithm 1.

The novelty of Algorithm 1 completely lies in the scheduling and settlement step. Thus, even though APM employs asynchronous settlement of energy transactions, energy trade itself is still based on the standard, synchronized PTU intervals $[t_n, t_{n+1})$, $n \in \mathbb{Z}$. Hence, BRPs may establish transactions with any other market actor, regardless of their respective time frames during the operational day. Also, note that the E-references $\hat{E}_i$ are dependent on the synchronous E-programs E_i only, such that no production is shifted from one BRP to an other one.

Remark 3.3.1 The time shifts employed in APM, i.e., $\varphi_j T_{\text{PTU}} = \frac{(1+2j)}{2M} T_{\text{PTU}}$, are nonzero for all $j \in \mathbb{Z}_{[0,M-1]}$. This avoids possible competitive advantages arising from market-synchronized settlement. ■

In what follows, it is assumed that production costs are strictly convex functions of power production, and all BRPs respond to incentives in a rational, cost-minimizing fashion. These assumptions are widely used in power system economics, see (Glachant and Lévêque, 2009). Moreover, for ease of presentation, in what follows we assume that $M = N$ and $\mathcal{I}_j := \{j\}$, such that the energy transactions of BRP i are settled with respect to time frame $\mathcal{P}_i$. Then, (3.8) reduces to

$$\hat{E}_i[n] := (1-\varphi_i)E_i[n] + \varphi_i E_i[n+1], \qquad i \in \mathcal{I}_{\text{BRP}}. \tag{3.9}$$

Now consider the following result.

Proposition 3.3.2 *Rescheduling of energy production according to* (3.8) *will not affect the nett energy exchange for the network as a whole.*

Proposition 3.3.2 is derived as follows. Consider a sequence of PTUs $n \in \mathbb{Z}_{[0,K-1]}$, for which the total energy exchange of BRP i under synchronous and asynchronous scheduling satisfies

$$\sum_{n=0}^{K-1} E_i[n] = \sum_{n=0}^{K-1} \big(\varphi_i E_i[n] + (1-\varphi_i)E_i[n]\big),$$
$$\sum_{n=0}^{K-1} \hat{E}_i[n] = \sum_{n=0}^{K-1} \big((1-\varphi_i)E_i[n] + \varphi_i E_i[n+1]\big).$$

Thus, the nett difference in energy exchange is given by

$$\Delta E_i(K) := \sum_{n=0}^{K-1} \Big(E_i[n] - \hat{E}_i[n]\Big) = \varphi_i(E_i[0] - E_i[K]). \tag{3.10}$$

In practice, the sequence of energy transactions will be highly periodic (e.g., over a day or a year). Hence, it follows that, for appropriate K^*, $E_i[0] \approx E_i[K^*]$ and thus $\Delta E_i(K^*) \approx 0$. Moreover, in accordance with (3.8), all transactions $E_i[n]$ are distributed over a period $\big[(\varphi_i + n - 1)T_{\mathrm{PTU}}, (\varphi_i + n + 1)T_{\mathrm{PTU}}\big)$ of length $2T_{\mathrm{PTU}}$. Note that this interval includes the PTU that was used for establishing $E_i[n]$, i.e., $\big[nT_{\mathrm{PTU}}, (n+1)T_{\mathrm{PTU}}\big)$. Since no transactions are shifted from one BRP to another, equivalence of total BRP energy exchange yields equivalence of total aggregated energy exchange, which supports Proposition 3.3.2.

Equation (3.10) also shows that for arbitrary K, the open-loop energy mismatch introduced by APM settlement is bounded, because the energy transactions $E_i[n]$ and time shifts φ_i are bounded in practice.

Next, we recall that under APM, the controllable generators of rational BRPs will track step-wise power profiles $\hat{P}_i(t) = \hat{P}_i[n]$ for $t \in \mathbb{T}_i[n]$, with

$$\hat{P}_i[n] := \frac{1}{T_{\mathrm{PTU}}} \left(\hat{E}_i[n] - \int_{t \in \mathbb{T}_i[n]} \mu_{P,i}(t)\, dt \right), \tag{3.11}$$

to comply with E-reference-based portfolios in a similar way as BRPs comply with E-programs under the present synchronous scheduling arrangements, due to the assumed strict convexity of the production costs. The resulting controllable power exchange profile for the network as a whole, i.e., the aggregation of the individual time-shifted step-wise power profiles, is given by

$$\hat{P}(t) = \hat{P}[k] := \sum_{i=0}^{N-1} \hat{P}_i \left[\left\lfloor \frac{k-i}{N} \right\rfloor \right] \qquad \text{for } t \in \hat{\mathbb{T}}[k], \tag{3.12}$$

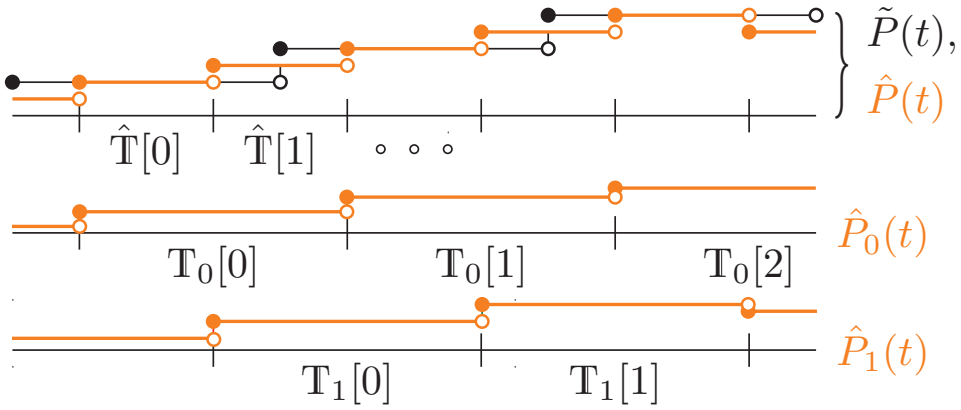

Figure 3.3: Controllable power production under APM, for $M = N = 2$.

where $\hat{\mathbb{T}}[k] := \left[\frac{1+2k}{2N} T_{\text{PTU}}, \frac{1+2(k+1)}{2N} T_{\text{PTU}}\right)$. Figure 3.3 illustrates this aggregation for $N = 2$. Note that even though the production profiles of individual BRPs are piecewise constant with steps of length T_{PTU}, the corresponding nett production on the aggregated system level is less coarse with steps of width $\frac{T_{\text{PTU}}}{N}$. Hence, in contrast to standard, synchronized scheduling, APM can induce an aggregated controlled power exchange profile that captures the smooth dynamics of $\mu_P(t)$ well and yields low open-loop imbalance, at any time instant $t \in \mathbb{R}$, in terms of *both energy and power*. The effectiveness of APM is dependent on the distribution of energy transactions over the individual BRPs, however. In what follows, we will describe two extreme scenarios to illustrate this dependency.

Firstly, suppose that BRP 0 is responsible for all the controllable production in the network. Accordingly, the aggregated controllable power production $\hat{P}(t) = \hat{P}_0(t) = \hat{P}_0[n]$ for $t \in [(\varphi_0 + n)T_{\text{PTU}}, (\varphi_0 + n + 1)T_{\text{PTU}})$ is step-wise with step width T_{PTU}, both under the present arrangements and under APM (regardless of the distribution of uncontrollable production over the BRPs). Thus, in this case, APM does not improve open-loop balancing performance.

Next, consider a second scenario where the controllable energy production is uniformly distributed over the BRPs $i \in \mathbb{Z}_{[0,N-1]}$, and let BRP 0 be responsible for all noncontrollable production (i.e., $\mu_{P,i}(t) \neq 0$ only for $i = 0$). Hence, $T_{\text{PTU}} \tilde{P}_i[n] = -\frac{1}{N} \int_{t_n}^{t_{n+1}} \mu_{P,0}(t)\,dt$ for all $i \in \mathcal{I}_{\text{BRP}}$. Moreover, suppose that

$$\int_{t \in \mathbb{T}_0[n]} \mu_P(t)\,dt = (1 - \varphi_0) \int_{t_n}^{t_{n+1}} \mu_P(t)\,dt + \varphi_0 \int_{t_{n+1}}^{t_{n+2}} \mu_P(t)\,dt. \tag{3.13}$$

It follows from (3.9)–(3.12) that

$$\hat{P}[k] = \frac{1}{N}\sum_{i=0}^{N-1}(1-\varphi_i)\widetilde{P}\left[\left\lfloor\frac{k-i}{N}\right\rfloor\right] + \varphi_i\widetilde{P}\left[\left\lfloor\frac{k-i}{N}\right\rfloor+1\right], \tag{3.14}$$

which is a weighted sum of time-shifted economically optimal production profiles for the present, synchronous settlement arrangements. From (3.14) it follows that in this second scenario, the aggregated controllable power production profile is step-wise with a step width of $\frac{T_{\mathrm{PTU}}}{N}$. Moreover, in Appendix A.1 it is shown that (3.14) is equivalent to convolving (3.3) with a *digital low-pass finite-impulse response filter*. This filter is specified by the coefficient vector/impulse response

$$\begin{aligned}\mathbf{h} &= \begin{bmatrix} h_0, & h_1, & \dots & h_{N-1}, & h_N, & \dots & h_{2N-2}, & h_{2N-1}\end{bmatrix} \\ &:= \frac{1}{2N^2}\begin{bmatrix} 1, & 1{+}2, & \dots & 1{+}2(N{-}1), & 1{+}2(N{-}1), & \dots & 1{+}2, & 1\end{bmatrix}.\end{aligned} \tag{3.15}$$

The low-pass character of APM illustrated by this example scenario ensures a smooth adjustment of controllable generation on the aggregated power system level. Instead of changing controllable production setpoints simultaneously at market-PTU boundaries, BRPs will adjust their production at different time instants, thus effectively tackling the issues discussed in Section 3.2.

Although, intuitively, the smoothing/de-synchronizing effect is expected to be optimal for evenly distributed controllable production capacity, APM will improve the open-loop balancing performance as long as the controllable load and generation is rescheduled over more than one time frame $\mathcal{P}_i$. This observation is formalized as follows.

Proposition 3.3.3 *APM provides BRPs with an incentive for delivering power in such a way that the aggregated dispatch profile yields an open-loop power imbalance that is at most as large as, but (under normal operating conditions) most likely less than the imbalance attained by a synchronous method with identical PTU length.*

The details on deriving Proposition 3.3.3 are provided in Appendix A.2; below, we list the main results only.

An upper bound on the worst-case open-loop power mismatch $\Delta P_{\mathrm{OL}}(t) := \widetilde{P}[n] - \mu_P(t)$ for $t \in [t_n, t_{n+1})$ induced by APM is

$$\left|\Delta P_{\mathrm{OL}}(t)\big|_{N=1}\right| \leq \frac{T_{\mathrm{PTU}}}{2}\left|\frac{\mathrm{d}\mu_P}{\mathrm{d}t}(t)\right| + \frac{T_{\mathrm{PTU}}^2}{6}\left|\frac{\mathrm{d}^2\mu_P}{\mathrm{d}t^2}(t)\right| + \mathcal{O}(T_{\mathrm{PTU}}^3), \tag{3.16}$$

see Appendix A.2. This bound applies to the current, synchronous settlement arrangements, or, equivalently, to APM with $N = 1$ or a scenario where all controllable energy production is concentrated in a single PTU partition $\mathcal{P}_j$. An upper bound on the best-case open-loop imbalance profile, as obtained for a uniform distribution of controllable exchange and $N \to \infty$, is

$$\left|\Delta P_{\mathrm{OL}}(t)\big|_{N\to\infty}\right| \leq \frac{T_{\mathrm{PTU}}^2}{6}\left|\frac{\mathrm{d}^2\mu_P}{\mathrm{d}t^2}(t)\right| + \mathcal{O}(T_{\mathrm{PTU}}^3). \tag{3.17}$$

From (3.16) and (3.17) it follows that APM gives an approximation of the actual noncontrollable power production profile that is at least as accurate as the profile induced by synchronous arrangements, which supports Proposition 3.3.3.

Remark 3.3.4 Proposition 3.3.3 (and the corresponding details in Appendix A.2) shows that a balanced distribution of controllable generation/load over the time frames $\mathcal{P}_j$ is crucial for optimizing APM's performance. Thus, a natural way of assigning the BRPs to the different partitions is based on their share of the total controllable production capacity. ■

Remark 3.3.5 In contrast to standard/synchronous scheduling, the open-loop power imbalance $\Delta P_{\mathrm{OL}}(t)$ attained by APM does not converge to zero for all $t \in \mathbb{R}$ if $N \to \infty$. This issue is inherent to establishing PTU-based energy (instead of continuous-time power) transactions on the market, which can be considered as sampling the smooth, expected noncontrollable production profiles at a nonuniform sampling rate. This is explained below.

The *mean value theorem* states that for continuous, differentiable $\mu_P(t)$, there exists a $t_n^* \in [t_n, t_{n+1})$ such that

$$\int_{t_n}^{t_{n+1}} \mu_P(t)dt = (t_{n+1} - t_n)\mu_P(t_n^*) = T_{\mathrm{PTU}}\mu_P(t_n^*).$$

In other words, $\mu_P(t)$ takes on its average value $\widetilde{P}[n]$ at some point of the n-th PTU, and thus, all $\widetilde{P}_i[n]$ are (weighted) samples of $\mu_P(t)$ taken at this unknown time instant $t_n^* \in [t_n, t_{n+1})$. This corresponds to nonuniform sampling of $\mu_P(t)$ at an average rate of $\frac{1}{T_{\mathrm{PTU}}}$.

In the literature, many methods are available for reconstructing nonuniformly, super-Nyquist sampled signals, see, e.g., (Sommen and Janse, 2008). Crucial to these approaches is that the sample instants t_n^* are distinct and known. PTU-based trade does not satisfy the latter condition. The nonuniform samples $E_i[n]$ are therefore not sufficient for perfect reconstruction of the power profile $\mu_P(t)$, and accordingly, the bound on the corresponding open-loop power imbalance $\Delta P_{\mathrm{OL}}(t)$ does not converge to 0 as $N \to \infty$. ■

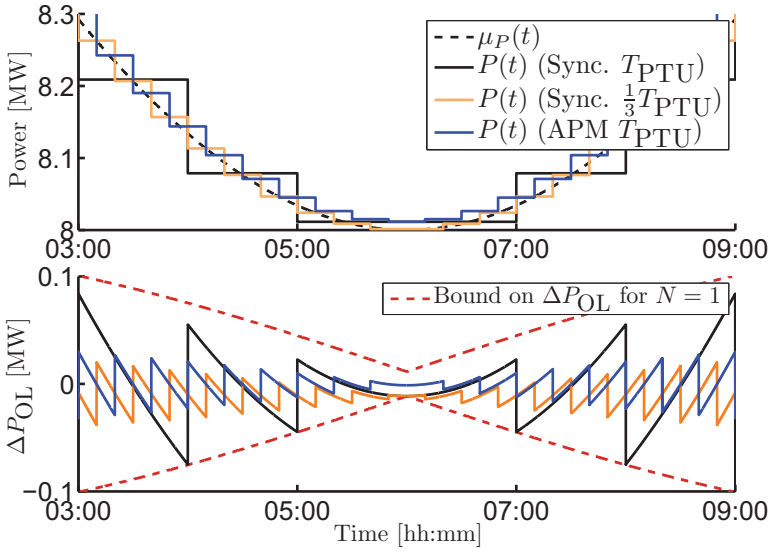

Figure 3.4: Open-loop power exchange and imbalance profiles for $N = 3$.

3.4 Simulation results

The effectiveness of APM is evaluated by comparing it with synchronous scheduling for different PTU lengths. We begin with open-loop scheduling performance, followed by a comparison of closed-loop simulation results.

3.4.1 Open-loop performance

The open-loop performance of a T_{PTU} and a $\frac{T_{\mathrm{PTU}}}{N}$ PTU-length synchronous settlement scheme are compared with the performance attained by an N-sequence APM scheme with a PTU-length of T_{PTU} =1 h and evenly-distributed controllable production. The asynchronous scheme is simulated for $N = 3$ and $N = 1000$, where the latter scenario provides an indication of the results for $N \to \infty$. In the simulation, for simplicity, the noncontrollable power exchange profile $\mu_P(t)$ is assumed to be sinusoidal with a period of one day.

Figure 3.4 shows the open-loop performance of the current arrangements, that of a synchronous scheme with PTU length $\frac{T_{\mathrm{PTU}}}{3}$ and that of a 3-sequence asynchronous scheme. The upper bound on the open-loop error $|\Delta P_{\mathrm{OL}}(t)|$ for the synchronous scheme, i.e., (3.16), is represented by the dashed lines in the lower subfigure. Both the APM and the synchronous scheme with PTU length $\frac{T_{\mathrm{PTU}}}{3}$ decrease the worst-case open-loop error by a factor of approximately 3. Fur-

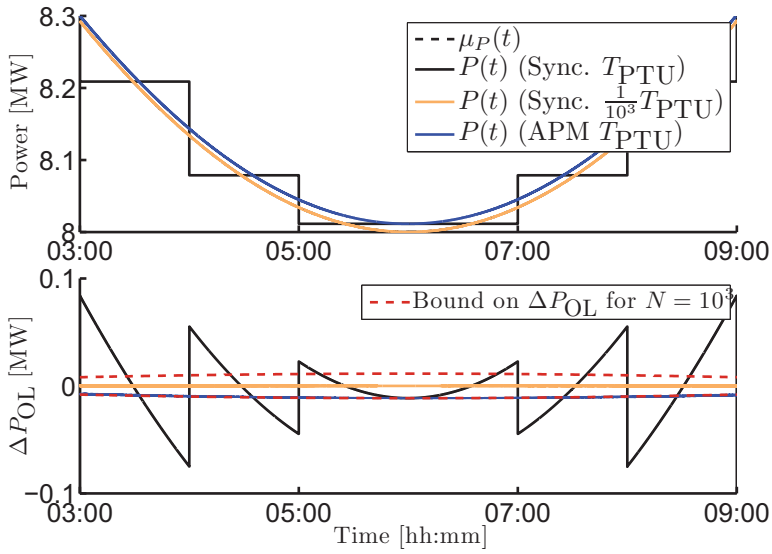

Figure 3.5: Open-loop power exchange and imbalance profiles for $N = 1000$.

thermore, note that the open-loop error resulting from $\frac{T_{\mathrm{PTU}}}{3}$-PTU scheduling is 0 whenever $\frac{\mathrm{d}\mu_P}{\mathrm{d}t}(t) = 0$ (for instance, at 06:00h), whereas a small error is apparent in the asynchronous case, due to nonzero higher order derivatives in (3.17).

Figure 3.5 shows the simulation results for $N = 1000$. The worst-case open-loop error envelope for the $N \to \infty$ APM settlement scheme, i.e., (3.17), is shown in the bottom plot. Although increasing N does not reduce the open-loop APM error to zero (see Remark 3.3.5), it is possible to get arbitrarily close to error bound (3.17) for all $t \in \mathbb{R}$ by choosing appropriate $N \in \mathbb{Z}_+$.

Now consider the root mean square imbalance/error criterion

$$e(T) := \sqrt{\int_0^T |\Delta P_{\mathrm{OL}}(t)|^2 dt}. \tag{3.18}$$

Evaluating this criterion for a period of one day (i.e., $T = 86400\,\mathrm{s}$) and $N = 3$ yields a 64% and 67% reduction in $e(T)$ for APM and $\frac{T_{\mathrm{PTU}}}{3}$-based synchronized settlement, respectively, measured with respect to the error induced by the standard T_{PTU}-based synchronous scheme. For $N = 1000$ this reduction is even larger, that is, 85% and 99%, respectively. These figures show that, even for relatively small values of N, both the APM-based and short-PTU schemes can outperform the current arrangements. However, although APM and PTU-shortening lead to similar improvement of the open-loop balancing quality, the

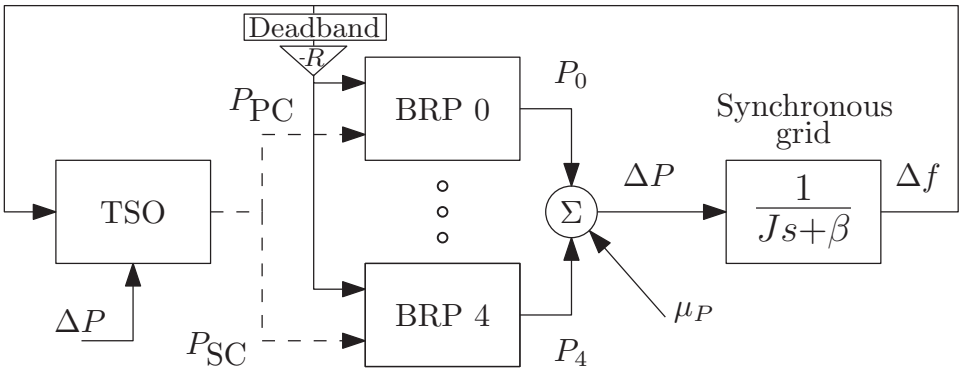

Figure 3.6: Benchmark power system.

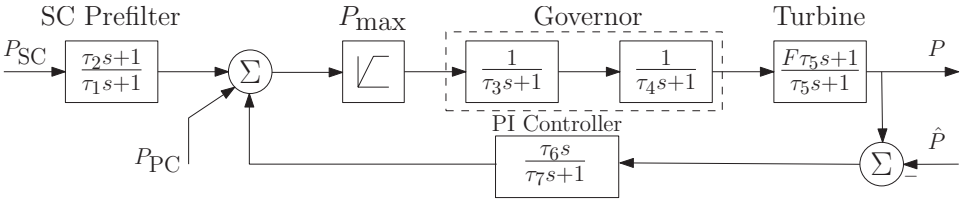

Figure 3.7: Linear BRP/generator model.

complexity of their implementation is quite different. In the shortened PTU case, large N values correspond to small PTU-lengths, and thus require highly accurate prediction models and many decisions for trade. This is not the case for the APM scheme, as the corresponding market is based on a PTU-length of T_{PTU} independent of $N \in \mathbb{Z}_+$.

3.4.2 Closed-loop performance

Next, we focus on real-time balancing. Figure 3.6 schematically depicts the simulated 5-BRP benchmark power network. Its closed-loop performance is evaluated during regular, unperturbed operation under the current, synchronized (ENTSO-E) settling arrangements and for APM with $N = 5$ and evenly-distributed energy transactions. All BRPs are described by a linear, lumped generator model, reproduced from (Anderson, 2003) and schematically shown in Figure 3.7. Frequency/imbalance control is implemented by two parallel feedback loops. The primary control law is $P_{\mathrm{PC}}(t) = -RD(\Delta f(t))$, with frequency

Table 3.1: Assessment of closed-loop performance

Settling method	$\Delta f_{\max}$ [mHz]	E_{PC} [GWh]	E_{SC} [GWh]
Synchronous	71.8	2.27	6.26
Asynchronous ($N=5$)	15.5	0.00	1.64

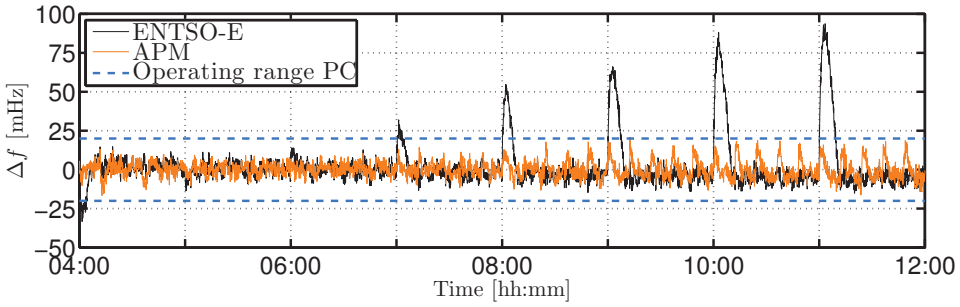

Figure 3.8: Evolution of the closed-loop grid frequency over time.

deviation $\Delta f(t) := f(t) - f_0$, $f_0 := 50\,\mathrm{Hz}$, and with dead-band function

$$D(x) := \begin{cases} 0 & \text{for } |x| \le d \\ x & \text{for } |x| > d, \end{cases} \tag{3.19}$$

where $d \in \mathbb{R}_+$ is some operating threshold. Secondary control power $P_{\mathrm{SC}}(t)$ is requested by the TSO through the classical feedback law $P_{\mathrm{SC}}(t) = K_{\mathrm{p,SC}}\mathrm{ACE}(t) + K_{\mathrm{i,SC}} \int \mathrm{ACE}(t)\,dt$, where $\mathrm{ACE}(t) := \Delta P(t) + K_f \Delta f(t)$ is the area control error. The system is considered to be a single control area, and thus, in this particular situation, $\Delta P(t)$ represents the network's total power imbalance. All network parameters, such as the total (normalized) inertia J, the load-damping coefficient β, the primary control operating range d and the gains of the primary and secondary control loops are taken from (ENTSO-E, 2009). BRP models 0–3 are dimensioned as (relatively slow) coal-fired generators; BRP 4 is modeled as a fast-responding gas-fueled power plant. All BRPs have equal production capacities $P_{\max}$.

The closed-loop performance is measured in terms of the maximum frequency deviation $\Delta f_{\max} := \max_t |f(t) - f_0|$ and the primary and secondary control effort, defined as $E_x(T) := \int_0^T |P_x(t)|\,dt$ [GWh], where x can be either "PC" or "SC" to denote primary or secondary balancing power/energy, respectively. Table 3.1 lists the corresponding performance results; Figure 3.8 depicts the evolution of the grid frequency over time. Firstly, note that the synchronous set-

tlement result in Figure 3.8 shows a clear resemblance with the actual ENTSO-E-grid measurements shown in Figure 3.2, which indicates that the simulation captures the relevant power system dynamics well. Secondly, it can be observed that the grid frequency is stabilized, i.e., is driven back to f_0 in case of disturbances, which, in this scenario, completely originate from finitely fast generator dynamics and the mismatch between the smooth sinusoidal load profile and the aggregated step-wise generation schedules. Table 3.1 shows that the daily APM-induced maximum frequency deviations are smaller than the deviations caused by the synchronous scheme. Moreover, as the closed-loop power imbalance induced by asynchronous settlement completely lies within the dead-band interval $[-d,d]$, APM avoids undesired activation of fast, primary balancing reserves. Also, the simulation illustrates that asynchronous scheduling reduces the need for secondary control energy (and thus, also the TSO's balancing costs), due to the corresponding improvement in open-loop scheduling efficiency.

3.5 Conclusions

In the deregulated electrical energy market, transmission system operators have to provide market participants with appropriate incentives to guarantee stable operation of the transmission network. In this chapter, it was shown that the currently employed incentive system does not necessarily induce power exchange profiles that contribute to balancing and security of supply, due to the fundamental inconsistency between energy-based trade and power-related control objectives. State-of-the-art solutions for tackling this issue can affect market flexibility or significantly increase complexity of trade. Therefore, an alternative scheduling concept was proposed that relies on standard market arrangements, but settles the energy transactions of different (clusters of) balance responsible parties in an asynchronous way. Open- and closed-loop simulations were provided to illustrate that by adopting this method, grid operation can become more robust and the strain on balancing reserves, and thus balancing costs, can be reduced considerably.

4

Non-centralized model predictive control for power systems

4.1 Introduction

With the ongoing deregulation of the electrical energy market and the growing share of intermittent, distributed generation, the efficiency of open-loop scheduling mechanisms such as the ones discussed in the previous chapters is declining steadily. Future power systems will be characterized by large, badly controllable and unpredictable fluctuations in power demand and supply, and thus, more and more balancing efforts are needed during the operational day. The trends in electrical power system design also imply that the common way of dealing with network and generator constraints, that is, by imposing sufficiently large security margins on the scheduling problem, tends to affect market performance to an unacceptable extent. Instead, it may be more efficient to handle these constraints also on a (near-)real-time basis, as short-run imbalance fluctuations can be predicted in a relatively accurate fashion (Frunt, 2011). However, this means that the conventional automatic generation control scheme needs to be replaced by a more advanced frequency control architecture that can both

guarantee stable and efficient operation of the power system, while explicitly accounting for the specific constraints and disturbances that are associated with the electrical power transmission and generation.[1]

The design of alternative real-time supply-demand balancing schemes will be the topic for the remainder of this thesis. We begin by evaluating the suitability of *model predictive control (MPC)* for frequency control in future power networks in this chapter, followed in Chapters 5 and 6 by a more detailed discussion of the key underlying control problem, i.e., the non-centralized stabilization of networks of interacting dynamical systems. The developed control methods are then applied to a number of non-trivial power system benchmark examples in Chapter 7.

4.1.1 Predictive frequency control

In various recent papers it is observed that model predictive control has the potential for solving some of the problems that will appear in future electrical power networks (Camponogara, 2000; Venkat, 2006; Jokić et al., 2007; Camponogara et al., 2002; Venkat et al., 2008). MPC is capable of handling control problems where off-line computation of a classical control law is difficult, particularly since MPC can explicitly take system constraints into account when computing the control action. Furthermore, MPC allows the use of disturbance models, which can be employed to counteract the fluctuations in power generation introduced by renewable energy sources. For a detailed survey of MPC and constrained optimal control, the interested reader is referred to (Mayne et al., 2000; Goodwin et al., 2005).

Yet, the fact that MPC is a centralized control mechanism is a major issue when considering power system applications. Centralized control implies that a single controller is able to measure all the system outputs, compute the optimal control input, and apply that action to all the actuators in the network, within one sampling period. As power networks are large-scale systems, both computationally and geographically, a centralized MPC controller is practically impossible to implement.

The difficulties with centralized predictive control for large-scale systems explain the increasing attention for *non-centralized* MPC implementations in the control literature, see for example (Camponogara, 2000; Camponogara et al., 2002; Keviczky et al., 2006; Alessio and Bemporad, 2007; Dunbar, 2007; Venkat et al., 2008). Roughly speaking, non-centralized MPC schemes can be divided

[1] For a detailed discussion on what is meant by stability in the electrical power systems setting, we refer the interested reader to (Kundur et al., 2004). The corresponding fundamental mathematical notions are provided in Chapter 5.

into two categories: *decentralized techniques*, which do not allow for communication between local controllers, and *distributed techniques*, where communication between different controllers is exploited to improve the prediction accuracy. Distributed MPC methods can be further categorized as techniques that require communication between all the controllers in the network and techniques that require communication solely with directly neighboring controllers.

In the literature on non-centralized predictive control, various power system implementations have been illustrated, see (Camponogara, 2000; Camponogara et al., 2002; Venkat et al., 2008). These methods differ in terms of computational complexity, the extent of communication and the size of the embedded prediction model, and, as a consequence, in terms of performance. In this chapter we consider *decentralized model predictive control* (DMPC; Alessio and Bemporad (2007)), *stability-constrained distributed model predictive control* (SC-DMPC; Camponogara et al. (2002)), and *feasible cooperation-based model predictive control* (FC-MPC; Venkat (2006)), all of which represent viable candidates for implementation in power systems. Alternative methods, such as strategies for enforcing constraints that involve the dynamics of multiple control areas (see for instance Jia and Krogh (2002); Keviczky et al. (2006); Richards and How (2007); Müller et al. (2012); Grüne and Worthmann (2012)) are not discussed, as the literature does not yet give a solid, practical solution for dealing with both coupled constraints and dynamics in a low-complexity and non-conservative fashion. For a discussion on the theoretical issues regarding non-centralized MPC in general, the interested reader is referred to (Camponogara, 2000; Camponogara et al., 2002; Jia and Krogh, 2002; Keviczky et al., 2006; Alessio and Bemporad, 2007; Dunbar, 2007; Richards and How, 2007; Venkat et al., 2008; Scattolini, 2009; Stewart et al., 2010; Liu et al., 2009a, 2010; Maestre et al., 2011; Stewart et al., 2011; Farina and Scattolini, 2012; Müller et al., 2012; Grüne and Worthmann, 2012) and the references therein.

The choice for DMPC, SC-DMPC and FC-MPC is further motivated by our main research goal, which is to study the correlation between the complexity and usefulness of non-centralized MPC schemes and their corresponding attainable performance. DMPC does not require communication and therefore belongs to the decentralized and simplest category of non-centralized MPC. Although specific implementations of DMPC do exploit an exchange of information between controllers, we will only consider the completely decentralized version in this chapter, to give an indication of the performance that can be obtained without communication. SC-DMPC and FC-MPC are distributed MPC schemes, as they both employ communication to increase the accuracy of their state predictions. The FC-MPC technique requires communication among all the local controllers and uses an iterative procedure to compute the control

action, while the SC-DMPC scheme employs communication between directly neighboring subsystems only.

The remainder of this chapter is organized as follows. Section 4.2 introduces the (centralized) MPC concept along with the method that is typically employed to guarantee closed-loop stability. In Section 4.3, we describe the DMPC, SC-DMPC and FC-MPC techniques from an engineering perspective, particularly focusing on the details that are relevant for controller implementation. Section 4.4 provides simulation results for the MPC algorithms under consideration, as obtained for a suitably constructed power network example. The non-centralized MPC schemes are compared with centralized MPC and classical AGC. Given the results of this benchmark test, we discuss the suitability of the considered methods for real-time balancing of electrical power networks. We finish with conclusions in Section 4.5.

4.2 Centralized model predictive control

Figure 4.1 illustrates the basic principles of model predictive control. In MPC, the control action is computed by solving a finite-horizon open-loop optimal control problem at each discrete-time instant. The controller employs a model to obtain a prediction of the state evolution over time, given the current state of the controlled system. Only the first sample of the optimal sequence of control actions is applied to the plant, after which the whole process is repeated the next time instant. This is the main difference with classical control methods, which normally use a pre-computed and fixed feedback law. The unique, distinguishing feature of MPC lies in its ability to compute the control input while explicitly taking input and state constraints into account.

In this chapter, we consider systems that can be accurately modeled using linear discrete-time state-space representations of the form

$$x(k+1) = Ax(k) + Bu(k), \tag{4.1}$$

where $A \in \mathbb{R}^{n\times n}$, $B \in \mathbb{R}^{n\times m}$, $x(k) \in \mathbb{R}^n$ is the state and $u(k) \in \mathbb{R}^m$ is the control input at discrete-time instant $k \in \mathbb{Z}_+$. Note that the number of states n in power networks that consist of thousands of nodes/buses can be very large, which corresponds to high-dimensional A and B matrices.

Let the control input and the predicted state at time instants $k+l \in \mathbb{Z}_+$, given $x(k)$, be denoted by $u(l|k)$ and $x(l|k)$, respectively. Moreover, let $\mathbf{u} = \{u(0|k), \ldots, u(N_\mathrm{p}-1|k)\}$ be a finite sequence of control moves, where $N_\mathrm{p} \in \mathbb{Z}_+$ is the prediction horizon. The optimal control problem that the MPC controller solves each sampling instant, is formally defined as follows.

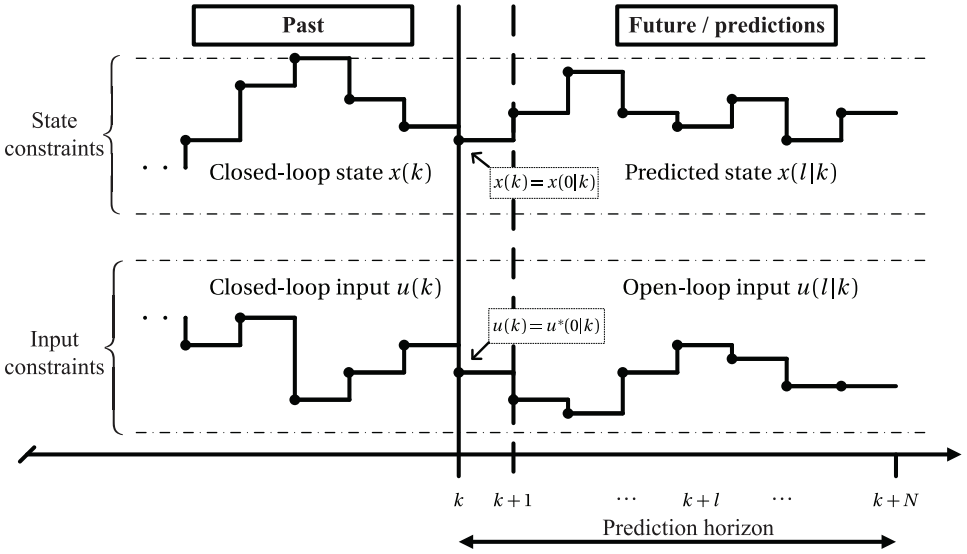

Figure 4.1: A schematic illustration of model predictive control.

Problem 4.2.1 Centralized MPC At discrete-time instant $k \in \mathbb{Z}_+$ let $x(k)$ and $N_\mathrm{p} \in \mathbb{Z}_{\geq 1}$ be given, set $x(0|k) := x(k)$ and solve

$$V^*_{N_\mathrm{p}}(x) = \min_{\mathbf{u}} \{ V_{N_\mathrm{p}}(x, \mathbf{u}) \mid \mathbf{u} \in \mathbb{U}_{N_\mathrm{p}}(x) \}, \tag{4.2a}$$

where

$$\begin{aligned} V_{N_\mathrm{p}}(x, \mathbf{u}) &= F(x(N_\mathrm{p}|k)) + \sum_{l=0}^{N_\mathrm{p}-1} \ell(x(l|k), u(l|k)) \\ &= x(N_\mathrm{p}|k)^\top P x(N_\mathrm{p}|k) + \sum_{l=0}^{N_\mathrm{p}-1} x(l|k)^\top Q x(l|k) + u(l|k)^\top R u(l|k) \end{aligned} \tag{4.2b}$$

$$x(l+1|k) = Ax(l|k) + Bu(l|k), \tag{4.2c}$$

for $l \in \mathbb{Z}_{[0,N_\mathrm{p}-1]}$. ■

The matrices $Q = Q^\top \succeq 0$ and $R = R^\top \succ 0$ are suitably chosen performance weights, i.e., tuning parameters, whereas the matrix $P = P^\top \succ 0$ that weighs the terminal state is usually computed off-line in such a way that closed-loop stability is guaranteed (Mayne et al., 2000).

Problem 4.2.1 minimizes the quadratic cost function $V_{N_\mathrm{p}}(x, \mathbf{u})$ over all input sequences $\mathbf{u}$ in the set $\mathbb{U}_{N_\mathrm{p}}(x)$. We assume that $\mathbb{U}_{N_\mathrm{p}}(x)$ can be defined by a finite

number of linear inequalities in $\mathbf{u}$, such that the MPC optimization problem can be formulated as a quadratic program (QP). The set of feasible input sequences is determined by the constraints on the states and inputs,

$$\mathbb{U}_{N_\mathrm{p}}(x) := \{\mathbf{u} \in \mathbb{U}^{N_\mathrm{p}} \,|\, x(l|k) \in \mathbb{X},\, l \in \mathbb{Z}_{[1,N_\mathrm{p}-1]},\, x(N_\mathrm{p}|k) \in \mathbb{X}_f\}, \tag{4.3}$$

where $\mathbb{U}^{N_\mathrm{p}} := \mathbb{U} \times \ldots \times \mathbb{U}$ is the N_p-times Cartesian product of $\mathbb{U}$. The set of feasible inputs $\mathbb{U}$ is a compact subset of $\mathbb{R}^m$ and $\mathbb{X}$ is a closed subset of $\mathbb{R}^n$. Asymptotic stability of the MPC controlled system can be guaranteed *a priori* by constraining the terminal state $x(N_\mathrm{p}|k)$ to an appropriately chosen terminal set $\mathbb{X}_f \subseteq \mathbb{X}$ and by using a specific terminal weight P (Mayne et al., 2000). To be precise, the set $\mathbb{X}_f$ must be positively invariant (Blanchini, 1994) and should satisfy the following property:

$$\mathbb{X}_f \subseteq \mathcal{O}_\infty := \{x \in \mathbb{R}^n \mid K(A+BK)^k x \in \mathbb{U}, (A+BK)^k x \in \mathbb{X}, k \in \mathbb{Z}_+\}, \tag{4.4}$$

where the pair $\{P, K\}$ is obtained as the solution of the unconstrained infinite horizon LQR problem (Mayne et al., 2000), i.e.,

$$P = (A+BK)^\top P (A+BK) + K^\top R K + Q, \tag{4.5a}$$

$$K = -(R + B^\top P B)^{-1} B^\top P A. \tag{4.5b}$$

After solving problem 4.2.1, the controller applies the first element of the optimal input sequence $\mathbf{u}^*$ to the system, i.e., $u(k) := u^*(0|k)$, and discards the rest of the sequence. At the next time instant, the state of the system is measured and the procedure described above is repeated. This *receding horizon strategy* acts as a feedback mechanism to increase robustness against prediction errors.

4.3 Non-centralized model predictive control

As explained in the introduction of this chapter, a centralized implementation of MPC is not well suited for control of power networks due to the complexity and the size of these systems. In this section, we describe three scalable MPC techniques that are more appropriate for power system control.

4.3.1 Decentralized MPC

The DMPC technique (Alessio and Bemporad, 2007) exploits the fact that many large-scale systems such as power networks consist of several subsystems (e.g., control areas) that are only loosely coupled. As a consequence, these systems

can be modeled by sparse state-space representations. In DMPC, the global state-space model is approximated via a state and input matrix partitioning that defines a set of N *decoupled* prediction models. Correspondingly, the DMPC control action is generated by the ensemble of N local MPC control laws that are independently designed for each decoupled subsystem.

Let the large-scale system that is to be controlled be described by the discrete-time state-space model given in (4.1). The division into N subsystems employed in DMPC is based on an explicit transformation via suitably defined matrices W_i and Z_i, $i \in \mathcal{I} := \{1,\dots,N\}$. These matrices collect the states and inputs assigned to subsystem i:

$$x_i = W_i^\top x, \qquad u_i = Z_i^\top u, \tag{4.6a}$$

where $x_i \in \mathbb{R}^{n_i}$ and $u_i \in \mathbb{R}^{m_i}$. The corresponding local, decoupled prediction models are given by

$$x_i(l+1|k) = A_i x_i(l|k) + B_i u_i(l|k) \tag{4.6b}$$

$$A_i = W_i^\top A W_i, \quad B_i = W_i^\top B Z_i, \tag{4.6c}$$

for $i \in \mathcal{I}$, where $A_i \in \mathbb{R}^{n_i \times n_i}$, $B_i \in \mathbb{R}^{n_i \times m_i}$.

W_i and Z_i are such that, by (4.6a), each element of x is assigned to one or more x_i and each element of u is assigned to one or more u_i. This allows for overlapping subsystems. However, in this chapter, we consider DMPC with non-overlapping partitions only, i.e., we restrict our attention to the case where each element of x is assigned to a single, unique x_i and each element of u is assigned to a unique u_i. Although DMPC performance is expected to benefit from subsystem overlap, this inherently comes with a requirement for communication among the systems in the network. The non-overlapping partitions considered in this section do not require subsystem coordination/communication, which is attractive from a practical perspective. For more information about the construction of the partitioning matrices, and for details on handling overlapping inputs in particular, the reader is referred to (Alessio and Bemporad, 2007).

In contrast to centralized MPC, where the control action for the full system is generated by a single computing unit, in DMPC the control action is computed by a set of local control laws, each assigned to a particular subsystem $i \in \mathcal{I} := \mathbb{Z}_{[1,N]}$. The corresponding subsystem-specific finite-horizon problem is given below.

Problem 4.3.1 DMPC At discrete-time instant $k \in \mathbb{Z}_+$ let $x_i(k)$ and $N_\mathrm{p} \in \mathbb{Z}_{\geq 1}$ be given, set $x_i(0|k) := x_i(k)$ and solve

$$V^*_{i,N_\mathrm{p}}(x_i) = \min_{\mathbf{u}_i} \{ V_{i,N_\mathrm{p}}(x_i, \mathbf{u}_i) \mid \mathbf{u}_i \in \mathbb{U}_{i,N_\mathrm{p}}(x_i) \}, \tag{4.7a}$$

with

$$V_{i,N_\mathrm{p}}(x_i,\mathbf{u}_i) = F_i(x_i(N_\mathrm{p}|k)) + \sum_{l=0}^{N_\mathrm{p}-1} \ell_i(x_i(l|k),u_i(l|k))$$
$$= x_i(N_\mathrm{p}|k)^\top P_i x_i(N_\mathrm{p}|k)$$
$$+ \sum_{l=0}^{N_\mathrm{p}-1} x_i(l|k)^\top Q_i x_i(l|k) + u_i(l|k)^\top R_i u_i(l|k) \tag{4.7b}$$
$$x_i(l+1|k) = A_i x_i(l|k) + B_i u_i(l|k), \quad l \in \mathbb{Z}_{[0,N_\mathrm{p}-1]}, \tag{4.7c}$$

where the penalty matrices used in each cost function, given the weights of centralized control problem (4.2), are $Q_i = W_i^\top Q W_i = Q_i^\top \succeq 0$, $R_i = Z_i^\top R Z_i = R_i^\top \succ 0$ and $P_i \succ 0$. ■

Problem 4.3.1 minimizes the local quadratic cost function $V_{i,N_\mathrm{p}}(x_i,\mathbf{u}_i)$ over input sequences $\mathbf{u}_i = \{u_i(0|k),\ldots,u_i(N_\mathrm{p}-1|k)\}$ in the set

$$\mathbb{U}_{i,N_\mathrm{p}}(x_i) := \{\mathbf{u}_i \in \mathbb{U}_i^{N_\mathrm{p}}\}, \tag{4.8}$$

where $\mathbb{U}_i^{N_\mathrm{p}} := \mathbb{U}_i \times \ldots \times \mathbb{U}_i$ is the N_p-times Cartesian product of the set of feasible local inputs. Assuming that $\mathbb{U}_{i,N_\mathrm{p}}$ is a polytope (i.e., can be described by a finite number of affine inequalities in $\mathbf{u}_i$), Problem 4.3.1 can be formulated as a quadratic program.

The ensemble of the optimal local control actions $u_i^*(0|k)$ of all N controllers, i.e.,

$$u(k) = \mathrm{col}(u_1^*(0|k),\ldots,u_i^*(0|k),\ldots,u_N^*(0|k)), \tag{4.9}$$

is applied as input to the full system (4.1). In line with the receding horizon principle, the whole procedure is repeated the next time instant.

In contrast to centralized MPC, the DMPC algorithm does not take (coupled) state constraints into account. This may be problematic if DMPC is to be employed for frequency control in electrical power networks, where state constraints such as bounds on transmission-line power flows are essential to guarantee safe operation.

Moreover, as described in Section 4.2, one can specifically design centralized MPC to provide an *a priori* guarantee for closed-loop stability, based on a suitably chosen terminal weight matrix and particular terminal state conditions. However, these centralized conditions do usually not allow for tractable, non-centralized implementation. Non-centralized predictive controllers such as DMPC exploit modified stabilization conditions on local inputs and states, while possibly providing a weaker guarantee for closed-loop stability of the full

network. In DMPC, an a priori guarantee of stability for each *decoupled* subsystem can be obtained by defining the terminal penalty matrix P_i for each subsystem i as

$$P_i = (A_i + B_i K_i)^\top P_i (A_i + B_i K_i) + K_i^\top R_i K_i + Q_i, \tag{4.10a}$$

$$K_i = -(R_i + B_i^\top P_i B_i)^{-1} B_i^\top P_i A_i, \tag{4.10b}$$

and constraining the terminal state $x_i(N_\mathrm{p}|k)$ to an invariant terminal set

$$\mathbb{X}_{f_i} \subseteq \{x \in \mathbb{R}^{n_i} \mid K_i(A_i + B_i K_i)^k x \in \mathbb{U}_i, (A_i + B_i K_i)^k x \in \mathbb{X}_i,\, k \in \mathbb{Z}_+\}, \tag{4.11}$$

where $\mathbb{X}_i$ is the set of feasible local states. If K_i is chosen to be 0, as is done in (Alessio and Bemporad, 2007), (4.10a) reduces to the Lyapunov equation. Note that if $Q_i \succ 0$, this implies that each subsystem has to be open-loop stable, i.e., that all eigenvalues of A_i must be within the unit circle. A more detailed study of decoupled stability conditions will be provided in Chapters 5 and 6.

Nonetheless, observe that condition (4.10) only implies closed-loop stability under the assumption that the subsystems are indeed decoupled. Still, it is possible to provide *a posteriori* verifiable stability conditions for the network under coupled operation, as shown in (Alessio and Bemporad, 2007). More precisely, the proposed stability test checks stability of the entire system (4.1) in closed loop with (4.9), if the matrices P_i are chosen according to (4.10a). This *a posteriori* stability test checks whether the sum of all cost functions is a Lyapunov function for the overall system, and is based on the explicit form of each MPC controller, see (Bemporad et al., 2002). Under certain conditions this reduces to a positive semi-definiteness check of a square $n \times n$ matrix. However, this test has to be carried out on a centralized level, which partly cancels out the attractive features of DMPC's decentralized structure.

The main merit of DMPC is that each local controller has to solve a relatively small and simple optimization problem, yielding low computational requirements per subsystem, while requiring no exchange of information with any of the other control units in the network. However, it is important to observe that the cost function associated with controller i solely depends on the local states $x_i(l|k)$ and inputs $u_i(l|k)$. This is a consequence of the fact that the DMPC prediction model (4.6) approximates the real system by ignoring the dynamic coupling between subsystems and uses only local state information to initialize the optimization problem. Therefore, (4.9) will generally not be optimal with respect to the centralized MPC optimization problem, i.e., Problem (4.2.1), unless $x = x_i$ and $u = u_i$, for all $i \in \mathcal{I}$. The state predictions generated by DMPC may be far from accurate, as subsystem coupling dynamics are not taken into account. DMPC is therefore expected to be outperformed by non-centralized

control schemes that employ a non-approximate model of the full network dynamics, such as the SC-DMPC and FC-MPC methods that are considered in what follows.

4.3.2 Stability-constrained distributed MPC

The SC-DMPC scheme (Camponogara et al., 2002) is a distributed predictive control method, in which each local controller exploits communication with neighboring subsystems to improve the accuracy of its local state predictions. As such, SC-DMPC is expected to outperform decentralized control schemes that neglect dynamic coupling and that do not exploit communication at all.

The prediction model employed by SC-DMPC is given by (4.1), with

$$A = \begin{bmatrix} A_{11} & \dots & A_{1N} \\ \vdots & \ddots & \vdots \\ A_{N1} & \dots & A_{MM} \end{bmatrix}, \quad B = \begin{bmatrix} B_{11} & \dots & 0 \\ \vdots & \ddots & \vdots \\ 0 & \dots & B_{MM} \end{bmatrix}, \tag{4.12}$$

where $A \in \mathbb{R}^{n\times n}$, $B \in \mathbb{R}^{n\times m}$, $A_{ij} \in \mathbb{R}^{n_i \times n_j}$, $B_{ii} \in \mathbb{R}^{n_i \times m_i}$, $x = \mathrm{col}(x_1, \dots, x_N) \in \mathbb{R}^n$, $x_i \in \mathbb{R}^{n_i}$, and $u = \mathrm{col}(u_1, \dots, u_N) \in \mathbb{R}^m$, $u_i \in \mathbb{R}^{n_i}$. B is block diagonal, such that input u_i only affects subsystem i directly (later on, we will show that this structure suits the models that are typically used in a frequency-control/power-system setting). Correspondingly, the neighbors of subsystem i are those systems for which $A_{ij} \neq 0$, $j \neq i$. In what follows, we denote the set of neighbors of system i by $\mathcal{N}_i = \{j \in \mathcal{I} | j \neq i, A_{ij} \neq 0\}$.

Let $N_\mathrm{p} \in \mathbb{Z}_{\geq 1}$ be a fixed prediction horizon. At all discrete-time instants $k \in \mathbb{Z}_+$, each SC-DMPC controller solves the following optimization problem:

Problem 4.3.2 SC-DMPC At discrete-time instant $k \in \mathbb{Z}_+$, let $x_i(k)$ and $x_j^{N_\mathrm{p}}(l|k)$ for $l \in \mathbb{Z}_{[0,N_\mathrm{p}-1]}$ and all $j \in \mathcal{N}_i$ be given. Set $x_i(0|k) := x_i(k)$ and solve

$$V^*_{i,N_\mathrm{p}}(x_i) = \min_{\mathbf{u}_i} \{ V_{i,N_\mathrm{p}}(x_i, \mathbf{u}_i) \mid \mathbf{u}_i \in \mathbb{U}_{i,N_\mathrm{p}}(x_i) \}, \tag{4.13a}$$

where

$$\begin{aligned} V_{i,N_\mathrm{p}}(x_i, \mathbf{u}_i) &= F_i(x_i(N_\mathrm{p}|k)) + \sum_{l=0}^{N_\mathrm{p}-1} \ell_i(x_i(l|k), u_i(l|k)) \\ &= x_i(N_\mathrm{p}|k)^\top P_i x_i(N_\mathrm{p}|k) \\ &\quad + \sum_{l=0}^{N_\mathrm{p}-1} x_i(l|k)^\top Q_i x_i(l|k) + u_i(l|k)^\top R_i u_i(l|k) \end{aligned} \tag{4.13b}$$

$$x_i(l+1|k) = A_{ii}x_i(l|k) + B_{ii}u_i(l|k) + \sum_{j\in\mathcal{N}_i} A_{ij}x_j^{N_\mathrm{p}}(l|k), \qquad (4.13c)$$

for $l \in \mathbb{Z}_{[0,N_\mathrm{p}-1]}$. ■

The weight matrices used in the cost function, i.e., $Q_i \succeq 0$, $R_i \succ 0$ and $P_i \succ 0$, can be chosen based on an underlying centralized problem, in a way that is analogous to the DMPC approach. The SC-DMPC controllers take the dynamic coupling among neighboring subsystems into account by including an open-loop state prediction of these subsystems, denoted by $x_j^{N_\mathrm{p}}(l|k)$, in their local model. A natural choice for $x_j^{N_\mathrm{p}}(l|k)$ would be $x_j(l|k)$, $l \in \mathbb{Z}_{[0,N_\mathrm{p}]}$. However, as the state predictions $x_j(l|k)$, $l \in \mathbb{Z}_{[0,N_\mathrm{p}]}$, are yet to be determined at instant k, the shifted predictions of the previous time instant $k-1$ are used instead:

$$x_j^{N_\mathrm{p}}(l|k) := x_j^*(l+1|k-1), \quad l \in \mathbb{Z}_{[0,N_\mathrm{p}-1]}, \qquad (4.14)$$

where $x_j^*(l+1|k-1)$ denotes the predicted state at time $k+l$, which is computed at subsystem j given the local state measurement $x_j(k-1)$ and corresponding optimal control actions $u_j^*(l|k-1)$, $l \in \mathbb{Z}_{[0,N_\mathrm{p}-1]}$.

Problem 4.3.2 minimizes the cost $V_{i,N_\mathrm{p}}(x_i, \mathbf{u}_i)$ over input sequences in the set

$$\mathbb{U}_{i,N_\mathrm{p}}(x_i) := \left\{ \mathbf{u}_i \in \mathbb{U}_i^{N_\mathrm{p}} \;\middle|\; \|x_i(1|k)\|_2^2 \le \hat{l}_i \right\}, \qquad (4.15)$$

where

$$\hat{l}_i := \max\left\{ \|x_i(1|k-1)\|_2^2, \|x_i(0|k)\|_2^2 \right\} - \beta_i \|x_i^1(0)\|_2^2, \qquad (4.16)$$

with tuning parameter $\beta_i \in \mathbb{R}_{(0,1)}$, and

$$x_i(1|k-1) := A_{ii}x_i(0|k-1) + B_{ii}u_i^*(0|k-1) + \sum_{j\in\mathcal{N}_i} A_{ij}x_j^{N_\mathrm{p}}(0|k). \qquad (4.17)$$

Here, $x_i^1(0)$ is related to $x(k)$ via a similarity transform that is based on the controllable companion form (Camponogara et al., 2002). In (Camponogara et al., 2002), it is shown that any $\mathbf{u}_{i,[N_\mathrm{p}-1]} \in \mathbb{U}_{i,N_\mathrm{p}}(x_i)$ induces state convergence for the local, *decoupled* system $x_i(k+1) = A_{ii}x_i(k) + B_{ii}u_i(k)$, $k \in \mathbb{Z}_+$, as a result of the contractive state constraint used in the definition of $\mathbb{U}_{i,N_\mathrm{p}}(x_i)$.

The ensemble of the optimal local control actions $u_i^*(0|k)$ of all N controllers, i.e.,

$$u(k) = \mathrm{col}(u_1^*(0|k), \ldots, u_i^*(0|k), \ldots, u_N^*(0|k)), \qquad (4.18)$$

is applied as input to the full system (4.1). Subsequently, all neighboring controllers exchange the shifted state prediction sequences, after which the whole procedure is repeated at the next time instant.

Except for the horizon-1 local-state contraction constraint in (4.15), the SC-DMPC scheme does not take state constraints into account. In (Camponogara et al., 2002), it is proven that the controllable-companion-form based construction of $\mathbb{U}_{i,N_p}(x_i)$ ensures the existence of control actions that satisfy (4.15). In addition, it is shown that (4.18) comprises a feasible solution for the overall system. This is the case even though SC-DMPC's state predictions are inexact due to the delayed and possibly inaccurate information on $x_j(l|k)$, $j \in \mathcal{N}_i$.

As observed above, the contraction constraint guarantees stability if the subsystems are decoupled, since it enforces strict decrease of the 2-norm of subsequent one-step-ahead subsystem state predictions. However, to conclude stability of the *overall* system, additional conditions on stability of a suitably defined full-state matrix A in a controllable companion form are required. More details on feasibility and stability of the SC-DMPC scheme can be found in (Camponogara et al., 2002).

SC-DMPC relies on a communication network to exchange information between neighboring controllers. Certain large-scale systems, such as power networks, consist of subsystems that are only loosely coupled, such that the number of neighbors per subsystem is small and the extent of communication is limited. Because SC-DMPC controllers communicate with direct neighbors only, the graph of the required communication network coincides with the graph that describes the dynamical subsystem interconnections. When considering control of electrical power networks, this implies that control areas that are not directly physically coupled do not require a communication link. Because transmission lines are typically equipped with a parallel communication link, the implementation of SC-DMPC may be more realistic than the application of control methods that require global communication/coordination, and thus, the construction of a network-wide dedicated communication infrastructure. Still, SC-DMPC does not include physical constraints that span multiple subsystems and cannot guarantee stability for the interconnected system dynamics, which is a considerable drawback when considering application in practice.

4.3.3 Feasible cooperation-based MPC

The DMPC and SC-DMPC controllers described in the previous sections solve locally different optimization problems. Such competitive strategies converge to *Nash equilibria* at best. A Nash equilibrium does not necessarily coincide with the global (*Pareto*) optimum attained by a centralized control scheme, i.e., Problem 4.2.1. Moreover, there are examples where these Nash equilibria are unstable, which means that competitive optimization algorithms may be divergent (Camponogara, 2000). The feasible cooperation-based MPC (FC-MPC) method

(Venkat, 2006; Venkat et al., 2008) on the other hand, cooperatively solves a single, *global* optimization problem, thus ensuring that the resulting equilibrium is stable and Pareto optimal. This is a key advantage of FC-MPC when comparing this method with DMPC and SC-DMPC, although this improvement in terms of performance comes at the cost of more extensive communication requirements.

Let the system to be controlled be of the form given in (4.1). In FC-MPC, a controller is assigned to each subsystem $i \in \mathcal{I}$. Because these controllers are only able to optimize the global cost over their own local manipulated variables (i.e. local control inputs), the globally optimal solution needs to be attained via an iterative optimization and communication procedure. A convenient choice for a global objective that measures the system-wide impact of local control actions is a strict convex combination of local cost functions, i.e.,

$$V^p_{N_\mathrm{p}}(\cdot) = \sum_{i\in\mathcal{I}} w_i V_{i,N_\mathrm{p}}(\cdot), \quad w_i \in \mathbb{R}_{>0}, \quad \sum_{i\in\mathcal{I}} w_i = 1. \tag{4.19}$$

Given a fixed prediction horizon $N_\mathrm{p} \in \mathbb{Z}_{\geq 1}$, the open-loop FC-MPC optimization problem of controller $i \in \mathcal{I}$ is defined as follows.

Problem 4.3.3 FC-MPC At time $k \in \mathbb{Z}_+$ and iteration $p \in \mathbb{Z}_{\geq 1}$, let $\mathbf{u}_j^{p-1}$ for $j \in \mathcal{J}_i := \mathcal{I} \setminus \{i\}$ be given, set $x^p(0|k) := x(k)$ and solve

$$V^{p*}_{i,N_\mathrm{p}}(x, \{\mathbf{u}_j^{p-1}\}_{j\in\mathcal{J}_i}) = \min_{\mathbf{u}_i} \left\{ V^p_{N_\mathrm{p}}(x, \{\mathbf{u}_j^{p-1}\}_{j\in\mathcal{J}_i}, \mathbf{u}_i) \;\middle|\; \mathbf{u}_i \in \mathbb{U}_{i,N_\mathrm{p}}(x) \right\}, \tag{4.20a}$$

where

$$\begin{aligned} &V^p_{N_\mathrm{p}}(x, \{\mathbf{u}_j^{p-1}\}_{j\in\mathcal{J}_i}, \mathbf{u}_i) \\ &\qquad = F(x^p(N_\mathrm{p}|k)) + \sum_{l=0}^{N_\mathrm{p}-1} \ell(x^p(l|k), u_i^p(l|k)) \\ &\qquad = x^p(N_\mathrm{p}|k)^\top P x^p(N_\mathrm{p}|k) \\ &\qquad\quad + \sum_{l=0}^{N_\mathrm{p}-1} x^p(l|k)^\top Q x^p(l|k) + u_i^p(l|k)^\top R_i u_i^p(l|k), \end{aligned} \tag{4.20b}$$

$$x^p(l+1|k) = Ax^p(l|k) + B\,\mathrm{col}(u_1^p(l|k), \ldots, u_i^p(l|k), \ldots, u_N^p(l|k)), \tag{4.20c}$$

for $l \in \mathbb{Z}_{[0,N_\mathrm{p}-1]}$. ■

The FC-MPC controller of subsystem i minimizes the global cost function $V^p_{N_\mathrm{p}}(\cdot)$ over the polytopic set of feasible local input sequences $\mathbf{u}_i \in \mathbb{U}_{i,N_\mathrm{p}}(x)$, which is defined as

$$\mathbb{U}_{i,N_\mathrm{p}}(x) := \{\mathbf{u}_i \in \mathbb{U}_i^{N_\mathrm{p}}\}. \tag{4.21}$$

The terminal penalty matrix P used in (4.20b) is the solution of the unconstrained infinite horizon LQR problem, i.e.,

$$P = (A+BK)^\top P(A+BK) + K^\top RK + Q, \tag{4.22a}$$

$$K = -(R+B^\top PB)^{-1}B^\top PA. \tag{4.22b}$$

Note that in (Venkat et al., 2008), attention is restricted to open-loop stable systems, such that K is chosen equal to zero, yielding the stability condition $P = A^\top PA + Q$.

Given the parameters $\varepsilon \in \mathbb{R}_{>0}$, $w_i \in \mathbb{R}_{(0,1)}$, $i \in \mathcal{I} := \mathbb{Z}_{[1,N]}$, and $p_{\max} \in \mathbb{Z}_+$, at each discrete time instant $k \in \mathbb{Z}_+$, the optimal control action is calculated in each controller via the following iterative procedure:

Algorithm 2 FC-MPC

1: Initialize the iteration counter $p := 1$.
2: Measure $x_i(k)$ and exchange this information with all other controllers.
3: Set $u_i^0(l|k) := u_i^{\bar{p}*}(l+1|k-1)$ for $l \in \mathbb{Z}_{[0,N_\mathrm{p}-1]}$ and $i \in \mathcal{I}$.
4: **while** $\rho_i > \varepsilon$ and $p \le p_{\max}$ **do**
5: Solve Problem 4.3.3 and let $\mathbf{u}_i^{p,*}(k)$ be the local optimizer.
6: Set $\mathbf{u}_i^{p,*}(k) := w_i\mathbf{u}_i^{p,*}(k) + (1-w_i)\mathbf{u}_i^{p-1,*}(k)$.
7: Set $\rho_i := \left\|\mathbf{u}_i^{p,*}(k) - \mathbf{u}_i^{p-1,*}(k)\right\|$.
8: Exchange the local input sequence $\mathbf{u}_i^{p,*}(k)$ with all other controllers.
9: Increase the iteration counter: $p := p+1$.
10: **end while**
11: Set $\bar{p}(k) := p$.

Whenever the stop criterion is satisfied in all nodes for some $p = \bar{p} \le p_{\max}$, the first element of the calculated control sequence is applied to the subsystem, i.e.,

$$u(k) = \mathrm{col}(u_1^{\bar{p}}(0|k), \ldots, u_i^{\bar{p}}(0|k), \ldots, u_N^{\bar{p}}(0|k)). \tag{4.23}$$

Then, the procedure is repeated at the next time instant $k+1$.

The FC-MPC algorithm starts by initializing the current state and the global input trajectory, using the shifted optimal input sequence of the previous time instant $k-1$ as an initial guess (statements 2–3). Based on this information, each controller computes a new sequence of local optimal control actions (statement 5). A weighted average of the current optimizer and the input computed

at the previous iteration $p-1$ is used as the next estimate of the control input (statement 6). This ensures convergence of the iterates (Venkat, 2006).

FC-MPC takes only local input constraints, thus no state constraints, into account. This guarantees the existence of a feasible control action sequence for Problem 4.3.3. It is possible to prove convergence of the iterative procedure, and to prove that FC-MPC control is globally stabilizing. In fact, only a single iteration of the algorithm is required to guarantee closed-loop stability (Venkat, 2006).

Both centralized MPC and FC-MPC employ full state information to guarantee optimal performance in terms of a single cost function, which requires extensive system-wide communication. However, note that in the FC-MPC scheme this information has to be communicated to a possibly large number of local control units, whereas in the case of centralized MPC this information is required at one location only. When considering frequency control, in both cases the communication distances can be very large, due to the large geographical scale that power systems typically have. Moreover, centralized MPC, SC-DMPC and DMPC with overlapping subsystems utilize the communication network only once per discrete-time instant, whereas the FC-MPC scheme requires exchange of information *each iteration*. However, it is proven in (Venkat et al., 2008) that the FC-MPC algorithm can be terminated prior to convergence, without compromising feasibility or closed-loop stability. We can therefore conclude that the iterative nature of the FC-MPC scheme is not necessarily a drawback compared to other, non-iterative communication-based methods.

4.4 Benchmark test

The frequency control problem in electrical power networks provides a suitable benchmark test for assessing and comparing the non-centralized MPC schemes described previously. Before presenting the simulation results, we describe the test setup in the next subsection.

4.4.1 Test network and simulation scenario

All simulations were performed on the power network setup given in (Venkat et al., 2008). A schematic representation of this test system is depicted in Figure 4.2. The system consists of $N = 4$ control areas, whose linearized dynamics are given by the following standard model (Kundur, 1994):

$$\frac{\mathrm{d}\Delta\omega_i}{\mathrm{d}t} = \frac{1}{J_i}(\Delta P_{M_i} - D_i\Delta\omega_i - \sum_{j\in\mathcal{N}_i}\Delta P_{\text{tie}}^{ij} - \Delta P_{L_i}), \tag{4.24a}$$

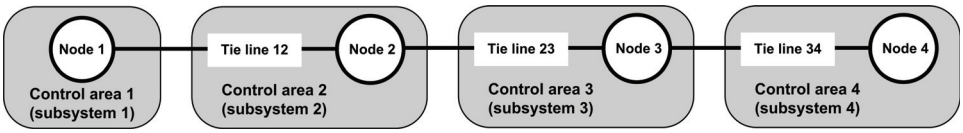

Figure 4.2: Schematic representation of a 4-control-area power network.

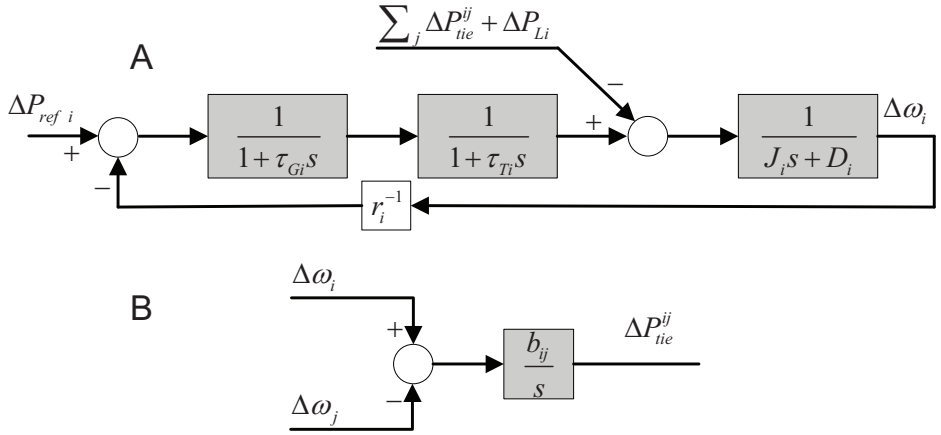

Figure 4.3: Block diagram of a generator (A) and a power transmission line (B).

$$\frac{\mathrm{d}\Delta P_{M_i}}{\mathrm{d}t} = \frac{1}{\tau_{T_i}}(\Delta P_{V_i} - \Delta P_{M_i}), \tag{4.24b}$$

$$\frac{\mathrm{d}\Delta P_{V_i}}{\mathrm{d}t} = \frac{1}{\tau_{G_i}}(\Delta P_{\mathrm{ref}_i} - \Delta P_{V_i} - \frac{1}{r_i}\Delta\omega_i), \tag{4.24c}$$

$$\frac{\mathrm{d}\Delta P_{\mathrm{tie}}^{ij}}{\mathrm{d}t} = b_{ij}(\Delta\omega_i - \Delta\omega_j), \tag{4.24d}$$

$$\Delta P_{\mathrm{tie}}^{ji} = -\Delta P_{\mathrm{tie}}^{ij}. \tag{4.24e}$$

Here, (4.24a)–(4.24c) describe the dynamics of a steam turbine generator (or the lumped equivalent of multiple generators in a control area). The power flow through a transmission line connecting two generators/control areas is modeled by (4.24d)–(4.24e). The corresponding block diagrams are shown in Figure 4.3. The control input to subsystem $i \in \mathbb{Z}_{[1,4]}$ is the signal $\Delta P_{\mathrm{ref}_i}$, which represents the change in the reference value for the power production in that area. The exogenous disturbance input ΔP_{L_i} represents the aggregated change of the power demand in control area i.

In the benchmark test, we compared the performance of MPC, DMPC, SC-

DMPC and FC-MPC with the results attained by a conventional AGC control law. The classical AGC method consists of local, i.e., area-specific, integral feedback controllers that drive the frequency and the transmission-line power flow deviations $\Delta\omega_i$ and $\Delta P_{\text{tie}}^{ij}$ to zero. The AGC feedback control law for area i is described by

$$\frac{\mathrm{d}\Delta P_{\text{ref}_i}}{\mathrm{d}t} = -K_i\Big(B_i\Delta\omega_i + \sum_{j\in\mathcal{N}_i}\Delta P_{\text{tie}}^{ij}\Big), \tag{4.25}$$

with tuning parameters K_i and B_i. Note that, in essence, similar to DMPC, SC-DMPC and FC-MPC, the European automatic generation control scheme is implemented in a non-centralized fashion as well. Each control area is governed by its own, local AGC law, that feeds back local frequency measurements and the aggregated cross-border power exchange, whereas the ultimate goal of AGC is to stabilize the European network as a whole. The interested reader is referred to (Kundur, 1994; Jaleeli et al., 1992) for a more detailed discussion on classical AGC.

The simulation scenario used to assess the closed-loop performance of the described control methods was the following. For time instants $k \in \mathbb{Z}_{[0,9]}$, the network was in steady-state with frequency and transmission-line flow deviations equal to zero, and $\Delta P_{L_i} = 0$ for $i \in \mathbb{Z}_{[1,4]}$. A step disturbance $\Delta P_{L_2} = 0.25$ was applied to control area 2 for $k \in \mathbb{Z}_{\geq 10}$, while simultaneously applying a step disturbance $\Delta P_{L_3} = -0.25$ to area 3.

For all control techniques, we used identical model and simulation parameter values, which are listed in Appendix B. All predictive optimization problems were formulated as quadratic programs of the form

$$\min_{v} \quad v^\top H v + f^\top v, \tag{4.26a}$$

$$\text{subject to} \quad A_{\text{ineq}} v \leq B_{\text{ineq}}, \tag{4.26b}$$

with $v \in \mathbb{R}^{n_v}$, positive definite $H \in \mathbb{R}^{n_v \times n_v}$, $f \in \mathbb{R}^{n_v}$, $A_{\text{ineq}} \in \mathbb{R}^{n_c \times n_v}$ and $B_{\text{ineq}} \in \mathbb{R}^{n_c}$. All QPs were evaluated using Matlab's `quadprog` solver. Note that we employed the 1-norm in (4.15) to allow for a linear formulation of this contraction constraint, and thus, to enable a QP-based implementation of SC-DMPC. The number of FC-MPC iterations was fixed to 2. In all non-centralized schemes, the global prediction model was partitioned according to the underlying division into control areas, which is a natural choice to obtain a low extent of coupling between the local models.

Finally, note that so far, we have assumed that the prediction models for the various methods do not explicitly account for exogenous disturbances, e.g., aggregated load changes ΔP_{L_i}. However, in the simulations, we used local state

perturbed models of the form

$$x(l+1|k) = Ax(l|k) + Bu(l|k) + \bar{d}_0, \quad l \in \mathbb{Z}_{[0,N_p]}, \tag{4.27}$$

where $\bar{d}_0 := \bar{d}(k) \in \mathbb{R}$ is an estimate of a constant additive disturbance, e.g., the aggregated load ΔP_{L_i}, given the measured and predicted state for discrete-time instant k. The inclusion of this disturbance model makes the state predictions more accurate, as constant load disturbances can be compensated for, whereas the stability and feasibility properties of the non-centralized algorithms discussed in Section 4.3 are preserved. The interested reader is referred to (Muske and Badgwell, 2002; Pannocchia and Rawlings, 2003) for further details on disturbance estimation and zero-offset tracking in MPC.

4.4.2 Simulation results

Figures 4.4–4.5 depict the closed-loop trajectories generated by centralized MPC and AGC, and the results obtained by the non-centralized DMPC, SC-DMPC and FC-MPC schemes, respectively. Both figures show the trajectories of network frequency deviation $\Delta\omega_2$ and transmission-line power flow deviation $\Delta P_{\text{tie}}^{23}$, together with the control inputs applied to control areas 2 and 3, i.e., ΔP_{ref_2} and ΔP_{ref_3}, respectively.

Table 4.1 lists the settling times of the penalized states,[2] i.e., the states for which the corresponding elements in Q_i are nonzero (see Appendix B), and the global performance cost over 200 samples, namely the value of

$$\sum_{k=0}^{200} x(k)^\top Q x(k) + u(k)^\top R u(k).$$

The results show that in this particular scenario, the centralized MPC scheme outperforms all the other simulated control methods. By contrast, the classical AGC method is characterized by the worst performance in terms of cost, settling time and overshoot; all the assessed non-centralized MPC schemes perform better than AGC. Moreover, the performance of the non-centralized control techniques appears to be directly correlated with the extent of inter-subsystem communication. The observed difference in the DMPC and SC-DMPC performance costs is relatively small, however, which is surprising given their significantly different communication requirements. Finally, note that FC-MPC performance is almost identical to that of centralized MPC, even though the number of FC-MPC iterations was fixed to only 2.

[2] With "settling time", we mean the time required for a transient to settle within an error band of $\pm 5.10^{-4}$ around the steady-state value (e.g., 0 rad/s). As all trajectories were generated by the same disturbance, it is not problematic that this measure relies on an absolute (rather than a usually employed relative) error band.

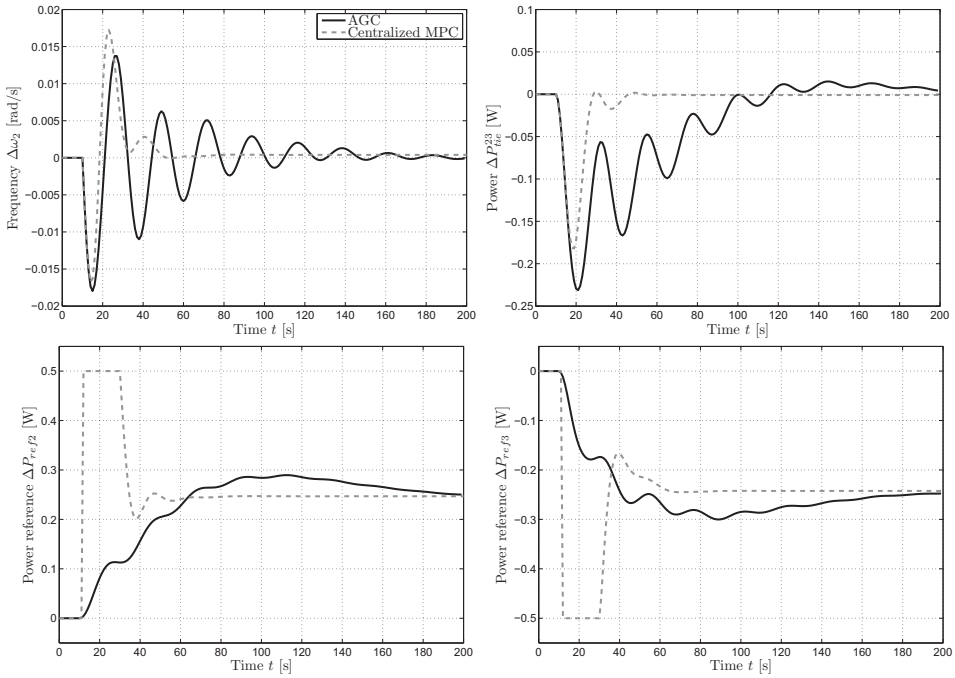

Figure 4.4: Simulation results for centralized MPC and classical AGC.

The computational complexity of each predictive control scheme can be expressed in terms of the dimensions of the corresponding local optimization problems. The computational burden for the control hardware depends on the number of manipulated variables n_v and the number of inequality constraints n_c. These values are listed in Table 4.2, for the considered simulation and for the general case (with prediction horizon N_p, number of local control inputs m_i and number of local states n_i). Table 4.2 shows that the complexity of the local DMPC, SC-DMPC and FC-MPC controllers is *independent of the number of subsystems present in the network*, whereas this is not the case for the centralized MPC controller, where the optimization problem scales quadratically with the total number of system inputs $\sum_i m_i$. This is a key motivation for research in the field of non-centralized predictive power network control, as scalability is an important aspect in light of the large and expanding character of today's power system.

Computational complexity can also be assessed by measuring the worst-case time that is required for computing the optimal input sequence of controller i. These values, obtained for a simulation on a 3.48 GB RAM, 2.66 GHz

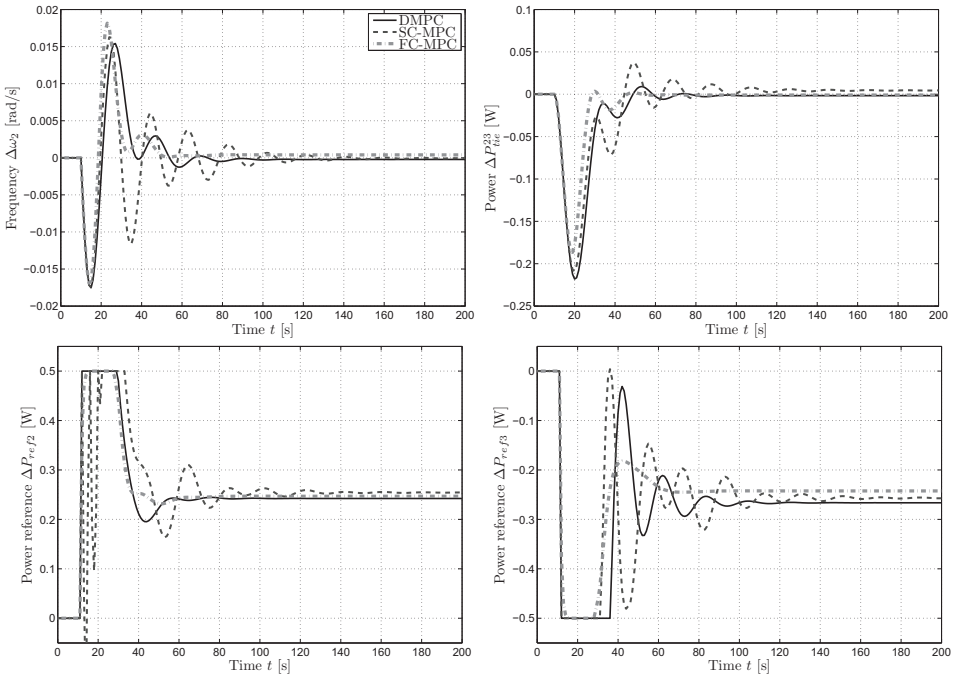

Figure 4.5: Simulation results for DMPC, SC-DMPC and FC-MPC.

Pentium-E PC, are shown in Figure 4.6. The computational burden is particularly high immediately after the change in load (occurring at time instant $k = 10$), when corrective action is needed to prevent violation of state and input constraints.

The above results clearly indicate that DMPC and SC-DMPC are attractive from a computational point of view, because these techniques require significantly less computational effort than centralized MPC. The computational burdens of DMPC and SC-DMPC are comparable, as their optimization problems are almost equally sized, except for the additional contraction constraints in SC-DMPC. The FC-MPC algorithm requires about twice as much computational time than SC-DMPC and DMPC if the maximum number of iterations is set to 2, because the local QPs that FC-MPC solves per iteration have dimensions that are comparable with those of the SC-DMPC and DMPC optimization problems. Thus, although in this simulation, the FC-MPC controller needs less computational effort than centralized MPC to compute a control action, from a complexity point of view, FC-MPC is only advantageous as long as the number of iterations per sampling instant is small.

Table 4.1: Performance characteristics

Method	Settling time (s)							Cost
	ω_1	ω_2	ω_3	ω_4	P_{tie}^{12}	P_{tie}^{23}	P_{tie}^{34}	
PC (open sec. loop)	130	131	129	140	167	214	170	2573.30
AGC	164	165	175	175	235	353	187	530.62
MPC	58	48	45	43	56	55	66	176.59
FC-MPC (2 iterations)	50	48	45	44	56	55	65	182.44
DMPC	64	63	65	72	72	98	79	270.73
SC-DMPC	88	114	105	105	138	158	50	260.13

Table 4.2: Dimensions of the local quadratic programs

Technique	Size of A ($n_v \times n_c$)	
	Example	General case
Centralized MPC	400×200	$2N_{\text{p}} \sum_i m_i \times N_{\text{p}} \sum_i m_i$
FC-MPC	100×50	$2N_{\text{p}} m_i \times N_{\text{p}} m_i$
SC-DMPC	108×50	$2(N_{\text{p}} m_i + n_i) \times N_{\text{p}} m_i$
DMPC	100×50	$2N_{\text{p}} m_i \times N_{\text{p}} m_i$

A summary of the results provided in this section is given in Figure 4.7, which indicates that performance is positively correlated with the extent of communication and the complexity of the prediction models/optimization problems that underlie the control scheme.

4.4.3 Assessment

The results obtained in Section 4.3 and Subsection 4.4.2 indicate two important aspects that determine the performance of a non-centralized MPC technique:

Prediction accuracy
A model that ignores the dynamic coupling between subsystems introduces a prediction error, i.e., a mismatch between the predicted (local) state trajectories and the state trajectories that would result from applying the ensemble of local control actions to the full network of interconnected systems. MPC controllers

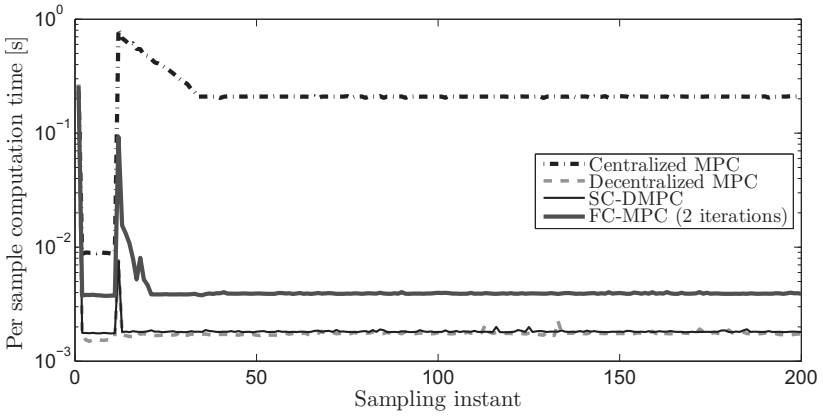

Figure 4.6: Computation time of all the assessed control algorithms.

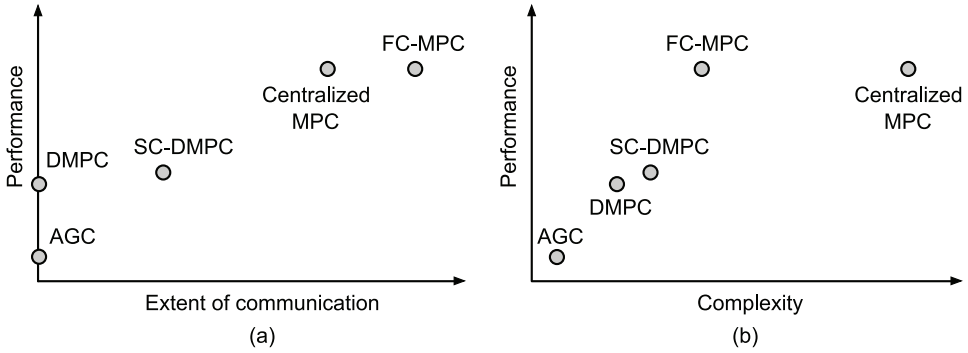

Figure 4.7: a) Qualitative comparison of performance and communication requirements; b) Qualitative comparison of performance and complexity.

can exchange their local state predictions to use them as a measure for the dynamic coupling, and exploit this for increasing prediction accuracy. Accurate predictions are important, as solving a control problem that is based on inexact predictions results in non-optimal closed-loop performance. Precise predictions are required also for state constraint handling, as a constrained optimal control action associated with inaccurate local predictions can be non-feasible for the actual coupled system.

Optimization strategy

The performance of a non-centralized control scheme depends on more than prediction accuracy alone. Schemes that rely on local control laws that seek

to non-cooperatively minimize their own objective functions, will induce Nash optimal performance at best, even if their prediction models are exact. Such a competitive equilibrium is in general not equal to the Pareto optimal solution, i.e., the solution of the centralized MPC problem.

A need for accurate predictions and globally optimal performance inevitably leads to the requirement of a full prediction model that exploits global state information. However, the large scale of real-life power networks prohibits a non-centralized implementation of MPC that requires fast and reliable communication with a large number of subsystems in the network. *It is therefore questionable whether Pareto-optimal non-centralized (predictive) control is a feasible goal in today's electrical power networks.* Future advances in communication technology and increasing processing power could bring this goal closer to realization, however. Communication with a small number of neighboring subsystems or control areas is currently more realistic and relatively easy to implement, as transmission lines are usually equipped with communication links.

Moreover, although a completely decentralized MPC implementation is usually outperformed by distributed methods, it may still perform better than conventional AGC. Hence, there is room for a tradeoff: one can use decentralized MPC if the corresponding performance is acceptable, and in this way avoid communication between neighboring control areas, or use distributed MPC with limited communication to improve performance by attaining higher prediction accuracy.

Even if optimal performance is not a major concern in power networks, control schemes for supply-demand matching should always be able to ensure stable and reliable operation of the grid. Of the non-centralized MPC methods considered in this chapter, only FC-MPC is able to provide a solid closed-loop stability guarantee, although this requires system-wide communication and centralized, and thus, impractical, synthesis of the terminal state penalty P, see (4.22). Due to the liberalization of the electrical energy market, efficient use of resources is becoming increasingly important and the system tends to be pushed towards its physical constraints and stability boundaries. In this respect, the non-centralized algorithms considered in this chapter all have the same flaw: they lack the ability of taking coupled state constraints into account, whereas ultimately, constraint handling for preventing inter-area transmission-line outages is one of the key reasons for considering MPC. Coupled constraints can only be satisfied if the prediction of all the constrained states coincides with

the predicted state trajectory of the centralized MPC scheme.[3] Consequently, network-wide communication among the subsystems to obtain accurate state predictions is crucial for constraint handling. Note, however, that this does not necessarily require the use of a global communication network, as state information can also be distributed via *iterative communication* among *neighboring subsystems only*. Promising directions for state-constraint satisfaction under non-centralized predictive control are considered in, e.g., (Doan et al., 2011a,b), where methods are studied for improving convergence of distributed, iterative optimization schemes.

Other important issues that electrical power system operators face when considering non-centralized predictive control algorithms for frequency control include the following:

- Electrical power networks are characterized by significant nonlinear and hybrid (i.e., both discrete and continuous) dynamics. The model (4.1) used to describe the network dynamics in this chapter can usually be obtained by linearizing a nonlinear first-principle model around some operating point. The accuracy of such a linearized model is only acceptable for relatively small power and frequency deviations, and these models are not able to capture the saturation or switching effects that are associated with larger disturbances. Moreover, with the ongoing liberalization of the electricity market, power generation control tends to become price-based (Jokić, 2007), which tends to introduce additional hybrid dynamics. These observations suggest a need for advanced, nonlinear models, which complicates the application of control algorithms in general.

- Due to their dependency on intensive communication, distributed control methods need to be robust against the typical disturbances that are associated with the exchange of information over large networks, such as varying time delays and packet loss. Stability must be guaranteed even in the presence of delayed or interrupted communications. A lot of effort is put in mastering networked control systems, which are characterized by delays and information loss in the feedback loop, see, for example, (Gielen et al., 2012).

- Market actors are unwilling to share non-public, market-sensitive information with their rivals, as this may provide them with a competitive advantage. Control algorithms for frequency control should therefore not

[3] If this is not the case, feasibility for interconnected systems can be guaranteed by tightening the coupling constraints using certain safety margins, see, e.g., (Jia and Krogh, 2002). However, such approaches tend to be conservative, such that their applicability is limited.

disclose such information, neither during synthesis nor during evaluation of the control law. This hampers, for example, the application of DMPC with overlapping subsystem models, as this would require competitors to share details on their generator equipment.

4.5 Conclusions

Model predictive control is a promising technique for real-time control of future electrical power networks that are characterized by highly fluctuating power flows, tight constraint margins and a strong demand for efficient, profitable operation. Since power networks are too large for centralized control to be feasible, in this chapter we assessed a number of non-centralized MPC schemes that differ in terms of decentralization, communication requirements and computational complexity. Now, the following conclusions can be drawn.

The large scale of electrical power systems hampers the application of non-centralized MPC schemes that require extensive communication among a large number of subsystems. As a result, Pareto optimal performing non-centralized MPC may not be a feasible goal for power networks. Alternative methods that rely on short-distance communication among neighboring subsystems only are more realistic, however.

A completely decentralized implementation of MPC can outperform conventional automatic generation control, whereas it offers a lower complexity and a higher extent of decentralization than the alternative non-centralized predictive control methods. Decentralized MPC is appropriate when acceptable performance can be achieved without knowledge of the state of neighboring subsystems, which is typically the case when the physical coupling between subsystems is weak. Distributed MPC can be employed to increase prediction accuracy, and thus, to improve closed-loop performance, in networks with strong system interactions, but only if the corresponding extent of communication is feasible in practice.

An important problem that is not yet solved by practical state-of-the-art non-centralized MPC schemes originates from coupled state constraints. It is challenging to enforce such constraints based on incomplete, local state measurements and thus, inaccurate predictions. This issue is of paramount significance to power systems, where coupled state constraints, such as bounds on transmission-line power flows, are inherent and of growing importance.

However, perhaps the most important issue associated with non-iterative, non-centralized MPC is that so far, there are no tractable and non-conservative ways to guarantee closed-loop stability based on local model and state infor-

mation only, even if other control objectives such as constraint handling and performance optimization are considered to be irrelevant. The design of scalable methods for a-priori guaranteeing closed-loop stability will be the topic of Chapters 5 and 6.

5

Distributed Lyapunov-based MPC

5.1 Introduction

The basic requirement of any control system is that the corresponding closed-loop dynamics are stable. In standard model predictive control schemes, this is typically guaranteed via monotonic convergence of the subsequent optimal performance cost values, see, e.g., Chapter 4 and (Mayne et al., 2000). Hence, in these cost-based approaches, attaining *globally (i.e., Pareto) optimal performance* is a key prerequisite for stability. Unfortunately, when non-centralized MPC for large-scale networks of interconnected dynamical systems (NDS) is the main focus, the demand for optimization of a system-wide performance cost function inherently comes with a need for intensive iterative exchange of information or global coordination among the agents that control the various subsystems in the network. Such coordination may be hampered by limitations of the communication infrastructure that is available in practice, or may be undesired in competitive environments such as the deregulated electrical power market (Chapter 4).

A promising alternative to cost-based stabilization is *Lyapunov-based MPC (L-MPC)*, see, e.g., (Bemporad, 1998; Mhaskar et al., 2006). L-MPC makes use of

an explicit control Lyapunov function (CLF) to characterize the set of stabilizing control actions, and therefore decouples the need for globally optimal performance from the desire for closed-loop stability. Although L-MPC has already been successfully applied to networked control systems in, for example, (Liu et al., 2009a,b), therein the focus is more on communication network effects such as time delays and packet dropouts, rather than on non-centralized stabilization of large-scale systems. However, as the dimensions and complexity of networked dynamical systems generally impede the application of centralized control laws, the search for non-centralized formulations of CLF-based stability conditions has become a major concern.

In this chapter we propose a non-centralized Lyapunov-based model predictive control scheme for discrete-time nonlinear NDS that are subject to coupled local dynamics and separable constraints. The key ingredient of the proposed approach is a set of *structured CLFs* with a particular type of convergence conditions. While these conditions do not impose that each of the structured functions should decrease monotonously, as typically required for a CLF (Artstein, 1983; Sontag, 1983), they provide a standard CLF for the overall network. Still, the conservatism associated with a demand for monotonous convergence of the overall CLF might be restrictive in practice. Therefore, we provide a solution for relaxing the temporal monotonicity of the global CLF based on an adaptation of the Lyapunov-Razumikhin technique (Hale, 1977; Liu and Marquez, 2008), which was originally developed for systems with time delays. The proposed L-MPC scheme needs no global coordination and can be implemented in an *almost decentralized fashion*. By this we mean that the controller requires only one round of information exchange between direct neighbors per sampling instant. This is in contrast to many of the existing non-centralized control schemes, which either require iterative computations or global information, see e.g., (Camponogara et al., 2002; Venkat et al., 2008), or, employ (possibly restrictive) contractive constraints or small gain conditions, see e.g., (Magni and Scattolini, 2006; Raimondo et al., 2009; Dashkovskiy et al., 2010), to guarantee closed-loop stability.

For systems that are affine in the control input, we show that by employing infinity-norm based structured CLFs, the proposed L-MPC setup can be implemented by solving a single linear problem per sampling instant and node. The effectiveness and computational complexity of the proposed scheme is assessed on a non-trivial nonlinear example.

The remainder of this chapter is organized as follows. We start, in Section 5.2, with a brief overview of the stability notions that are instrumental for defining our control problem. In Section 5.3, we define the class of systems and the control problem considered in this and the following chapter. The L-MPC

framework is described and analyzed in Section 5.4, and simulation results are provided in Section 5.5. We finish with conclusions in Section 5.6.

5.2 Preliminary stability notions

Consider the discrete-time, time-invariant nonlinear system described by the difference inclusion

$$x(k+1) \in \Phi(x(k)), \qquad k \in \mathbb{Z}_+, \tag{5.1}$$

where $x(k) \in \mathbb{X} \subseteq \mathbb{R}^n$ with $0_n \in \text{int}(\mathbb{X})$ is the state at the discrete-time instant $k \in \mathbb{Z}_+$. The set-valued mapping $\Phi : \mathbb{R}^n \rightrightarrows \mathbb{R}^n$ is such that $\Phi(x)$ is compact and nonempty for all $x \in \mathbb{X}$. We assume that the origin is an equilibrium of (5.1), i.e., $\Phi(0_n) = \{0_n\}$.

Now consider the following notions (Lyapunov, 1907; Kundur et al., 2004).

Definition 5.2.1 The set $\mathbb{X} \subseteq \mathbb{R}^n$ is *positively invariant (PI)* for system (5.1) if for all $x \in \mathbb{X}$ it holds that $\Phi(x) \subseteq \mathbb{X}$. ■

Definition 5.2.2 System (5.1) is *Lyapunov stable* if for all $\varepsilon \in \mathbb{R}_+$ there is a $\delta(\varepsilon) \in \mathbb{R}_+$ such that the corresponding trajectories of (5.1) satisfy

$$\|x(0)\| \leq \delta(\varepsilon) \quad \Rightarrow \quad \|x(k)\| \leq \varepsilon$$

for all $k \in \mathbb{Z}_+$. ■

Definition 5.2.3 The origin 0_n is *attractive in* $\mathbb{X}$ if for any $x(0) \in \mathbb{X}$ it holds that the trajectories generated by (5.1) satisfy $\lim_{k\to\infty} \|x(k)\| = 0$. ■

Definition 5.2.4 System (5.1) is *asymptotically stable in* $\mathbb{X}$ (denoted by AS($\mathbb{X}$)) if it is Lyapunov stable and attractive in $\mathbb{X}$; then there is a $\mathcal{KL}$-function $\beta(\cdot,\cdot)$ such that the trajectories of (5.1) satisfy $\|x(k)\| \leq \beta(\|x(0)\|, k)$ for all $k \in \mathbb{Z}_+$ and $x(0) \in \mathbb{X}$. ■

Definition 5.2.5 System (5.1) is *exponentially stable in* $\mathbb{X}$ (denoted by ES($\mathbb{X}$)) if it is AS($\mathbb{X}$) with $\beta(s,k) := cs\mu^k$, for some $c \in \mathbb{R}_{\geq 1}$ and $\mu \in \mathbb{R}_{[0,1)}$. ■

The above provided notions of attractivity and asymptotical/exponential stability are defined with respect to a subset $\mathbb{X}$ of the state space. In case attractivity holds for the full state space, i.e., for $\mathbb{X} = \mathbb{R}^n$, system (5.1) is said to be *globally attractive*. Similarly, system (5.1) is *globally asymptotically stable (GAS)* and *globally exponentially stable (GES)* if it is AS($\mathbb{R}^n$) and ES($\mathbb{R}^n$), respectively.

Theorem 5.2.6 *Let $\mathbb{X}$ be a PI set for system* (5.1)*. Furthermore, let $\alpha_1, \alpha_2 \in \mathcal{K}_\infty$, $\rho \in \mathbb{R}_{[0,1)}$ and let $V : \mathbb{R}^n \to \mathbb{R}_+$ be a function such that*

$$\alpha_1(\|x\|) \leq V(x) \leq \alpha_2(\|x\|) \tag{5.2a}$$

$$V(x^+) \leq \rho V(x) \tag{5.2b}$$

for all $x \in \mathbb{X}$ and all $x^+ \in \Phi(x)$. Then system (5.1) *is AS($\mathbb{X}$).*

A function V that satisfies the conditions of Theorem 5.2.6 is called a *Lyapunov function (LF)*. The proof of Theorem 5.2.6 can be obtained from (Kellett and Teel, 2005), Theorem 2.8. Note that in (Kellett and Teel, 2005) continuity of the function V on $\mathbb{X}$, i.e., not solely at the origin as specified by Theorem 5.2.6, is required only to show certain robustness properties.

Next, consider the discrete-time constrained system

$$x(k+1) = \Psi(x(k), u(k)), \quad k \in \mathbb{Z}_+, \tag{5.3}$$

where $x(k) \in \mathbb{X} \subseteq \mathbb{R}^n$ is the state and $u(k) \in \mathbb{U} \subseteq \mathbb{R}^m$ is the control input at the discrete-time instant $k \in \mathbb{Z}_+$. The function $\Psi : \mathbb{R}^n \times \mathbb{R}^m \to \mathbb{R}^n$ is nonlinear with $\Psi(0_n, 0_m) = 0_n$. We assume that $\mathbb{X}$ and $\mathbb{U}$ are bounded sets with $0_n \in \text{int}(\mathbb{X})$ and $0_m \in \text{int}(\mathbb{U})$. Next, let $\alpha_1, \alpha_2 \in \mathcal{K}_\infty$ and let $\rho \in \mathbb{R}_{[0,1)}$.

Definition 5.2.7 A function $V : \mathbb{R}^n \to \mathbb{R}_+$ that satisfies

$$\alpha_1(\|x\|) \leq V(x) \leq \alpha_2(\|x\|), \quad \forall x \in \mathbb{R}^n, \tag{5.4}$$

and for which there exists a possibly set-valued control law $\pi : \mathbb{R}^n \rightrightarrows \mathbb{U}$ such that

$$V(\Psi(x, u)) \leq \rho V(x), \quad \forall x \in \mathbb{X}, \forall u \in \pi(x), \tag{5.5}$$

is called a control Lyapunov function in $\mathbb{X}$ for (5.3). ■

5.3 Modeling framework and problem definition

A useful way of dealing with the complexity of many large-scale dynamical systems is to model them as a network of (sparsely) interconnected subsystems, which are typically of much lower order than the full network. In what follows, we describe this modeling framework in detail.

Consider a *directed connected graph* $\mathcal{G} = (\mathcal{S}, \mathcal{E})$ with a finite number of vertices $\mathcal{S} = \{\varsigma_1, \ldots, \varsigma_N\}$ and a set of directed edges $\mathcal{E} \subseteq \{(\varsigma_i, \varsigma_j) \in \mathcal{S} \times \mathcal{S} \mid i \neq j\}$.

In input-driven NDS, a dynamical system is assigned to each vertex $\varsigma_i \in \mathcal{S}$, that is described by the difference equation

$$x_i(k+1) = \psi_i(x_i(k), v_i(x_{\mathcal{N}_i}(k)), u_i(k)), \quad k \in \mathbb{Z}_+, \tag{5.6}$$

for vertex indices $i \in \mathcal{I} := \mathbb{Z}_{[1,N]}$. In (5.6), $x_i \in \mathbb{X}_i \subseteq \mathbb{R}^{n_i}$ denotes the state and $u_i \in \mathbb{U}_i \subseteq \mathbb{R}^{m_i}$ represents the control input of the i-th system, i.e., the system assigned to vertex ς_i. With each directed edge $(\varsigma_j, \varsigma_i) \in \mathcal{E}$ we associate a function $v_{ij} : \mathbb{R}^{n_j} \to \mathbb{R}^{n_{v_{ij}}}$ that defines the interconnection signal $v_{ij}(x_j) \in \mathbb{R}^{n_{v_{ij}}}$, between system j and system i, i.e., $v_{ij}(x_j)$ characterizes how the states of system j influence the dynamics of system i. We use $\mathcal{N}_i := \{j \mid (\varsigma_j, \varsigma_i) \in \mathcal{E}\}$ to denote the set of indices corresponding to the *direct neighbors* of system i. Thus, a direct neighbor of system i is any system in the network whose dynamics (e.g., states or outputs) appear explicitly (via the function $v_{ij}(\cdot)$) in the state equations that govern the dynamics of system i. Clearly, if system j is a direct neighbor of system i, this does not necessarily imply the reverse. Let $\overline{\mathcal{N}}_i := \mathcal{N}_i \cup \{i\}$. We define $x_{\mathcal{N}_i}(k) := \mathrm{col}(\{x_j(k)\}_{j \in \mathcal{N}_i})$ as the vector that collects all the state vectors of the direct neighbors of system i and $v_i(x_{\mathcal{N}_i}(k)) := \mathrm{col}(\{v_{ij}(x_j(k))\}_{j \in \mathcal{N}_i}) \in \mathbb{R}^{n_{v_i}}$ as the vector that collects all the vector-valued interconnection signals that "enter" system i. The functions $\psi_i : \mathbb{R}^{n_i} \times \mathbb{R}^{n_{v_i}} \times \mathbb{R}^{m_i} \to \mathbb{R}^{n_i}$ and $v_{ij} : \mathbb{R}^{n_j} \to \mathbb{R}^{n_{v_{ij}}}$ satisfy $\psi_i(0_{n_i}, 0_{n_{v_i}}, 0_{m_i}) = 0_{n_i}$ for all $i \in \mathcal{I}$ and $v_{ij}(0_{n_j}) = 0_{n_{v_{ij}}}$ for all $(i,j) \in \mathcal{I} \times \mathcal{N}_i$. For all $i \in \mathcal{I}$ we assume that $0_{n_i} \in \mathrm{int}(\mathbb{X}_i)$ and $0_{m_i} \in \mathrm{int}(\mathbb{U}_i)$. System (5.6) is said to be *decoupled* if $v_i(x_{\mathcal{N}_i}(k))$ is set to $0_{n_{v_i}}$ for all $k \in \mathbb{Z}_+$. Hence, under decoupled operation, system i is described by the difference equation $x_i(k+1) = \psi_i(x_i(k), 0_{n_{v_i}}, u_i(k))$.

The following standing assumption is instrumental for obtaining the results presented in this chapter.

Assumption 5.3.1 The values of all the interconnection signals $\{v_{ij}(x_j(k))\}_{j \in \mathcal{N}_i}$ are known at each discrete-time instant $k \in \mathbb{Z}_+$, for any system $i \in \mathcal{I}$. ■

Notice that Assumption 5.3.1 does not require knowledge of any of the interconnection signals at future time instants. From a technical point of view, Assumption 5.3.1 is satisfied, e.g., if all the interconnection signals $v_{ij}(x_j(k))$ are directly measurable at all $k \in \mathbb{Z}_+$.[1] Alternatively, Assumption 5.3.1 is satisfied if all directly neighboring systems $j \in \mathcal{N}_i$ are able to communicate their local

[1] For example, in the modeling framework for electrical power systems considered in this thesis, where the dynamical system at node i is a (lumped set of) generator(s), the interconnection signal is the power (or current) flow in the connected power lines, which can be directly measured.

measured state $x_j(k)$ to system $i \in \mathcal{I}$, which can then compute $v_{ij}(x_j(k))$ if it has knowledge of the function $v_{ij}(\cdot)$.

Finally, let

$$x(k+1) = \Psi(x(k), u(k)), \qquad k \in \mathbb{Z}_+, \tag{5.7}$$

denote the dynamics of the overall network of interconnected systems (5.6), written in a compact form. In (5.7), $x = \text{col}(\{x_i\}_{i\in\mathcal{I}}) \in \mathbb{R}^n$, $n = \sum_{i\in\mathcal{I}} n_i$, and $u = \text{col}(\{u_i\}_{i\in\mathcal{I}}) \in \mathbb{R}^m$, $m = \sum_{i\in\mathcal{I}} m_i$, are vectors that collect all local states and inputs, respectively.

Now, our objective is to find a tractable solution to the following control problem.

Problem 5.3.2 Given NDS (5.6), design a set of control laws $\mu_i(x_i, \{x_j\}_{j\in\mathcal{N}_i})$, $\mu_i : \mathbb{X}_i \times \left(\prod_{j\in\mathcal{N}_i} \mathbb{X}_j\right) \to \mathbb{U}_i$, $i \in \mathcal{I}$, such that the corresponding closed-loop dynamics

$$x(k+1) = \Psi(x(k), \mu(x(k))), \quad k \in \mathbb{Z}_+, \tag{5.8}$$

with $\mu(x) := \text{col}(\{\mu_i(x_i, \{x_j\}_{j\in\mathcal{N}_i})\}_{i\in\mathcal{I}})$, are asymptotically stable and $x_i(k) \in \mathbb{X}_i$ for all $k \in \mathbb{Z}_+$, $i \in \mathcal{I}$. ■

Problem 5.3.2 belongs to the class of *structured control problems*. This is reflected by the feedback laws $\mu_i(x_i, \{x_j\}_{j\in\mathcal{N}_i})$, which define local control actions based on local and neighboring state information only.

5.4 Main result: structured max-CLFs

To solve Problem 5.3.2, we introduce the notion of a set of "structured max-CLFs", which provides an alternative to the structured CLFs defined recently in (Jokić and Lazar, 2009).

Definition 5.4.1 Let $\alpha_1^i, \alpha_2^i \in \mathcal{K}_\infty$ for $i \in \mathcal{I}$ and let $\{V_i\}_{i\in\mathcal{I}}$ be a set of functions $V_i : \mathbb{R}^{n_i} \to \mathbb{R}_+$ that satisfy

$$\alpha_1^i(\|x_i\|) \le V_i(x_i) \le \alpha_2^i(\|x_i\|), \ \forall x_i \in \mathbb{R}^{n_i}, \ \forall i \in \mathcal{I}. \tag{5.9a}$$

Then, given $\rho_i \in \mathbb{R}_{[0,1)}$ for $i \in \mathcal{I}$, if there exists a non-empty set of possibly set-valued control laws $\pi_i : \mathbb{R}^{n_i} \times \mathbb{R}^{n_{v_i}} \rightrightarrows \mathbb{U}_i$ such that

$$V_i(\psi_i(x_i, v_i(x_{\mathcal{N}_i}), u_i)) \le \rho_i \max_{j\in\overline{\mathcal{N}}_i} V_j(x_j), \tag{5.9b}$$

$\forall x_i \in \mathbb{X}_i$, $\forall u_i \in \pi_i(x_i, v_i(x_{\mathcal{N}_i}))$, the set of functions $\{V_i\}_{i\in\mathcal{I}}$ is called a set of "structured max control Lyapunov functions" (max-CLFs) in $\mathbb{X} := \{\text{col}(\{x_i\}_{i\in\mathcal{I}}) \mid x_i \in \mathbb{X}_i\}$ for (5.7). ■

In the above definition the term *structured* emphasizes the fact that each V_i is a function of x_i only, i.e., the structural decomposition of the dynamics of the overall interconnected system (5.6) is reflected in the functions $\{V_i\}_{i\in\mathcal{I}}$. Moreover, the term *max* originates from the corresponding convergence condition, i.e., (5.9b). Next, based on Definition 5.4.1, we formulate the following feasibility problem.

Problem 5.4.2 Let $\rho_i \in \mathbb{R}_{[0,1)}$, $i \in \mathcal{I}$ and a set of "structured max-CLFs" $\{V_i\}_{i\in\mathcal{I}}$ be given. At time $k \in \mathbb{Z}_+$, let the state vector $\{x_i(k)\}_{i\in\mathcal{I}}$, the set of interconnection signals $\{v_i(x_{\mathcal{N}_i}(k))\}_{i\in\mathcal{I}}$ and the values $\{V_i(x_i(k))\}_{i\in\mathcal{I}}$ be known, and calculate a set of control actions $\{u_i(k)\}_{i\in\mathcal{I}}$, such that:

$$u_i(k)\in\mathbb{U}_i,\ \psi_i(x_i(k),v_i(x_{\mathcal{N}_i}(k)),u_i(k))\in\mathbb{X}_i, \tag{5.10a}$$

$$V_i(\psi_i(x_i(k),v_i(x_{\mathcal{N}_i}(k)),u_i(k)))\leq\rho_i\max_{j\in\overline{\mathcal{N}}_i}V_j(x_j(k)), \tag{5.10b}$$

for all $i\in\mathcal{I}$. ■

Let $\pi(x(k)) := \{\mathrm{col}(\{u_i(k)\}_{i\in\mathcal{I}}) \mid (5.10) \text{ holds}\}$ and let

$$x(k+1)\in\phi_{\mathrm{CL}}(x(k),\pi(x(k))) := \{\Psi(x(k),u(k)) \mid u(k)\in\pi(x(k))\} \tag{5.11}$$

denote the difference inclusion corresponding to system (5.7) in "closed loop" with the set of feasible solutions obtained by solving Problem 5.4.2 at each discrete-time instant $k\in\mathbb{Z}_+$.

Theorem 5.4.3 *Let $\alpha_1^i,\alpha_2^i\in\mathcal{K}_\infty$ and $\rho_i\in\mathbb{R}_{[0,1)}$, $\forall i\in\mathcal{I}$ be given and choose a set of structured max-CLFs $\{V_i\}_{i\in\mathcal{I}}$ in $\mathbb{X}=\{\mathrm{col}(\{x_i\}_{i\in\mathcal{I}}) \mid x_i\in\mathbb{X}_i\}$ for system* (5.7)*. Suppose that Problem 5.4.2 is feasible for all $x(k)\in\mathbb{X}$ and the corresponding signals $\{v_i(x_{\mathcal{N}_i}(k))\}_{i\in\mathcal{I}}$. Then the difference inclusion* (5.11) *is AS($\mathbb{X}$).*

See Appendix C.1 for the proof. Notice that in Problem 5.4.2 the functions V_i do not need to be CLFs (in conformity with Definition 5.2.7) in $\mathbb{X}_i$ for each system $i\in\mathcal{I}$, respectively. Condition (5.10b) permits a *spatially* non-monotonous evolution of V_i. More precisely, the local functions are allowed to increase, as long as for each system the value of its function V_i at the next time instant is less than ρ_i times the maximum over the current values of its own function and those of its direct neighbors.

Moreover, observe that Problem 5.4.2 is separable in $\{u_i\}_{i\in\mathcal{I}}$. The set of feasible control inputs defined by (5.10) only contains inequalities at a local, subsystem-specific level. Therefore, it is possible to solve Problem 5.4.2 by independently solving N feasibility problems, each assigned to a single local controller, i.e., the controller associated to one of the systems $i\in\mathcal{I}$. To compute

$u_i(k)$, each controller needs to measure or estimate the current state $x_i(k)$ of its system, and have knowledge of the interconnection signals $\{v_i(x_{\mathcal{N}_i})\}_{i\in\mathcal{N}_i}$ and the values $\{V_i(x_i(k))\}_{i\in\mathcal{N}_i}$. A single round of information exchange among direct neighbors per sampling instant is sufficient to acquire this knowledge. Therefore, an attractive feature of the control scheme considered in this chapter is that it can be implemented in an almost decentralized fashion.

5.4.1 Temporal non-monotonicity

In general, it may be difficult to find functions $\{V_i\}_{i\in\mathcal{I}}$ that satisfy (5.9) for all $x_i \in \mathbb{X}_i$. Systematic methods for synthesizing CLFs for an arbitrary nonlinear system do not exist, although candidate CLFs can often be generated using linearized system dynamics. However, the region of validity for these CLFs is often limited to a neighborhood of the origin. Supposing that we have a set of structured max-CLFs in $\widetilde{\mathbb{X}} \subset \mathbb{X}$, we propose a method to relax the conditions on the candidate CLFs, based on an adaptation of the Lyapunov-Razumikhin (LR) technique for time-delay systems (Hale, 1977; Liu and Marquez, 2008). The LR method allows the Lyapunov function to be non-monotonous to compensate for the effects of the delay. Next, we show how the LR technique can be applied to discrete-time systems as well, to permit a *temporal* non-monotonous evolution of the candidate CLF for the full network.

Problem 5.4.4 Let $N_\tau \in \mathbb{Z}_{\geq 1}$ be given. Consider Problem 5.4.2 for a set of "structured max-CLFs" $\{V_i\}_{i\in\mathcal{I}}$ in $\widetilde{\mathbb{X}} \subset \mathbb{X}$, with (5.10b) replaced by

$$V_i(\psi_i(x_i(k), v_i(x_{\mathcal{N}_i}(k)), u_i(k))) \leq \rho_i \max_{\tau\in\mathbb{Z}_{[0,N_\tau-1]}} \max_{j\in\overline{\mathcal{N}}_i} V_j(x_j(k-\tau)), \tag{5.12}$$

for all $k \in \mathbb{Z}_{\geq N_\tau - 1}$ and $i \in \mathcal{I}$. ■

Let $\bar{\pi}(x(k)) := \{\mathrm{col}(\{u_i(k)\}_{i\in\mathcal{I}}) \mid \text{(5.10a) and (5.12) hold}\}$ and let

$$x(k+1) \in \bar{\phi}_{\mathrm{CL}}(x(k), \bar{\pi}(x(k))) := \{\Psi(x(k), u(k)) \mid u(k) \in \bar{\pi}(x(k))\} \tag{5.13}$$

denote the difference inclusion corresponding to system (5.7) in "closed loop" with the set of feasible solutions obtained by solving Problem 5.4.4 at each time instant $k \in \mathbb{Z}_+$.

Theorem 5.4.5 *Let $\alpha_1^i, \alpha_2^i \in \mathcal{K}_\infty$, $N_\tau \in \mathbb{Z}_{\geq 1}$ and $\rho_i \in \mathbb{R}_{[0,1)}$, $\forall i \in \mathcal{I}$ be given and choose a set of structured max-CLFs $\{V_i\}_{i\in\mathcal{I}}$ in $\widetilde{\mathbb{X}} \subseteq \mathbb{X} = \{\mathrm{col}(\{x_i\}_{i\in\mathcal{I}}) \mid x_i \in \mathbb{X}_i\}$ for system* (5.7)*. Suppose that Problem 5.4.4 is feasible for all $x(k) \in \mathbb{X}$, all $k \in \mathbb{Z}_+$ and the corresponding signals $\{v_i(x_{\mathcal{N}_i}(k))\}_{i\in\mathcal{I}}$. Then* (5.13) *is AS($\mathbb{X}$).*

For the proof of Theorem 5.4.5, see Appendix C.2. The distinctive feature of Problem 5.4.4 is that it allows the trajectories of the local functions $V_i(x_i(k))$ to be non-monotonous, and relaxes the convergence condition on the corresponding candidate CLF for the overall network, i.e., $V(x) := \max_{i\in\mathcal{I}} V_i(x_i)$, as well. The evolution of $V(x(k))$ can be arbitrary, as long as it remains within the asymptotically converging envelope generated by (5.12) and the first N_τ values of $V(x(k))$.

Note that if we combine Problem 5.4.2 or Problem 5.4.4 with the optimization of a set of local cost functions, the feasibility-based stability guarantee and the possibility of an almost decentralized implementation still hold. This enables the formulation of a one-step-ahead predictive control algorithm in which stabilization is decoupled from performance, and in which the controllers do not need to attain Pareto optimal cost at each sampling instant, as typically required for stability in classical MPC (Mayne et al., 2000).

For the remainder of this chapter we therefore consider the following almost decentralized Lyapunov-based MPC algorithm, supposing that a set of local objective functions $\{J_i(u_i, x_i)\}_{i\in\mathcal{I}}$ is known.

Algorithm 3 Distributed L-MPC

At each instant $k \in \mathbb{Z}_+$ and node $i \in \mathcal{I}$:
Step 1: Measure or estimate the current local state $x_i(k)$ and transmit $v_{ji}(x_i(k))$ and $V_i(x_i(k))$ to nodes $\{j \in \mathcal{I} \mid i \in \mathcal{N}_j\}$.
Step 2: Specify the set of feasible local control actions $\bar{\pi}_i(x_i(k), v_i(x_{\mathcal{N}_i}(k))) := \{u_i(k) \mid \text{(5.10a) and (5.12) hold}\}$. Minimize the cost $J_i(u_i(k), x_i(k))$ over the set of actions $\bar{\pi}_i(x_i(k), v_i(x_{\mathcal{N}_i}(k)))$ and denote the optimizer by $u_i^*(k)$;
Step 3: Use $u_i(k) = u_i^*(k)$ as control action.

Remark 5.4.6 In Algorithm 3, each controller optimizes its own local performance. However, many distributed MPC schemes (see, for instance, Camponogara et al. (2002); Venkat et al. (2008)) optimize a global cost function (e.g., some convex combination of local objectives) and aim for optimization of global performance by employing network-wide information or iterations. Therein, stability is attained by assuming optimality (for example, in Venkat et al. (2008)) or by imposing a contractive constraint on the norm of the local states (e.g., in Camponogara et al. (2002)). The L-MPC conditions proposed in this chapter can be used in those implementations as well, as an alternative way to achieve stability that is less conservative than contractive constraints, whereas multiple time-consuming iterations per sampling instant would only be required for improving global performance. ■

Remark 5.4.7 The dependence of conditions (5.10b) and (5.12) on $V_j(\cdot)$ for j in the set $\overline{\mathcal{N}}_i$ is convenient, because the corresponding communication graph coincides with the graph that characterizes the exchange of $v_{ij}(x_j)$ as required by the local state predictions, i.e., (5.6). However, in fact, stability also follows if (5.10a) and

$$V_i(\psi_i(x_i(k), v_i(x_{\mathcal{N}_i}(k)), u_i(k))) \leq \rho_i \max_{\tau \in \mathbb{Z}_{[0,N_\tau-1]}} \max_{j \in \mathcal{P}_i} V_j(x_j(k-\tau)) \tag{5.14}$$

hold $\forall k \in \mathbb{Z}_{\geq N_\tau - 1}$, where $\{\mathcal{P}_i\}_{i\in\mathcal{I}}$ is an *arbitrary* collection of non-empty sets of nodes such that

$$\textstyle\bigcup_{i\in\mathcal{I}} \mathcal{P}_i = \mathcal{I}. \tag{5.15}$$

As $\max_{j\in\overline{\mathcal{N}}_i} V_j \leq \max_{j\in\mathcal{P}_i} V_j$ for $\overline{\mathcal{N}}_i \subseteq \mathcal{P}_i$, enlarging the set over which the maximum V_j value is evaluated is an attractive method of relaxing the local CLF convergence conditions if this is supported by the available communication infrastructure.

Analogously, it can be shown that Problem 5.4.2 and Problem 5.4.4 provide some robustness against communication failures such as packet loss. As long as the perturbed communication graph is characterized by a collection of sets $\{\mathcal{P}_i\}_{i\in\mathcal{I}}$ that satisfies (5.15), the asymptotic stability guarantee is retained. ■

5.4.2 Implementation Issues

In what follows, we consider nonlinear NDS that are affine in the control input, i.e.,

$$\begin{aligned} x_i(k+1) &= \psi_i(x_i(k), v_i(x_{\mathcal{N}_i}(k)), u_i(k)) \\ &= f_i(x_i(k), v_i(x_{\mathcal{N}_i}(k))) + g_i(x_i(k), v_i(x_{\mathcal{N}_i}(k)))u_i(k), \end{aligned} \tag{5.16}$$

with $f_i : \mathbb{R}^{n_i} \times \mathbb{R}^{n_{v_i}} \to \mathbb{R}^{n_i}$, $f_i(0_{n_i}, 0_{n_{v_i}}) = 0_{n_i}$, $g_i : \mathbb{R}^{n_i} \times \mathbb{R}^{n_{v_i}} \to \mathbb{R}^{n_i \times m_i}$ and $g_i(0_{n_i}, 0_{n_{v_i}}) = 0$ for all $i \in \mathcal{I}$. For these systems and polytopic state and input sets $\mathbb{X}_i$ and $\mathbb{U}_i$, respectively, it is possible to implement Step 2 of Algorithm 3 by solving a single linear program, without introducing conservatism.

For this, we restrict our attention to infinity-norm based structured CLFs, i.e.,

$$V_i(x_i) = \|P_i x_i\|_\infty, \tag{5.17}$$

where $P_i \in \mathbb{R}^{p_i \times n_i}$ is a full-column rank matrix. Note that this type of structured max-CLFs satisfies (5.9a), for $\alpha_1^i(s) := \frac{\sigma_{P_i}}{\sqrt{p_i}} s$, where $\sigma_{P_i} > 0$ is the smallest singular value of P_i, and $\alpha_2^i(s) := \|P_i\|_\infty s$.

By definition of the infinity norm, for $\|x\|_\infty \leq c$ to be satisfied for some vector $x \in \mathbb{R}^n$ and constant $c \in \mathbb{R}$, it is necessary and sufficient to require that $\pm[x]_j \leq c$

for all $j \in \mathbb{Z}_{[1,n]}$. So, for (5.12) to be satisfied, it is necessary and sufficient to require that

$$\pm[P_i\{g_i(x_i(k), v_i(x_{\mathcal{N}_i}(k)))u_i(k)\}]_j \leq \zeta_i(k) \mp [P_i\{f_i(x_i(k), v_i(x_{\mathcal{N}_i}(k)))\}]_j, \quad (5.18)$$

for $j \in \mathbb{Z}_{[1,p_i]}$ and $k \in \mathbb{Z}_{\geq N_\tau - 1}$, and where

$$\zeta_i(k) := \rho_i \max_{\tau \in \mathbb{Z}_{[0,N_\tau-1]}} \max_{j \in \overline{\mathcal{N}}_i} V_j(x_j(k-\tau)) \in \mathbb{R}_+ \quad (5.19)$$

is constant at any $k \in \mathbb{Z}_{\geq N_\tau - 1}$. This yields a total of $2p_i$ linear inequalities in u_i.

Then, by choosing infinity-norm based local cost functions of the form

$$J_i(x_i, u_i) := \|Q_1^i \psi_i(x_i, v_i(x_{\mathcal{N}_i}), u_i)\|_\infty + \|Q_0^i x_i\|_\infty + \|R^i u_i\|_\infty, \quad (5.20)$$

with full-rank matrices $Q_1^i \in \mathbb{R}^{n_{q_{1,i}} \times n_i}, Q_0^i \in \mathbb{R}^{n_{q_{0,i}} \times n_i}$ and $R^i \in \mathbb{R}^{n_{r_i} \times m_i}$, we can reformulate Step 2 of Algorithm 3 as the linear program

$$\min_{u_i(k), \varepsilon_1, \varepsilon_2} \varepsilon_1 + \varepsilon_2 \quad (5.21)$$

subject to (5.10a), (5.18) and

$$\pm\left[Q_1^i \psi_i(x_i(k), v_i(x_{\mathcal{N}_i}(k)), u_i(k))\right]_j + \|Q_0^i x_i(k)\|_\infty \leq \varepsilon_1$$
$$\pm[R^i u_i(k)]_l \leq \varepsilon_2,$$

for $j \in \mathbb{Z}_{[1,n_{q_{1,i}}]}$ and $l \in \mathbb{Z}_{[1,n_{r_i}]}$.

5.5 Illustrative example

Consider NDS (5.6) with $\mathcal{S} = \{\varsigma_1, \varsigma_2\}$, $\mathcal{N}_1 = \{2\}$, $\mathcal{N}_2 = \{1\}$, $\mathbb{X}_1 = \mathbb{X}_2 = \{x \in \mathbb{R}^2 \mid \|x\|_\infty \leq 5\}$ and $\mathbb{U}_1 = \mathbb{U}_2 = \{u \in \mathbb{R} \mid |u| \leq 2\}$. Its dynamics are given by:

$$\psi_1(x_1, v_1(x_{\mathcal{N}_1}), u_1) := \begin{bmatrix} 1 & 0.7 \\ 0 & 1 \end{bmatrix} x_1 + \begin{bmatrix} \sin([x_1]_2) \\ 0 \end{bmatrix} + \begin{bmatrix} 0.245 \\ 0.7 \end{bmatrix} u_1 + \begin{bmatrix} 0 \\ ([x_2]_1)^2 \end{bmatrix}, \quad (5.22a)$$

$$\psi_2(x_2, v_2(x_{\mathcal{N}_2}), u_2) := \begin{bmatrix} 1 & 0.5 \\ 0 & 1 \end{bmatrix} x_2 + \begin{bmatrix} \sin([x_2]_2) \\ 0 \end{bmatrix} + \begin{bmatrix} 0.125 \\ 0.5 \end{bmatrix} u_2 + \begin{bmatrix} 0 \\ [x_1]_1 \end{bmatrix}. \quad (5.22b)$$

The method of (Lazar et al., 2006) was used to compute the weights $P_1, P_2 \in \mathbb{R}^{2\times 2}$ of two local infinity-norm based candidate CLFs, i.e., $V_1(x_1) = \|P_1 x_1\|_\infty$ and $V_2(x_2) = \|P_2 x_2\|_\infty$ with $\rho = \rho_1 = \rho_2 = 0.8$ and linearizations of (5.22a), (5.22b),

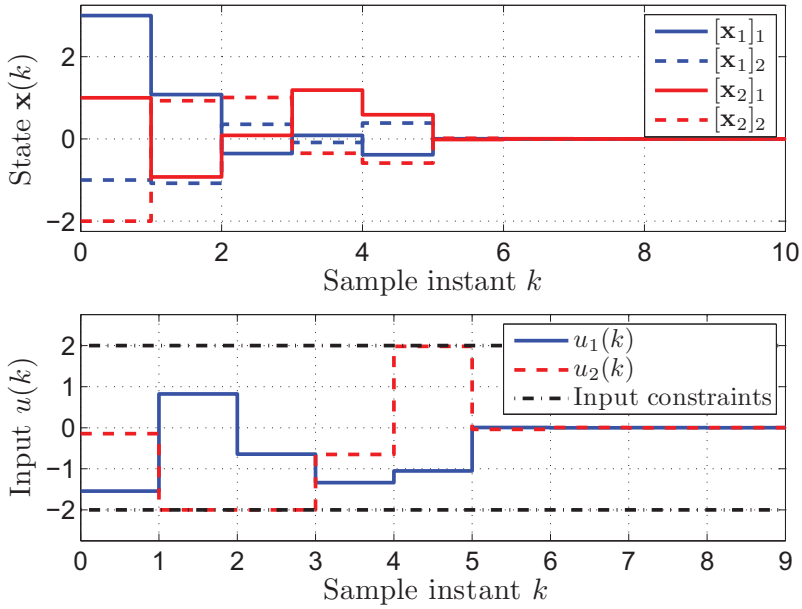

Figure 5.1: Input trajectories for $\rho = 0.8$ and $N_\tau = 3$.

respectively, around the origin, in closed-loop with the local state-feedback laws $u_1(k) := K_1 x_1(k)$, $u_2(k) := K_2 x_2(k)$, $K_1, K_2 \in \mathbb{R}^{1\times 2}$, yielding

$$P_1 = \begin{bmatrix} 2.56 & 0.33 \\ 1.86 & 5.02 \end{bmatrix}, \; K_1 = \begin{bmatrix} -0.97 \\ -2.12 \end{bmatrix}^\top, \; P_2 = \begin{bmatrix} -0.39 & -0.38 \\ 0.27 & 0.98 \end{bmatrix}, \; K_2 = \begin{bmatrix} -0.39 \\ -2.78 \end{bmatrix}^\top.$$

Note that the control laws $u_1(k) = K_1 x_1(k)$ and $u_2(k) = K_2 x_2(k)$ are only employed off-line, to calculate the weight matrices P_1, P_2 and they are not used for controlling the system. For each system $i \in \mathcal{I}$, we employed cost function (5.20), where $Q_1^1 = Q_1^2 = 4I_2$, $Q_0^1 = Q_0^2 = 0.1 I_2$ and $R^1 = R^2 = 0.4$.

In the simulation scenario we tested the system response in closed-loop with Algorithm 3 for $x_1(0) = [3,\ -1]^\top$, $x_2(0) = [1,\ -2]^\top$ and $N_\tau = 3$. Figure 5.1 shows the control inputs for system 1 and system 2, along with the input constraints that are represented by the dash-dotted lines. Note that these constraints are not violated, although they are active at some time instants. The corresponding evolutions of $V_1(x_1(k))$, $V_2(x_2(k))$, $V(x(k))$ and the upper bounds generated by (5.12) are shown in Figure 5.2. The simulation illustrates that $V(x(k))$ is allowed to vary arbitrarily within the asymptotically converging envelope defined by (5.12), thus inducing state convergence. Moreover, the proposed L-MPC algorithm allows a spatially non-monotonous evolution of the structured max-CLFs (at

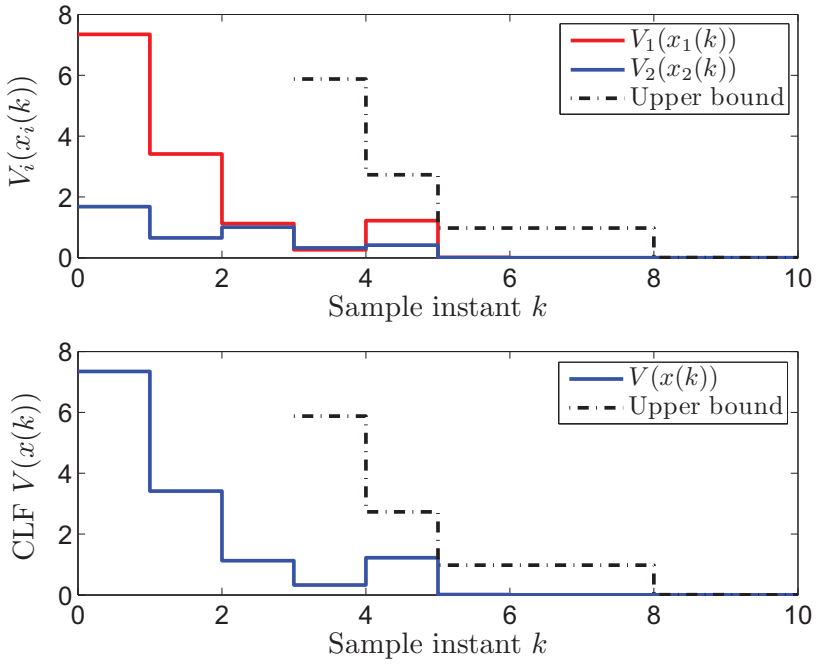

Figure 5.2: $V_1(x_1(k))$, $V_2(x_2(k))$ *and* $V(x(k))$ *trajectories for* $\rho = 0.8$ *and* $N_\tau = 3$.

time instant $k = 2$, $V_2(x_2(k))$ increases although $V(x(k))$ does not), whereas the candidate CLF itself can be non-decreasing as well (which is the case for $k = 4$). The closed-loop convergence rate is similar to the one attained by the method in (Jokić and Lazar, 2009) for the same example and initial conditions. However, the technique in (Jokić and Lazar, 2009) requires global coordination and iterative optimization to guarantee closed-loop stability, whereas the method proposed in this chapter does not.

5.6 Conclusions

This chapter proposed an almost decentralized solution to the problem of stabilizing a network of discrete-time nonlinear systems with coupled dynamics that are subject to local state/input constraints. By "almost decentralized" we mean that each local controller is allowed to use the states of neighboring systems for feedback, whereas it is not permitted to employ iterations between the systems in the network to compute the control action. The stabilization conditions were decentralized via a set of structured control Lyapunov functions for which the

maximum over all the functions in the set is a CLF for the overall network of systems. However, this does not necessarily imply that each function is a local CLF for its corresponding system. Additionally, we provided a solution for relaxing the temporal monotonicity of the CLF for the overall network. An example illustrated the effectiveness of the developed scheme and demonstrated that the proposed L-MPC technique can perform as well as more complex distributed, iteration-based MPC algorithms.

6

Stabilization of interconnected dynamical systems by on-line convex optimization

6.1 Introduction

The analysis of large-scale dynamical systems has intrigued researchers for more than four decades, see, for instance, (Šiljak, 1978; Sandell et al., 1978; Šiljak, 1991) and the references therein. The general way of dealing with the complexity of such systems is to model them as a network of interconnected dynamical systems (NDS; see Chapter 5). Then, the objective is to deduce characteristics for the interconnected system in a non-centralized fashion, i.e., based on conditions that are defined with respect to the individual systems in the network.

A similar need for decentralization arises when considering stability analysis (and, consequently, controller design) for networks of unconstrained systems, which is the main focus of this chapter. The most common, centralized way of determining asymptotic stability by verifying the existence of a quadratic Lyapunov function (LF) is not a viable option in this case, as the required full-system model is usually not available and the corresponding synthesis problem,

formulated as a semi-definite program (SDP), comes with a computational burden that can be prohibitively large.

Non-centralized stability analysis typically relies on small-gain conditions or dissipativity theory. As an example of the first class of methods, we mention (Dashkovskiy et al., 2007, 2010), where conditions are provided by which stability of a nonlinear network can be deduced from input-to-state stability (ISS) of the individual subsystems. More specifically, the existence of an ISS Lyapunov function for the interconnected subsystems is established if the combined gains of these systems satisfy a certain upper bound.

In this paper, however, the focus is on dissipation theory to generate a full-network LF from a set of system-specific *storage and supply functions* (Willems, 1972). As an example, we mention the scheme proposed in (Langbort et al., 2004), where the synthesis procedure is based on finding "fixed" storage and supply functions, that is, functions with a fixed, in this case quadratic structure and off-line calculated parameters that apply to the complete state-space region of interest. Further decentralization of the stability conditions is possible by considering, for example, constant (i.e., state, input and time independent) supply rates, zero supply rates, and decoupled local system dynamics. Although this may simplify synthesis and loosen communication requirements, the conservatism of such decentralized approaches can be considerable, see, e.g., (Sandell et al., 1978; Šiljak, 1991).

More recent methods aim to increase flexibility of non-centralized Lyapunov synthesis by employing *state-parameterized supply functions*, see, e.g., (Jokić and Lazar, 2009). A similar approach was pursued in Chapter 5, where the supply-rate parameterization is based on "max-type dissipativity conditions" that allow for max-type construction of a LF for the interconnected dynamics. As observed in (Dashkovskiy et al., 2010), this type of construction provides more flexibility than the common way of constructing Lyapunov candidates by summing over the storage functions,[1] which is instrumental in, e.g., (Langbort et al., 2004; Jokić and Lazar, 2009). Even so, all of the above described schemes suffer from the possible impediments that are characteristic to the *off-line synthesis of fixed-parameter quadratic storage functions*.

In terms of non-centralized stability analysis, the contribution of this chapter is twofold. Firstly, we formalize the conservatism associated with state-of-the-art, tractable methods for noncentralized stability analysis in a theorem that applies to the broad and common class of networks with one or more sys-

[1] It is worth to point out that for certain types of stability, such as integral input-to-state stability (iISS), sum-based constructions of Lyapunov functions are less conservative than max-based constructions (Ito et al., 2012).

tems that are unstable under decoupled operation. Then, the consequences for synthesis are illustrated by providing a linear and time-invariant motivating example network that does not admit construction of a (control) Lyapunov function from a set of fixed-parameter quadratic storage functions, but that is stabilizable nonetheless. Secondly, the objective is to find a solution to this issue, by endowing the storage functions with a finite set of state-dependent parameters. It was already shown in, e.g., (Lazar and Gielen, 2010) that enriching the set of admissible parameters for a system-wide LF leads to less conservative centralized synthesis conditions for nonlinear and constrained linear systems. However, in the context of this chapter, the relaxation is specifically employed to obtain non-conservative system-specific *non-centralized* convergence conditions that establish the existence of a Lyapunov function for the full, interconnected network.

Synthesis conditions analogous to the ones provided in Chapter 5 are used to allow for max-type construction of a Lyapunov candidate for the full network, whereas the employed parameterized storage functions are not required to be system-specific LFs. The merit of the provided approach is that the storage functions can be constructed *during operation*, i.e., along the closed-loop trajectory, via a collection of coupled convergence conditions. Thus, the impediment of off-line LF synthesis via fixed storage functions is removed. The provided stability conditions are efficiently exploited in devising a non-centralized, trajectory-dependent control law that relies on non-iterative communication among directly coupled systems only. For input-affine NDS and quadratic parameterized storage functions, the synthesis scheme can be implemented by solving a single low-complexity SDP problem at each node, in a receding horizon fashion. Moreover, we show that for linear and time-invariant networks, an even simpler, explicit control law can be derived by interpolating a collection of a-priori generated trajectories in a distributed fashion. This yields a unique, scalable way to extend the trajectory-specific convergence property associated with parameterized-storage-function based synthesis to a much stronger guarantee of closed-loop asymptotical stability. We use the motivating example to demonstrate that the concepts proposed in this chapter may allow for stabilization in cases where conventional non-centralized methods based on off-line generated, fixed quadratic storage functions fail.

Remark 6.1.1 A *non-conservative, set-theoretic* approach to stability and stabilization of interconnected systems was recently proposed in (Raković et al., 2010). Therein, the concept of invariant families of sets along with several practical parameterizations were introduced. In contrast to decentralized, standard invariant sets, this concept does not require existence of a local invariant set for

each subsystem and, as such, it may be of use to construct parameterized (Lyapunov) storage functions. Fully exploring this possibility is, however, beyond the scope of this chapter. ■

The remainder of this chapter is structured as follows. We begin with preliminary notions on parameterized Lyapunov functions in Section 6.2, followed by the motivating example and theorem in Section 6.3. The main results on parameterized stability analysis and stabilization are described in Section 6.4. Details on non-centralized interpolation are given in Section 6.5. We then provide simulation results in Section 6.6 and end with conclusions.

We recommend to read the preliminary notions on stability and networked dynamical systems provided in Sections 5.2–5.3 before starting with this chapter.

6.2 Parameterized Lyapunov functions

Consider the discrete-time autonomous (i.e., time-invariant) nonlinear system

$$x(k+1) = \Phi(x(k)), \quad k \in \mathbb{Z}_+, \tag{6.1}$$

where $x(k) \in \mathbb{R}^n$ is the state at discrete-time instant k and $\Phi : \mathbb{R}^n \to \mathbb{R}^n$ is an arbitrary function. For simplicity, let the origin be an equilibrium of (6.1), i.e., $\Phi(0_n) = 0_n$. Next, we describe the notion of parameterized Lyapunov functions (see Lazar and Gielen (2010) and the references therein), which will be instrumental in the subsequent sections.

Let $\mathbb{P}$ denote a set of real-valued parameter sets, where each element of $\mathbb{P}$ contains a finite number of parameters with a predefined, but otherwise arbitrary structure (for instance, a matrix of certain fixed dimensions). Now consider a function $V : \mathbb{P} \times \mathbb{R}^n \to \mathbb{R}_+$ and consider the following inequalities, given $\alpha_1, \alpha_2 \in \mathcal{K}_\infty$, $\rho \in \mathbb{R}_{[0,1)}$, $(P_1, P_2) \in \mathbb{P} \times \mathbb{P} = \mathbb{P}^2$ and some $x \in \mathbb{R}^n$:

$$\alpha_1(\|x\|) \leq V(P_1, x) \leq \alpha_2(\|x\|) \tag{6.2a}$$

$$V(P_2, \Phi(x)) \leq \rho\, V(P_1, x). \tag{6.2b}$$

Consider the set-valued map $\mathcal{P} : \mathbb{R}^n \rightrightarrows \mathbb{P}^2$, i.e.,

$$\mathcal{P}(x) := \{(P_1, P_2) \in \mathbb{P}^2 \mid (6.2) \text{ holds}\}. \tag{6.3}$$

For any $x \in \mathbb{R}^n$, $\mathcal{P}(x) \neq \emptyset$ means that there is at least one pair $(P_1, P_2) \in \mathbb{P}^2$ that satisfies (6.2). To distinguish between the two outputs of $\mathcal{P}$, we use $[\mathcal{P}(x)]_1 \subseteq \mathbb{P}$ and $[\mathcal{P}(x)]_2 \subseteq \mathbb{P}$ to denote the sets where the first and second component of a pair (P_1, P_2) satisfying (6.2) take values, respectively. With slight abuse of notation, let $P(x)$ represent any $P_1 \in [\mathcal{P}(x)]_1$.

Definition 6.2.1 A function $V(P(x),x)$ with $P(x)\in[\mathcal{P}(x)]_1$ is called a *parameterized Lyapunov function (p-LF)* for (6.1) if

$$\mathcal{P}(x)\neq\emptyset \tag{6.4a}$$

$$[\mathcal{P}(x)]_2\cap[\mathcal{P}(\Phi(x))]_1\neq\emptyset, \tag{6.4b}$$

for all $x\in\mathbb{R}^n$. ■

In what follows, we restrict our attention to *parameterized quadratic Lyapunov functions (p-qLFs)*, i.e., p-LFs of the form $V(P,x):=x^\top Px$, where $\mathbb{P}\subseteq\mathbb{R}^{n\times n}$. Now, consider the following result from (Lazar and Gielen, 2010).

Corollary 6.2.2 *The following statements are equivalent:*

(i) System (6.1) *is GES.*

(ii) System (6.1) *admits a p-qLF.*

Based on Corollary 6.2.2, in (Lazar and Gielen, 2010) p-qLFs were used to derive a set of non-conservative stability conditions for discrete-time, possibly constrained nonlinear systems, which pose a non-trivial challenge to the off-line synthesis of conventional "fixed" Lyapunov functions, that is, functions with a fixed structure (e.g., quadratic; $V(x)=x^\top P(x)x$) and parameter set (e.g., a common weight matrix $P(x)=P$ for the full state-space region of interest). In this chapter, we exploit the flexibility offered by p-qLFs to establish closed-loop stability for a network of unconstrained interconnected dynamical systems via a set of decentralized convergence conditions that are defined with respect to the individual, local system dynamics. However, first, we specify the need for improved decentralized stability approaches based on a motivating example network.

6.3 A motivating result

In what follows, we consider unconstrained and autonomous NDS, i.e., networks described by a connected and directed graph $\mathcal{G}=(\mathcal{S},\mathcal{E})$ and subsystem dynamics

$$x_i(k+1)=\phi_i(x_i(k),v_i(x_{\mathcal{N}_i}(k))),\quad k\in\mathbb{Z}_+,\quad i\in\mathcal{I}, \tag{6.5}$$

with local states $x_i\in\mathbb{R}^{n_i}$ and $\phi_i:\mathbb{R}^{n_i}\times\mathbb{R}^{n_{v_i}}\to\mathbb{R}^{n_i}$ such that $\phi_i(0_{n_i},0_{n_{v_i}})=0_{n_i}$. The interconnection terms $v_i(x_{\mathcal{N}_i})$ are as defined in Section 5.3. Thus, the overall interconnected dynamics can be written in compact form as

$$x(k+1)=\Phi(x(k)),\qquad k\in\mathbb{Z}_+, \tag{6.6}$$

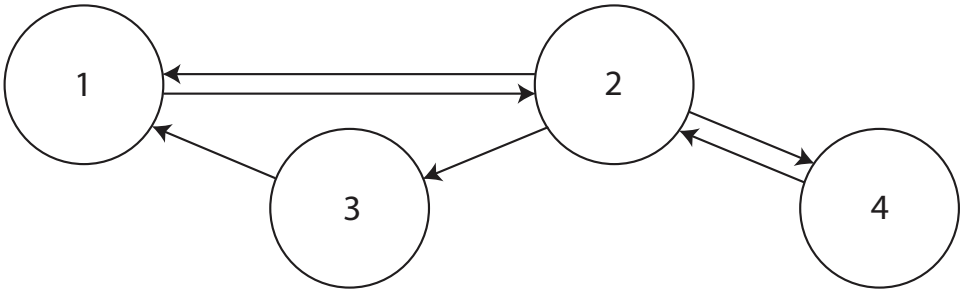

Figure 6.1: Topology of the example network.

where $x = \text{col}(\{x_i\}_{i\in\mathcal{I}}) \in \mathbb{R}^n$, $n = \sum_{i\in\mathcal{I}} n_i$, and where $\Phi : \mathbb{R}^n \to \mathbb{R}^n$ is defined as $\Phi(x) := \text{col}(\{\phi_i(x_i, v_i(x_{\mathcal{N}_i}))\}_{i\in\mathcal{I}})$. From the assumptions on $\phi_i(\cdot)$ and $v_i(\cdot)$ it readily follows that the origin is an equilibrium of (6.6), i.e., $\Phi(0_n) = 0_n$.

Now consider the following theorem.

Theorem 6.3.1 *Let* (6.6) *be linear and time-invariant, i.e.,* $\Phi(x) := Ax$ *for some* $A \in \mathbb{R}^{n\times n}$. *Assume that* (6.6) *is GAS, and that systems* (6.5), $i \in \mathcal{J} \subseteq \mathcal{I}$, $\mathcal{J} \neq \emptyset$, *are such that they do not admit Lyapunov candidates* $V_i(x_i) = x_i^\top P_i x_i$ *under decoupled operation. Then, there is no block-diagonal* $P = \text{diag}(\{P_i\}_{i\in\mathcal{I}}) \in \mathbb{R}^{n\times n}$, $P_i \in \mathbb{R}^{n_i\times n_i}$, *such that* $V(x) = x^\top Px$ *is a quadratic LF for* (6.6).

Theorem 6.3.1 is proven in Appendix D.1. Note that this theorem applies to a broad class of linear and autonomous network dynamics. Thus, the above observation has considerable consequences for the applicability of off-line controller synthesis methods that rely on fixed-parameter quadratic storage functions to establish closed-loop stability, regardless of the type of feedback (e.g., static or dynamic) used. In what follows, we illustrate these consequences for a simple motivating example network.

Consider the following set of systems, interconnected as shown in Figure 6.1 and having states and inputs $x_i \in \mathbb{R}^2$ and $u_i \in \mathbb{R}$, respectively, for $i \in \mathbb{Z}_{[1,4]}$:

$$x_i(k+1) = A_{ii}x_i(k) + \sum_{j\in\mathcal{N}_i} A_{ij}x_j(k) + B_i u_i(k), \tag{6.7}$$

where $\mathcal{N}_1 = \{2,3\}$, $\mathcal{N}_2 = \{1,4\}$, $\mathcal{N}_3 = \{2\}$, $\mathcal{N}_4 = \{2\}$,

$$A = \begin{bmatrix} A_{11} & A_{12} & A_{13} & A_{14} \\ A_{21} & A_{22} & A_{23} & A_{24} \\ A_{31} & A_{32} & A_{33} & A_{34} \\ A_{41} & A_{42} & A_{43} & A_{44} \end{bmatrix}$$

$$= \left[\begin{array}{cc|cc|cc|cc} -\frac{3}{4} & -1 & \frac{1}{2} & \frac{1}{4} & -\frac{1}{2} & \frac{1}{2} & 0 & 0 \\ \frac{1}{4} & 0 & \frac{1}{4} & 0 & 1 & \frac{1}{2} & 0 & 0 \\ \hline -\frac{3}{4} & -\frac{1}{2} & -\frac{1}{2} & -1 & 0 & 0 & -\frac{1}{2} & -\frac{1}{4} \\ \frac{1}{4} & \frac{1}{4} & 0 & -\frac{3}{4} & 0 & 0 & \frac{1}{2} & 1 \\ \hline 0 & 0 & -1 & \frac{3}{4} & \frac{3}{4} & 0 & 0 & 0 \\ 0 & 0 & \frac{3}{4} & -\frac{3}{4} & 0 & 1 & 0 & 0 \\ \hline 0 & 0 & 0 & -\frac{1}{2} & 0 & 0 & -\frac{1}{2} & \frac{1}{4} \\ 0 & 0 & 0 & \frac{1}{4} & 0 & 0 & -\frac{1}{2} & -\frac{1}{4} \end{array}\right]$$

and

$$B = \begin{bmatrix} B_1 & 0 & 0 & 0 \\ 0 & B_2 & 0 & 0 \\ 0 & 0 & B_3 & 0 \\ 0 & 0 & 0 & B_4 \end{bmatrix} = \operatorname{diag}\left(\begin{bmatrix} 0 \\ -\frac{1}{2} \end{bmatrix}, \begin{bmatrix} 0 \\ \frac{1}{2} \end{bmatrix}, \begin{bmatrix} \frac{1}{2} \\ 0 \end{bmatrix}, \begin{bmatrix} -1 \\ -1 \end{bmatrix} \right).$$

The interconnected network dynamics are written in compact form as

$$x(k+1) = Ax(k) + Bu(k), \tag{6.8}$$

where $x = \operatorname{col}(x_1, \ldots, x_4) \in \mathbb{R}^8$ and $u = \operatorname{col}(u_1, \ldots, u_4) \in \mathbb{R}^4$. System (6.7) is not open-loop stable; some of the eigenvalues of A lie outside the open unit disk $\mathcal{B} := \{\varepsilon \in \mathbb{C} \mid |\varepsilon| < 1\}$. Moreover, it can be shown that system 3 (see Figure 6.1) is neither open-loop asymptotically stable nor stabilizable under decoupled operation, i.e., if $x_j(k)$ is zero for all $j \in \mathcal{N}_3$ and $k \in \mathbb{Z}_+$. Decentralized controller synthesis based on local state feedback is therefore not applicable here. However, since A and B satisfy the Kalman rank condition for controllability (i.e., $\operatorname{rank}([\,B\ AB\ \ldots\ A^7B\,]) = 8$), it is still possible to stabilize system (6.7) using a static full-state feedback law $u = Kx$, for some $K \in \mathbb{R}^{4\times 8}$.

In what follows, let us consider the design of such a control law for (6.7). State-of-the-art non-centralized schemes for assessing closed-loop stability usually employ a set of storage functions $\{V_i(\cdot)\}_{i\in\mathcal{I}}$ with $V_i(x_i) = x_i^\top P_i x_i$, $P_i \in \mathbb{R}^{n_i \times n_i}$, to construct a LF candidate $V(x) := \sum_{i\in\mathcal{I}} V_i(x_i) = x^\top P x$ with block-diagonal and fixed $P := \operatorname{diag}(\{P_i\}_{i\in\mathcal{I}}) \in \mathbb{R}^{n\times n}$. Note that in many approaches, the functions $V_i(\cdot)$ are not required to be a LF for their corresponding system, see, e.g., (Langbort et al., 2004; Jokić and Lazar, 2009). In this example, methods based on static feedback succeed if there exist matrices $P := \operatorname{diag}(\{P_i\}_{i\in\mathbb{Z}_{[1,4]}}) \in \mathbb{R}^{8\times 8}$, $K \in \mathbb{R}^{4\times 8}$ such that $P \succ 0$ and

$$(A + BK)^\top P (A + BK) - P \prec 0, \tag{6.9}$$

in accordance with (5.2b), i.e., the requirement that $V(x)$ monotonically decreases to 0 along the system trajectories. Verifying the existence of matrices

P, K that satisfy the above inequality amounts to solving a semi-definite program ((6.9) can be rewritten into linear form via the Schur complement rule), which is tractable for the small NDS considered here. Using this approach, it can be shown that there is no block-diagonal $P := \mathrm{diag}(\{P_i\}_{i\in\mathbb{Z}_{[1,4]}})$ with $P_i \in \mathbb{R}^{2\times 2}$, $i \in \mathbb{Z}_{[1,4]}$, that satisfies (6.9). This is in line with Theorem 6.3.1 and the observation that system 3 cannot be stabilized under decoupled operation. As a result, conventional scalable design of fixed state-feedback control schemes, including non-centralized approaches that rely on structured (e.g., block-diagonal) K, see (Sandell et al., 1978; Šiljak, 1991), fails. However, note that the above described impediment is not merely applicable to fixed state-feedback — Theorem 6.3.1 implies that scalable stabilization techniques that belong to the framework of model predictive control, see, e.g., (Dunbar, 2007; Alessio and Bemporad, 2007; Raimondo et al., 2007), and dynamic feedback schemes such as the dissipativity-based scheme provided in (Langbort et al., 2004) are not able to stabilize network (6.7) either.[2] For all of these methods, the stability guarantee completely depends on the existence of fixed quadratic storage functions.

Motivated by the above observations, the aim of this chapter is to provide a scalable, numerical method for synthesizing, on-line, trajectory-dependent stabilizing control sequences for discrete-time NDS (6.7). This is attained by relaxing the conditions for closed-loop stability using *parameterized storage functions*.

6.4 Main results

Let $c_1 \in \mathbb{R}_{>0}$, $c_2 \in \mathbb{R}_{\geq c_1}$ and consider a Lyapunov function with quadratic bounds, i.e., a LF $V : \mathbb{R}^n \to \mathbb{R}_+$ that satisfies $\alpha_1(\|x\|) \leq V(x) \leq \alpha_2(\|x\|)$ with $\alpha_1(s) := c_1 s^2$ and $\alpha_2(s) := c_2 s^2$.

Lemma 6.4.1 *The following two statements are equivalent:*

(i) System (6.6) *is GES.*

(ii) System (6.6) *admits a LF with quadratic bounds.*

[2] The approach provided in (Langbort et al., 2004) is designed for continuous-time dynamics, yet the corresponding stability guarantee carries over *mutatis mutandis* to a discrete-time version of the method. Note that in contrast to the class of networks considered in (Langbort et al., 2004), in our modeling framework we do not allow for direct feed-through of local control actions u_i or interconnection terms $v_i(x_{\mathcal{N}_i})$ to the systems $\{j \in \mathcal{I} \mid i \in \mathcal{N}_j\}$. Theorem 6.3.1 applies to the reduced models that are obtained when all algebraic loops associated with this kind of direct feed-through are eliminated.

Lemma 6.4.1 is proven in (Jiang and Wang, 2002, Thm. 2), for the general case of time-varying V and system dynamics. Next, we extend this result by showing that every LF with quadratic bounds can be decomposed into a set of local, quadratic storage functions, each parameterized by a full-state-dependent matrix $\widetilde{P}_i(x) \in \mathbb{R}^{n_i \times n_i}$, $i \in \mathcal{I}$.

Lemma 6.4.2 *Let $V(x)$ be a LF for* (6.6) *with quadratic bounds. Then there exist $\widetilde{P}_i(x) \in \mathbb{R}^{n_i \times n_i}$, $i \in \mathcal{I}$, such that $V(x) = \max_{i\in\mathcal{I}} V_i(\widetilde{P}_i(x), x_i)$ with $V_i(\widetilde{P}_i(x), x_i) = x_i^\top \widetilde{P}_i(x) x_i$, for all $x_i \in \mathbb{R}^{n_i}$.*

For the proof, see Appendix D.2. Next, let $\mathbb{P} := \mathbb{P}_1 \times \ldots \mathbb{P}_N$, with $\mathbb{P}_i := \mathbb{R}^{n_i \times n_i}$, $i \in \mathcal{I}$, denote a set of real-valued parameter matrices. Given $c_{1,i} \in \mathbb{R}_{>0}$, $c_{2,i} \in \mathbb{R}_{\geq c_{1,i}}$ and $\rho_i \in \mathbb{R}_{[0,1)}$ for all $i \in \mathcal{I}$, consider a collection of functions $\{V_i\}_{i\in\mathcal{I}}$ with $V_i(P_i, x_i) := x_i^\top P_i x_i$, $P_i \in \mathbb{P}_i$, $x_i \in \mathbb{R}^{n_i}$, that satisfy

$$c_{1,i}\|x_i\|_2^2 \leq V_i(P_{1,i}, x_i) \leq c_{2,i}\|x_i\|_2^2 \tag{6.10a}$$

$$V_i(P_{2,i}, x_i^+) \leq \rho_i \max_{j\in\mathcal{I}} V_j(P_{1,j}(x), x_j), \tag{6.10b}$$

for all $i \in \mathcal{I}, x \in \mathbb{R}^n, x^+ = \Phi(x)$, and some $\big(\{P_{1,i}\}_{i\in\mathcal{I}}, \{P_{2,i}\}_{i\in\mathcal{I}}\big) \in \mathbb{P}^2$. Moreover, let $\mathcal{P}_\mathrm{s} : \mathbb{R}^n \rightrightarrows \mathbb{P}^2$ be the set-valued map

$$\mathcal{P}_\mathrm{s}(x) := \left\{ \big(\{P_{1,i}\}_{i\in\mathcal{I}}, \{P_{2,i}\}_{i\in\mathcal{I}}\big) \in \mathbb{P}^2 \;\middle|\; (6.10) \text{ holds} \right\}. \tag{6.11}$$

For arbitrary $x \in \mathbb{R}^n$, $\mathcal{P}_\mathrm{s}(x) \neq \emptyset$ means that there is at least one pair

$$(\{P_{1,i}\}_{i\in\mathcal{I}}, \{P_{2,i}\}_{i\in\mathcal{I}}) \in \mathbb{P}^2$$

that satisfies (6.10). To distinguish between the outputs of $\mathcal{P}_\mathrm{s}$, we use $[\mathcal{P}_\mathrm{s}(x)]_1 \subseteq \mathbb{P}$ and $[\mathcal{P}_\mathrm{s}(x)]_2 \subseteq \mathbb{P}$ to denote the sets where the first and second component of a pair $(\{P_{1,i}\}_{i\in\mathcal{I}}, \{P_{2,i}\}_{i\in\mathcal{I}})$ satisfying (6.10) take values, respectively. With slight abuse of notation, let $P_\mathrm{s}(x) := \{P_{\mathrm{s},i}(x)\}_{i\in\mathcal{I}}$ represent any $\{P_{1,i}\}_{i\in\mathcal{I}} \in [\mathcal{P}_\mathrm{s}(x)]_1$.

Definition 6.4.3 A set of functions $V_i(P_{\mathrm{s},i}(x), x_i) := x_i^\top P_{\mathrm{s},i}(x) x_i$, $i \in \mathcal{I}$, that satisfy

$$\mathcal{P}_\mathrm{s}(x) \neq \emptyset, \quad \forall x \in \mathbb{R}^n, \tag{6.12a}$$

$$[\mathcal{P}_\mathrm{s}(x)]_2 \cap [\mathcal{P}_\mathrm{s}(\Phi(x))]_1 \neq \emptyset, \quad \forall x \in \mathbb{R}^n, \tag{6.12b}$$

is called a set of *parameterized quadratic storage functions (p-qSFs)* for (6.6). ■

Clearly, p-qSFs are comparable to p-qLFs (cf. Definition 6.2.1) that act on local state vectors only. Both types of functions are endowed with a set of parameters to obtain convergence constraints (i.e., (6.10b) and (6.2b), respectively)

that are less conservative than the convergence conditions associated with conventional, fixed-parameter LFs. However, note that in contrast to p-qLFs, we do not require p-qSFs to decrease monotonically. Indeed, (6.10b) permits V_i to increase, as long as its subsequent value does not exceed ρ_i times the maximum over all the current V_i values in the network. This relaxation is crucial for non-centralized stability analysis: it allows local states x_i (and thus, by construction, the corresponding $V_i(\cdot, x_i)$) that are zero at time instant k to attain non-zero values at instant $k+1$ as a consequence of system interactions and non-zero $x_{\mathcal{N}_i}(k)$.

Now consider the following result for a network of interconnected (closed-loop) dynamics, i.e., (6.6).

Corollary 6.4.4 *The following statements are equivalent:*

(i) System (6.6) *is GES.*

(ii) System (6.6) *admits a set of p-qSFs.*

Corrolary 6.4.4 directly follows from Lemma 6.4.1 and Lemma 6.4.2, by observing that $V_i(P_{\mathrm{s},i}(x), x_i)$ with $P_{\mathrm{s},i}(x) := \widetilde{P}_i(x)$ as defined by (D.3) yields p-qSFs that satisfy (6.10) with $c_{1,i} = c_1$, $c_{2,i} = c_2$, and $\rho_i = \rho$, $i \in \mathcal{I}$. Thus, given a set of parameterized quadratic storage functions, it is possible to construct a LF for the full, interconnected system by selecting, at each time instant, the largest of their values. Local functions whose maximum defines a LF are frequently used in NDS stability studies, see, e.g., (Dashkovskiy et al., 2010), which deals with establishing input-to-state stability for networked systems that are subject to disturbances. However, in contrast to the method employed in (Dashkovskiy et al., 2010), (6.10b) does not require any of the functions V_i to be a LF for its corresponding local system dynamics, which decreases conservatism considerably.

6.4.1 Distributed controller synthesis

Based on the above results, we now provide two non-centralized synthesis solutions for the stabilization of NDS. Firstly, we focus on a full-state feedback scheme that serves as the starting point for both approaches. For this, consider a NDS with graph $\mathcal{G} = (\mathcal{S}, \mathcal{E})$, and let each system $\varsigma_i \in \mathcal{S}$ be governed by the dynamics

$$x_i(k+1) = \psi_i(x_i(k), v_i(x_{\mathcal{N}_i}(k)), u_i(k)), \quad k \in \mathbb{Z}_+. \tag{6.13}$$

Here, $x_i(k) \in \mathbb{R}^{n_i}$, $v_i(x_{\mathcal{N}_i}(k)) \in \mathbb{R}^{n_{v_i}}$ and $u_i(k) \in \mathbb{R}^{m_i}$. The functions $\psi_i : \mathbb{R}^{n_i} \times \mathbb{R}^{n_{v_i}} \times \mathbb{R}^{m_i} \to \mathbb{R}^{n_i}$ satisfy $\psi_i(0_{n_i}, 0_{n_{v_i}}, 0_{m_i}) = 0_{n_i}$ for all $i \in \mathcal{I}$. Note that this modeling framework does not allow for direct feed-through of the local input signals

to the neighbors, i.e., we necessarily have $v_i(x_{\mathcal{N}_i}(k))$, and not $v_i(x_{\mathcal{N}_i}(k), u_{\mathcal{N}_i}(k))$ with $u_{\mathcal{N}_i}(k) := \text{col}(\{u_j(k)\}_{j\in\mathcal{N}_i})$.

Given Definition 6.4.3, let us formulate an optimization control problem to be solved on-line, in a receding horizon fashion, that yields *trajectory-dependent* p-qSFs. This means that the computed sequences $\{P_i(x(k))\}_{k\in\mathbb{Z}_+}$ can be used to establish asymptotic convergence only for the corresponding closed-loop trajectory $\{x(k)\}_{k\in\mathbb{Z}_+}$.

Problem 6.4.5 *Centralized p-qSF-based synthesis*
At each $k \in \mathbb{Z}_+$, let $x(k) := \text{col}(\{x_i(k)\}_{i\in\mathcal{I}})$ be known. Let $c_{1,i} \in \mathbb{R}_{>0}$, $c_{2,i} \in \mathbb{R}_{\geq c_{1,i}}$, $\rho_i \in \mathbb{R}_{[0,1)}$, $i \in \mathcal{I}$, be given and consider the following inequalities

$$c_{1,i}\|x_i(0)\|_2^2 \leq V_i(P_i(x(0)), x_i(0)) \quad \leq c_{2,i}\|x_i(0)\|_2^2 \tag{6.14a}$$

$$c_{1,i}\|x_i^+(k)\|_2^2 \leq V_i(P_i(x^+(k)), x_i^+(k)) \leq c_{2,i}\|x_i^+(k)\|_2^2 \tag{6.14b}$$

$$V_i(P_i(x^+(k)), x_i^+(k)) \leq \rho_i \max_{j\in\mathcal{I}} V_j(P_j(x(k)), x_j(k)), \tag{6.14c}$$

for all $x_i^+(k) = \psi_i(x_i(k), v_i(x_{\mathcal{N}_i}(k)), u_i(k))$, $i \in \mathcal{I}$. If $k = 0$, find $u_i(0) \in \mathbb{R}^{m_i}$ and $P_i(x(0)), P_i(x^+(0)) \in \mathbb{P}_i$ that satisfy (6.14). If $k \in \mathbb{Z}_{\geq 1}$, set $P_i(x(k)) = P_i(x^+(k-1))$ and find $u_i(k) \in \mathbb{R}^{m_i}, P_i(x^+(k)) \in \mathbb{P}_i$ that satisfy (6.14b)–(6.14c). ■

Notice that apart from the $\max_{j\in\mathcal{I}} V_j(\cdot)$-term in (6.14c), conditions (6.14) concern subsystem parameters only. This allows for a non-centralized implementation of Problem 6.4.5, by assigning the synthesis of $P_i(x(k))$ and $u_i(k)$ to network node $i \in \mathcal{I}$, while providing it with knowledge of the i-th subsystem model, i.e., (6.13), state information $(x_i, v_i(x_{\mathcal{N}_i}))$ and the value of $\max_{j\in\mathcal{I}} V_j(\cdot)$. The latter can be determined efficiently via multi-branched recursive communication, see (Cormen et al., 2001).

Next, let $\overline{\pi}_i : \mathbb{R}^n \times \mathbb{P} \to \mathbb{R}^{m_i}$ and $\overline{\phi}_i^P : \mathbb{R}^n \times \mathbb{P} \to \mathbb{P}$ be a feedback law and control function that select an arbitrary control action u_i and set of parameters $P_i(x^+)$, $i \in \mathcal{I}$, out of the set of solutions to Problem 6.4.5 for each $x \in \mathbb{R}^n$ and $P(x) := \{P_i(x)\}_{i\in\mathcal{I}} \in \mathbb{P}$, respectively. Moreover, let

$$x_i(k+1) = \overline{\phi}_i(x(k), P(x(k))) \tag{6.15a}$$

$$P_i(x(k+1)) = \overline{\phi}_i^P(x(k), P(x(k))), \quad k \in \mathbb{Z}_+, \tag{6.15b}$$

with $\overline{\phi}_i(x) := \psi_i(x_i, v_i(x_{\mathcal{N}_i}), \overline{\pi}_i(x, P(x)))$, describe system (6.13) in closed-loop with global-state feedback law $\overline{\pi}_i$ and control function $\overline{\phi}_i^P$.

Let $\mathbb{X}$ be some subset of $\mathbb{R}^n$. In what follows, for all considered state, control action and parameter sequences $\{x(k)\}_{k\in\mathbb{Z}_+}$, $\{u(k)\}_{k\in\mathbb{Z}_+}$ and $\{P(x(k))\}_{k\in\mathbb{Z}_+}$, respectively, we adopt the following standing assumption.

Assumption 6.4.6 For every $x(0) \in \mathbb{X}$ and $k \in \mathbb{Z}_+$, the sequences $\{u(l)\}_{l\in\mathbb{Z}_{[0,k-1]}}$, $\{x(l)\}_{l\in\mathbb{Z}_{[0,k]}}$ and $\{P(x(l))\}_{l\in\mathbb{Z}_{[0,k-1]}}$ are such that Problem 6.4.5 is feasible at all $k \in \mathbb{Z}_{\geq 1}$. ■

Now consider the following result.

Theorem 6.4.7 *Let $\{x(k)\}_{k\in\mathbb{Z}_+}$, $\{P(x(k))\}_{k\in\mathbb{Z}_+}$ with $x(0) = x_0 \in \mathbb{X}$ be state and parameter trajectories generated by* (6.15)*. Then, $\lim_{k\to\infty} \|x(k)\| = 0$; more specifically, $\|x(k)\|$ converges exponentially to the origin.*

Theorem 6.4.7 is proven in Appendix D.3. Even though methods for evaluating $\max_{j\in\mathcal{I}} V_j(\cdot)$ in an efficient, distributed fashion exist, the corresponding extent of communication might still be infeasible for certain large-scale applications. In what follows, we will therefore propose a way to further decentralize the parameterized stabilization problem, by generating $V_i(P_i(x(k)), x_i(k))$ and $u_i(k)$ based on local information only.

Let $\{J_i(\cdot)\}_{i\in\mathcal{I}}$ with $J_i(\lambda_i) := \lambda_i$ for $\lambda_i \in \mathbb{R}_+$ be a set of cost functions. Now consider the following problem.

Problem 6.4.8 *Almost-decentralized p-qSF-based synthesis*
Consider Problem 6.4.5, but replace (6.14c) by

$$V_i(P_i(x^+(k)), x_i^+(k)) \leq \rho_i \max_{j\in\overline{\mathcal{N}}_i} V_j(P_j(x(k)), x_j(k)) + \lambda_i(k) \tag{6.16a}$$

$$\lambda_i(k) \geq 0, \tag{6.16b}$$

for all $x_i^+(k) = \psi_i(x_i(k), v_i(x_{\mathcal{N}_i}(k)), u_i(k))$, $i \in \mathcal{I}$. If $k = 0$, minimize $J_i(\lambda_i(0))$ over $u_i(0) \in \mathbb{R}^{m_i}$, $P_i(x(0)), P_i(x^+(0)) \in \mathbb{P}_i$ and $\lambda_i(0)$ such that (6.14a)–(6.14b) and (6.16) hold. If $k \in \mathbb{Z}_{\geq 1}$, set $P_i(x(k)) = P_i(x^+(k-1))$ and minimize $J_i(\lambda_i(k))$ over $u_i(k) \in \mathbb{R}^{m_i}$, $P_i(x^+(k)) \in \mathbb{P}_i$ and $\lambda_i(k)$ such that (6.14b) and (6.16) hold. ■

Note that in Problem 6.4.8, only subsystem model (6.13) and the values of x_i, $v_i(x_{\mathcal{N}_i})$ and $\max_{j\in\overline{\mathcal{N}}_i} V_j(\cdot)$ are required to synthesize $P_i(x^+)$, u_i and λ_i. From $\overline{\mathcal{N}}_i := \mathcal{N}_i \cup \{i\}$, it follows that a single run of information exchange among direct neighbors is sufficient to acquire this knowledge.

Next, let $\pi_i : \mathbb{R}^{n_i} \times \mathbb{R}^{n_{v_i}} \times \mathbb{P}_{\overline{\mathcal{N}}_i} \to \mathbb{R}^{m_i}$ and $\phi_i^P : \mathbb{R}^{n_i} \times \mathbb{R}^{n_{v_i}} \times \mathbb{P}_{\overline{\mathcal{N}}_i} \to \mathbb{P}_i$ be a feedback law and control function that select an arbitrary control action u_i and set of parameters $P_i(x^+)$, $i \in \mathcal{I}$, from the solution set of Problem 6.4.8 for each $(x_i, v_i(x_{\mathcal{N}_i})) \in \mathbb{R}^{n_i} \times \mathbb{R}^{n_{v_i}}$ and $P_{\overline{\mathcal{N}}_i}(x) := \{P_j(x)\}_{j\in\overline{\mathcal{N}}_i} \in \mathbb{P}_{\overline{\mathcal{N}}_i}$, respectively. Since $\lambda_i(k)$ is unbounded from above for all $k \in \mathbb{Z}_+$, Problem 6.4.8 is recursively

feasible and π_i is well-defined for all $i \in \mathcal{I}$. Let

$$x_i(k+1) = \phi_i(x_i(k), v_i(x_{\mathcal{N}_i}(k)), P_{\overline{\mathcal{N}}_i}(x(k))) \tag{6.17a}$$

$$P_i(x(k+1)) = \phi_i^P(x_i(k), v_i(x_{\mathcal{N}_i}(k)), P_{\overline{\mathcal{N}}_i}(x(k))) \tag{6.17b}$$

with $\phi_i(x_i, v_i(x_{\mathcal{N}_i}), P_{\overline{\mathcal{N}}_i}(x)) := \psi_i(x_i, v_i(x_{\mathcal{N}_i}), \pi_i(x_i, v_i(x_{\mathcal{N}_i}), P_{\overline{\mathcal{N}}_i}(x)))$, denote the difference equation corresponding to (6.13) in closed-loop with local-state feedback law π_i and control function ϕ_i^P. Let $\lambda_i^*(k)$ denote the λ_i that optimizes Problem 6.4.8 at instant $k \in \mathbb{Z}_+$.

Now consider the following theorem.

Theorem 6.4.9 *Let $\{x(k)\}_{k\in\mathbb{Z}_+}$ with $x(0) = x_0 \in \mathbb{X}$ and $\{P(x(k))\}_{k\in\mathbb{Z}_+}$ be a state and parameter trajectory generated by* (6.17)*. Then,* $\lim_{k\to\infty} \|x(k)\| = 0$*; more specifically,* $\|x(k)\|$ *converges exponentially to the origin.*

Theorem 6.4.9 is proven in Appendix D.4. In contrast to (6.14), conditions (6.14a)–(6.14b) and (6.16) concern local/neighbor system parameters only. Thus, we have obtained a scalable control scheme that guarantees closed-loop stability based on *non-iterative neighbor-to-neighbor communication only*.

Remark 6.4.10 Assumption 6.4.6, that is, recursive feasibility of (6.14b)–(6.14c), is crucial in showing that the control law defined by Problem 6.4.5 (and consequently, Problem 6.4.8) yields converging closed-loop trajectories. Guaranteeing that Problem 6.4.5 is feasible for all $x(k) \in \mathbb{R}^n$, $k \in \mathbb{Z}_+$, can be challenging, as it implies feasibility for all $P_i(x(k))$ such that

$$c_{1,i}\|x_i(k)\|_2^2 \leq V_i(P_i(x(k)), x_i(k)) \leq c_{2,i}\|x_i(k)\|_2^2.$$

Still, recursive feasibility may be facilitated by selecting $P_i(x^+(k))$ in a way that relaxes conditions (6.14b)–(6.14c) as much as possible *at the next time instant*. More specifically, for the quadratic storage functions $V_i(P_i(x), x_i) = x_i^\top P_i(x) x_i$ considered here, this involves maximizing the eigenvalues of $P_i(x^+(k))$ or minimizing the decrease in $V_i(\cdot)$, i.e., by extending Problem 6.4.5 with the following separable objective and constraints:

$$\max_{\{\varepsilon_i, \delta_i\}_{i\in\mathcal{I}}} \sum_{i\in\mathcal{I}} (\varepsilon_i - w_\delta \delta_i) \tag{6.18a}$$

subject to

$$\varepsilon_i I_{n_i} \preceq P_i(x^+(k)) \tag{6.18b}$$

$$V_i(P_i(x^+(k)), x_i^+(k)) - \rho_i \max_{j\in\mathcal{I}} V_j(P_j(x(k)), x_j(k)) \leq \delta_i, \tag{6.18c}$$

where $w_\delta \in \mathbb{R}_+$ is some scalar weight. ■

6.4.2 Implementation via on-line convex optimization

Next, we show that for input-affine NDS and quadratic parameterized storage functions, Problem 6.4.8 is equivalent to solving, on-line, a set of low-complexity semi-definite programming problems. Such problems can be efficiently solved using interior-point methods. These algorithms typically find the solution to an SDP up to an additive error ϵ within a time frame that is polynomial in the program size (and thus, in this case subsystem order n_i, as shown below) and $\log(1/\epsilon)$, see, e.g., (Todd, 2001).

Consider NDS dynamics (6.13) with

$$\psi_i(x_i, v_i(x_{\mathcal{N}_i}), u_i) := f_i(x_i, v_i(x_{\mathcal{N}_i})) + g_i(x_i, v_i(x_{\mathcal{N}_i}))u_i, \tag{6.19}$$

for $i \in \mathcal{I}$, where $x_i \in \mathbb{R}^{n_i}$, $u_i \in \mathbb{R}^{m_i}$, $f_i : \mathbb{R}^{n_i} \times \mathbb{R}^{n_{v_i}} \to \mathbb{R}^{n_i}$, $g_i : \mathbb{R}^{n_i} \times \mathbb{R}^{n_{v_i}} \to \mathbb{R}^{n_i \times m_i}$, such that $f_i(0_{n_i}, 0_{n_{v_i}}) = 0_{n_i}$. Let $\gamma_i \in \mathbb{R}_{>0}$, $\Gamma_i \in \mathbb{R}_{\geq \gamma_i}$ and let $P_i(x(0)) = \Gamma_i I_{n_i}$. Now consider the linear matrix inequalities

$$Z_i(k) \succeq \Gamma_i^{-1} I_{n_i}, \quad Z_i(k) \preceq \gamma_i^{-1} I_{n_i}, \quad \lambda_i(k) \geq 0 \tag{6.20a}$$

$$\begin{bmatrix} \rho_i \max\limits_{j \in \overline{\mathcal{N}}_i} x_j(k)^\top P_j(x(k)) x_j(k) + \lambda_i(k) & * \\ \widetilde{f}_i(x(k)) + \widetilde{g}_i(x(k)) u_i(k) & Z_i(k) \end{bmatrix} \succeq 0, \tag{6.20b}$$

where $\widetilde{f}_i(x) := f_i(x_i, v_i(x_{\mathcal{N}_i}))$ and $\widetilde{g}_i(x) := g_i(x_i, v_i(x_{\mathcal{N}_i}))$.

Lemma 6.4.11 *At time $k \in \mathbb{Z}_+$ and node $i \in \mathcal{I}$, let $x_i(k)$, $x_{\mathcal{N}_i}(k)$, ρ_i, γ_i, Γ_i and $\{P_j(x(k))\}_{j \in \overline{\mathcal{N}}_i}$ be given. Suppose that $\{Z_i(k), u_i(k), \lambda_i(k)\}$ is a solution of* (6.20)*. Then $P_i(x^+(k)) = Z_i(k)^{-1}$, $u_i(k)$ and $\lambda_i(k)$ is a solution of* (6.14b) *and* (6.16a)–(6.16b) *with $c_{1,i} := \gamma_i$ and $c_{2,i} := \Gamma_i$.*

The above result is proven in Appendix D.5. Lemma 6.4.11 provides a scalable SDP-based control scheme for networks of interconnected input-affine systems. The resulting set of local control laws is stabilizing under recursive feasibility of Problem 6.4.5, or, if Problem 6.4.8 is considered, under optimality with respect to the linear local cost functions $J_i(\lambda_i)$ for all time instants $k \in \mathbb{Z}_+$.

6.5 Stabilization via distributed interpolation

In what follows, we describe how the exponentially converging sequences generated by Problem 6.4.5 and Problem 6.4.8 can be used to obtain a practical, non-centralized stabilizing control law for a network of linear, time-invariant systems. Such networks are described by (6.13) with

$$\psi_i(x_i, v_i(x_{\mathcal{N}_i}), u_i) := A_{ii} x_i + v_i(x_{\mathcal{N}_i}) + B_i u_i, \tag{6.21}$$

for $i \in \mathcal{I}$, $v_i(x_{\mathcal{N}_i}) := \sum_{j\in\mathcal{N}_i} A_{ij}x_j$ and matrices $A_{ij} \in \mathbb{R}^{n_i\times n_j}$, $B_i \in \mathbb{R}^{n_i\times m_i}$.

For each system $i \in \mathcal{I}$ in the network, let there be a finite collection of $L_i \in \mathbb{Z}_+$ vectors, i.e., $\mathcal{X}_i := \{x_i^l\}_{l\in\mathbb{Z}_{[1,L_i]}}$, $x_i^l \in \mathbb{R}^{n_i}$. These vectors are used to construct the set

$$\mathcal{X} = \{x_0^q\}_{q\in\mathbb{Z}_{[1,Q]}} := \mathcal{X}_1 \times \ldots \times \mathcal{X}_N \subset \mathbb{R}^n, \tag{6.22}$$

where $Q := L_1 \times \ldots \times L_N$. With each $x_0^q := \mathrm{col}(\{x_{0,i}^q\}_{i\in\mathcal{I}}) \in \mathcal{X}$ we associate a control sequence $\mathbf{u}^q := \{u^q(k)\}_{k\in\mathbb{Z}_+}$, $u^q(k) = \mathrm{col}(\{u_i^q(k)\}_{i\in\mathcal{I}}) \in \mathbb{R}^m$. These sequences are such that the closed-loop dynamics

$$\begin{aligned} x_i(k+1) &= \psi_i(x_i(k), v_i(x_{\mathcal{N}_i}(k)), u_i^q(k)) \\ &= A_{ii}x_i(k) + v_i(x_{\mathcal{N}_i}(k)) + B_i u_i^q(k), \qquad k \in \mathbb{Z}_+,\ i \in \mathcal{I}, \end{aligned} \tag{6.23}$$

and initial condition $x(0) = x_0^q$ generate a state sequence $\mathbf{x}(x_0^q, \mathbf{u}^q) := \{x^q(k)\}_{k\in\mathbb{Z}_+}$ that satisfies

$$\|x^q(k)\| \le c_q \|x_0^q\| \mu_q^k, \tag{6.24}$$

for some $c_q \in \mathbb{R}_{\ge 1}$ and $\mu_q \in \mathbb{R}_{[0,1)}$. By Theorem 6.4.7 (or Theorem 6.4.9), it follows that any infinite sequence of control actions generated by Problem 6.4.5 (or Problem 6.4.8) for $x(0) = x_0^q$, given Assumption 6.4.6, satisfies this exponential convergence condition (see (D.6)). From these trajectories, it is possible to extract the multisets $\mathcal{S}_i(k) \subset \mathbb{R}^{2n_i}$ of tuples

$$\xi_i(x^q(k)) := \begin{bmatrix} x_i^q(k) \\ v_i(x_{\mathcal{N}_i}^q(k)) \end{bmatrix}$$

for $q \in \mathbb{Z}_{[1,Q]}$, and where $x_{\mathcal{N}_i}^q := \mathrm{col}(\{x_j^q\}_{j\in\mathcal{N}_i})$. Note that the elements of $\mathcal{S}_i(k)$ may be non-unique; this is the case if $\xi_i(x^q(k)) = \xi_i(x^p(k))$ for some $p \ne q$, with $p, q \in \mathbb{Z}_{[1,Q]}$.

Now consider the following problem.

Problem 6.5.1 *Distributed interpolation*
Let $\mathcal{S}_i(k) = \{\xi_i(x^q(k))\}_{q\in\mathbb{Z}_{[1,Q]}}$ be given for all $k \in \mathbb{Z}_+$ and $i \in \mathcal{I}$. At time instant $k \in \mathbb{Z}_+$ and node $i \in \mathcal{I}$, obtain $\xi_i(x(k))$ and compute a combination of scalars $\alpha_i^q \in \mathbb{R}$, $q \in \mathbb{Z}_{[1,Q]}$, such that

$$\xi_i(x(k)) = \sum_{q\in\mathbb{Z}_{[1,Q]}} \alpha_i^q \xi_i(x^q(k)). \tag{6.25}$$

Then, apply the local control actions

$$u_i(k) := \sum_{q\in\mathbb{Z}_{[1,Q]}} \alpha_i^q u_i^q(k) \tag{6.26}$$

to (6.21), where $u_i^q(k)$ is the control action associated with $\xi_i(x^q(k))$. ■

Now, consider the set $\mathbb{S}_i := \{(\xi_i, k) \in \mathbb{R}^{2n_i} \times \mathbb{Z}_+ \mid \xi_i \in \text{span}(\mathcal{S}_i(k))\}$. Note that the solution to (6.25), given $\xi_i(x(k))$ is not necessarily unique; this requires linear independence of the vectors $\xi_i(x^q(k)) \in \mathcal{S}_i(k)$. Therefore, let $\pi_i^{\text{ip}} : \mathbb{S}_i \to \mathbb{R}^{m_i}$ be a feedback law that selects an arbitrary control action $u_i(k)$ out of the set of solutions to (6.25)–(6.26) for each $(\xi_i(x(k)), k) \in \mathbb{S}_i$.[3] The time-variant closed-loop dynamics associated with Problem 6.5.1 and NDS (6.21) are then given by

$$x_i(k+1) = A_{ii}x_i(k) + v_i(x_{\mathcal{N}_i}(k)) + B_i\pi_i^{\text{ip}}(\xi_i(x(k)), k), \qquad k \in \mathbb{Z}_+,\ i \in \mathcal{I}. \quad (6.27)$$

Now consider the following assumption.

Assumption 6.5.2 The feedback laws $\{\pi_i^{\text{ip}}\}_{i\in\mathcal{I}}$ are such that for all $i \in \mathcal{I}$,

$$\pi_i^{\text{ip}}(\xi_i(x(k)), k) = \textstyle\sum_{q\in\mathbb{Z}_{[1,Q]}} \alpha^q u_i^q(k)$$

if $x(k) = \sum_{q\in\mathbb{Z}_{[1,Q]}} \alpha^q x^q(k)$. ■

Assumption 6.5.2 implies that local state information, i.e., $\xi_i(x(k))$, is sufficient to recover the ensemble of local control actions $u^q(k) = \text{col}(\{u_i^q(k)\}_{i\in\mathcal{I}}) \in \mathbb{R}^m$ for the full network of interconnected systems.[4] Thus, based on a similar hypothesis as the one that was used to decentralize Problem 6.4.5/Theorem 6.4.7 and obtain a convergence guarantee for Problem 6.4.8, it is possible to derive the following result.

Theorem 6.5.3 *Suppose that Assumption 6.5.2 holds and consider* $\{x^q(k)\}_{q\in\mathbb{Z}_{[1,Q]}}$ *that satisfy* (6.24)*. Then system* (6.27) *is asymptotically stable in* $\text{span}(\mathcal{X})$*.*

For the proof, see Appendix D.6. Theorem 6.5.3 demonstrates that, for linear time-invariant network dynamics, Problem 6.5.1 can be used to extend the *trajectory-specific convergence guarantee* provided by Problem 6.4.5 and Problem 6.4.8 to a much stronger guarantee of *asymptotical stability with respect to a subset of the state space*. Now consider the following implication of Theorem 6.5.3.

Corollary 6.5.4 *Let* $\mathcal{X} = \{x_0^q\}_{q\in\mathbb{Z}_{[1,Q]}}$ *contain* $n \leq Q$ *linear independent vectors* $x_0^q \in \mathbb{R}^n$*, and suppose that Assumption 6.5.2 and* (6.24) *hold. Then, system* (6.27) *is GAS.*

[3] Note that the control law defined by Problem 6.5.1 is time variant, as the set of vectors $\xi_i(x^q(k))$, i.e., $\mathcal{S}_i(k)$, employed in (6.25) depends on k.

[4] Note that in case of system-wide communication/coordination, e.g., if $\overline{\mathcal{N}}_i = \mathcal{I}$ for all $i \in \mathcal{I}$, it is rather easy to fulfil this requirement.

Corollary 6.5.4 readily follows from Theorem 6.5.3 and the observation that $\text{span}(\mathcal{X}) = \mathbb{R}^n$. This result implies that, by employing Problem 6.4.5 (or, Problem 6.4.8) to generate trajectories for appropriate initial conditions $x_0^q \in \mathbb{R}^n$, we can obtain a *global stabilizing control law* for the corresponding network of interconnected systems using a non-centralized interpolation procedure. Problem 6.5.1 relies on feedback of local and neighboring states only, and the solution of a simple set of linear equations, i.e., (6.25), is sufficient for obtaining stabilizing control actions. Thus, no online optimization is required; for n linearly independent tuples $\xi_i(x^q(k))$, the explicit solution to (6.25)–(6.26) is given by the linear relation

$$u_i(k) = \begin{bmatrix} u_i^1(k) & \dots & u_i^n(k) \end{bmatrix} \begin{bmatrix} \xi_i(x^1(k)) & \dots & \xi_i(x^n(k)) \end{bmatrix}^{-1} \xi_i(x(k)). \tag{6.28}$$

Implementation of Problem 6.5.1 is tractable only if there exists a finite integer $k^* \in \mathbb{Z}_+$ such that $x^q(k) = 0$ and $u^q(k) = 0$ for $k \in \mathbb{Z}_{\geq k^*}$. Then, all trajectories consist of a finite number of non-zero elements and as such, the memory required for implementing Problem 6.5.1 on dedicated computing hardware is bounded. Note also that in this case, finite-time convergence is obtained, i.e., the corresponding closed-loop trajectories satisfy $x(k) = 0_n$ and $u(k) = 0_m$ for $k \in \mathbb{Z}_{\geq k^*}$.

Remark 6.5.5 So far, we have only considered the stabilization of unconstrained networks of dynamical systems. Yet in practice, many NDS applications come with strict constraints on the state and control actions. Problem 6.4.5 and Problem 6.4.8 can be readily extended with a set of system-specific, separable constraints (i.e., by requiring that $\psi_i(x_i(k), v_i(x_{\mathcal{N}_i}(k)), u_i(k)) \in \mathbb{X}_i \subset \mathbb{R}^{n_i}$ and $u_i(k) \in \mathbb{U}_i \subset \mathbb{R}^{m_i}$ for all $k \in \mathbb{Z}_+$) to synthesize converging, feasible trajectories in a non-centralized, non-iterative fashion. For linear dynamics and convex sets $\mathbb{X}_i$ and $\mathbb{U}_i$, this feasibility guarantee can be inherited by the distributed interpolation scheme, if (6.25) is extended with the requirement that $\alpha_i^q \in \mathbb{R}_{[0,1]}$ and $\sum_{i\in\mathcal{I}} \alpha_i^q = 1$. Then, (6.26) and (D.9) imply that $u_i(k) \in \text{conv}(\{u_i^q(k)\}_{q\in\mathbb{Z}_{[1,Q]}}) \subseteq \mathbb{U}_i$ and $x_i(k) \in \text{conv}(\{x_i^q(k)\}_{q\in\mathbb{Z}_{[1,Q]}}) \subseteq \mathbb{X}_i$ for all $k \in \mathbb{Z}_+$. ■

6.6 Simulation results

First, p-qSF-based controller synthesis is illustrated for the network of linear time-invariant systems provided in Section 6.3, using the SDP-based implementation given in Section 6.4.2. Network (6.7) is described by (6.19) with

$$\begin{aligned} f_i(x_i, v_i(x_{\mathcal{N}_i})) &:= A_{ii}x_i + \textstyle\sum_{j\in\mathcal{N}_i} A_{ij}x_j \\ g_i(x_i, v_i(x_{\mathcal{N}_i})) &:= B_i, \end{aligned} \tag{6.29}$$

for $i \in \mathbb{Z}_{[1,4]}$. In the simulations, the values $\gamma_i = 0.1$, $\Gamma_i = 1$ and $\rho_i = 0.95$ were used for all $i \in \mathbb{Z}_{[1,4]}$. Figure 6.2 shows the trajectories of $x(k)$, $u_i(k)$ and $\lambda_i(k)$ as generated by Problem 6.4.8 in closed-loop with (6.7) for initial condition $x(0) = [-0.59\ -0.91\ -0.05\ -0.76\ 0.65\ -0.96\ 0.46\ 0.50]^\top$. The numbers in the $\lambda_i(k)$ plot denote the index of the "dominant subsystem", i.e., $\arg\max_{i\in\mathbb{Z}_{[1,4]}} V_i(P_i(x(k)), x_i(k))$ at discrete-time instants $k \in \mathbb{Z}_{[0,15]}$. The evolution of $V_i(P_i(x(k)), x_i(k))$ and $V(P(x(k)), x(k)) := \max_{i\in\mathbb{Z}_{[1,4]}} V_i(P_i(x(k)), x_i(k))$ is depicted in Figure 6.3. Therein, it can be observed that even though the functions $V_i(\cdot)$ are not enforced to decrease monotonically, the corresponding full-network Lyapunov candidate $V(\cdot)$ does, which in turn results in asymptotically converging state trajectories. Also, note that $\lambda_3(k) \neq 0$ for $k \in \{4, 9\}$, to relax convergence condition (6.16a) on $V_3(\cdot)$ as $\arg\max_{j\in\mathbb{Z}_{[1,4]}} V_j(P_j(x(k)), x_j(k)) = 1 \notin \overline{\mathcal{N}}_3$ at these time instants. Consequently, the control problem remains feasible and asymptotically converging closed-loop state trajectories are obtained even though each controller employs local information only. Figure 6.4 shows the level sets of $V_i(P_i(x(k)), x_i(k))$, $i \in \mathbb{Z}_{[1,4]}$, i.e.,

$$\left\{ z \in \mathbb{R}^2 \,\middle|\, V_i(P_i(x(k)), z) = \frac{1}{2} \right\}_{k\in\mathbb{Z}_{[0,15]}}.$$

Note that the change in $P_4(x(k))$, corresponding to the sparsely-connected system 4, is rather small. Still, the strong variation of the level sets for the other systems shows that in this simulation, the flexibility associated with p-qSF parameterization is amply exploited by controllers 1–3. This enabled synthesis of stabilizing control actions, whereas standard Lyapunov techniques that rely on fixed storage functions failed.

To illustrate the potential of Problem 6.4.8 in terms of stabilizing *nonlinear dynamics*, we summarize the results obtained by repeating the above described simulation for a network that is described by (6.19) with

$$\begin{aligned} f_i(x_i, v_i(x_{\mathcal{N}_i})) &:= A_{ii} \begin{bmatrix} \sin([x_i]_1) \\ \sin([x_i]_2) \end{bmatrix} + \sum_{j\in\mathcal{N}_i} A_{ij} \begin{bmatrix} \sin([x_j]_1) \\ \sin([x_j]_2) \end{bmatrix} \\ g_i(x_i, v_i(x_{\mathcal{N}_i})) &:= B_i, \end{aligned} \tag{6.30}$$

for $i \in \mathbb{Z}_{[1,4]}$, and where A_{ii} and B_i are given in (6.7). Existing dissipation-based stabilization techniques typically rely on off-line synthesized fixed-parameter quadratic storage functions for a *linearized* version of the plant dynamics around a particular equilibrium. The so-obtained storage functions are valid for states that lie in a certain neighborhood of this equilibrium. However, it is straightforward to see that linearization of (6.30) around its equilibrium, i.e., the origin, yields the dynamics of the motivating example network, that is, (6.7), for which

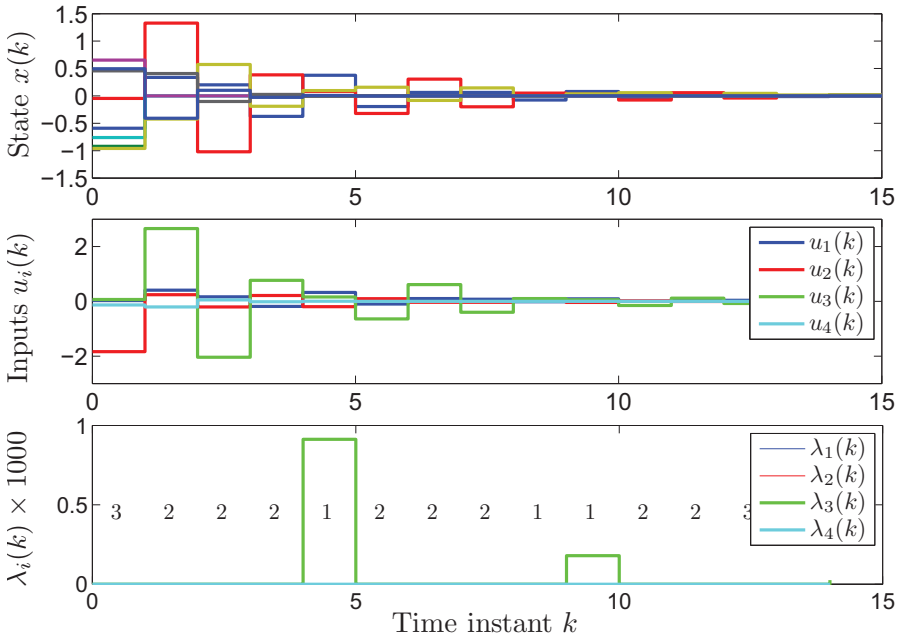

Figure 6.2: Simulated state, input and λ_i trajectories.

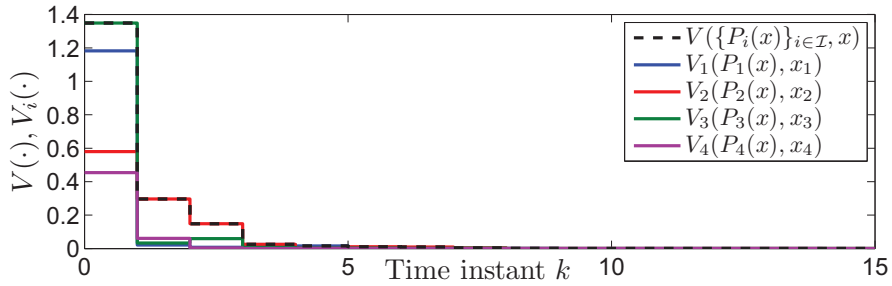

Figure 6.3: Simulated evolution of $V_i(\cdot)$ and $V(\cdot)$ over time.

synthesis of fixed-parameter quadratic SFs is not possible. Figure 6.5 depicts the trajectories of $x(k)$, $u_i(k)$ and $\lambda_i(k)$ generated by Problem 6.4.8 for the nonlinear network, which shows that synthesis of converging closed-loop trajectories is possible nevertheless, if online parameterized SF-based control is considered.

For the considered network and using the SeDuMi solver in Matlab 7 on a 2.66 GHz 3.48 GB RAM PC, the single system-specific SDPs can be solved, in parallel, within 0.1 s. The computation time is expected to be considerably lower if the control scheme is implemented on dedicated hardware.

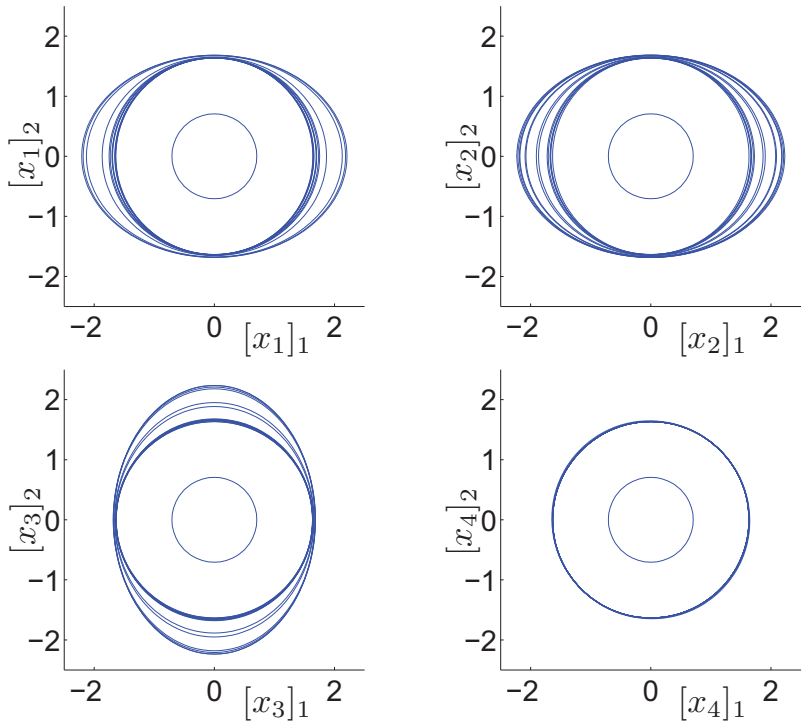

Figure 6.4: Level sets of $V_i(P_i(x(k)), x_i(k))$ for $k \in \mathbb{Z}_{[0,15]}$.

Next, we provide simulation results for the motivating example network and the distributed interpolation scheme described in Section 6.5. The multisets of trajectories $\mathcal{S}_i(k)$ employed by the algorithm were generated using Problem 6.4.8 for initial conditions in the finite set $\mathcal{X} := \mathcal{X}_1 \times \ldots \times \mathcal{X}_4 \subset \mathbb{R}^8$ with

$$\mathcal{X}_1 = \left\{ \begin{bmatrix} -\frac{1}{4} \\ 0 \end{bmatrix}, \begin{bmatrix} \frac{1}{4} \\ 0 \end{bmatrix}, \begin{bmatrix} 0 \\ -\frac{1}{4} \end{bmatrix}, \begin{bmatrix} 0 \\ \frac{1}{4} \end{bmatrix} \right\}, \quad \mathcal{X}_2 = \mathcal{X}_3 = \left\{ \begin{bmatrix} -\frac{1}{4} \\ -\frac{1}{4} \end{bmatrix}, \begin{bmatrix} \frac{1}{4} \\ \frac{1}{4} \end{bmatrix} \right\}, \quad \mathcal{X}_4 = \left\{ \begin{bmatrix} \frac{1}{10} \\ 0 \end{bmatrix} \right\}.$$

In addition, the off-line synthesized control action sequences were enforced to satisfy $u_1^q(k) \in \mathbb{U}_1 := \mathbb{R}_{[-1,1]}$ for all $i \in \mathcal{I}$ and $k \in \mathbb{Z}_+$. Figure 6.6 shows the closed-loop state and control action trajectories generated by the non-centralized interpolation scheme, i.e., Problem 6.5.1, for initial condition

$$x(0) = \begin{bmatrix} 0 & -\frac{1}{8} & -\frac{1}{10} & -\frac{1}{10} & \frac{1}{10} & \frac{1}{10} & \frac{1}{10} & 0 \end{bmatrix}^\top.$$

Note that $x(0) \in \text{conv}(\mathcal{X})$. Hence, in accordance with Remark 6.5.5, the simulations show that $u_i(k) \in \text{conv}(\{u_i^q(k)\}_{q \in \mathbb{Z}_{[1,Q]}})$, and consequently, because all $u_1^q(k)$ lie in the convex set $\mathbb{U}_1$, it holds that $u_1(k) \in \mathbb{U}_1$ for all $k \in \mathbb{Z}_+$.

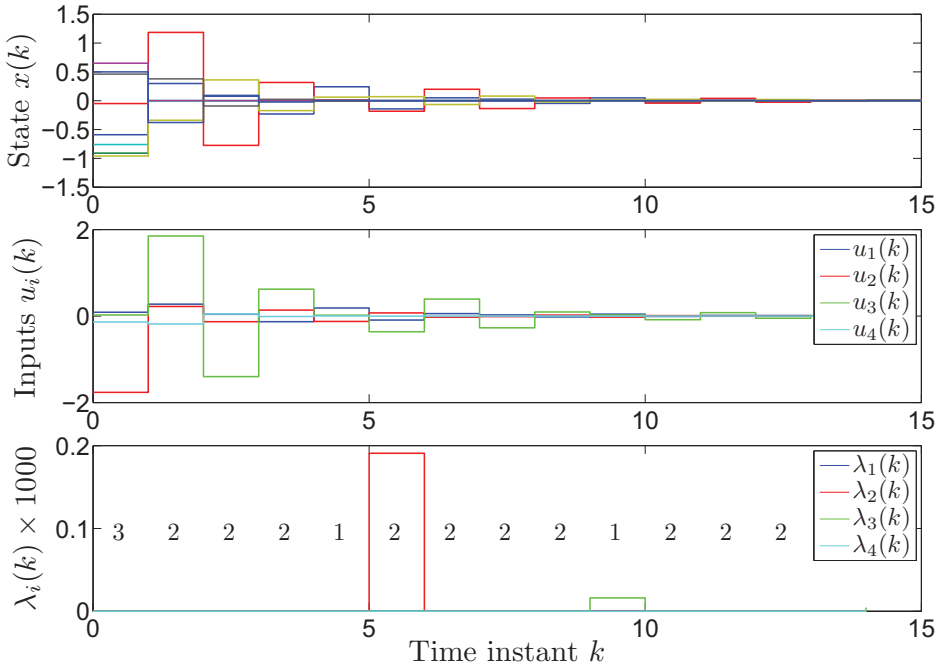

Figure 6.5: Simulated state, input and λ_i trajectories for the nonlinear network example.

6.7 Conclusions

This chapter addressed the problem of stabilizing networks of interconnected dynamical systems in a scalable way. As a first contribution, an example was provided to illustrate that standard dissipation-based NDS stabilization methods can fail even for simple unconstrained linear time-invariant dynamics. Then, a solution to this issue was proposed, by decentralizing the synthesis of stabilizing control actions via a set of parameterized storage functions. The employed convergence conditions allow for max-type construction of a trajectory-specific Lyapunov function for the full closed-loop network, whereas the parameterized functions are not required to be LFs for their respective system. The provided approach was shown to be non-conservative, in the sense that it can generate converging closed-loop trajectories for the motivating example network and a prescribed set of initial conditions. For input-affine NDS and quadratic parameterized storage functions, the synthesis scheme can be implemented by solving a single low-complexity SDP problem at each node, in a receding horizon fashion.

As additional contribution, it was shown that for linear and time-invariant networks, an even simpler, explicit control law can be constructed by interpolating a collection of a-priori generated trajectories in a distributed fashion. In combination with non-centralized trajectory synthesis, this yields a unique, scalable tool to extend the corresponding trajectory-specific convergence property to a much stronger closed-loop stability guarantee.

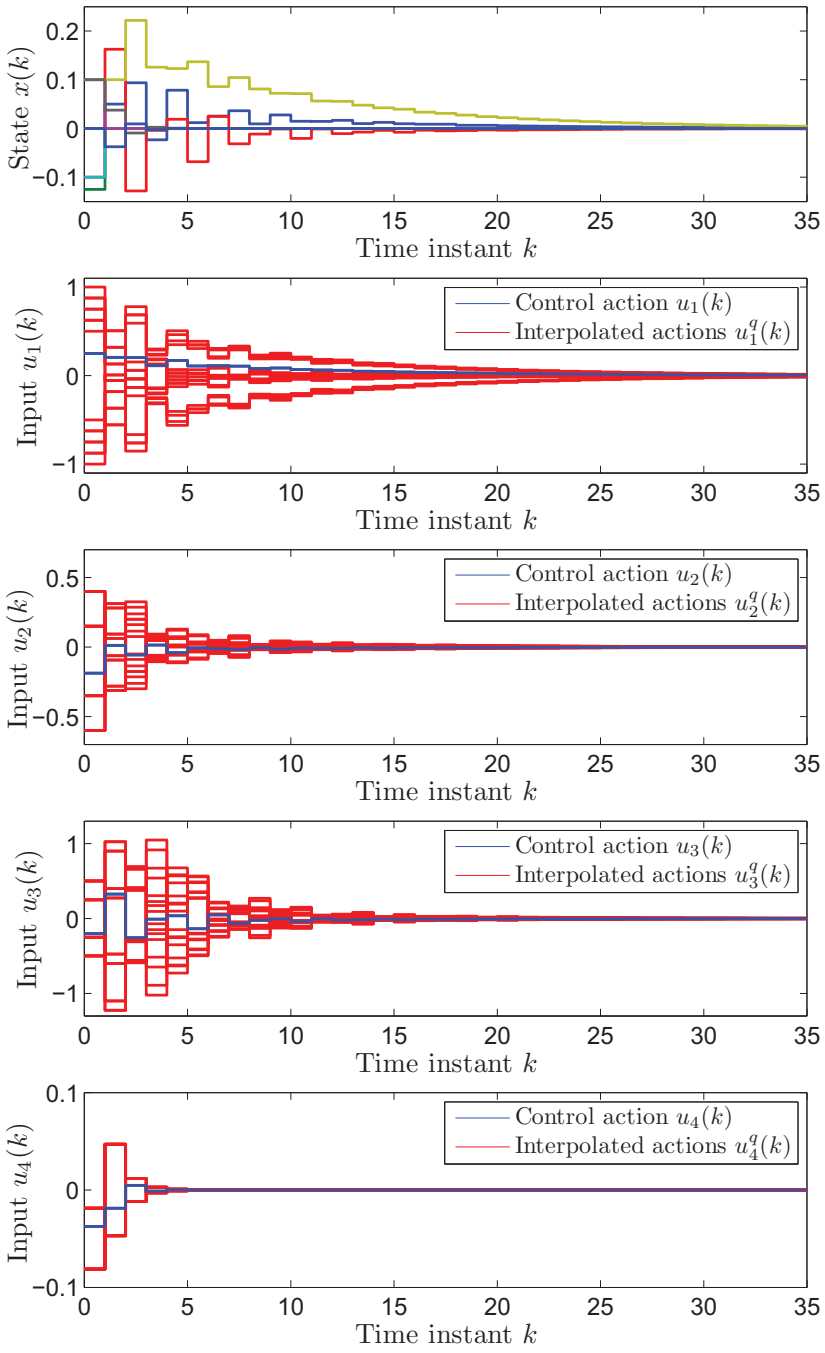

Figure 6.6: State and control action sequences generated by distributed interpolation.

7

Competitive frequency control: a case study

7.1 Introduction

In the previous two chapters, we have introduced a number of non-centralized techniques for the stabilization of networks of interacting dynamical systems (NDS). In this chapter, we return to the problem of real-time balancing or frequency control in deregulated electrical power systems. It is shown that multimachine power systems fit the NDS-modeling framework, which enables the application of the previously introduced L-MPC and p-qSF schemes for stabilization of the network power balance and frequency. Moreover, given that electrical power generators are operated by competitive, profit-driven market agents, we provide an algorithm for improving closed-loop performance in a non-cooperative fashion, by embedding the p-qSF stability conditions in a distributed, iterative optimal control scheme that relies on neighbor-to-neighbor communication only. We evaluate the suitability of the distributed Lyapunov-based predictive control and parameterized storage function algorithms as an alternative to the conventional automatic generation control method. This assessment is based on simulations in closed-loop with the 7-machine CIGRÉ benchmark system (Pai, 1981).

7.2 Multimachine power systems

N-machine power systems, such as the network shown in Figure 7.1, consist of N generator buses and a finite number of load buses that are interconnected by a grid of transmission lines. Such a network can be described by a connected graph $\bar{\mathcal{G}} = (\bar{\mathcal{S}}, \bar{\mathcal{E}}, A)$, with a collection of buses/nodes $\bar{\mathcal{S}} := \{\mathcal{S}_{\text{Generator}}, \mathcal{S}_{\text{Load}}\} = \{\{\varsigma_1, \ldots, \varsigma_N\}, \{\varsigma_{N+1}, \ldots, \varsigma_M\}\}$, a set of tie lines/directed edges $\bar{\mathcal{E}} \subseteq \{(\varsigma_i, \varsigma_j) \in \bar{\mathcal{S}} \times \bar{\mathcal{S}} \mid i \neq j\}$ and a weighted adjacency matrix $A \in \mathbb{R}^{M \times M}$. Directed edges are denoted by $\varepsilon_{ij} := (\varsigma_i, \varsigma_j)$ and A satisfies $[A]_{ij} \neq 0 \Leftrightarrow \varepsilon_{ij} \in \bar{\mathcal{E}}$ and $[A]_{ij} = 0 \Leftrightarrow \varepsilon_{ij} \notin \bar{\mathcal{E}}$. For convenience, we define the weights in the adjacency matrix as $[A]_{ij} := -\frac{1}{z_{ij}} = -b_{ij}$, where z_{ij} [Ω] is the inductive reactance, and b_{ij} [Ω^{-1}] is the susceptance of the line corresponding to the edges $\varepsilon_{ij}, \varepsilon_{ji}$.

The linearized continuous-time dynamics of steam-valve controlled generators can be described by the following standard model for load-frequency control studies, see (Kundur, 1994):

$$\dot{\delta}_i = \omega_i, \tag{7.1a}$$

$$\dot{\omega}_i = \frac{1}{H_i}\Big(P_{\text{M}_i} - D_i\omega_i - P_{\text{L}_i} - \textstyle\sum_{\{j \mid (\varsigma_i, \varsigma_j) \in \bar{\mathcal{E}}\}} P_{\text{tie}}^{ij}\Big), \tag{7.1b}$$

$$\dot{P}_{\text{M}_i} = \frac{1}{\tau_{\text{T}_i}}\big(P_{\text{G}_i} - P_{\text{M}_i}\big), \tag{7.1c}$$

$$\dot{P}_{\text{G}_i} = \frac{1}{\tau_{G_i}}\big(P_{\text{ref}_i} - P_{\text{G}_i} - \frac{1}{r_i}\omega_i\big). \tag{7.1d}$$

Here, δ_i [rad], ω_i [rad/s], P_{M_i} [MW] and P_{G_i} [MW], $i \in \mathcal{I} := \mathbb{Z}_{[1,N]}$, are the rotor/voltage phase angle, the rotor/voltage frequency, and the turbine and governor states of the machine (or lumped set of machines) at bus $\varsigma_i \in \mathcal{S}_{\text{Generator}}$, respectively, all measured with respect to the a-priori scheduled values $\delta_{i,0}$, ω_0, $P_{\text{M}_{i,0}}$ and $P_{\text{G}_{i,0}}$. The control input of system i is P_{ref_i} [MW], which represents a change in the reference value for power production, while the exogenous disturbance input P_{L_i} [MW] represents the deviation in power demand with respect to the nominal operating point. The parameters associated with generator bus i are H_i, D_i, τ_{T_i}, τ_{G_i} and r_i, i.e., the (normalized) inertia, damping coefficient, turbine and governor time constants, and the regulation constant of the decentralized primary feedback loop, respectively. The power flow from bus ς_i to the connected nodes $\{\varsigma_j \in \bar{\mathcal{S}} | (\varsigma_i, \varsigma_j) \in \bar{\mathcal{E}}\}$ is determined using a "DC power flow" model (see, e.g., (Christie et al., 2000) for more details), which is an acceptable approximation of the first-principles based nonlinear "AC power flow" equations if small voltage phase differences are considered. Hence, the flow in line $\varepsilon_{ij} \in \bar{\mathcal{E}}$ is given by $P_{\text{tie}}^{ij} = b_{ij}(\delta_i - \delta_j) = -P_{\text{tie}}^{ji}$, where $P_{\text{tie}}^{ij} > 0$ indicates positive power flow from i to j.

At the time scale relevant for frequency control, the dynamics of load-bus voltage angles can be ignored, as the inertia connected to these nodes is negligibly small compared to the inertia of the generators. Therefore, we model the coupling between $\delta_j, j \in \{j | \varsigma_j \in \mathcal{S}_{\text{Load}}\}$ and generator-bus angles and frequencies $\delta_i, \omega_i, i \in \{i | \varsigma_i \in \mathcal{S}_{\text{Generator}}\}$ by approximating the overall network power balance as

$$\begin{bmatrix} H_1\dot{\omega}_1 \\ \vdots \\ \frac{H_N\dot{\omega}_N}{0} \\ \vdots \\ 0 \end{bmatrix} = \begin{bmatrix} P_{\text{M}_1} - D_1\omega_1 - P_{\text{L}_1} \\ \vdots \\ \frac{P_{\text{M}_N} - D_N\omega_N - P_{\text{L}_N}}{-P_{\text{L}_{N+1}}} \\ \vdots \\ -P_{\text{L}_M} \end{bmatrix} - \left[\begin{array}{c|c} B_{11} & B_{12} \\ \hline B_{21} & B_{22} \end{array}\right] \begin{bmatrix} \delta_1 \\ \vdots \\ \frac{\delta_N}{\delta_{N+1}} \\ \vdots \\ \delta_M \end{bmatrix}, \tag{7.2}$$

where the matrix $B = \left[\begin{smallmatrix} B_{11} & B_{12} \\ B_{21} & B_{22} \end{smallmatrix}\right] \in \mathbb{R}^{M\times M}$ is given by $B := A - \text{diag}(A\mathbf{1}_M)$. Note that (7.2) includes the nodal balance equations (7.1b) for all generator buses in the network. Eliminating $\delta_{N+1}, \ldots, \delta_M$ from (7.2) transforms (7.1b) into

$$\begin{bmatrix} H_1\dot{\omega}_1 \\ \vdots \\ H_N\dot{\omega}_N \end{bmatrix} = \begin{bmatrix} P_{\text{M}_1} - D_1\omega_1 \\ \vdots \\ P_{\text{M}_N} - D_N\omega_N \end{bmatrix} - \Gamma \begin{bmatrix} \delta_1 \\ \vdots \\ \delta_N \end{bmatrix} + \Upsilon \begin{bmatrix} P_{\text{L}_1} \\ \vdots \\ P_{\text{L}_M} \end{bmatrix}, \tag{7.3}$$

where $\Gamma := (B_{11} - B_{12}B_{22}^{-1}B_{21}) \in \mathbb{R}^{N\times N}$ and $\Upsilon := [-I_N \;\; B_{12}B_{22}^{-1}]$. This node elimination procedure is also known as *Kron reduction* (Grainger and Stevenson, 2003).

Given the sets $\mathcal{S} := \mathcal{S}_{\text{Generator}}$ and $\mathcal{E} := \{(\varsigma_i, \varsigma_j) \in \mathcal{S}\times\mathcal{S} \mid i \neq j, [\Gamma]_{ij} \neq 0\}$, the power system can now be defined as a network of dynamical systems (see Chapter 5) with connected graph representation $\mathcal{G} = (\mathcal{S}, \mathcal{E})$, and where the continuous-time dynamics of the systems assigned to vertices $\varsigma_i \in \mathcal{S}$ are given by (7.1a), (7.1c)–(7.1d) and (7.3). Let

$$x := \text{col}\left(\left\{\begin{bmatrix}\delta_i & \omega_i & P_{\text{M}_i} & P_{\text{G}_i}\end{bmatrix}^\top\right\}_{i\in\mathcal{I}}\right) \in \mathbb{R}^{4N}$$

and

$$u := \text{col}\left(\left\{P_{\text{ref}_i}\right\}_{i\in\mathcal{I}}\right) \in \mathbb{R}^N$$

be the state and control input of the multimachine network and consider a control law $\mu : \mathbb{R}^{4N} \to \mathbb{R}^N$. The corresponding closed-loop dynamics of the machine at bus i are described by (7.1a), (7.1c)–(7.1d) and (7.3) with $P_{\text{ref}_i} := [\mu(x)]_i$.

Now consider the following control problem.

Problem 7.2.1 *Single-area load-frequency control:* Design a feedback control law $\mu(x)$ for a single-area multimachine power system that asymptotically stabilizes the frequency of all generator and load buses at nominal value 0. ■

Load-frequency control (secondary control) is indispensable for stable operation of electrical power networks, because asymptotic stabilization of the network frequency corresponds to maintaining the balance between (active) power supply and demand, and therefore also the balance in produced and consumed energy. In single control-area power systems, imbalances are compensated by the system as a whole, irrespective of the bus where they occur. In other words, no generator is supposed to counterbalance the change in load at a particular, predefined bus by itself, but in general all generators may contribute.

In this chapter, we consider *isolated* single-area multi-machine networks that have no connection to other areas, and in which each local control law describes the actions of the (lumped set of) prosumer(s) at a certain bus. Note that the current European synchronous power system actually consists of several *interconnected* control areas, which, for historical and political reasons, typically coincide with individual nations. Therein, rather than stabilization of the internal frequency, secondary control actually involves stabilization of the area control error (ACE; see Chapter 1). In fact, this implies that the individual areas are decoupled in steady state and do not fully benefit from continent-wide aggregation. Today, TSOs therefore intend to harmonize the national balancing markets and couple their control areas also in real-time, to improve security of supply and market efficiency, see, e.g., (Van der Veen, 2012). In the near future, the individual European control areas will thus be merged to form a single-area power system. Because the large size and complexity of this area hamper the implementation of a centralized load-frequency control scheme, the distributed algorithms evaluated in this chapter may particularly be of use there.[1]

Given the network-wide character of Problem 7.2.1, it is natural that the design and evaluation of $\mu(x)$ is left to an area-wide transmission system operator. The TSO may motivate market participants to supply $\mu(x)$ balancing power by providing them with appropriate incentives (or, if $\mu(x)$ is set valued, by rewarding actions that lie in the corresponding set), see (Jokić, 2007). Note that in large deregulated electrical power systems, full-state feedback may be prohibitive, as it requires the TSO to have knowledge not only of the network states δ_i, ω_i, but also of the market-agent operated generator states P_{M_i} and P_{G_i}. Consequently, in large-scale and deregulated systems, sparse (i.e., decentralized or distributed) feedback laws μ are preferred.

Automatic generation control (AGC), which is based on proportional-integral feedback of ω_i (or the ACE, if interconnected areas are considered) is a possible

[1]For example, by assuming that each node of the considered multi-machine network is representative of a partition of the European network that is governed by a specific "regional TSO", which has a specific local objective and relies on neighbor-to-neighbor communication only. Together, these TSOs are responsible for stabilization of the *full* European power system.

solution to the above problem. However, because the performance of conventional load-frequency control schemes is affected by deregulation, network growth and the increasing penetration of DG, here, our aim is to solve Problem 7.2.1 with the non-centralized stabilization schemes that were proposed in Chapters 5 and 6 instead. Next, we continue by combining the p-qSF based stability conditions from Chapter 6 with the non-cooperative optimization of a set of local objective functions, to demonstrate that this stabilization technique may be particularly useful in competitive environments such as the electrical energy market.

7.3 Two-step competitive p-qSF control

To improve closed-loop performance, p-qSF based stabilization (Problem 6.4.5 and Problem 6.4.8) can be combined with the optimization of a (set of) cost function(s) over a finite receding prediction horizon. Whereas stability of the corresponding closed-loop system would then only require a single round of information exchange among the network nodes per sampling instant, additional iterations could be exploited to optimize performance in a non-centralized way.

Perhaps the best-known techniques for non-centralized receding-horizon optimization are based on decomposition of a global predictive control problem, see, e.g., (Bertsekas, 1999; Giselsson and Rantzer, 2010) and the FC-MPC scheme described in Chapter 4 (Venkat, 2006; Venkat et al., 2008). The corresponding local control laws employ iterative and global communication or coordination to cooperatively minimize a system-wide performance cost (e.g., a weighted sum of local objective functions). Consequently, the local iterates are guaranteed to converge asymptotically to the global optimum, although the convergence rate of these schemes may be rather slow in practice. In applications that admit system-wide communication while allowing for sufficient time to converge over iterations, besides optimal performance with respect to a network-wide objective function, a guarantee for closed-loop stability is often inherited from the underlying centralized predictive control problem, which typically relies on terminal-cost based stabilization, see, for example, Chapter 4 and (Mayne et al., 2000; Lazar, 2006). Such applications are, for instance, the control of relatively slow large-scale plants in chemical and process industry.

Still, there are many other examples of networked systems in which the need for system-wide communication/coordination associated with cooperative optimization is overly restrictive or undesired. Instead, these systems rely on competitive mechanisms for their operation, such that, rather than pursuing system-wide optimal performance, the local control laws aim at minimizing ex-

clusively their own cost. A particular example of these applications is the deregulated electrical power system, in which multiple market actors compete for the supply and demand of energy, while communication is restricted to the exchange of bids/offers with a neutral market operator and non-market-sensitive information with competitors over short distances.

There are several examples where competitive optimal control is shown not to be stabilizing, see, e.g., (Camponogara et al., 2002). The "feasibility-implies-stability guarantee" provided by p-qSF synthesis is therefore particularly appealing for use with non-cooperative, uncoordinated optimization methods. Hence, in what follows, we provide a two-step competitive NDS control scheme: *step one*, a set of p-qSFs is synthesized via Problem 6.4.8 to define a set of stabilizing control actions; *step two*, if time permits, additional iterations are employed to improve local performance in a competitive receding horizon fashion, all based on information exchange only between directly connected systems.

To define the competitive receding horizon problem, the following notation is introduced. For a finite prediction horizon $N_k \in \mathbb{Z}_{\geq 1}$, let

$$\mathbf{x}_i^p\left(x_i(k), \mathbf{x}_{\mathcal{N}_i}^{p-1}(k), \mathbf{u}_i^p(k)\right) := \left\{x_i^p(l \mid k)\right\}_{l \in \mathbb{Z}_{[0,N_k]}}$$

denote the predicted local state sequence as generated by NDS (6.13) at time instant $k \in \mathbb{Z}_+$ and iteration $p \in \mathbb{Z}_{\geq 1}$, from initial local state $x_i^p(0 \mid k) = x_i(0 \mid k) =: x_i(k)$, neighbor-system state sequence $\mathbf{x}_{\mathcal{N}_i}^{p-1}(k) := \left\{x_{\mathcal{N}_i}^{p-1}(l \mid k)\right\}_{l \in \mathbb{Z}_{[0,N_k-1]}}$ (computed during iteration $p-1 \in \mathbb{Z}_+$) and local control sequence $\mathbf{u}_i^p(k) := \left\{u_i^p(l \mid k)\right\}_{l \in \mathbb{Z}_{[0,N_k-1]}}$. Next, let $C_i : (\mathbb{R}^{n_i})^{N_k+1} \times (\mathbb{R}^{m_i})^{N_k} \to \mathbb{R}$, $i \in \mathcal{I}$, be a strictly convex performance cost function assigned to system $i \in \mathcal{I}$. Let $p_{\max} \in \mathbb{Z}_{\geq 1}$ be the maximum number of iterations allowed per sampling period and consider the following problem.

Problem 7.3.1 *Decentralized performance optimization*
At iteration $p \in \mathbb{Z}_{[1,p_{\max}]}$, given $x_i(k) \in \mathbb{R}^{n_i}$, $\mathbf{x}_{\mathcal{N}_i}^{p-1}(k)$, $P_i(x^+(k)) \in \mathbb{P}_i$ and $\Lambda_i^p \in \mathbb{R}_+$, solve

$$\begin{aligned}
\min_{\mathbf{u}_i^p(k)} \quad & C_i\left(\mathbf{x}_i^p\left(x_i(k), \mathbf{x}_{\mathcal{N}_i}^{p-1}(k), \mathbf{u}_i^p(k)\right), \mathbf{u}_i^p(k)\right) && \text{(7.4a)}\\
\text{s.t.} \quad & V_i(P_i(x^+(k)), x_i^+(k)) \leq \Lambda_i^p && \text{(7.4b)}\\
& x_i^+(k) \in \mathbb{X}_i, && \text{(7.4c)}
\end{aligned}$$

where $x_i^+(k) = x_i^p(1 \mid k)$. ■

In what follows, denote the optimizer of Problem 7.3.1 and the correspond-

Algorithm 4 Two-step competitive p-qSF control

1: **for** $k \in \mathbb{Z}_+$ **do**
2: Obtain $x_i(k)$;
3: Transmit $x_i(k)$ and $V_i\big(P_i(x(k)), x_i(k)\big)$ to neighbors;
4: *(I) Almost-decentralized p-qSF synthesis*:
Solve Problem 6.4.8 to find $P_i(x^+(k))$ and $\lambda_i^*(k)$;
5: Set $\Lambda_i^0 := \rho_i \max_{j\in\overline{\mathcal{N}}_i} V_j\big(P_j(x(k)), x_j(k)\big) + \lambda_i^*(k)$ and $\mathbf{x}_{\mathcal{N}_i}^0(k) := \{x_{\mathcal{N}_i}(k), 0, \ldots, 0\}$;
6: **for** $p \in \mathbb{Z}_{[1,p_{\max}]}$ **do**
7: Set $\Lambda_i^p := \max\Big\{\Lambda_i^{p-1}, \max_{j\in\mathcal{N}_i} \Lambda_j^{p-1}\Big\}$;
8: *(II) Decentralized performance optimization*:
Solve Problem 7.3.1 to find $\mathbf{u}_i^{p*}(k)$ and $\mathbf{x}_i^{p*}(k)$;
9: Transmit $\mathbf{x}_i^{p*}(k)$ and Λ_i^p to neighbors, construct $\mathbf{x}_{\mathcal{N}_i}^p(k)$;
10: **end for**
11: Apply $\bar{u}_i(k) := u_i^{p*}(0 \mid k)$ to the system;
12: **end for**

ing state prediction by

$$\mathbf{u}_i^{p*}(k) := \big\{u_i^{p*}(l \mid k)\big\}_{l\in\mathbb{Z}_{[0,N_k-1]}}$$

and

$$\mathbf{x}_i^{p*}(k) := \mathbf{x}_i^p\Big(x_i(k), \mathbf{x}_{\mathcal{N}_i}^{p-1}(k), \mathbf{u}_i^{p*}(k)\Big) := \big\{x_i^{p*}(l \mid k)\big\}_{l\in\mathbb{Z}_{[0,N_k]}},$$

respectively.

The competitive control scheme is now described by Algorithm 4. Each sampling instant, during the first iteration Problem 6.4.8 is solved to determine a set of stabilizing local control actions based on the synthesis of a collection of p-qSFs (statements 2–5). The corresponding parameters $P_i(x^+(k))$ and Λ_i^0, i.e., the value of the right-hand side in (6.16a), are then employed by Problem 7.3.1 to competitively optimize local performance over the set of stabilizing control actions using the subsequent iterations $p \in \mathbb{Z}_{[1,p_{\max}]}$ (see statements 6–10). If the maximum number of iterations $p_{\max}$ has been performed, the first sample of the last computed control sequence $\bar{u}_i(k)$ is applied to the system; the rest is discarded (statement 11). Observe that the for-condition in statement 6 may be extended with a convergence test to avoid unnecessary iterations and to speed up the algorithm.

Note that even though the parameters $P_i(x^+(k))$ and Λ_i^0 are generated and defined based on the local information $\max_{j\in\overline{\mathcal{N}}_i} V_j(P(x(k)), x_j(k))$ and (6.16a), it straightforwardly follows from Theorem 6.4.7 that constraints (7.4b)–(7.4c)

with $P_i(x^+(k))$ and $\max_{i\in\mathcal{I}}\Lambda_i^0$ are feasible and define stabilizing control actions as well. As each increase in Λ_i^p provides additional relaxation of the stability conditions, i.e., (7.4b), the iterations of Algorithm 4 are not only exploited for decentralized optimization, but also to communicate the value $\max_{j\in\mathcal{I}}\Lambda_i^0$ to all the nodes in the network. This is the purpose of statement 7: for connected communication graphs and finite N, repeated application of this statement will monotonically increase Λ_i^p over p such that it attains the value $\max_{i\in\mathcal{I}}\Lambda_i^0$ within a finite number of iterations, thereby relaxing the local stability conditions accordingly.

7.3.1 Two-step competitive p-qSF control: convergence

In what follows, the convergence and performance characteristics of Algorithm 4 are analyzed for the particular case of linear NDS dynamics and quadratic cost functions. Let the local cost functions employed in Problem 7.3.1 be given by

$$\begin{aligned}
&C_i\left(\mathbf{x}_i^p\left(x_i(k),\mathbf{x}_{\mathcal{N}_i}^{p-1}(k),\mathbf{u}_i^p(k)\right),\mathbf{u}_i^p(k)\right)\\
&\quad:=x_i(k)^\top Q_i x_i(k)+\sum_{l=1}^{N_k}\left\{x_i^p(l\mid k)^\top Q_i x_i^p(l\mid k)+u_i^p(l-1\mid k)^\top R_i u_i^p(l-1\mid k)\right\}\\
&\quad=(\underline{x}_i^p(k))^\top\mathcal{Q}_i\underline{x}_i^p(k)+(\underline{u}_i^p(k))^\top\mathcal{R}_i\underline{u}_i^p(k),
\end{aligned}\tag{7.5}$$

where $Q_i\in\mathbb{R}^{n_i\times n_i}, Q_i\succeq 0$, $R_i\in\mathbb{R}^{m_i\times m_i}, R_i\succ 0$, and

$$\begin{aligned}
\underline{x}_i^p(k)&:=\operatorname{col}\left(\{x_i^p(l\mid k)\}_{l\in\mathbb{Z}_{[0,N_k]}}\right)\\
&=\operatorname{col}\left(\mathbf{x}_i^p(x_i(k),\mathbf{x}_{\mathcal{N}_i}^{p-1}(k),\mathbf{u}_i^p(k))\right)\in\mathbb{R}^{(N_k+1)n_i},\\
\underline{u}_i^p(k)&:=\operatorname{col}\left(\{u_i^p(l\mid k)\}_{l\in\mathbb{Z}_{[0,N_k-1]}}\right)\\
&=\operatorname{col}\left(\mathbf{u}_i^p(k)\right)\in\mathbb{R}^{N_k m_i},\\
\mathcal{Q}_i&:=\operatorname{diag}(\{Q_i,\ldots,Q_i\})\in\mathbb{R}^{(N_k+1)n_i\times(N_k+1)n_i},\\
\mathcal{R}_i&:=\operatorname{diag}(\{R_i,\ldots,R_i\})\in\mathbb{R}^{N_k m_i\times N_k m_i}.
\end{aligned}$$

Now consider network dynamics (6.13) and suppose that $\psi_i(x_i,v_i(x_{\mathcal{N}_i}),u_i)$ is affine in the state and input. Then, Problem 7.3.1 relies on the prediction model

$$\begin{aligned}
x_i^p(l+1\mid k)&=\psi_i\left(x_i^p(l\mid k),v_i(x_{\mathcal{N}_i}^{p-1}(l\mid k)),u_i^p(l\mid k)\right)\\
&:=A_{ii}x_i^p(l\mid k)+\sum_{j\in\mathcal{N}_i}A_{ij}x_j^{p-1}(l\mid k)+B_i u_i^p(l\mid k)\\
&=:A_{ii}x_i^p(l\mid k)+A_{\mathcal{N}_i}x^{p-1}(l\mid k)+B_i u_i^p(l\mid k),
\end{aligned}\tag{7.6}$$

with $A_{ij} \in \mathbb{R}^{n_i \times n_j}$, $B_i \in \mathbb{R}^{n_i \times m_i}$ and $A_{\mathcal{N}_i} \in \mathbb{R}^{n_i \times n}$, and where $x^{p-1}(l \mid k) := \operatorname{col}\left(\{x_i^{p-1}(l \mid k)\}_{i \in \mathcal{I}}\right) \in \mathbb{R}^n$. Note that the last equality is introduced for notational convenience only, and does not imply that the predictions $x_i^p(l+1 \mid k)$ require full-state knowledge; the neighbor state predictions, i.e., $x_{\mathcal{N}_i}^{p-1}(l \mid k)$, are sufficient for predicting the future local states. The above dynamics allow for a linear expression of the local state prediction $\underline{x}_i^p(k)$, which can be substituted in (7.5) to solve Problem 7.3.1 explicitly. Recursive application of (7.6) yields

$$\underline{x}_i^p(k) = H_i x_i(k) + H_{\mathcal{N}_i} \underline{x}^{p-1}(k) + T_i \underline{u}_i^p(k), \tag{7.7}$$

where the transition matrices $H_i \in \mathbb{R}^{(N_k+1)n_i \times n_i}$, $H_{\mathcal{N}_i} \in \mathbb{R}^{(N_k+1)n_i \times (N_k+1)n}$ and $T_i \in \mathbb{R}^{(N_k+1)n_i \times N_k m_i}$ are defined as

$$H_i := \begin{bmatrix} I \\ A_{ii} \\ A_{ii}^2 \\ \vdots \\ A_{ii}^{N_k} \end{bmatrix}, H_{\mathcal{N}_i} := \begin{bmatrix} 0 & 0 & \dots & 0 & 0 \\ A_{\mathcal{N}_i} & 0 & \dots & 0 & 0 \\ A_{ii}A_{\mathcal{N}_i} & A_{\mathcal{N}_i} & \dots & 0 & 0 \\ \vdots & \vdots & \ddots & \vdots & \vdots \\ A_{ii}^{N_k-1}A_{\mathcal{N}_i} & A_{ii}^{N_k-2}A_{\mathcal{N}_i} & \dots & A_{\mathcal{N}_i} & 0 \end{bmatrix}, T_i := \begin{bmatrix} 0 & 0 & \dots & 0 \\ B_i & 0 & \dots & 0 \\ A_{ii}B_i & B_i & \dots & 0 \\ \vdots & \vdots & \ddots & \vdots \\ A_{ii}^{N_k-1}B_i & A_{ii}^{N_k-2}B_i & \dots & B_i \end{bmatrix},$$

and where $\underline{x}^{p-1}(k) := \operatorname{col}(\{x^{p-1}(l \mid k)\}_{l \in \mathbb{Z}_{[0,N_k]}})$ denotes the full-state sequence prediction generated at iteration $p-1 \in \mathbb{Z}_+$ and time instant $k \in \mathbb{Z}_+$. Combining the above result for all $i \in \mathcal{I}$, yields the full-state prediction vector

$$\underline{x}^p(k) = Hx(k) + H_{\mathcal{N}} \underline{x}^{p-1}(k) + T\underline{u}^p(k), \tag{7.8}$$

where $H \in \mathbb{R}^{(N_k+1)n \times n}$, $H_{\mathcal{N}} \in \mathbb{R}^{(N_k+1)n \times (N_k+1)n}$ and $T \in \mathbb{R}^{(N_k+1)n \times N_k m}$ are defined as

$$H := \begin{bmatrix} I & 0 & \dots & 0 \\ \vdots & \vdots & \ddots & \vdots \\ 0 & 0 & \dots & I \\ A_{11} & 0 & \dots & 0 \\ 0 & A_{22} & \dots & 0 \\ \vdots & \vdots & \ddots & \vdots \\ 0 & 0 & \dots & A_{NN} \\ A_{11}^2 & 0 & \dots & 0 \\ 0 & A_{22}^2 & \dots & 0 \\ \vdots & \vdots & \ddots & \vdots \\ A_{11}^{N_k} & 0 & \dots & 0 \\ \vdots & \vdots & \ddots & \vdots \\ 0 & 0 & \dots & A_{NN}^{N_k} \end{bmatrix}, \qquad H_{\mathcal{N}} := \begin{bmatrix} 0 & 0 & \dots & 0 & 0 \\ \vdots & \vdots & \ddots & \vdots & \vdots \\ 0 & 0 & \dots & 0 & 0 \\ A_{\mathcal{N}_1} & 0 & \dots & 0 & 0 \\ A_{\mathcal{N}_2} & 0 & \dots & 0 & 0 \\ \vdots & \vdots & \ddots & \vdots & \vdots \\ A_{\mathcal{N}_N} & 0 & \dots & 0 & 0 \\ A_{11}A_{\mathcal{N}_1} & A_{\mathcal{N}_1} & \dots & 0 & 0 \\ A_{22}A_{\mathcal{N}_2} & A_{\mathcal{N}_2} & \dots & 0 & 0 \\ \vdots & \vdots & \ddots & \vdots & \vdots \\ A_{11}^{N_k-1}A_{\mathcal{N}_1} & A_{11}^{N_k-2}A_{\mathcal{N}_1} & \dots & A_{\mathcal{N}_1} & 0 \\ \vdots & \vdots & \ddots & \vdots & \vdots \\ A_{NN}^{N_k-1}A_{\mathcal{N}_N} & A_{NN}^{N_k-2}A_{\mathcal{N}_N} & \dots & A_{\mathcal{N}_N} & 0 \end{bmatrix},$$

$$T := \begin{bmatrix}
0 & 0 & \dots & 0 & 0 & 0 & \dots & 0 & \dots & 0 & 0 & \dots & 0 \\
\vdots & \vdots & \ddots & \vdots & \vdots & \vdots & \ddots & \vdots & \vdots & \vdots & \ddots & \vdots & \\
0 & 0 & \dots & 0 & 0 & 0 & \dots & 0 & \dots & 0 & 0 & \dots & 0 \\
B_1 & 0 & \dots & 0 & 0 & 0 & \dots & 0 & \dots & 0 & 0 & \dots & 0 \\
0 & 0 & \dots & 0 & B_2 & 0 & \dots & 0 & \dots & 0 & 0 & \dots & 0 \\
\vdots & \vdots & \ddots & \vdots & \vdots & \vdots & \ddots & \vdots & \vdots & \vdots & \ddots & \vdots & \\
0 & 0 & \dots & 0 & 0 & 0 & \dots & 0 & \dots & B_N & 0 & \dots & 0 \\
A_{11}B_1 & B_1 & \dots & 0 & 0 & 0 & \dots & 0 & \dots & 0 & 0 & \dots & 0 \\
0 & 0 & \dots & 0 & A_{22}B_2 & B_2 & \dots & 0 & \dots & 0 & 0 & \dots & 0 \\
\vdots & \vdots & \ddots & \vdots & \vdots & \vdots & \ddots & \vdots & \vdots & \vdots & \ddots & \vdots & \\
A_{11}^{N_k-1}B_1 & A_{11}^{N_k-2}B_1 & \dots & B_1 & 0 & 0 & \dots & 0 & \dots & 0 & 0 & \dots & 0 \\
\vdots & \vdots & \ddots & \vdots & \vdots & \vdots & \ddots & \vdots & \vdots & \vdots & \ddots & \vdots & \\
0 & 0 & \dots & 0 & 0 & 0 & \dots & 0 & \dots & A_{NN}^{N_k-1}B_N & A_{NN}^{N_k-2}B_N & \dots & B_N
\end{bmatrix},$$

and with full-system control sequence vector $\underline{u}^p(k) := \operatorname{col}\left(\{\underline{u}_i^p(k)\}_{i\in\mathcal{I}}\right)$. Note that $\underline{u}^p(k)$ is differently structured than the state sequence vector, i.e., $\underline{x}^p(k)$.

Next, given some $x_i \in \mathbb{R}^{n_i}$ and $\underline{x}^{p-1} \in \mathbb{R}^{(N_k+1)n}$, let

$$\begin{aligned}
&\underline{u}_i^{p*}(x_i, \underline{x}^{p-1}) \\
&\quad := -(T_i^\top \mathcal{Q}_i T_i + \mathcal{R}_i)^{-1} T_i^\top \mathcal{Q}_i \left(H_i x_i + H_{\mathcal{N}_i} \underline{x}^{p-1}\right) \\
&\quad =: L_i x_i + L_{\mathcal{N}_i} \underline{x}^{p-1},
\end{aligned} \tag{7.9}$$

where $L_i \in \mathbb{R}^{N_k m_i \times n_i}$ and $L_{\mathcal{N}_i} \in \mathbb{R}^{N_k m_i \times (N_k+1)n}$. Note that since $T_i^\top \mathcal{Q}_i T_i + \mathcal{R}_i \succ 0$, $T_i^\top \mathcal{Q}_i T_i + \mathcal{R}_i$ is nonsingular and L_i and $L_{\mathcal{N}_i}$ are well-defined. Now consider the following theorem.

Theorem 7.3.2 *At time $k \in \mathbb{Z}_+$, suppose that at each iteration $p \in \mathbb{Z}_{[1,p_{\max}]}$ and node $i \in \mathcal{I}$ the vector $\underline{u}_i^{p*}(x_i(k), \underline{x}^{p-1}(k))$ is included in the set of feasible control actions defined by* (7.4b)–(7.4c)*. Also, let*

$$\varepsilon_{\max}\left(H_{\mathcal{N}} + T \begin{bmatrix} L_{\mathcal{N}_1} \\ \vdots \\ L_{\mathcal{N}_N} \end{bmatrix}\right) < 1. \tag{7.10}$$

Then, the iterates $\underline{x}^p(k)$ generated by Algorithm 4 asymptotically converge over iteration number p.

Theorem 7.3.2 is proven in Appendix E.1. It provides a convergence certificate for the iterates generated by Algorithm 4 assuming that $\underline{u}_i^{p*}\left(x_i(k), \underline{x}_{\mathcal{N}_i}^{p-1}(k)\right)$ is feasible for all $p \in \mathbb{Z}_{[1,p_{\max}]}$. In practice, this assumption may be rather strong, and moreover, the full system knowledge required for verifying condition (7.10) may not be available. Still, even if convergence (and thus, Nash optimal performance) cannot be guaranteed based on Theorem 7.3.2, the control actions computed via Algorithm 4 will be stabilizing as long as the p-qCLF synthesis problem, i.e., Problem 6.4.8, is recursively feasible over time.

7.3.2 Two-step competitive p-qSF control: implementation

Problem 7.3.1 can be implemented by extending the SDP-based framework described in Section 6.4.2 with objective (7.4a), while using

$$\rho_i \max_{j\in\overline{\mathcal{N}}_i} x_j(k)^\top P_j(x(k))x_j(k) + \lambda_i(k) =: \Lambda_i^p$$

and $$Z_i(k) := \big(P_i(x^+(k))\big)^{-1}$$

as given parameters. For polytopic/ellipsoidal $\mathbb{X}_i$, and quadratic cost functions and affine NDS dynamics as given in (7.5) and (7.6), respectively, this yields the following SDP problem in $\underline{u}_i^p(k)$:

$$\min_{\underline{u}_i^p(k)\in\underline{\mathbb{U}}_i^{\mathrm{s}}(k)} f_i\big(x_i(k), \underline{x}^{p-1}(k), \underline{u}_i^p(k)\big), \tag{7.11}$$

with $f_i(\cdot)$ as defined in (E.1), and where $\underline{\mathbb{U}}_i^{\mathrm{s}}(k) := \mathbb{U}_i^{\mathrm{s}}(k)\times\mathbb{R}^{(N_k-1)m_i}$, with

$$\mathbb{U}_i^{\mathrm{s}}(k) := \left\{ \upsilon\in\mathbb{R}^{m_i} \;\middle|\; \begin{bmatrix} \Lambda_i^p & * \\ \widetilde{f}_i(x(k))+\widetilde{g}_i(x(k))\upsilon & (P_i(x^+(k)))^{-1} \end{bmatrix} \succeq 0, \widetilde{f}_i(x(k))+\widetilde{g}_i(x(k))\upsilon\in\mathbb{X}_i \right\}.$$

Here, $\widetilde{f}_i(x(k)) := A_{ii}x_i(k) + A_{\mathcal{N}_i}x(k)$ and $\widetilde{g}_i(x(k)) := B_i$. In practice, a fully SDP-based implementation of Problem 7.3.1 may be too complex to allow for a satisfactory amount of iterations per sampling period. A computationally efficient realization can be obtained based on the explicit solution to unconstrained optimization problem (E.1), as described by Algorithm 5.

Algorithm 5 Semi-explicit implementation of Problem 7.3.1

1: Compute $\underline{u}_i^{p*}(x_i(k), \underline{x}^{p-1}(k))$ via (7.9);
2: **if** $\underline{u}_i^{p*}(x_i(k), \underline{x}^{p-1}(k)) \notin \underline{\mathbb{U}}_i^{\mathrm{s}}(k)$ **then**
3: Set $\underline{u}_i^{p*}(x_i(k), \underline{x}^{p-1}(k)) := \arg\min_{\underline{u}_i^p(k)\in\underline{\mathbb{U}}_i^{\mathrm{s}}(k)} f_i\big(x_i(k), \underline{x}^{p-1}(k), \underline{u}_i^p(k)\big)$;
4: **end if**
5: Set $u_i^{p*}(l \mid k) := \big[\underline{u}_i^{p*}(x_i(k), \underline{x}^{p-1}(k))\big]_l$, $l\in\mathbb{Z}_{[0,N_k-1]}$.

Algorithm 5 minimizes the need for SDP programming by employing the explicit solution to (E.1) whenever it is feasible (and consequently, whenever it is optimal, as demonstrated in the proof of Theorem 7.3.2). Thus, whenever $\underline{u}_i^{p*}(x_i(k), \underline{x}^{p-1}(k)) \in \underline{\mathbb{U}}_i^{\mathrm{s}}(k)$, Algorithm 5 amounts to evaluating *a simple explicit local feedback law*, i.e., (7.9). Note that this local control law can be evaluated in an almost-decentralized way: the non-neighbor state information in $\underline{x}^{p-1}$ is not used, as the corresponding entries of $H_{\mathcal{N}_i}$ are 0.

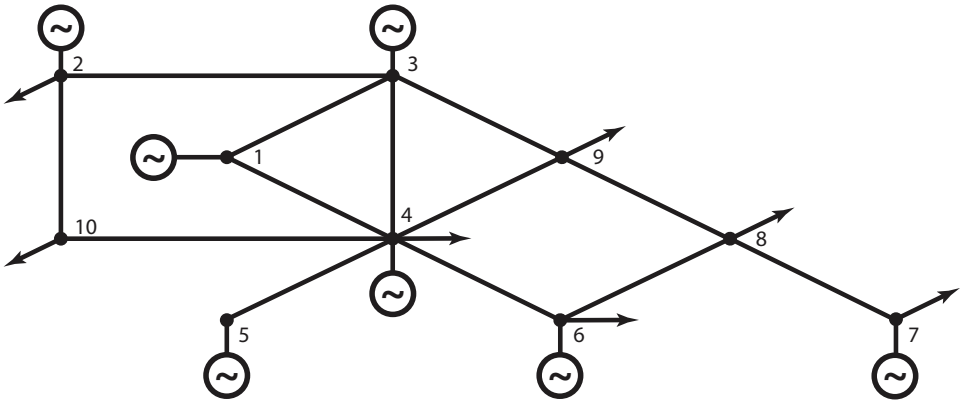

Figure 7.1: Single-line representation of the seven-machine CIGRÉ test system.

Algorithm 5 provides a low-complexity control framework that allows for both competitive performance optimization and almost-decentralized stabilization of large-scale NDS. Although p-qSF-based stabilization is particularly attractive in combination with decentralized control schemes that are not inherently stabilizing, such as the competitive method described above, it may also be of use in cooperative techniques that rely on global communication and optimal performance to provide stabilizing control actions. Therein, the "feasibility-implies-stability guarantee" associated with p-qSF synthesis may relax the need for optimal performance with respect to a system-wide cost, which can be exploited to render these schemes less vulnerable to failures of the communication network.

7.4 Application case study

Next, we illustrate the potential of Algorithm 3 (distributed L-MPC; see Chapter 5) and Algorithm 4 (two-step competitive p-qSF based control) for frequency control by simulating these schemes in closed-loop with the 7-machine CIGRÉ (International Council on Large Electric Systems) benchmark system reproduced from (Pai, 1981). The network is schematically depicted in Figure 7.1, and consists of $N = 7$ generator buses and 3 load buses that are interconnected via 13 transmission lines. Each generator is modeled in accordance with (7.1a), (7.1c)–(7.1d) and (7.3). The system parameters used in the simulation are listed in Table E.1.

The prediction model employed by the controllers, i.e., (5.6), is obtained via time discretization of (7.1a), (7.1c)–(7.1d) and (7.3), using a sampling period of

$T_\mathrm{s} = 1$ s. This yields the discrete-time linear state-space representation

$$\begin{aligned} x_i(k+1) &= \psi_i(x_i(k), v_i(x_{\mathcal{N}_i}(k)), u_i(k)) \\ &:= A_{ii}x_i(k) + v_i(x_{\mathcal{N}_i}(k)) + B_i u_i(k), \\ v_i(x_{\mathcal{N}_i}(k)) &:= \textstyle\sum_{j\in\mathcal{N}_i} A_{ij}x_j(k), \end{aligned} \tag{7.12}$$

with $x_i := [\,\delta_i \;\; \omega_i \;\; P_{\mathrm{M}_i} \;\; P_{\mathrm{G}_i}\,]^\top$, $u_i := P_{\mathrm{ref}_i}$, $i \in \mathcal{I} := \mathbb{Z}_{[1,7]}$, and where $A_{ii} \in \mathbb{R}^{n_i \times n_i}$, $B_i \in \mathbb{R}^{n_i \times m_i}$, $A_{ij} \in \mathbb{R}^{n_i \times n_j}$. The sets of direct neighbors $\mathcal{N}_i$ for the CIGRÉ network (after load-bus elimination) are given in Table E.1.

7.4.1 Distributed L-MPC based frequency control

First, we consider L-MPC based stabilization of the network frequency, by simulating the CIGRÉ network in closed-loop with Algorithm 3. The controllers employ quadratic local performance cost functions, i.e.,

$$J_i(x_i(k), u_i(k)) := x_i(1|k)^\top F_i x_i(1|k) + x_i(k)^\top Q_i x_i(k) + u_i(k)^\top R_i u_i(k), \quad i \in \mathcal{I},$$

with one-step-ahead state prediction $x_i(1|k) := \psi_i(x_i(k), v_i(x_{\mathcal{N}_i}(k)), u_i(k))$. The values for $F_i \succ 0$, $Q_i \succeq 0$ and $R_i \succ 0$ are listed in Table E.2. F_i satisfies the discrete-time Riccati equation $F_i = A_i^\top F_i A_i + A_i^\top F_i B_i L_i + Q_i$, with linear quadratic regulator feedback gain $L_i = (R_i + B_i^\top F_i B_i)^{-1} B_i^\top F_i A_i$. This specific value was chosen to optimize performance in terms of $\sum_{k\in\mathbb{Z}_+} \sum_{i\in\mathcal{I}} x_i(k)^\top Q_i x_i(k) + u_i(k) R_i u_i(k)$, where Q_i penalizes δ_i and ω_i to induce adequate damping on frequency and tie-line flow oscillations. Note however that, in contrast to classical MPC, the choice for F_i does not play a role in guaranteeing closed-loop stability.

The method of (Lazar et al., 2006) was used to compute the weights $P_i \in \mathbb{R}^{n_i \times n_i}$, $i \in \mathcal{I}$, of the local infinity-norm based candidate CLFs for Algorithm 3, i.e., $V_i(x_i) = \|P_i x_i\|_\infty$ with $\rho_i = 0.9$, $\forall i \in \mathcal{I}$, and systems (7.12) (under decoupled operation), in closed-loop with local feedback laws $u_i(k) := K_i x_i(k)$, $K_i \in \mathbb{R}^{1\times n_i}$, yielding

$$P_1 = \begin{bmatrix} -0.62979 & 17.158 & 7.3639 & -6.5897 \\ -1.2466 & 38.485 & 0.68023 & 2.3994 \\ 3.0898 & 33.119 & 0.35449 & 0.94405 \\ -0.41334 & -14.006 & 0.11274 & 0.99418 \end{bmatrix}, \qquad K_1 = \begin{bmatrix} -0.056146 \\ 17.013 \\ 0.17313 \\ 0.63512 \end{bmatrix}^\top,$$

$$P_2 = \begin{bmatrix} -7.7327 & 24.86 & -0.45184 & -1.3596 \\ 9.6994 & 62.824 & 10.53 & -11.793 \\ 9.7231 & 72.123 & -2.791 & 9.8619 \\ -8.0183 & 4.4586 & 7.5088 & 1.19 \end{bmatrix}, \qquad K_2 = \begin{bmatrix} -0.1415 \\ 17.27 \\ -0.42816 \\ 1.1958 \end{bmatrix}^\top,$$

$$P_3 = \begin{bmatrix} -0.94289 & 34.854 & -6.4203 & 10.729 \\ -5.7409 & -16.222 & 1.6906 & -0.96636 \\ 6.8157 & 44.128 & 4.5873 & -3.129 \\ 12.125 & 10.053 & 0.8673 & 0.68066 \end{bmatrix}, \qquad K_3 = \begin{bmatrix} -1.9488 \\ 10.154 \\ 0.15808 \\ 0.20908 \end{bmatrix}^\top,$$

$$P_4 = \begin{bmatrix} 1.6663 & 7.5646 & -5.1264 & 13.222 \\ 4.0893 & -20.416 & -0.89703 & -0.58409 \\ -1.9142 & 2.2781 & 7.2915 & -1.6996 \\ 4.0666 & 29.068 & 0.84367 & 0.18502 \end{bmatrix}, \qquad K_4 = \begin{bmatrix} 0.11742 \\ 17.745 \\ 0.37284 \\ 0.12559 \end{bmatrix}^\top$$

$$P_5 = \begin{bmatrix} 5.7046 & 5.5612 & -5.5749 & 7.2372 \\ 6.5151 & 25.236 & 1.0041 & -0.082996 \\ -5.2836 & 18.191 & 1.1193 & 1.9971 \\ 4.8618 & -12.936 & 0.42708 & 0.18429 \end{bmatrix}, \qquad K_5 = \begin{bmatrix} -0.13866 \\ 14.185 \\ 0.5927 \\ -0.20511 \end{bmatrix}^\top,$$

$$P_6 = \begin{bmatrix} -2.7264 & 10.554 & 1.1353 & 3.9908 \\ 2.5412 & -12.799 & 0.68144 & -0.30603 \\ 2.7504 & 4.5373 & -4.8496 & 3.1844 \\ 3.4173 & 21.908 & 0.28121 & 0.062939 \end{bmatrix}, \qquad K_6 = \begin{bmatrix} -0.17089 \\ 11.615 \\ 0.072399 \\ 0.038927 \end{bmatrix}^\top,$$

$$P_7 = \begin{bmatrix} 5.6752 & 54.244 & 4.6571 & -0.39439 \\ -0.26188 & 23.17 & -3.3943 & 13.382 \\ 8.5394 & 28.707 & 2.5505 & 4.1042 \\ 0.044767 & 3.4706 & 9.2078 & -2.4838 \end{bmatrix}, \qquad K_7 = \begin{bmatrix} -0.4908 \\ 15.387 \\ 0.62681 \\ -0.229 \end{bmatrix}^\top.$$

It is important to stress that the control laws $u_i(k) = K_i x_i(k)$ are only employed off-line, to calculate the matrices P_i and they are never used for controlling the system. Moreover, we set $N_\tau = 5$ in Algorithm 3. Note that by choosing infinity-norm CLFs, it is possible to formulate Algorithm 3 as a quadratic program (QP), by writing the structured CLF conditions as linear constraints in $u_i(k)$ (see Section 5.4.2).

In the simulation we evaluated the performance of the closed-loop network when recovering from a state perturbation (or imbalance) given by

$$x_1(0) = \begin{bmatrix} -0.1 \\ 0.025 \\ -0.4 \\ 0.1 \end{bmatrix}, \qquad x_2(0) = \begin{bmatrix} 0.15 \\ -0.035 \\ 0.015 \\ 0.1 \end{bmatrix}, \quad x_3(0) = \begin{bmatrix} 0.05 \\ -0.005 \\ 0 \\ 0.01 \end{bmatrix},$$

$$x_4(0) = \begin{bmatrix} 0.1 \\ -0.0025 \\ 0.01 \\ 0.0005 \end{bmatrix}, \quad x_5(0) = \begin{bmatrix} -0.25 \\ 0.004 \\ 0 \\ 0.05 \end{bmatrix}, \quad x_6(0) = \begin{bmatrix} -0.2 \\ 0.02 \\ -0.5 \\ 0.001 \end{bmatrix}, \qquad x_7(0) = \begin{bmatrix} 0.25 \\ 0.005 \\ 0.015 \\ -0.045 \end{bmatrix}.$$

Furthermore, we assume a nominal, static load, i.e., we set $P_{\mathrm{L}_i}(k) := 0$ for $k \in \mathbb{Z}_+$ and $i \in \mathcal{I}$. Since power networks are generally subject to constraints, for physical, performance or security reasons, we constrain the control inputs as

$$-0.2 \le u_i \le 0.2, \quad i \in \mathcal{I}. \tag{7.13}$$

The relevant system outputs $(\omega_i,\, P_{\mathrm{tie}_i})$, where $P_{\mathrm{tie}_i}(k) := \sum_{\{j|(\varsigma_i,\varsigma_j)\in\mathcal{E}\}} P_{\mathrm{tie}}^{ij}(k)$, are shown in Figure 7.2, along with the corresponding control actions P_{ref_i}, $i \in \mathcal{I}$. Clearly, the frequency and power flow trajectories converge to 0 as k goes to infinity. Note that input constraint (7.13) is not violated, although it is active for some time instants. Figure 7.3 depicts the evolution of $V_i(x_i(k))$ for buses $i \in \mathbb{Z}_{[1,4]} \subset \mathcal{I}$, $V(x(k))$ and the corresponding upper bound as generated by condition (5.12) in Algorithm 3. The simulation shows that $V(x(k))$ is allowed to

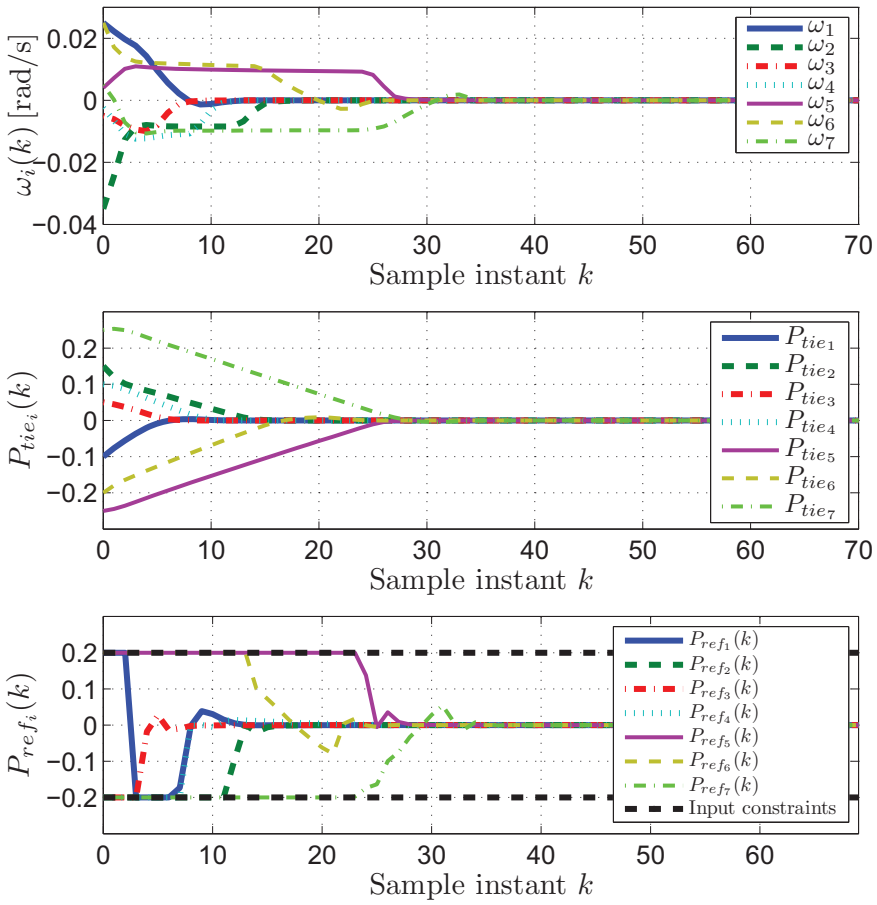

Figure 7.2: Frequency, flow and input trajectories under distributed L-MPC.

vary arbitrarily within the asymptotically converging envelope defined by (5.12), resulting in closed-loop stability. The results clearly illustrate the effectiveness of Algorithm 3 for load-frequency control.

7.4.2 Competitive p-qSF based frequency control

Next, we simulate the CIGRÉ network in closed-loop with Algorithm 4, to demonstrate that p-qSF based synthesis is able to induce converging state trajectories even under competitive subsystem operation. The local control laws employed quadratic cost functions (7.5) with prediction horizon $N_k = 5$, state and input penalty matrices Q_i, R_i listed in Table E.3, and $p_{\max} = 8$ iterations per sample

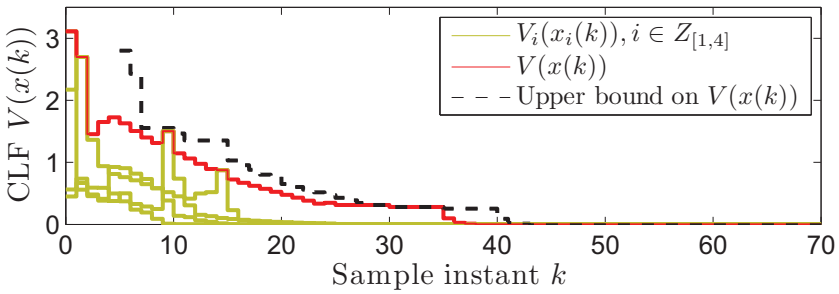

Figure 7.3: Evolution of structured LFs $V_i(x_i(k))$, $V(x(k))$ and the upper bound on $V(x(k))$ over time.

instant. These parameters satisfy condition (7.10) as $\varepsilon_{\max}(W) = 0.0020$. Note also that Q_1 is negative definite: consequently, generator 1 aims to increase the frequency and voltage angle deviations at its respective bus. This destabilizing behavior complicates real-time balancing of the network.

First, consider a simulation of the network under *non-p-qSF-constrained* competitive control, that is, in closed-loop with (7.9), for initial condition

$$x_1(0) = \begin{bmatrix} 0 \\ -0.005 \\ -0.575 \\ 0.755 \end{bmatrix}, \quad x_2(0) = \begin{bmatrix} -0.11 \\ 0.1 \\ 0 \\ -0.01 \end{bmatrix}, \quad x_3(0) = \begin{bmatrix} 0.045 \\ -0.02 \\ 0.085 \\ -0.04 \end{bmatrix},$$

$$x_4(0) = \begin{bmatrix} 0.465 \\ -0.305 \\ -4.3 \\ 5.055 \end{bmatrix}, \quad x_5(0) = \begin{bmatrix} 0.005 \\ 0 \\ 0.065 \\ 0.095 \end{bmatrix}, \quad x_6(0) = \begin{bmatrix} -0.04 \\ 0.025 \\ -0.61 \\ 0.31 \end{bmatrix}, \quad x_7(0) = \begin{bmatrix} 0.075 \\ 0 \\ -0.005 \\ -0.005 \end{bmatrix}.$$

The load $P_{L_i}(k)$ was set to 0 for all $k \in \mathbb{Z}_+$ and $i \in \mathcal{I}$. Figure 7.4 shows that the corresponding closed-loop state and input trajectories do not converge; competition among the generators pushes the network towards instability.

Now consider the results obtained for the above scenario, when simulating the network in closed-loop with competitive p-qSF based control (Algorithm 4). In contrast to L-MPC, there is no need for a-priori synthesis of a set of (structured) Lyapunov functions; p-qSF based control generates both the control actions $u_i(k)$ and the p-qSF parameter matrices $P_i(x(k))$ on-line, i.e., during operation. As explained in Chapter 6, this synthesis requires solving, in parallel, a set of $N = 7$ subsystem-specific semi-definite programs per time instant. Each program involves optimization over the scalar local control action $u_i(k)$, and, in case of synthesis during the first iteration, also over a 4 by 4

parameter matrix $P_i(x(k))$ and a scalar slack variable $\lambda_i(k)$. In the simulation, we employed synthesis parameter values $\rho_i = 0.999$, $\gamma_i = 0.1$ and $\Gamma_i = 5$. Constraint (7.4c) was ignored as no local state and input constraints were considered in this simulation scenario. Problem 6.4.8 remained feasible for all time instants $k \in \mathbb{Z}_{[0,200]}$. Figure 7.5 depicts the associated $x(k)$ and $u(k)$ trajectories. In the simulation, the unconstrained competitive control laws (7.9) were feasible with respect to p-qSF constraint (7.4b) for 29.9 %, 92.7 %, 100 %, 99.0 %, 100 %, 100 % and 42.2 % of the iterations performed by controllers 1, ..., 6 and 7, respectively (in the transient phase, i.e., for $k \in \mathbb{Z}_{[0,10]}$, these numbers are 98.75 %, 100 %, 100 %, 80 %, 100 %, 100 % and 96.25 %). This indicates that the computational benefit associated with embedding the explicit solution to problem (7.4a) in the implementation of Algorithm 4 can be considerable.

Most importantly, the simulation demonstrates that Algorithm 4 is able to generate converging closed-loop state sequences, despite the non-stabilizing competing objectives of the local controllers.

7.4.3 Assessment

In what follows, we will evaluate the suitability of structured max-CLF and p-qSF based control for frequency control in deregulated and decentralized electrical power systems.

As discussed in Chapter 4, control methods for future electrical power systems should be able to deal with complex system dynamics, handle state/input constraints, and guarantee efficient, and, most importantly, stable network operation. The large and deregulated nature of electrical power systems asks for non-centralized ways of achieving these objectives. The structured max-CLF and p-qSF based methods described in Chapters 5 and 6 were specifically designed for distributed stabilization of large-scale networks of dynamical systems. However, by expressing the system-wide aim for closed-loop stability via sets of local input constraints (rather than by minimizing a certain cost function), these methods can easily be combined with techniques for achieving one of the other operational goals, such as constraint satisfaction and optimal performance. For instance, in a max-CLF/p-qSF based balancing scheme, market actors are free to select their actions from the set of stabilizing max-CLF/p-qSF controls based on an arbitrary optimization objective. Note also that synthesis of the max-CLF and p-qSF control laws does not require knowledge of the full network dynamics; each controller requires merely a model of its respective subsystem. This is particularly attractive in competitive environments such as the electrical energy market, where actors are unwilling to share the details on their generating equipment with competitors. Moreover, it was shown that

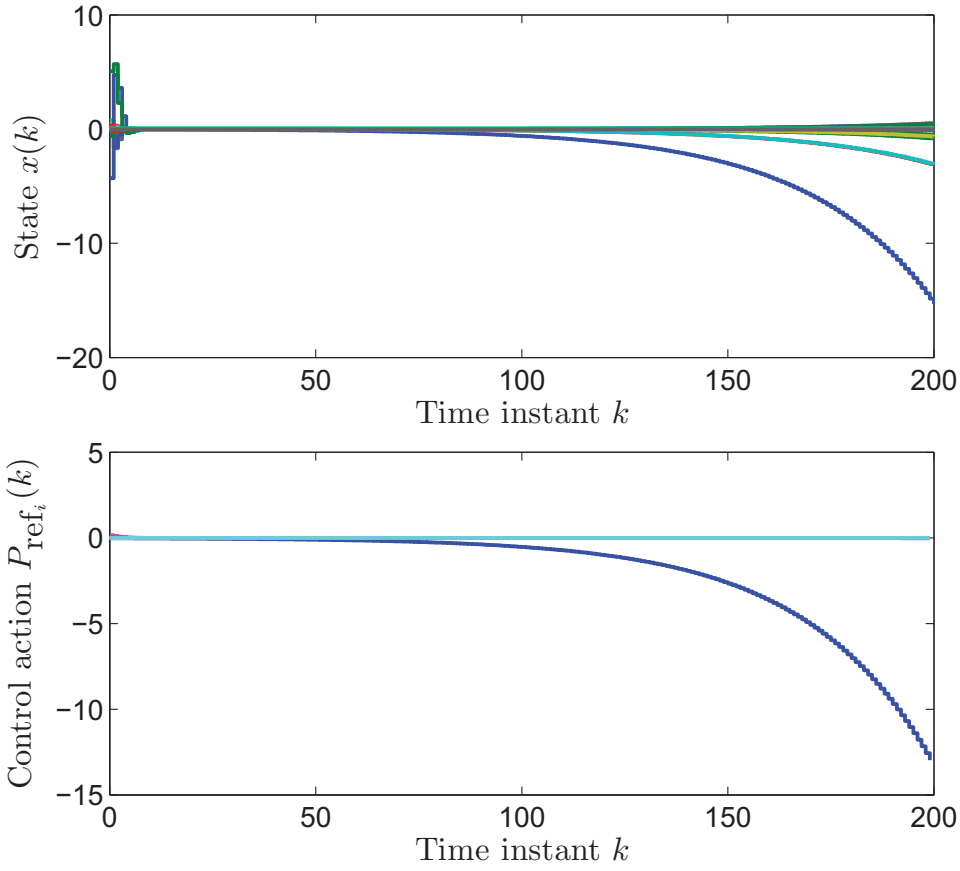

Figure 7.4: State and input trajectories under (non-p-qSF-constrained) competitive control.

both the max-CLF and p-qSF methods are non-conservative, in the sense that they are able to induce converging closed-loop trajectories for networks where standard, non-relaxed monotonic CLF methods or fixed-parameter quadratic storage function based approaches fail. By specifying sets of actions that contribute to network-wide stability that are larger than the solution space defined by conventional, non-flexible CLF-based schemes, the methods provided in this thesis allow for increased market efficiency.

Another important aspect of non-centralized control for deregulated electrical power systems is the need for communication. To compute the local control actions $u_i(k)$, both L-MPC and p-qSF based controllers i need to exchange information with nodes $j \in \mathcal{N}_i$, each sampling instant. Note that due to the

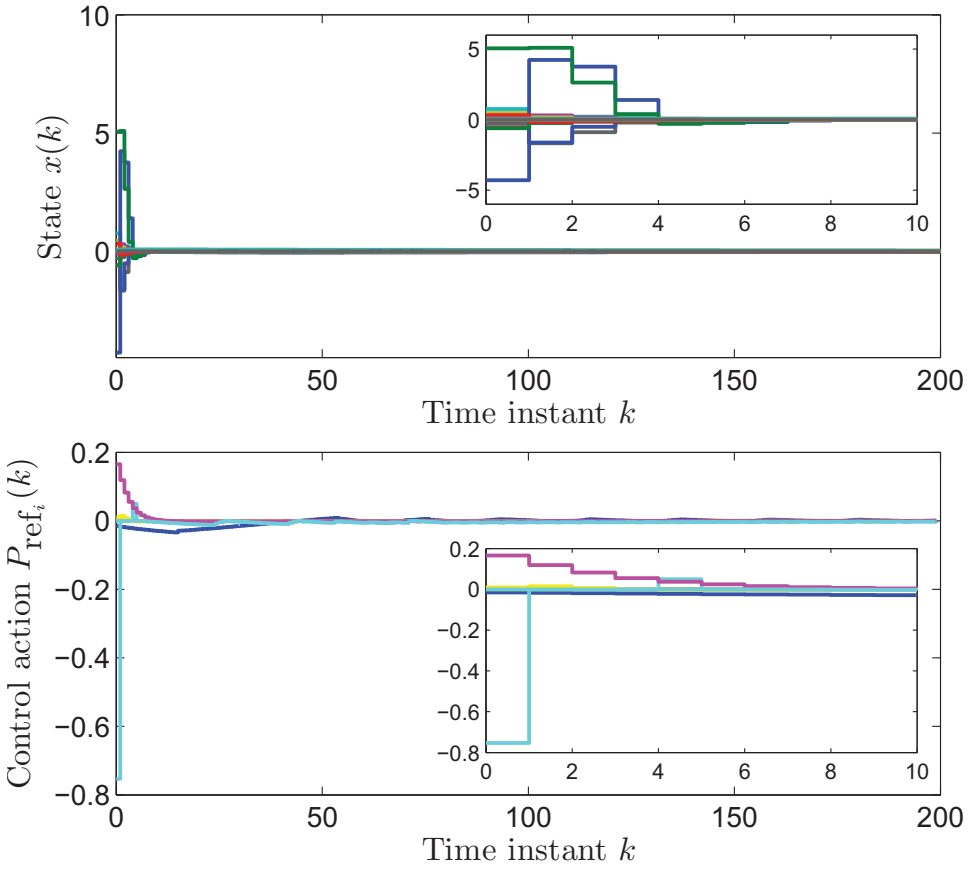

Figure 7.5: State and input trajectories under competitive p-qSF based control (inset: transient phase in detail).

load-bus elimination, the direct neighbors of generator i are not only those generator buses j that are connected via a single edge $\varepsilon_{ij} \in \bar{\mathcal{E}}$, but also those that are connected by a path in single-line diagram $\bar{\mathcal{G}}$ from generator i to generator j via load-buses only (see Figure 7.1 and Table E.1). Consequently, some of the sparsity of the non-reduced network graph $\bar{\mathcal{G}}$ is lost. For certain networks, even the exchange of information among neighbors therefore implies system-wide communication. However, regardless of the network topology, L-MPC or p-qSF based stabilization does not require iterations to guarantee closed-loop stability. Such control schemes are less dependent on high-speed information exchange and more robust against (short-lived/sub-T_s) failures of the communication network than iterative techniques.

It is important to stress that the communication among competitors required by max-CLF or p-qSF based stabilization is restricted to the exchange of low market-sensitive or public information only. In the modeling framework considered in this thesis, the interconnection term between generator nodes, i.e., the power (or current) flow in the connected power lines, is directly measurable by either one of the corresponding interacting agents, whereas knowledge of V_i and $P_i(x)$ does not provide neighboring market players with a significant competitive advantage.

The stabilization techniques discussed in this thesis guarantee closed-loop stability as long as the corresponding control problems keep on admitting a feasible solution, each time instant, which is referred to as *recursive feasibility* in the MPC literature. In Section 6.5 it was shown that this is not an issue for linear and time-invariant networks, where the p-qSF method can be used to synthesize, off-line, a number of converging trajectories, which are then interpolated in real-time to obtain an explicit control scheme with a strong closed-loop stability guarantee. One way of establishing recursive feasibility for the *implicit* max-CLF or p-qSF control schemes and a set of initial conditions relies on generating a region of attraction in the full state space, based on an off-line generated explicit form of the corresponding closed-loop dynamics (see, e.g., (Hermans et al., 2012f), where recursive feasibility is established for a non-linearly constrained electromagnetic actuator in closed-loop with a centralized, flexible-CLF control law). Application of this technique to the max-CLF and p-qSF methods is subject of further research.

The simulation results and observations provided in this section clearly indicate that Lyapunov- and storage-function based stabilization is a promising way of solving the frequency control problem in future electrical power systems.

7.5 Conclusions

In this chapter, the problem of real-time balancing or frequency control in a single-area multimachine electrical power system was considered. It was shown that such power networks fit the NDS-modeling framework, which enables the application of max-CLF and p-qSF based schemes for stabilization of the network frequency. Also, given that generators are operated by non-cooperative, profit-driven market agents, the p-qSF stabilization scheme introduced in Chapter 6 was extended with the competitive optimization of a set of local performance cost functions over a finite, receding prediction horizon. In this control algorithm, firstly, parameterized stability conditions are employed to define a set of stabilizing control actions, and secondly, additional iterations are used

to competitively improve performance, all based on information from directly connected systems only.

We evaluated the suitability of the distributed Lyapunov-based predictive control and parameterized storage function methods as an alternative to the conventional automatic generation control arrangements by simulating them in closed-loop with the 7-machine CIGRÉ benchmark system. The control laws were shown to be particularly suitable for NDS that are situated in competitive environments, as state-of-the-art non-cooperative optimal control is generally not inherently stabilizing, whereas communication is restricted to the exchange of low market-sensitive information only.

8 Conclusions

We conclude this thesis by summarizing the main contributions and describing a number of possible directions and starting points for future research.

8.1 Contributions

The main contributions of this thesis are:

- The observation that optimal nodal pricing and cost-based congestion redispatch can induce identical, economically efficient nodal power injections, whereas the transactions needed to establish this market equilibrium differ and result in different aggregated prosumer profits;
- A multiobjective modeling framework to decouple and analyze the effects of TSO/regulator and producer behavior on power system security and short-run market efficiency;
- A novel, asynchronous energy transaction settlement procedure for reducing the power imbalance fluctuations associated with energy-based production scheduling;
- The observation that optimal performance with respect to a system-wide objective function, and thus, cost-based stabilization, is not a feasible goal when considering predictive control for electrical power systems;

- A scalable method for stabilizing a network of coupled discrete-time nonlinear systems via a set of a-priori generated structured control Lyapunov functions;
- A theorem proving that stability analysis that relies on the construction of a Lyapunov function from a set of fixed-parameter quadratic storage functions may fail even for simple unconstrained, linear time-invariant network dynamics;
- A non-centralized method for synthesizing stabilizing control action trajectories via a set of parameterized quadratic storage functions, which can be interpolated to obtain an explicit control law for linear, time-invariant networks.

8.1.1 Managing congestion in the deregulated electricity market

In Chapter 2, the maximization of *reliability* and *economic efficiency* were identified as the two key objectives of electrical power system operation. Neither of the two objectives can be pursued while fully ruling out the other; a reliable transmission network is essential for the exchange of electrical energy among market participants, whereas the costs of transmission network operation and expansion need to be recovered from the market. In the deregulated electrical power system, the conflicting nature of both objectives is reflected by the actions of the main actors involved, i.e., the transmission system operator, who is entrusted with the expansion, maintenance and operation of the electricity grid, and energy prosumers, whose aim is to maximize profit via suitably chosen energy transactions and power prosumption profiles.

The tension between network reliability and market performance is particularly apparent in the congestion management problem. This was illustrated by comparing the effects of two fundamentally different congestion management procedures, namely, locational marginal pricing and cost-based redispatch. In the first scheme, market actors are confronted with the limitations of the transmission network during trade, whereas in the second, a possible overloading of the network by the unconstrained market outcome is relieved, after gate closure, by the TSO, at socialized costs. It was shown that even though both schemes can induce identical, optimal power injections, the transactions needed to establish this market equilibrium differ, and thus, the methods will generally induce different aggregated prosumer profits.

As a second contribution of Chapter 2, we addressed the non-transparency of thermal transmission-line limit and safety-margin computations that provides network operators with the possibility to exploit flow-capacity estima-

tion in their own benefit. Naturally, TSOs tend to minimize the chance of network overloading by choosing security margins as large as possible, whereas the society demands maximum transmission capacity, i.e., minimum margins, to optimize social welfare. A multiobjective modeling framework was therefore presented to decouple and analyze the effects of TSO and prosumer behavior on short-run network security and dispatch market efficiency.

All the results provided in Chapter 2 were illustrated via simulation of the IEEE 39-bus New-England benchmark network.

8.1.2 Asynchronous settlement of energy transactions

In the deregulated electrical energy market, transmission system operators have to provide market participants with appropriate incentives to guarantee stable operation of the transmission network. Since the main electricity market commodity is energy rather than power, the market and TSO can only provide energy-based financial incentives, at a limited number of discrete-time instants, i.e., at the end of each program time unit, even though real-time control objectives actually require a continuous balancing of power.

In Chapter 3, it was observed that the currently employed energy-based incentive system promotes coarse, step-wise power production profiles that cause large imbalances with respect to the smooth variations in power demand. These imbalances need to be compensated by considerable control effort during the operational day, even if no unexpected disturbances act on the system. It was shown that already today, these market-induced power imbalances give rise to grid frequency deviations that can be alarmingly large.

State-of-the-art solutions for improving open-loop scheduling performance can constrain trade and significantly increase market complexity. Hence, an alternative scheduling concept was proposed that relies on standard market arrangements, but settles the energy exchange of different market participants in an asynchronous way. Open- and closed-loop simulations were provided to illustrate that by adopting this method, network operation can become more robust and the strain on balancing reserves, and thus balancing costs, can be reduced considerably.

8.1.3 Model predictive control for large-scale power systems

With the increasing share of intermittent, badly-predictable distributed generation, the share of electrical energy production that can be effectively scheduled is decreasing steadily. As a result, there is a growing need for efficient balancing mechanisms that can account for generator and transmission network capacity

constraints in real-time. In Chapter 4 it was shown that a promising candidate for real-time operation of future electrical power systems is model predictive control. Because the large dimensions and complexity of these networks hamper a standard, centralized implementation of MPC, we assessed the suitability of a number of scalable schemes, differing in terms of decentralization, communication requirements and computational complexity, instead.

Simulation results showed a positive correlation between the extent of communication among local controllers and state-prediction accuracy and, thus, attainable closed-loop performance. Iterative, system-wide communication or coordination is usually not feasible for large-scale networks, however, and consequently, optimal performance with respect to a system-wide objective function and coupled-constraint handling are currently out of reach. This also hampers the application of cost-based stabilization schemes, in which closed-loop stability is guaranteed via monotonic convergence of a single, optimal system-wide performance cost. The observations made in Chapter 4 thus motivate the search for non-centralized control schemes that can ensure stability based on local model and state information only.

8.1.4 Stabilization of networked dynamical systems

Motivated by the results provided in Chapter 4, in Chapters 5–7 the focus was on non-centralized stabilization methods for networks of interconnected discrete-time dynamical systems, with power systems as particular field of application.

Distributed Lyapunov-based model predictive control
In Chapter 5, a distributed, constraint-based stabilization technique was proposed, in which the set of stabilizing control actions is specified via separable convergence conditions for a set of a-priori synthesized *structured max-control Lyapunov functions (max-CLFs)*. These conditions were shown to be non-conservative, in the sense that non-monotonic convergence of the structured functions along closed-loop trajectories is allowed, whereas their construction establishes the existence of a control Lyapunov function, and thus, stability, for the full, interconnected dynamics. Secondly, an alternative method was provided in which also the demand for a monotonically converging full-system CLF was relaxed while retaining the stability certificate. Then, the conditions were embedded in an almost-decentralized Lyapunov-based MPC scheme, in which the local control laws rely on non-iterative neighbor-to-neighbor communication only.

Scalable stabilization via parameterized quadratic storage functions
In Chapter 6, a theorem and an example system were provided, which showed that stabilization methods that rely on the off-line synthesis of a Lyapunov candidate via fixed quadratic storage functions fail for even the simplest of networks, if those networks contain one or more subsystems that do not admit a quadratic Lyapunov function under decoupled operation. A solution to this issue was found by considering storage functions that are endowed with a finite set of state-dependent parameters. Max-type convergence conditions similar to the ones used in the L-MPC scheme discussed in Chapter 5 were employed to construct a Lyapunov function for the full network, whereas monotonic convergence of the individual storage functions is not required. The merit of the provided approach is that the storage functions can be constructed during operation, i.e., along a closed-loop trajectory, thus removing the impediment of centralized, off-line LF synthesis associated with fixed-parameter storage functions.

We showed that the p-qSF synthesis conditions can be efficiently exploited to obtain a scalable, trajectory-dependent control scheme that relies on non-iterative communication among directly-connected systems only. For input-affine network dynamics and quadratic storage functions, the procedure can be implemented by solving a single semi-definite program per node and sampling instant, in a receding horizon fashion. Moreover, by interpolating a collection of so-obtained input trajectories, it is possible to obtain a low-complexity explicit control law for linear, time-invariant systems and extend the trajectory-specific convergence property to a much stronger guarantee of closed-loop asymptotic stability for a particular set of initial conditions.

Application to frequency control in a competitive environment
In Chapter 7, we considered the application of max-CLF and p-qSF-based control for real-time balancing, i.e., stabilization of the network frequency, in multi-machine electrical power networks. Given that generators are operated by competitive, profit-driven market agents, the p-qSF stabilization scheme introduced in Chapter 6 was extended with the competitive optimization of a set of arbitrarily chosen, local performance cost functions over a finite, receding prediction horizon. In this control algorithm, firstly, the parameterized stability conditions are employed to define a set of stabilizing control actions, and secondly, additional iterations are used to competitively improve performance, all based on information from directly connected systems only. The suitability of the distributed Lyapunov-based predictive control and parameterized storage function algorithms was assessed as an alternative to conventional load-frequency control, by simulating them in closed-loop with the 7-machine CIGRÉ benchmark

system. The control schemes were shown to be particularly suitable for NDS that are situated in competitive environments, as state-of-the-art non-cooperative optimal control is generally not inherently stabilizing, whereas communication is restricted to the exchange of low market-sensitive information only.

8.2 Open problems and ideas for future research

There are several open problems and interesting research directions in connection to the results presented in this thesis. In what follows, we will briefly describe a few future lines of research that can be pursued.

8.2.1 Non-centralized handling of coupled constraints

In Chapter 4, we briefly mentioned the challenges associated with distributed control of networks that are subject to coupled constraints (i.e., constraints that affect the state and input trajectories of multiple subsystems) if the design and evaluation of the corresponding local feedback laws is based on partial model and state knowledge only. Coupled constraints are particularly relevant in the real-time balancing of electrical power systems, for example, to avoid overloading of inter-area transmission lines. In decentralized MPC for interconnected systems, coupled constraint feasibility can for example be guaranteed by considering system interactions as disturbance inputs and tightening the coupling constraints via worst-case safety margins (Jia and Krogh, 2002). A similar approach is pursued in the operation of electrical power networks, where TSOs reduce the inter-area congestion risk by adjusting the forward market's available transfer capacity based on expected dispatch scenarios and approximate power flow computations, see Chapter 2. Such methods tend to be conservative, however, and have a considerable impact on market efficiency when deregulated power systems are considered. The development of alternative, less conservative methods for dealing with coupled constraints and dynamics, while keeping communication requirements within practical limits, is therefore of great interest.

8.2.2 A-posteriori verification of recursive feasibility

The closed-loop stability guarantees provided by both the max-CLF and p-qSF methods proposed in this thesis require the corresponding open-loop optimization problems to be feasible at each discrete-time instant. Verification of this property, also referred to as *recursive feasibility* in the MPC literature, is nontrivial. Still, in particular cases, it may be possible to obtain a tractable ex-

plicit formulation of the closed-loop network dynamics. This allows for the a-posteriori computation of an attractive set, and thus, a set of initial state conditions for which asymptotic stability holds. For an example of such an approach, we refer to (Hermans et al., 2012f), where a flexible CLF method is used for non-conservative stabilization of an electromagnetic actuator. However, for large networks, such an approach is expected to be computationally demanding, while requiring a centralized knowledge of the full network dynamics, which prohibits application in competitive environments such as the deregulated electrical energy market. Further research into scalable stability analysis techniques for general networks of dynamical systems, and the electrical power system in particular, is therefore highly needed.

8.2.3 Design of a real-time multi-area energy market

The European electricity market currently allows energy transactions to be established up to a few hours before operation. The so-obtained values for nett inter-area power exchange are used during the operational day as setpoints for the secondary control loops (more specifically, for computing the area control error), and consequently, each control area is required to internally compensate for its real-time energy imbalance. In terms of load-frequency control, this implies that the individual areas are in fact decoupled in steady state and do not fully benefit from continental-scale aggregation.

If we consider each machine bus to be representative of a full control area, the competitive framework for real-time power balancing provided in Chapter 7 is similar to how control areas are managed today. For instance, coordination of real-time inter-area power exchange typically involves TSOs of neighboring control areas only, and network operators have much freedom in designing the internal balancing scheme for their respective areas. By contrast, the scheme proposed in Chapter 7 does allow for real-time balancing of the European network as a whole, i.e., not just on a control area level, which provides the TSOs with more flexibility than they have today. Still, more research is needed to evaluate the effects of continent-wide load-frequency balancing on system-stability, transmission-constraint handling and market efficiency.

Bibliography

Aguado, M., Bourgeois, R., Bourmaud, J. Y., Casteren, J. V., Ceratto, M. A., Jäkel, M., Malfliet, B., Mestdag, C., Noury, P., Pool, M., den Reek, W. V., Rohleder, M., Schavemaker, P. H., Scolari, S., Weis, O., Wolpert, J., 2012. Flow-based market coupling in the central western European region: on the eve of implementation. Tech. rep., CIGRÉ, Paris, France.

Alessio, A., Bemporad, A., July 2007. Decentralized model predictive control of constrained linear systems. In: European Control Conference. Kos, Greece, pp. 2813–2818.

Anderson, P., 2003. Power System Control and Stability. IEEE Press, New York, NY, USA.

Artstein, Z., 1983. Stabilization with relaxed controls. Nonlinear Analysis 7 (11), 1163–1173.

Atwa, Y. M., El-Saadany, E. F., November 2010. Optimal allocation of ESS in distribution systems with a high penetration of wind energy. IEEE Transactions on Power Systems 25 (4), 1815–1822.

Bemporad, A., 1998. A predictive controller with artificial Lyapunov function for linear systems with input/state constraints. Automatica 34 (10), 1255–1260.

Bemporad, A., Morari, M., Dua, V., Pistikopoulos, E. N., 2002. The explicit linear quadratic regulator for constrained systems. Automatica 38 (1), 3–20.

Bertsekas, D. P., 1999. Nonlinear Programming. Athena Scientific, Belmont, MA, USA.

Blanchini, F., 1994. Ultimate boundedness control for uncertain discrete-time systems via set-induced Lyapunov functions. IEEE Transactions on Automatic Control 39 (2), 428–433.

Bompard, E., Correia, P., Gross, G., Amelin, M., 2002. A comparative analysis of congestion management schemes under a unified framework. IEEE Power Engineering Review 22 (11), 59–60.

Camponogara, E., 2000. Controlling networks with collaborative nets. Ph.D. thesis, Carnegie Mellon University, Pittsburgh, PA, USA.

Camponogara, E., Jia, D., Krogh, B. H., Talukdar, S., 2002. Distributed model predictive control. IEEE Control Systems Magazine 22 (1), 44–52.

Chen, S. X., Gooi, H. B., Wang, M. Q., March 2012. Sizing of energy storage for microgrids. IEEE Transactions on Smart Grid 3 (1), 142–151.

Chowdhury, A. A., Koval, D. O., 2010. Quantitative transmission-system-reliability assessment. IEEE Transactions on Industry Applications 46 (1), 304–312.

Christie, R. D., Wollenberg, B. F., Wangensteen, I., 2000. Transmission management in the deregulated environment. Proceedings of the IEEE 88 (2), 170–195.

Cormen, T. H., Leiserson, C. E., Rivest, R. L., Stein, C., 2001. Introduction to Algorithms. The MIT Press, Cambridge, MA, USA.

Dashkovskiy, S., Rüffer, B., Wirth, F., 2007. An ISS small gain theorem for general networks. Mathematics of Control, Signals, and Systems 19 (2), 93–122.

Dashkovskiy, S. N., Rüffer, B. S., Wirth, F. R., 2010. Small gain theorems for large scale systems and construction of ISS Lyapunov functions. SIAM Journal on Control and Optimization 48 (6), 4089–4118.

Doan, M. D., Keviczky, T., Schutter, B. D., December 2011a. A distributed optimization-based approach for hierarchical MPC of large-scale systems with coupled dynamics and constraints. In: IEEE Conference on Decision and Control. Orlando, FL, USA, pp. 5236–5241.

Doan, M. D., Keviczky, T., Schutter, B. D., 2011b. An iterative scheme for distributed model predictive control using Fenchel's duality. Journal of Process Control 21 (5), 746–755.

Driessen, P. A. A., Hermans, R. M., Van den Bosch, P. P. J., December 2012. Distributed economic model predictive control of networks in competitive environments. In: IEEE Conference on Decision and Control. Maui, HI, USA.

Dunbar, W. B., 2007. Distributed receding horizon control of dynamically coupled nonlinear systems. IEEE Transactions on Automatic Control 52 (7), 1249–1263.

ENTSO-E, March 2009. Policy 1: Load-Frequency Control and Performance. ENTSO-E, Brussels, Belgium, 3rd Edition.

ETSO, March 2000. Net transfer capacities and available transfer capacities in the internal market of electricity in Europe. Tech. rep., ETSO/ENTSO-E, Brussels, Belgium.

ETSO, April 2005. An evaluation of preventive countertrade as a means to guarantee firm transmission capacity. Tech. rep., ETSO/ENTSO-E, Brussels, Belgium.

European Commission, March 2011. A roadmap for moving to a competitive low carbon economy in 2050. Tech. rep., European Union, Brussels, Belgium.

Farina, M., Scattolini, R., 2012. Distributed predictive control: A non-cooperative algorithm with neighbor-to-neighbor communication for linear systems. Automatica 48 (6), 1088–1096.

Frunt, J., June 2011. Analysis of balancing requirements in future sustainable and reliable power systems. Ph.D. thesis, Eindhoven University of Technology, Eindhoven, The Netherlands.

Gielen, R., Lazar, M., Teel, A., 2012. Input-to-state stability analysis for interconnected difference equations with delay. Mathematics of Control, Signals, and Systems 24 (1), 33–54.

Giselsson, P., Rantzer, A., December 2010. Distributed model predictive control with suboptimality and stability guarantees. In: IEEE Conference on Decision and Control. Atlanta, GA, USA, pp. 7272–7277.

Glachant, J.-M., Lévêque, F., 2009. Electricity Reform in Europe - Towards a Single Energy Market. Edward Elgar Publishing Ltd, Cheltenham, UK.

Glachant, J.-M., Pignon, V., 2005. Nordic congestion's arrangement as a model for Europe? Physical constraints vs. economic incentives. Utilities Policy 13 (2), 153–162.

Goodwin, G. C., Seron, M. M., De Doná, J. A., 2005. Constrained control and estimation: an optimization approach. Communications and control engineering. Springer, London, UK.

Grainger, J. J., Stevenson, W. D., 2003. Power system analysis. McGraw-Hill, Columbus, OH, USA.

Grüne, L., Worthmann, K., 2012. A Distributed NMPC Scheme without Stabilizing Terminal Constraints. In: Johansson, R., Rantzer, A. (Eds.), Distributed Decision Making and Control. Springer, Berlin/Heidelberg, Germany, pp. 261–287.

Hale, J., 1977. Theory of functional differential equations. Springer, Berlin/Heidelberg, Germany.

Heath, M., 2002. Scientific Computing. McGraw-Hill, New York, NY, USA.

Hermans, R. M., Almassalkhi, M. R., Hiskens, I. A., June 2012a. Incentive-based coordinated charging control of plug-in electric vehicles at the distribution-transformer level. In: American Control Conference. Montréal, QC, Canada, pp. 264–269.

Hermans, R. M., Jokić, A., Lazar, M., Alessio, A., Van den Bosch, P. P. J., Hiskens, I. A., Bemporad, A., 2012b. Assessment of non-centralised model predictive control techniques for electrical power networks. International Journal of Control 85 (8), 1162–1177.

Hermans, R. M., Jokić, A., Van den Bosch, P. P. J., Frunt, J., Kamphuis, I. G., Warmer, C. J., June 2010a. Limitations in the design of ancillary service markets imposed by communication network delays. In: International Conference on the European Energy Market. Madrid, Spain.

Hermans, R. M., Lazar, M., Jokić, A., 2010b. Almost decentralized Lyapunov-based nonlinear model predictive control. In: American Control Conference. Baltimore, MD, USA, pp. 3932–3938.

Hermans, R. M., Lazar, M., Jokić, A., July 2011a. Distributed predictive control of the 7-machine CIGRÉ power system. In: American Control Conference. San Francisco, CA, USA, pp. 5225–5230.

Hermans, R. M., Lazar, M., Jokić, A., 2012c. Competitive model predictive control for networks of interconnected dynamical systems, submitted to a conference (invited).

Hermans, R. M., Lazar, M., Jokić, A., 2012d. Distributed MPC Made Easy. Springer, Berlin/Heidelberg, Germany, Ch. Distributed Lyapunov-based Model Predictive Control, in press.

Hermans, R. M., Lazar, M., Jokić, A., 2012e. Stabilization of interconnected dynamical systems by on-line convex optimization. Submitted to a journal.

Hermans, R. M., Lazar, M., Jokić, A., Gielen, R. H., August 2011b. On parameterized stabilization of networked dynamical systems. In: IFAC World Congress. Milano, Italy, pp. 1416–1421.

Hermans, R. M., Lazar, M., Jokić, A., Van den Bosch, P. P. J., April 2010c. Almost decentralized model predictive control of power networks. In: IEEE Mediterranean Electrotechnical Conference. Valletta, Malta, pp. 1551–1556.

Hermans, R. M., Lazar, M., Kolmanovsky, I. V., Di Cairano, S., 2012f. Horizon-1 predictive control of automotive electromagnetic actuators. IEEE Transactions on Control Systems Technology. In press.

Hermans, R. M., Van den Bosch, P. P. J., Jokić, A., Giesbertz, P., Boonekamp, P., Virag, A., May 2011c. Congestion management in the deregulated electricity market: An assessment of locational pricing, redispatch and regulation. In: International Conference on the European Energy Market. Zagreb, Croatia, pp. 8–13.

Hermans, R. M., Verberk, J. H., Van den Bosch, P. P. J., Jokić, A., Frunt, J., 2012g. Systematic design of market-based balancing arrangements for deregulated power systems: an asynchronous solution, to be submitted to a journal. Based on conference paper (Verberk et al., 2011) that was awarded with an IEEE PES PowerTech'11 High Quality Paper Certificate.

Hill, C. A., Such, M., Chen, D., Gonzalez, J., Grady, W. M., 2012. Battery energy storage for enabling integration of distributed solar power generation. IEEE Transactions on Smart Grid 3 (2), 850–857.

Ilić, M. D., 1998. Electric Power Systems Restructuring: Engineering and Economics. Kluwer Academic Publishers, Dordrecht, The Netherlands.

Ito, H., Dashkovskiy, S., Wirth, F., 2012. Capability and limitation of max- and sum-type construction of Lyapunov functions for networks of iISS systems. Automatica 48 (6), 1197–1204.

Jaleeli, N., VanSlyck, L. S., Ewart, D. N., Fink, L. H., Hoffmann, A. G., 1992. Understanding automatic generation control. IEEE Transactions on Power Systems 7 (3), 1106–1122.

Jia, D., Krogh, B., May 2002. Min-max feedback model predictive control for distributed control with communication. In: American Control Conference. Achorage, AK, USA, pp. 4507–4512.

Jiang, Z.-P., Wang, Y., 2002. A converse Lyapunov theorem for discrete-time systems with disturbances. Systems & Control Letters 45 (1), 49–58.

Jokić, A., 2007. Price-based optimal control of electrical power systems. Ph.D. thesis, Eindhoven University of Technology, Eindhoven, The Netherlands.

Jokić, A., Lazar, M., June 2009. On decentralized stabilization of discrete-time nonlinear systems. In: American Control Conference. St. Louis, MO, USA, pp. 5777–5782.

Jokić, A., Lazar, M., Van den Bosch, P. P. J., 2007. Price-based optimal control of power flow in electrical energy transmission networks. In: Bemporad, A., Bicchi, A., Buttazzo, G. (Eds.), Hybrid Systems: Computation and Control. Vol. 4416 of Lecture Notes in Computer Science. Springer, Berlin/Heidelberg, Germany, pp. 315–328.

Kellett, C. M., Teel, A. R., 2005. On the robustness of $\mathcal{KL}$-stability for difference inclusions: Smooth discrete-time Lyapunov functions. SIAM Journal on Control and Optimization 44 (3), 777–800.

Keviczky, T., Borrelli, F., Balas, G. J., 2006. Decentralized receding horizon control for large scale dynamically decoupled systems. Automatica 42 (12), 2105–2115.

Kundur, P., 1994. Power System Stability and Control. McGraw-Hill, New York, NY, USA.

Kundur, P., Paserba, J., Ajjarapu, V., Andersson, G., Bose, A., Canizares, C., Hatziargyriou, N., Hill, D., Stankovic, A., Taylor, C., Van Cutsem, T., Vittal, V., 2004. Definition and classification of power system stability. IEEE Transactions on Power Systems 19 (3), 1387–1401, IEEE/CIGRÉ joint task force on stability terms and definitions.

Langbort, C., Chandra, R. S., D'Andrea, R., 2004. Distributed control design for systems interconnected over an arbitrary graph. IEEE Transactions on Automatic Control 49 (9), 1502–1519.

Lazar, M., 2006. Model predictive control of hybrid systems: Stability and robustness. Ph.D. thesis, Eindhoven University of Technology, Eindhoven, The Netherlands.

Lazar, M., Gielen, R. H., December 15–17 2010. On parameterized Lyapunov and control Lyapunov functions for discrete-time systems. In: IEEE Conference on Decision and Control. Atlanta, GA, USA, pp. 3264–3270.

Lazar, M., Heemels, W. P. M. H., Weiland, S., Bemporad, A., 2006. Stabilizing model predictive control of hybrid systems. IEEE Transactions on Automatic Control 51 (11), 1813–1818.

Lévêque, F. (Ed.), 2006. Competitive electricity markets and sustainability. Edward Elgar Publishing, Cheltenham, UK.

Liu, B., Marquez, H. J., 2008. Uniform stability of discrete delay systems and synchronization of discrete delay dynamical networks via Razumikhin technique. IEEE Transactions on Circuits and Systems I: Regular Papers 55 (9), 2795–2805.

Liu, J., Chen, X., Muñoz de la Peña, D., Christofides, P. D., 2010. Sequential and iterative architectures for distributed model predictive control of nonlinear process systems. AIChE Journal 56 (8), 2137–2149.

Liu, J., Muñoz de la Peña, D., Christofides, P. D., 2009a. Distributed model predictive control of nonlinear systems with input constraints. In: American Control Conference. St. Louis, MO, USA, pp. 2319–2326.

Liu, J., Muñoz de la Peña, D., Christofides, P. D., Davis, J. F., 2009b. Lyapunov-based model predictive control of nonlinear systems subject to time-varying measurement delays. International Journal of Adaptive Control and Signal Processing 23 (8), 788–807.

Lyapunov, A. M., 1907. Problème général de la stabilité du mouvement. Ann. Fac. Sci. Toulouse 9, 203–474, reprinted in Ann. Math. Study No. 17, 1949, Princeton University Press, Princeton, NJ, USA.

Maestre, J. M., Muñoz de la Peña, D., Camacho, E. F., Alamo, T., 2011. Distributed model predictive control based on agent negotiation. Journal of Process Control 21 (5), 685–697.

Magni, L., Scattolini, R., 2006. Stabilizing decentralized model predictive control of nonlinear systems. Automatica 42 (7), 1231–1236.

Mayne, D. Q., Rawlings, J. B., Rao, C. V., Scokaert, P. O. M., 2000. Constrained model predictive control: Stability and optimality. Automatica 36 (6), 789–814.

Mhaskar, P., El-Farra, N. H., Christofides, P. D., 2006. Stabilization of nonlinear systems with state and control constraints using Lyapunov-based predictive control. Systems & Control Letters 55 (8), 650–659.

Müller, M. A., Reble, M., Allgöwer, F., 2012. Cooperative control of dynamically decoupled systems via distributed model predictive control. International Journal of Robust and Nonlinear Control 22 (12), 1376–1397.

Muske, K. R., Badgwell, T. A., 2002. Disturbance modeling for offset-free linear model predictive control. Journal of Process Control 12 (5), 617–632.

Nicholson, W., Snyder, C. M., 2012. Microeconomic Theory: Basic Principles and Extensions. South-Western, Mason, OH, USA.

Pai, M. A., 1981. Power System Stability by Lyapunov's Method. North-Holland Publishing Company, Amsterdam, The Netherlands.

Pannocchia, G., Rawlings, J. B., 2003. Disturbance models for offset-free model-predictive control. AIChE Journal 49 (2), 426–437.

Raimondo, D. M., Hokayem, P., Lygeros, J., Morari, M., September 2009. An iterative decentralized MPC algorithm for large-scale nonlinear systems. In: IFAC Workshop on Estimation and Control of Networked Systems. Venice, Italy, pp. 162–167.

Raimondo, D. M., Magni, L., Scattolini, R., 2007. Decentralized MPC of nonlinear systems: An input-to-state stability approach. International Journal of Robust and Nonlinear Control 17 (17), 1651–1667.

Raković, S. V., Kern, B., Findeisen, R., December 15–17 2010. Practical set invariance for decentralized discrete time systems. In: IEEE Conference on Decision and Control. Atlanta, GA, USA, pp. 3283–3288.

Richards, A., How, J. P., 2007. Robust distributed model predictive control. International Journal of Control 80 (9), 1517–1531.

Sandell, N. R., Varaiya, P., Athans, M., Safonov, M. G., 1978. Survey of decentralized control methods for large scale systems. IEEE Transactions on Automatic Control 23 (2), 108–128.

Sawaragi, Y., Nakayama, H., Tanino, T., 1985. Theory of Multiobjective Optimization. Vol. 176 of Mathematics in Science and Engineering. Academic Press Inc., Orlando, FL, USA.

Scattolini, R., 2009. Architectures for distributed and hierarchical model predictive control: a review. Journal of Process Control 19 (5), 723–731.

Schavemaker, P., Croes, A., Otmani, R., Bourmaud, J., Zimmermann, U., Wolpert, J., Reyer, F., Weis, O., Druet, C., 2008. Flow-based allocation in the central western European region. Tech. rep., CIGRÉ, Paris, France.

Schweppe, F. C., Caraminis, M. C., Tabors, R. D., Bohn, R. E., 1988. Spot Pricing of Electricity. Kluwer Academic Publishers, Alphen aan den Rijn, The Netherlands.

Šiljak, D. D., 1978. Large-scale dynamic systems: stability and structure. Systems Sciences and Engineering Series. North-Holland, Amsterdam, The Netherlands.

Sommen, P., Janse, K., 2008. On the relationship between uniform and recurrent nonuniform discrete-time sampling schemes. IEEE Transactions On Signal Processing 56 (10), 5147–5156.

Sontag, E. D., 1983. A Lyapunov-like characterization of asymptotic controllability. SIAM Journal of Control and Optimization 21 (3), 462–471.

Stewart, B. T., Venkat, A. N., Rawlings, J. B., Wright, S. J., Pannocchia, G., 2010. Cooperative distributed model predictive control. Systems & Control Letters 59 (8), 460–469.

Stewart, B. T., Wright, S. J., Rawlings, J. B., 2011. Cooperative distributed model predictive control for nonlinear systems. Journal of Process Control 21 (5), 698–704.

Stoft, S., 2002. Power System Economics: Designing Markets for Electricity. IEEE Press/Wiley-Interscience, Piscataway, NJ, USA.

TenneT TSO, 2009. Operational data (website). TenneT TSO, Arnhem, The Netherlands.
URL `www.tennet.org/english/operational_management/`

Todd, M. J., 2001. Semidefinite optimization. Acta Numerica 2001 (10), 515–560.

Tractebel Engineering, February 2009. Study of the interactions and dependencies of balancing markets, intraday trade and automatically activated reserves. Tech. rep., Tractebel Engineering, Brussels, Belgium.

UCTE, August 2008. Frequency control investigation. Tech. rep., UCTE/ENTSO-E, Brussels, Belgium.

Van den Bosch, P. P. J., Jokić, A., Frunt, J., Kling, W. L., Nobel, F., Boonekamp, P., de Boer, W., Hermans, R. M., Virag, A., 2011. Price-based control of ancillary services for power balancing. European Transactions on Electrical Power 21 (6), 1889–1901.

Van der Veen, R. A. C., 2012. Designing multinational electricity balancing markets. Ph.D. thesis, Delft University of Technology, Delft, The Netherlands.

Venkat, A. N., 2006. Distributed model predictive control: Theory and applications. Ph.D. thesis, University of Wisconsin-Madison, Madison, WI, USA.

Venkat, A. N., Hiskens, I. A., Rawlings, J. B., Wright, S. J., 2008. Distributed MPC strategies with application to power system automatic generation control. IEEE Transactions on Control Systems Technology 16 (6), 1192–1206.

Verberk, J. H., Hermans, R. M., Van den Bosch, P. P. J., Jokić, A., Frunt, J., June 2011. Systematic design of market-based balancing arrangements for deregulated power systems: an asynchronous solution. In: IEEE PowerTech 2011. Trondheim, Norway, awarded with an IEEE PES PowerTech'11 High Quality Paper Certificate.

Šiljak, D. D., 1991. Decentralized Control of Complex Systems. Vol. 184 of Mathematics in Science and Engineering. Academic Press, Boston, MA, USA.

Weissbach, T., Welfonder, E., March 2009. High frequency deviations within the European power system: Origins and proposals for improvement. In: Power Systems Conference and Exposition. Seattle, WA, USA, pp. 1–6.

Willems, J. C., 1972. Dissipative dynamical systems. Archive for Rational Mechanics and Analysis 45, 321–393.

Wood, A. J., Wollenberg, B. F., 1996. Power generation, operation, and control, 2nd Edition. Wiley-Interscience, New York, NY, USA.

A

Appendix to Chapter 3

A.1 *Derivation of* (3.15)

Consider the second scenario in Section 3.3, where all controllable generation is uniformly distributed over BRPs $i \in \mathcal{I}_{\text{BRP}}$, and where BRP 0 is responsible for all noncontrollable production (i.e., $\mu_{P,i}(t) \neq 0$ only for $i = 0$). Let

$$\overline{P}[k] := \widetilde{P}[n], \qquad \text{for } n \leq \frac{k}{N} < n+1,\ k \in \mathbb{Z}, \tag{A.1}$$

be the result of up-sampling $\widetilde{P}[n] := \sum_i \widetilde{P}_i[n]$ with the strictly positive, integer factor N. Using (3.11)–(3.12), (3.14) is rewritten as

$$\hat{P}[k] = \sum_{i=0}^{N-1} \frac{1+2i}{2N^2} \Big(\overline{P}[k-N+i] + \overline{P}[k+N-i-1] \Big). \tag{A.2}$$

Thus, $\hat{P}[k]$ is a weighted sum of successive samples of $\overline{P}[k]$, or, equivalently, the result of convolving $\overline{P}[k]$ with a symmetric finite impulse response h_k, $k = 0, \ldots, 2N-1$. This impulse response is specified by the vector

$$\begin{aligned} \mathbf{h} &= \begin{bmatrix} h_0, & h_1, & \ldots & h_{N-1}, & h_N, & \ldots & h_{2N-2}, & h_{2N-1} \end{bmatrix} \\ &:= \frac{1}{2N^2} \begin{bmatrix} 1, & 1+2, & \ldots & 1+2(N-1), & 1+2(N-1), & \ldots & 1+2, & 1 \end{bmatrix}. \end{aligned} \tag{A.3}$$

Given (A.3), we observe the following. Firstly, note that the sum of the coefficients of $\mathbf{h}$ equals

$$\sum_{k=0}^{2N-1} h_k = 2 \cdot \frac{1}{2N^2} \left(\frac{1+(1+2(N-1))}{2} \cdot N \right) = 1. \tag{A.4}$$

This implies that all E-program transactions are contained in the E-references. Secondly, observe that **h** describes a $2N$-wide low-pass digital filter applied to the aggregated controlled power profile for the power system as a whole, which is sampled at a rate of $\frac{N}{T_{\text{PTU}}}$. Hence, under APM scheduling, transaction $E_i[n]$ is distributed over 2 PTUs of the market time frame. Both observations are in accordance with Proposition 3.3.2.

A.2 Derivation of Proposition 3.3.3

A.2.1 Synchronized settlement

An expression for the open-loop power exchange error associated with the currently-employed, T_{PTU}-based synchronous scheduling arrangements, and an upper bound thereon, is derived as follows. Let the aggregated step-wise power production profile be described by

$$\widetilde{P}[n] := \frac{1}{T_{\text{PTU}}} \int_{t_n}^{t_{n+1}} \mu_P(\tau)\mathrm{d}\tau = \frac{E(t_{n+1}) - E(t_n)}{T_{\text{PTU}}}, \tag{A.5}$$

where

$$E(\tau) = \int_0^{\tau} \mu_P(t)dt + E(0) \quad \Leftrightarrow \quad \frac{\mathrm{d}E}{\mathrm{d}t}(\tau) = \mu_P(\tau). \tag{A.6}$$

Assuming that $E(\tau)$ is infinitely differentiable for all $\tau \in \mathbb{R}$, its Taylor series representation around $t \in [t_n, t_{n+1})$ is

$$E(\tau) = E(t) + \frac{\mathrm{d}E}{\mathrm{d}t}(t)(\tau - t) + \frac{1}{2}\frac{\mathrm{d}^2E}{\mathrm{d}t^2}(\tau - t)^2 + \mathcal{O}((\tau - t)^3), \tag{A.7}$$

see, e.g., (Heath, 2002). From this, it follows that

$$E(t_n) = E(t) + \frac{\mathrm{d}E}{\mathrm{d}t}(t)(t_n - t) + \frac{1}{2}\frac{\mathrm{d}^2E}{\mathrm{d}t^2}(t_n - t)^2 + \mathcal{O}((t_n - t)^3) \tag{A.8a}$$

$$E(t_{n+1}) = E(t) + \frac{\mathrm{d}E}{\mathrm{d}t}(t)(t_{n+1} - t) + \frac{1}{2}\frac{\mathrm{d}^2E}{\mathrm{d}t^2}(t_{n+1} - t)^2 + \mathcal{O}((t_{n+1} - t)^3). \tag{A.8b}$$

By combining $t_n := nT_{\text{PTU}}$, $t_{n+1} := (n+1)T_{\text{PTU}}$, (A.6) and the above expressions for E_n and E_{n+1}, (A.5) is rewritten as

$$\begin{aligned}\widetilde{P}[n] = \mu_P(t) &- \frac{1}{2}\left((2n+1)T_{\text{PTU}} - 2t\right)\frac{\mathrm{d}\mu_P}{\mathrm{d}t}(t) \\ &+ \frac{1}{6}\left((1+3n+3n^2)T_{\text{PTU}}^2 - 3t(2n+1)T_{\text{PTU}} + 3t^2\right)\frac{\mathrm{d}^2\mu_P}{\mathrm{d}t^2}(t) \\ &+ \mathcal{O}(T_{\text{PTU}}^3).\end{aligned} \tag{A.9}$$

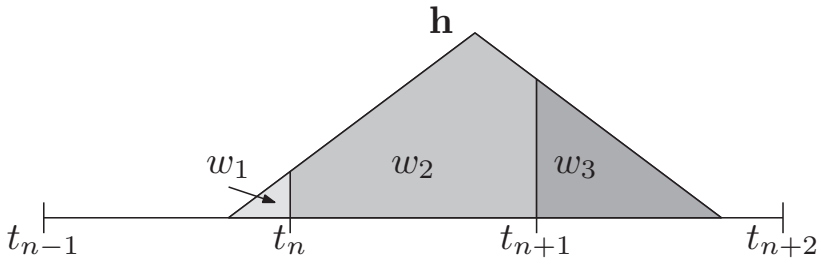

Figure A.1: Impulse response of APM filter $\mathbf{h}$ *for* $N \to \infty$ ($\frac{T_{PTU}}{N} \to 0$).

Introducing $t^* := t - t_n \in [0, T_{\text{PTU}})$ yields

$$\begin{aligned}\widetilde{P}[n] = \mu_P(t) - \frac{1}{2}\left(T_{\text{PTU}} - 2t^*\right)\frac{\mathrm{d}\mu_P}{\mathrm{d}t}(t) \\ + \frac{1}{6}\left(T_{\text{PTU}}^2 - 3t^*T_{\text{PTU}} + 3(t^*)^2\right)\frac{\mathrm{d}^2\mu_P}{\mathrm{d}t^2}(t) + \mathcal{O}(T_{\text{PTU}}^3).\end{aligned} \tag{A.10}$$

Hence, it follows that the open-loop error $\Delta P_{\text{OL}}(t) := \widetilde{P}[n] - \mu_P(t)$ for $t \in [t_n, t_{n+1})$ is given by

$$\begin{aligned}\Delta P_{\text{OL}}(t) = -\frac{1}{2}\left(T_{\text{PTU}} - 2t^*\right)\frac{\mathrm{d}\mu_P}{\mathrm{d}t}(t) \\ + \frac{1}{6}\left(T_{\text{PTU}}^2 - 3t^*T_{\text{PTU}} + 3(t^*)^2\right)\frac{\mathrm{d}^2\mu_P}{\mathrm{d}t^2}(t) + \mathcal{O}(T_{\text{PTU}}^3).\end{aligned} \tag{A.11}$$

Now, the upper bound on $|\Delta P_{\text{OL}}(t)|$, i.e., (3.16), follows by recalling the triangle and Cauchy-Schwarz inequalities, and the fact that $t^* := t - t_n \in [0, T_{\text{PTU}})$:

$$\begin{aligned}\left|\Delta P_{\text{OL}}(t)\right| &\le \frac{1}{2}\left|T_{\text{PTU}} - 2t^*\right|\left|\frac{\mathrm{d}\mu_P}{\mathrm{d}t}(t)\right| \\ &\quad + \frac{1}{6}\left|T_{\text{PTU}}^2 - 3t^*T_{\text{PTU}} + 3(t^*)^2\right|\left|\frac{\mathrm{d}^2\mu_P}{\mathrm{d}t^2}(t)\right| + \mathcal{O}(T_{\text{PTU}}^3) \\ &\le \frac{T_{\text{PTU}}}{2}\left|\frac{\mathrm{d}\mu_P}{\mathrm{d}t}(t)\right| + \frac{T_{\text{PTU}}^2}{6}\left|\frac{\mathrm{d}^2\mu_P}{\mathrm{d}t^2}(t)\right| + \mathcal{O}(T_{\text{PTU}}^3).\end{aligned} \tag{A.12}$$

A.2.2 Evenly-distributed APM

For $N \to \infty$ and evenly distributed controllable generation/load, the expression for $\Delta P_{\text{OL}}(t)$ under APM is derived as follows. In Appendix A.1, it was shown that

$\hat{P}[k]$ is the result of convolving $\overline{P}[k]$ with discrete-time impulse response h_k. Figure A.1 shows that for $N \to \infty$/infinitesimally small sampling period $\frac{T_{\mathrm{PTU}}}{N}$, this impulse response is triangular with width $2T_{\mathrm{PTU}}$ and height $\frac{1}{T_{\mathrm{PTU}}}$ (such that (A.4) holds). Accordingly, it is possible to express $\hat{P}(t)$ for $t \in [t_n, t_{n+1})$ as a weighted sum of $\widetilde{P}[n-1]$, $\widetilde{P}[n]$ and $\widetilde{P}[n+1]$, i.e.,

$$\hat{P}(t) = w_1(t)\widetilde{P}[n-1] + w_2(t)\widetilde{P}[n] + w_3(t)\widetilde{P}[n+1], \tag{A.13}$$

for $t \in [t_n, t_{n+1})$, with

$$w_1(t) := \frac{1}{2}\left(\frac{T_{\mathrm{PTU}} - t^*}{T_{\mathrm{PTU}}}\right)^2,\ w_2(t) := \frac{3}{4} - \left(\frac{1}{2} - \frac{T_{\mathrm{PTU}} - t^*}{T_{\mathrm{PTU}}}\right)^2,\ w_3(t) := \frac{1}{2}\left(\frac{t^*}{T_{\mathrm{PTU}}}\right)^2.$$

Combining (A.9) and (A.13) yields

$$\hat{P}(t) = \mu_P(t) + \frac{T_{\mathrm{PTU}}^2}{6}\frac{\mathrm{d}^2\mu_P}{\mathrm{d}t^2}(t) + \mathcal{O}(T_{\mathrm{PTU}}^3), \tag{A.14}$$

such that the open-loop error $\Delta P_{\mathrm{OL}}(t)$ is given by

$$\Delta P_{\mathrm{OL}}(t) = \hat{P}(t) - \mu_P(t) = \frac{T_{\mathrm{PTU}}^2}{6}\frac{\mathrm{d}^2\mu_P}{\mathrm{d}t^2}(t) + \mathcal{O}(T_{\mathrm{PTU}}^3). \tag{A.15}$$

Now, the upper bound on $|\Delta P_{\mathrm{OL}}(t)|$, i.e., (3.17), follows:

$$\left|\Delta P_{\mathrm{OL}}(t)\right| \leq \frac{T_{\mathrm{PTU}}^2}{6}\left|\frac{\mathrm{d}^2\mu_P}{\mathrm{d}t^2}(t)\right| + \mathcal{O}(T_{\mathrm{PTU}}^3). \tag{A.16}$$

Appendix to Chapter 4

Table B.1 lists the parameter values used in the simulation described in Section 4.4.

Table B.1: Simulation parameters

Parameter	Value (per unit)
Sampling period	1 s
Simulation time	200 s
Prediction horizon N	50
Iterations (FC-MPC)	2
State of subsystem 1	$x_1 = \text{col}(\Delta P_{V1}, \Delta P_{M1}, \Delta\omega_1)$
State of subsystem 2	$x_2 = \text{col}(\Delta\delta_{12}, \Delta P_{V2}, \Delta P_{M2}, \Delta\omega_2)$
State of subsystem 3	$x_3 = \text{col}(\Delta\delta_{23}, \Delta P_{V3}, \Delta P_{M3}, \Delta\omega_3)$
State of subsystem 4	$x_4 = \text{col}(\Delta\delta_{34}, \Delta P_{V4}, \Delta P_{M4}, \Delta\omega_4)$
Disturbance ΔP_{L_1}	$0,\ \forall t$
Disturbance ΔP_{L_2}	0 for $t < 10,\ +0.25$ for $t \geq 10$
Disturbance ΔP_{L_3}	0 for $t < 10,\ -0.25$ for $t \geq 10$
Disturbance ΔP_{L_4}	$0,\ \forall t$
Constraint on $\Delta P_{\text{ref}_i},\ i = 1, \ldots, 4$	$-0.5 \leq \Delta P_{\text{ref}_i} \leq 0.5$
Generator damping: D_1, D_2, D_3, D_4	$3, 0.275, 2, 2.75$
Generator inertia: J_1, J_2, J_3, J_4	$4, 40, 35, 10$
Speed regulation: r_1, r_2, r_3, r_4	$0.12, 0.28, 0.16, 0.12$
Governor time constant: $\tau_{G1}, \tau_{G2}, \tau_{G3}, \tau_{G4}$	$4, 25, 15, 5$ s
Turbine time constant: $\tau_{T1}, \tau_{T2}, \tau_{T3}, \tau_{T4}$	$5, 10, 20, 10$ s
Tie-line gain: b_{12}, b_{23}, b_{34}	2.54, 1.5, 2.5
AGC gain 1: K_1, K_2, K_3, K_4	0.01, 0.02, 0.03, 0.01
AGC gain 2: B_1, B_2, B_3, B_4	36.33, 14.56, 27.00, 36.08
Q_1, Q_2	$100 \cdot \text{diag}(0,0,5), 100 \cdot \text{diag}(5,0,0,5)$
Q_3, Q_4	$100 \cdot \text{diag}(5,0,0,5), 100 \cdot \text{diag}(5,0,0,5)$
R_1, R_2, R_3, R_4	$1, 1, 1, 1$

C

Appendix to Chapter 5

C.1 Proof of Theorem 5.4.3

Let $x(k) \in \mathbb{X}$ for some $k \in \mathbb{Z}_+$. Then, feasibility of Problem 5.4.2 ensures that $x(k+1) \in \phi_{\mathrm{CL}}(x(k), \pi(x(k))) \subseteq \mathbb{X}$ due to constraint (5.10a). Hence, Problem 5.4.2 remains feasible and thus, $\mathbb{X}$ is a PI set for system (5.11). Now consider the function $V(x) := \max_{i\in\mathcal{I}} V_i(x_i)$. Together with condition (5.10b) this yields

$$\begin{aligned} V(x(k+1)) &= \max_{i\in\mathcal{I}} V_i(x_i(k+1)) \\ &\leq \rho \max_{i\in\mathcal{I}} \max_{j\in\overline{\mathcal{N}}_i} V_j(x_j(k)) = \rho \max_{i\in\mathcal{I}} V_i(x_i(k)) = \rho\, V(x(k)), \end{aligned} \tag{C.1}$$

for all $x(k) \in \mathbb{X}$, where $\rho := \max_{i\in\mathcal{I}} \rho_i \in \mathbb{R}_{[0,1)}$.

Next, we derive a lower bound for $V(x)$. Observing that the maximum element of a set always equals or exceeds the average value of the elements and using (5.9a) yields

$$V(x) := \max_{i\in\mathcal{I}} V_i(x_i) \geq \frac{1}{N} \sum_{i\in\mathcal{I}} V_i(x_i) \geq \frac{1}{N} \sum_{i\in\mathcal{I}} \alpha_1^i(\|x_i\|). \tag{C.2}$$

Next, note that

$$\sum_{i\in\mathcal{I}} \alpha_1^i(\|x_i\|) \geq \sum_{i\in\mathcal{I}} \tilde{\alpha}_1(\|x_i\|) \geq \tilde{\alpha}_1(\max_{i\in\mathcal{I}} \|x_i\|) \geq \tilde{\alpha}_1\left(\frac{1}{N} \sum_{i\in\mathcal{I}} \|x_i\|\right), \tag{C.3}$$

where $\tilde{\alpha}_1(s) := \min_{i\in\mathcal{I}} \alpha_1^i(s) \in \mathcal{K}_\infty$. With $\hat{x}_i := \mathrm{col}(0_{n_1}, \ldots, 0_{n_{i-1}}, x_i, 0_{n_{i+1}}, \ldots, 0_{n_N})$ we have that

$$\sum_{i\in\mathcal{I}} \|x_i\| = \sum_{i\in\mathcal{I}} \|\hat{x}_i\| \geq \left\| \sum_{i\in\mathcal{I}} \hat{x}_i \right\| = \|x\|. \tag{C.4}$$

Using this property, the fact that $\tilde{\alpha}_1 \in \mathcal{K}_\infty$ is strictly increasing and (C.2) gives the desired lower bound, i.e.,

$$V(x) \geq \frac{1}{N}\sum_{i\in\mathcal{I}} \alpha_1^i(\|x_i\|) \geq \frac{1}{N}\tilde{\alpha}_1\left(\frac{1}{N}\|x\|\right) =: \alpha_1(\|x\|), \tag{C.5}$$

for all $x \in \mathbb{R}^n$ and where $\alpha_1 \in \mathcal{K}_\infty$.

Next, we search for an upper bound on $V(x)$. For this, we first prove that $\|x_i\| \leq \|x\|$, $\forall x = \text{col}(\{x_i\}_{i\in\mathcal{I}}) \in \mathbb{R}^n$, $\forall i \in \mathcal{I}$, and any p-norm. For $1 \leq p < \infty$, the inequality follows from the definition of the p-norm:

$$\|x\|_p^p := \sum_{j=1}^{n} |[x]_j|^p = \sum_{l\in\mathcal{I}}\sum_{j=1}^{n_l} |[x_l]_j|^p = \sum_{l\in\mathcal{I}} \|x_l\|_p^p. \tag{C.6}$$

Hence

$$\|x_i\|_p^p = \|x\|_p^p - \sum_{l\in\{\mathcal{I}\setminus i\}} \|x_l\|_p^p \leq \|x\|_p^p, \ \forall i \in \mathcal{I}. \tag{C.7}$$

From this and the observation that $f(s) : \mathbb{R}_+ \to \mathbb{R}_+$, $f(s) := s^{\frac{1}{p}}$ and $p \geq 1$ is strictly increasing it follows that $\|x_i\|_p \leq \|x\|_p$ for $1 \leq p < \infty$. It is straightforward to see that the inequality holds for the ∞-norm as well:

$$\|x\|_\infty = \max_{j\in\mathbb{Z}_{[1,n]}} |[x]_j| = \max_{l\in\mathcal{I}} \max_{j\in\mathbb{Z}_{[1,n_l]}} |[x_l]_j| = \max_{l\in\mathcal{I}} \|x_l\|_\infty \geq \|x_i\|_\infty, \ \forall i \in \mathcal{I}. \tag{C.8}$$

Next, using (5.9a), the fact that α_2^i is strictly increasing for all $i \in \mathcal{I}$ and (C.7), (C.8), we obtain the desired upper bound, i.e.,

$$V(x) := \max_{i\in\mathcal{I}} V_i(x_i) \leq \max_{i\in\mathcal{I}} \alpha_2^i(\|x_i\|) \leq \max_{i\in\mathcal{I}} \alpha_2^i(\|x\|) =: \alpha_2(\|x\|), \tag{C.9}$$

for all $x \in \mathbb{R}^n$ and where $\alpha_2 \in \mathcal{K}_\infty$.

The result now follows directly from Theorem 5.2.6, with $V(x) := \max_{i\in\mathcal{I}} V_i(x_i)$ as CLF for the overall system. □

C.2 Proof of Theorem 5.4.5

Let $x(k) \in \mathbb{X}$ for some $k \in \mathbb{Z}_+$. Positive invariance of $\mathbb{X}$ follows from feasibility of (5.10a), as shown in the proof of Theorem 5.4.3. Now consider the function $V(x) := \max_{i\in\mathcal{I}} V_i(x_i)$. Condition (5.12) implies that

$$\begin{aligned} V(x(k+1)) &= \max_{i\in\mathcal{I}} V_i(x_i(k+1)) \\ &\leq \rho \max_{i\in\mathcal{I}} \max_{\tau\in\mathbb{Z}_{[0,N_\tau-1]}} \max_{j\in\overline{\mathcal{N}}_i} V_j(x_j(k-\tau)) \\ &= \rho \max_{\tau\in\mathbb{Z}_{[0,N_\tau-1]}} \max_{i\in\mathcal{I}} V_i(x_i(k-\tau)) = \rho \max_{\tau\in\mathbb{Z}_{[0,N_\tau-1]}} V(x(k-\tau)), \end{aligned} \tag{C.10}$$

for all $k \in \mathbb{Z}_{\geq N_\tau - 1}$ and $\rho := \max_{i\in\mathcal{I}} \rho_i \in \mathbb{R}_{[0,1)}$. Recursive application of (C.10) gives

$$\begin{aligned} V(x(k)) &\leq \rho \max_{l\in\mathbb{Z}_{[0,N_\tau-1]}} V(x(l)), \quad k \in \mathbb{Z}_{[N_\tau,2N_\tau-1]}, \\ V(x(k)) &\leq \rho \max_{l\in\mathbb{Z}_{[N_\tau,2N_\tau-1]}} V(x(l)) \\ &\leq \rho^2 \max_{l\in\mathbb{Z}_{[0,N_\tau-1]}} V(x(l)), \ k \in \mathbb{Z}_{[2N_\tau,3N_\tau-1]}, \\ &\vdots \\ V(x(k)) &\leq \rho^{\left\lfloor \frac{k}{N_\tau} \right\rfloor} \max_{l\in\mathbb{Z}_{[0,N_\tau-1]}} V(x(l)), \quad \forall k \in \mathbb{Z}_+. \end{aligned} \tag{C.11}$$

Furthermore, we derived in the proof of Theorem 5.4.3 that

$$\alpha_1(\|x\|) \leq V(x) \leq \alpha_2(\|x\|), \quad \forall x \in \mathbb{R}^n, \tag{C.12}$$

with $\alpha_1(s) := \frac{1}{N} \min_{i\in\mathcal{I}} \alpha_1^i(\frac{1}{N}s) \in \mathcal{K}_\infty$ and $\alpha_2(s) := \max_{i\in\mathcal{I}} \alpha_2^i(s) \in \mathcal{K}_\infty$. As $\mathcal{K}_\infty$-functions are strictly increasing, we know that

$$\max_{l\in\mathbb{Z}_{[0,N_\tau-1]}} V(x(l)) \leq \max_{l\in\mathbb{Z}_{[0,N_\tau-1]}} \alpha_2(\|x(l)\|) = \alpha_2\left(\left\|\mathbf{x}_{[0,N_\tau-1]}\right\|\right). \tag{C.13}$$

Combining this bound with (C.11) and (C.12) gives

$$\|x(k)\| \leq \alpha_1^{-1}\left(\rho^{\left\lfloor \frac{k}{N_\tau} \right\rfloor} \alpha_2\left(\left\|\mathbf{x}_{[0,N_\tau-1]}\right\|\right)\right). \tag{C.14}$$

The fact that

$$\lim_{k\to\infty} \|x(k)\| \leq \lim_{k\to\infty} \alpha_1^{-1}\left(\rho^{\left\lfloor \frac{k}{N_\tau} \right\rfloor} \alpha_2\left(\left\|\mathbf{x}_{[0,N_\tau-1]}\right\|\right)\right) = 0 \tag{C.15}$$

proves attractivity of the closed-loop system (5.13). Lyapunov stability follows, as for every $\varepsilon > 0$ we can find a $\delta(\varepsilon) := \alpha_2^{-1}(\alpha_1(\varepsilon)) > 0$, such that

$$\|x(0)\| \leq \left\|\mathbf{x}_{[0,N_\tau-1]}\right\| < \delta$$

implies that $\|x(k)\| < \alpha_1^{-1}(\rho^{\left\lfloor \frac{k}{N_\tau} \right\rfloor} \alpha_2(\delta)) \leq \varepsilon$ for all $k \in \mathbb{Z}_+$. This proves asymptotic stability of (5.13) in $\mathbb{X}$. □

D

Appendix to Chapter 6

D.1 Proof of Theorem 6.3.1

For simplicity, we begin by considering a network of only 2 vertices. Such a network is described by

$$x(k+1)=Ax(k)=\begin{bmatrix}A_{1,1} & A_{1,2}\\ A_{2,1} & A_{2,2}\end{bmatrix}x(k),\quad k\in\mathbb{Z}_+,\ x\in\mathbb{R}^n,$$

with non-zero $A_{i,j}\in\mathbb{R}^{n_i\times n_j}$, for all $i,j\in\mathcal{I}:=\mathbb{Z}_{[1,2]}$. Let $\mathcal{J}:=\{1\}$, such that by assumption, there exists no $P_1\in\mathbb{R}^{n_1\times n_1}$ that satisfies $P_1\succ 0$ and $A_{1,1}^\top P_1 A_{1,1}-P_1\prec 0$.

Next, we prove the result by contradiction. Suppose that there exist block-diagonal matrices $P=\mathrm{diag}(P_1,P_2)$, $P_i\in\mathbb{R}^{n_i\times n_i}$, such that $V(x)=x^\top Px$ is a Lyapunov function for the full network, i.e., there are $P=\mathrm{diag}(P_1,P_2)\succ 0$ that satisfy

$$\begin{aligned}&A^\top PA-P\\ &=\begin{bmatrix}A_{1,1}^\top P_1A_{1,1}+A_{2,1}^\top P_2A_{2,1} & A_{1,1}^\top P_1A_{1,2}+A_{2,1}^\top P_2A_{2,2}\\ * & A_{1,2}^\top P_1A_{1,2}+A_{2,2}^\top P_2A_{2,2}\end{bmatrix}-\begin{bmatrix}P_1 & 0\\ 0 & P_2\end{bmatrix}\prec 0.\end{aligned}\tag{D.1}$$

Since $A_{2,1}\neq 0$ and $P_2\succ 0$, this requires that

$$A_{1,1}^\top P_1A_{1,1}-P_1\prec -A_{2,1}^\top P_2A_{2,1}\prec 0.\tag{D.2}$$

Thus, for this 2-subsystem network, the result follows: we have obtained a contradiction, since by assumption, (D.2) does not admit a solution $P_1\succ 0$. The result readily extends to the general N-systems case, by assuming that subsystems 1 and 2 are representative of a "subnetwork", i.e., multiple interconnected

subsystems, in such a way that none of the subsystems in network 1 admits quadratic Lyapunov candidates under decoupled operation. In this case, (D.2) does not admit a block-diagonal solution $P_1 \succ 0$, where the blocks correspond to the individual systems in subnetwork 1. □

D.2 Proof of Lemma 6.4.2

To prove Lemma 6.4.2, let us construct functions $V_i(\widetilde{P}_i(x), x_i)$ that equal $V(x)$ except when x_i lies within a particular neighborhood of the origin, whose size is determined by the full network state x. Since $\|x_i\|_2^2 \leq \|x\|_2^2 = \sum_{i\in\mathcal{I}} \|x_i\|_2^2 \leq N \max_{i\in\mathcal{I}} \|x_i\|_2^2$, define for all $x \in \mathbb{R}^n$ and $i \in \mathcal{I}$,

$$\widetilde{P}_i(x) := \begin{cases} V(x)\|x_i\|_2^{-2} I_{n_i}, & \|x_i\|_2^2 \geq \frac{1}{N}\|x\|_2^2, \\ NV(x)\|x\|_2^{-2} I_{n_i}, & \|x_i\|_2^2 < \frac{1}{N}\|x\|_2^2, \|x\|_2^2 \neq 0, \\ Nc_2 I_{n_i}, & \|x\|_2^2 = 0. \end{cases} \tag{D.3}$$

In what follows, we show that $\widetilde{P}_i(x)$ is well-defined for all $x = \mathrm{col}(\{x_i\}_{i\in\mathcal{I}}) \in \mathbb{R}^n$. If $\|x_i\|_2^2 > \frac{1}{N}\|x\|_2^2$ (and thus, $\|x\|_2^2 > 0$), by (5.2a) and the definition of V we obtain

$$c_1 I_{n_i} \preceq \frac{c_1\|x\|_2^2}{\|x_i\|_2^2} I_{n_i} \preceq \widetilde{P}_i(x) \preceq \frac{c_2\|x\|_2^2}{\|x_i\|_2^2} I_{n_i} \preceq Nc_2 I_{n_i}.$$

Similarly, for $\|x_i\|_2^2 \leq \frac{1}{N}\|x\|_2^2$, $\|x\|_2^2 \neq 0$, it holds that

$$c_1 I_{n_i} \preceq Nc_1 I_{n_i} \preceq \widetilde{P}_i(x) \preceq Nc_2 I_{n_i}.$$

Moreover, for $\|x\|_2^2 = 0$ (and thus, $\|x_i\|_2^2 = 0$ for $i \in \mathcal{I}$), we obtain

$$c_1 I_{n_i} \preceq Nc_1 I_{n_i} \preceq \widetilde{P}_i(x) = Nc_2 I_{n_i} \preceq Nc_2 I_{n_i}.$$

Hence, $\widetilde{P}_i(x)$ is well-defined for all $x \in \mathbb{R}^n$.

Next, we show by contradiction that for any $x \in \mathbb{R}^n$, $\|x_i\|_2^2 \geq \frac{1}{N}\|x\|_2^2$ for at least one $i \in \mathcal{I}$. Suppose that $\|x_i\|_2^2 < \frac{1}{N}\|x\|_2^2$ for all $i \in \mathcal{I}$. This implies that

$$\|x\|_2^2 = \sum_{i\in\mathcal{I}} \|x_i\|_2^2 < N\frac{1}{N}\|x\|_2^2 = \|x\|_2^2.$$

Since this assumption yields a contradiction, for all $x \in \mathbb{R}^n$, there exists a non-empty set $\widetilde{\mathcal{I}} \subseteq \mathcal{I}$ such that $\|x_l\|_2^2 \geq \frac{1}{N}\|x\|_2^2$ for $l \in \widetilde{\mathcal{I}}$. Now consider the functions $V_i : \mathbb{R}^{n_i\times n_i} \times \mathbb{R}^{n_i} \to \mathbb{R}_+$, with $V_i(\widetilde{P}_i(x), x_i) := x_i^\top \widetilde{P}_i(x) x_i$ for all $i \in \mathcal{I}$. From the above result and the construction of $\widetilde{P}_i(x)$, it follows that

$$\max_{i\in\mathcal{I}} V_i(\widetilde{P}_i(x), x_i) = V_l(\widetilde{P}_l(x), x_l) = V(x),\ l \in \widetilde{\mathcal{I}}, x \in \mathbb{R}^n,$$

which concludes the proof. □

D.3 Proof of Theorem 6.4.7

By construction, any pair of state sequences $\{x(k)\}_{k\in\mathbb{Z}_+}, \{P(x(k))\}_{k\in\mathbb{Z}_+}$ that is generated by (6.15) satisfies (6.14) for all $k \in \mathbb{Z}_+$. This allows for recursive application of (6.14c), which yields

$$V(P(x(k)),x(k)) := \max_{i\in\mathcal{I}} V_i(P_i(x(k)),x_i(k)) \leq \overline{\rho}^k V(P(x_0),x_0), \tag{D.4}$$

where $\overline{\rho} := \max_{i\in\mathcal{I}} \rho_i$. Then, (6.14a)–(6.14b) yield

$$V(P(x(k)),x(k)) \geq \tfrac{1}{N}\textstyle\sum_{i\in\mathcal{I}} c_{1,i}\|x_i(k)\|_2^2 \geq \tfrac{\underline{c}_1}{N}\|x(k)\|_2^2 \tag{D.5a}$$

$$V(P(x(k)),x(k)) \leq \max_{i\in\mathcal{I}} \left(c_{2,i}\|x_i(k)\|_2^2\right) \leq \overline{c}_{2,i}\|x(k)\|_2^2, \tag{D.5b}$$

where $\underline{c}_1 := \min_{i\in\mathcal{I}} c_{1,i}$ and $\overline{c}_2 := \max_{i\in\mathcal{I}} c_{2,i}$. Therefore

$$\|x(k)\|_2^2 \leq \overline{\rho}^k \frac{N\overline{c}_2}{\underline{c}_1}\|x(0)\|_2^2, \tag{D.6}$$

for all $x(0) \in \mathbb{X}$ and $k \in \mathbb{Z}_+$. Since $\overline{\rho} \in \mathbb{R}_{[0,1)}$, $\|x(k)\|$ is bounded by an exponentially decreasing function of time and $\lim_{k\to\infty}\|x(k)\| \leq \lim_{k\to\infty}\overline{\rho}^k \frac{N\overline{c}_2}{\underline{c}_1}\|x(0)\|_2^2 = 0$. □

D.4 Proof of Theorem 6.4.9

First, we relate Problem 6.4.8, and consequently, (6.17), to Problem 6.4.5, given Assumption 6.4.6. Given that Problem 6.4.5 is feasible for $x(k)$ and $P_i(x(k)) \in \mathbb{P}_i$, $k \in \mathbb{Z}_+$, there exist $\bar{u}_i(k) \in \mathbb{R}^{m_i}$ and $\bar{P}_i(x^+(k)) \in \mathbb{P}_i$, $i \in \mathcal{I}$, that satisfy (6.14b)–(6.14c). Now consider the functions $\Delta_i : \mathbb{P}\times\mathbb{R}^n \to \mathbb{R}_+$, with

$$\Delta_i(P(x),x) := \rho_i\left(\max_{j\in\mathcal{I}} V_j(P_j(x),x_j) - \max_{j\in\overline{\mathcal{N}}_i} V_j(P_j(x),x_j)\right).$$

By feasibility of (6.14c) for $x(k) \in \mathbb{R}^n$ and $P_i(x(k)) \in \mathbb{P}_i$, $k \in \mathbb{Z}_+$, there is a $\lambda_i(k)$ such that

$$0 \leq \lambda_i(k) \leq \Delta_i(P(x(k)),x(k))$$

that satisfies (6.16a)–(6.16b) for $\bar{P}_i(x^+(k))$ and $\bar{u}_i(k)$.

Next, we prove that (6.17) yields exponentially converging state sequences. Minimization of $J_i(\lambda_i(k))$ over $\lambda_i(k)$ yields $0 \leq \lambda_i^*(k) \leq \Delta_i(P(x(k)),x(k)) < \infty$ and consequently

$$V_i(P_i(x^+(k)),x_i^+(k)) \leq \rho_i \max_{j\in\mathcal{I}} V_j(P_j(x(k)),x_j(k))$$

for all $x_i^+(k) = \phi_i(x_i(k), v_i(x_{\mathcal{N}_i}(k)), P_{\overline{\mathcal{N}}_i}(x(k)))$, $i \in \mathcal{I}$ and $k \in \mathbb{Z}_+$. Then, exponential convergence of $\|x(k)\|$ straightforwardly follows along the lines of the proof of Theorem 6.4.7. □

D.5 Proof of Lemma 6.4.11

As $P_i(x(0)) = \Gamma_i I_{n_i}$, (6.14a) follows with $c_{1,i} := \gamma_i$ and $c_{2,i} := \Gamma_i$. Also, the Schur complement of (6.20b) gives

$$\begin{aligned} &\rho_i \max_{j\in\overline{\mathcal{N}}_i} x_j^\top P_j(x) x_j + \lambda_i \\ &\quad - \big(\widetilde{f}_i(x) + \widetilde{g}_i(x) u_i\big)^\top Z_i^{-1} \big(\widetilde{f}_i(x) + \widetilde{g}_i(x) u_i\big) \geq 0, \end{aligned} \tag{D.7}$$

where the time-dependence was omitted for brevity. Combining (6.19) and (D.7) yields (6.16a) with $P_i(x^+(k)) = Z_i(k)^{-1}$. Moreover, (6.20a) yields (6.16b) and $\gamma_i I_{n_i} \preceq Z_i(k)^{-1} = P_i(x^+(k)) \preceq \Gamma_i I_{n_i}$, which is (6.14b). □

D.6 Proof of Theorem 6.5.3

We begin by showing that $x \in \operatorname{span}(\{x_0^q\}_{q\in\mathbb{Z}_{[1,Q]}})$ for some $x \in \mathbb{R}^n$ implies that $\xi_i(x) \in \operatorname{span}(\{\xi_i(x_0^q)\}_{q\in\mathbb{Z}_{[1,Q]}})$ for all $i \in \mathcal{I}$. This is a consequence of linearity of $v_i(x_{\mathcal{N}_i})$ and $\xi_i(x)$, i.e.,

$$\begin{aligned} x = \sum_{q\in\mathbb{Z}_{[1,Q]}} \alpha^q x_0^q &= \operatorname{col}\left(\left\{ \sum_{q\in\mathbb{Z}_{[1,Q]}} \alpha^q x_{0,i}^q \right\}_{i\in\mathcal{I}} \right) \\ \Rightarrow \quad \xi_i(x) = \begin{bmatrix} x_i \\ \sum_{j\in\mathcal{N}_i} A_{ij} x_j \end{bmatrix} &= \begin{bmatrix} \sum_{q\in\mathbb{Z}_{[1,Q]}} \alpha^q x_{0,i}^q \\ \sum_{j\in\mathcal{N}_i} A_{ij} \left(\sum_{q\in\mathbb{Z}_{[1,Q]}} \alpha^q x_{0,j}^q \right) \end{bmatrix} \\ &= \sum_{q\in\mathbb{Z}_{[1,Q]}} \alpha^q \begin{bmatrix} x_{0,i}^q \\ \sum_{j\in\mathcal{N}_i} A_{ij} x_{0,j}^q \end{bmatrix} = \sum_{q\in\mathbb{Z}_{[1,Q]}} \alpha^q \xi_i(x_0^q). \end{aligned} \tag{D.8}$$

Now consider arbitrary $x(0) \in \operatorname{span}(\mathcal{X})$ and the corresponding sets $\mathcal{S}_i(0)$, $i \in \mathcal{I}$. Then, the subsequent local states $x_i(1)$ can be expressed as

$$\begin{aligned} &x_i(1) \\ &= A_{ii} x_i(0) + v_i(x_{\mathcal{N}_i}(0)) + B_i \pi_i^{\mathrm{ip}}(\xi_i(x(0)), 0) \\ &= A_{ii} \left(\sum_{q\in\mathbb{Z}_{[1,Q]}} \alpha^q x_i^q(0) \right) + \left(\sum_{q\in\mathbb{Z}_{[1,Q]}} \alpha^q v_i(x_{\mathcal{N}_i}^q(0)) \right) + B_i \left(\sum_{q\in\mathbb{Z}_{[1,Q]}} \alpha^q u_i^q(0) \right) \\ &= \sum_{q\in\mathbb{Z}_{[1,Q]}} \alpha^q \left(A_{ii} x_i^q(0) + v_i(x_{\mathcal{N}_i}^q(0)) + B_i u_i^q(0) \right) = \sum_{q\in\mathbb{Z}_{[1,Q]}} \alpha^q x_i^q(1), \end{aligned} \tag{D.9}$$

where Assumption 6.5.2 was used to obtain the second equality. The above result implies that the closed-loop states $x_i(1) \in \text{span}(\{x_i^q(1)\}_{q\in\mathbb{Z}_{[1,Q]}})$, and thus, by (D.8), it holds that $\xi_i(x(1)) \in \text{span}(\mathcal{S}_i(1))$. Along the same lines, it follows that $x(k) = \sum_{q\in\mathbb{Z}_{[1,Q]}} \alpha^q x^q(k) \in \text{span}(\{x^q(k)\}_{q\in\mathbb{Z}_{[1,Q]}})$ and $\xi_i(x(k)) \in \text{span}(\mathcal{S}_i(k))$ for all $k \in \mathbb{Z}_+$.

Now the result follows, i.e., for $x(0) = x_0 \in \text{span}(\mathcal{X})$,

$$\begin{aligned} \|x(k)\| = \left\| \sum_{q\in\mathbb{Z}_{[1,Q]}} \alpha^q x^q(k) \right\| &\leq \sum_{q\in\mathbb{Z}_{[1,Q]}} |\alpha^q| \cdot \|x^q(k)\| \\ &\leq \sum_{q\in\mathbb{Z}_{[1,Q]}} |\alpha^q| \cdot c_q \|x_0^q\| \mu_q^k \\ &\leq \overline{c} \left(\sum_{q\in\mathbb{Z}_{[1,Q]}} |\alpha^q| \cdot \|x_0^q\| \right) \overline{\mu}^k, \qquad k \in \mathbb{Z}_+, \end{aligned} \tag{D.10}$$

where $\overline{c} := \max_q c_q \in \mathbb{R}_{\geq 1}$ and $\overline{\mu} := \max_q \mu_q \in \mathbb{R}_{[0,1)}$. Thus, it holds that

$$\lim_{k\to\infty} \|x(k)\| \leq \lim_{k\to\infty} \overline{c} \left(\sum_{q\in\mathbb{Z}_{[1,Q]}} |\alpha^q| \cdot \|x_0^q\| \right) \overline{\mu}^k = 0, \tag{D.11}$$

which implies asymptotic convergence. □

E

Appendix to Chapter 7

E.1 Proof of Theorem 7.3.2

The result follows by demonstrating that (7.9) defines the explicit solution to Problem 7.3.1 in case (7.4b) and (7.4c) are not active at the optimum. We start by eliminating $\underline{x}_i^p(k)$ from (7.5) using difference equation (7.7). If (7.4b)–(7.4c) are inactive, this yields the equivalent, unconstrained optimization problem

$$\min_{\underline{u}_i^p(k)} f_i\big(x_i(k), \underline{x}^{p-1}(k), \underline{u}_i^p(k)\big), \tag{E.1}$$

where

$$\begin{aligned} &f_i(x_i, \underline{x}^{p-1}, \underline{u}_i^p) := \\ &\quad (\underline{u}_i^p)^\top (T_i^\top \mathcal{Q}_i T_i + \mathcal{R}_i) \underline{u}_i^p + 2\left(x_i^\top H_i^\top + (\underline{x}^{p-1})^\top H_{\mathcal{N}_i}^\top\right) \mathcal{Q}_i T_i \underline{u}_i^p. \end{aligned}$$

Note that (E.1) is a strictly convex optimization problem, as $\nabla^2 f_i(x_i, \underline{x}^{p-1}, \underline{u}_i^p) = 2(T_i^\top \mathcal{Q}_i T_i + \mathcal{R}_i) \succ 0$. Therefore, the corresponding optimizer is unique and follows by solving $\nabla f_i(x_i, \underline{x}^{p-1}, \underline{u}_i^p) = 0$ for $\underline{u}_i^p$. This solution is $\underline{u}_i^{p*}(x_i, \underline{x}^{p-1})$, as defined in (7.9).

Given the explicit solution to Problem 7.3.1, it is possible to describe the state prediction vector $\underline{x}^p(k)$ as an explicit function of the prediction vector that was generated at iteration $p-1$. Hence, by combining (7.9) and (7.8) it follows that the predictions $\{\underline{x}^p(k)\}_{p \in \mathbb{Z}_{[1,p_{\max}]}}$ generated by Alg. 4 satisfy the linear

difference equation

$$\begin{aligned}&\underline{x}^p(k) \\ &= Hx(k)+H_{\mathcal{N}}\underline{x}^{p-1}(k)+T\,\mathrm{col}\left(\{L_i x_i(k)+L_{\mathcal{N}_i}\underline{x}^{p-1}(k)\}_{i\in\mathcal{I}}\right) \\ &= \left(H_{\mathcal{N}}+T\begin{bmatrix}L_{\mathcal{N}_1}\\ \vdots \\ L_{\mathcal{N}_N}\end{bmatrix}\right)\underline{x}^{p-1}(k)+\left(H+T\begin{bmatrix}L_1 & \dots & 0\\ \vdots & \ddots & \vdots \\ 0 & \dots & L_N\end{bmatrix}\right)x(k),\end{aligned} \tag{E.2}$$

for all $p \in \mathbb{Z}_{[1,p_{\max}]}$, and with initial condition $\underline{x}^0 := \begin{bmatrix} x(k)^\top & 0 & \dots & 0\end{bmatrix}^\top$ (see Alg. 4, statement 5).

Now the result straightforwardly follows from linear system stability theory. Thus, state predictions described by (E.2) asymptotically converge to a fixed-point $\underline{x}^*(k) \in \mathbb{R}^{(N_k+1)n}$ that satisfies

$$\left\{I-\left(H_{\mathcal{N}}+T\begin{bmatrix}L_{\mathcal{N}_1}\\ \vdots \\ L_{\mathcal{N}_N}\end{bmatrix}\right)\right\}\underline{x}^*(k)=\left(H+T\begin{bmatrix}L_1 & \dots & 0\\ \vdots & \ddots & \vdots \\ 0 & \dots & L_N\end{bmatrix}\right)x(k),$$

if all eigenvalues of

$$W := \left(H_{\mathcal{N}}+T\begin{bmatrix}L_{\mathcal{N}_1}\\ \vdots \\ L_{\mathcal{N}_N}\end{bmatrix}\right)$$

lie in the open unit circle of the complex plane, i.e., in $\{\varepsilon \in \mathbb{C} \mid |\varepsilon| < 1\}$. □

E.2 Simulation parameters

Tables E.1-E.3 list the parameter values used in the simulations described in Section 7.4.

Table E.1: CIGRÉ-7 model parameters

Parameter	Value (per unit)
Inertia $H_1, \ldots, H_7$	$100, 30.3, 35.8, 28.6, 26, 34.8, 26.4$
Damping constant $D_1, \ldots, D_7$	$0.8, 0.85, 0.8, 0.8, 0.9, 0.7, 0.8$
Governor time constant $\tau_{G_1}, \ldots, \tau_{G_7}$	$0.2, 0.15, 0.2, 0.2, 0.25, 0.2, 0.2$ s
Turbine time constant $\tau_{T_1}, \ldots, \tau_{T_7}$	$0.5, 0.4, 0.5, 0.5, 0.4, 0.5, 0.5$ s
Line susceptance b_{ij}	$b_{1,3} = 24.5, b_{1,4} = 24.5,$ $b_{2,3} = 62.6, b_{2,10} = 32.3,$ $b_{3,4} = 39.5, b_{3,9} = 28, b_{4,5} = 10,$ $b_{4,6} = 10, b_{4,9} = 97, b_{4,10} = 33,$ $b_{6,8} = 31.8, b_{7,8} = 39.5, b_{8,9} = 97$
Speed regulation $r_1, \ldots, r_7$	$\frac{1}{20}, \frac{1}{23}, \frac{1}{19}, \frac{1}{21}, \frac{1}{21}, \frac{1}{18}, \frac{1}{20}$
Direct neighbors $\mathcal{N}_1, \ldots, \mathcal{N}_7$	$\{3,4\}, \{3,4\}, \{1,2,4,6,7\},$ $\{1,2,3,5,6,7\}, \{4\}, \{3,4,7\}, \{3,4,6\}$

Table E.2: L-MPC parameters

Parameter	Value
One-step cost $F_1, \ldots, F_7$	$F_1 = \begin{bmatrix} 7130.3 & 47356 & 232.22 & 88.47 \\ 47356 & 638310 & 3244.7 & 1252.4 \\ 232.22 & 3244.7 & 16.517 & 6.3785 \\ 88.47 & 1252.4 & 6.3785 & 502.46 \end{bmatrix},$ $F_2 = \begin{bmatrix} 3823.9 & 12451 & 184.86 & 70.147 \\ 12451 & 74740 & 1172.7 & 452.61 \\ 184.86 & 1172.7 & 18.49 & 7.1462 \\ 70.147 & 452.61 & 7.1462 & 502.76 \end{bmatrix},$ $F_3 = \begin{bmatrix} 4250.6 & 15931 & 226.93 & 86.658 \\ 15931 & 117320 & 1777.4 & 693.15 \\ 226.93 & 1777.4 & 27.06 & 10.57 \\ 86.658 & 693.15 & 10.57 & 504.13 \end{bmatrix},$ $F_4 = \begin{bmatrix} 3396.2 & 9841.4 & 178.96 & 68.283 \\ 9841.4 & 66787 & 1341.1 & 528.51 \\ 178.96 & 1341.1 & 27.173 & 10.738 \\ 68.283 & 528.51 & 10.738 & 504.25 \end{bmatrix},$ $F_5 = \begin{bmatrix} 3568.1 & 10869 & 179.85 & 103.66 \\ 10869 & 63683 & 1119 & 662.76 \\ 179.85 & 1119 & 19.766 & 11.733 \\ 103.66 & 662.76 & 11.733 & 506.97 \end{bmatrix},$ $F_6 = \begin{bmatrix} 4156.4 & 15254 & 221.7 & 84.452 \\ 15254 & 113550 & 1761.1 & 686.02 \\ 221.7 & 1761.1 & 27.454 & 10.712 \\ 84.452 & 686.02 & 10.712 & 504.18 \end{bmatrix},$ $F_7 = \begin{bmatrix} 3794.9 & 12148 & 246.41 & 94.912 \\ 12148 & 69797 & 1511.5 & 594.48 \\ 246.41 & 1511.5 & 32.969 & 12.996 \\ 94.912 & 594.48 & 12.996 & 505.13 \end{bmatrix},$
Current cost $Q_1, \ldots, Q_7$	$Q_i = 100 \cdot \mathrm{diag}(5,5,0,0),\ i \in \mathcal{I}$
Input cost $R_1, \ldots, R_7$	$R_i = 0.1,\ i \in \mathcal{I}$

Table E.3: Competitive p-qSF parameters

Parameter	Value
State cost $Q_1, \ldots, Q_7$	$Q_1 = -\operatorname{diag}(10, 10, 0, 0)$, $Q_2 = \operatorname{diag}(1, 1, 1, 1)$, $Q_3 = \operatorname{diag}(0.1, 0.1, 0, 0)$, $Q_4 = \operatorname{diag}(1, 1, 0, 0)$, $Q_5 = \operatorname{diag}(1, 1, 0, 1)$, $Q_6 = \operatorname{diag}(0, 1, 1, 1)$, $Q_7 = \operatorname{diag}(1, 1, 0, 0)$
Input cost $R_1, \ldots, R_7$	$R_1 = 1$, $R_2 = 1000$, $R_3 = 10$, $R_4 = 100$, $R_5 = 1$, $R_6 = 1$, $R_7 = 1000$
Prediction horizon N_k	5
Iterations per time instant $p_{\max}$	8

Acknowledgements

Iucundi acti labores
Work that is all done is delightful
— Cicero

Now that the formal parts of my thesis have been written, one last section remains. Although some of the people mentioned below may actually oppose it, writing the acknowledgements section is perhaps more delicate than what I have written so far — after all, for many readers, this is the first (yet, hopefully, not the only) part they are interested in.

The writing of this final section marks the end of 4 years of intensive study of the fascinating world of electrical power systems and control theory. Four years in which I have learned a lot, on both a professional and a personal level. I owe a great deal to many people who have continuously guided and supported me during my research, to whom I would like to express my deepest gratitude.

First of all, I would like to thank my promotor, prof. P. P. J. Van den Bosch, and copromotors, dr. M. Lazar and dr. A. Jokić. Paul, thank you for giving me the opportunity to work on the interesting topic of electrical power system control, and for guiding me so kindly and patiently through this important period of my life. You are a great teacher and mentor. Mircea, I very much admire your dedication to research and your hard-working attitude. Thank you very much for the nice and fruitful collaboration we had over the past 5 years, and for your trust in me during all phases of my PhD. Andrej, you taught me to be critical

of my work, and showed me how to attack research problems in a systematic, logical way. It has been a great pleasure to work with you.

I am also very grateful to the other members of my PhD defense committee. Prof. Frank Allgöwer, prof. Gerard Doorman, prof. Wil Kling and ir. Paul Giesbertz, thank you for the time and efforts you spent on reading and discussing my thesis; your comments and suggestions have certainly helped in improving the quality of my work.

My appreciation goes out to SenterNovem/Agentschap NL, for funding my PhD research as part of the EOS-LT Regelduurzaam project.

Throughout the past four years, I have been privileged to meet many inspiring scholars and experts from industry. In particular, the collaboration with our project partners at APX (Paul Boonekamp), ECN (René Kamphuis, Frans Nieuwenhout and Cor Warmer), KEMA (Wouter de Boer, Gerben Dekker, Martijn Duvoort), and TenneT (Frank Nobel) proved to be very valuable in getting grip on the issues that the power system industry is dealing with today. My gratitude also goes to the other PhD students working on the Regelduurzaam and E-Price projects. Jasper, Ana, Ioannis and Barry, thank you for the nice discussions, your critical input and support.

Special thanks go out to prof. Ian Hiskens and Mads Almassalkhi from the University of Michigan. My three-month visit to Ann Arbor has truly been a rewarding and pleasant experience, and I was very happy to learn that there is much more to power system control than supply and demand balancing.

I sincerely enjoyed the rewarding discussions, conference visits and nice get togethers with my colleagues of the Control Systems Group. A special word of appreciation goes out to my office mate Rob: thanks for the interesting discussions we had regarding several mathematical problems, and thanks for teaching me to appreciate jazz music. Also, I had the pleasure of supervising a number of master and bachelor students. Joost, Roy, Maryam, Peter and Theo, I really enjoyed working with you. Moreover, I should not forget to thank our secretary Barbara and technical assistants Udo and Will for their friendly support.

Ten slotte zou ik graag mijn vrienden en familie willen bedanken. Bij hen kon ik altijd terecht voor de nodige afleiding en gezelligheid. Pap, Mam en Marc, een bijzonder woord van waardering gaat uit naar jullie. Zonder jullie onvoorwaardelijke liefde en steun was het schrijven van dit proefschrift stukken moeilijker, zo niet onmogelijk, geweest. Ik zeg het misschien niet zo vaak, maar het doet me veel dat jullie altijd voor me klaar staan.

Ralph Hermans
Eindhoven, October 2012

Curriculum Vitae

Ralph Hermans (born in Stein, The Netherlands, 16 March 1985) received his M.Sc. degree (cum laude) in Electrical Engineering from the Eindhoven University of Technology (TU/e), Eindhoven, The Netherlands, in 2008. His master thesis was selected as the winning paper of the IEEE Region 8 Student Paper Contest in 2008. Ralph Hermans's fundamental research interests include stability analysis and stabilizing controller synthesis for large-scale networks of dynamical systems, non-centralized model predictive control and optimization, and control problems in automotive, mechatronic and electrical power system applications.